RESIDENTIAL WOOD COMBUSTION AEROSOL CHARACTERIZATION AS A FUNCTION OF SIZE AND SOURCE APPORTIONMENT USING CHEMICAL MASS BALANCE MODELING

John Anthony Rau
B. S., Rensselaer Polytechnic Institute, 1958
M. S., University of Michigan, 1967
M. S., Oregon Graduate Center, 1981

A dissertation presented to the faculty
of the Oregon Graduate Center
in partial fulfillment of the
requirements for the degree
Doctor of Philosophy
in
Environmental Science

May, 1986

The dissertation "Residential Wood Combustion Aerosol Characterization as a Function of Size and Source Apportionment Using Chemical Mass Balance Modeling" by John A. Rau has been examined and approved by the following Examination Committee:

James J. Huntzicker
Dissertation Research Advisor
Professor

M. A. K. Khalil
Professor

Reinhold A. Rasmussen
Professor

John G. Watson
Associate Research Professor
Desert Research Institute
University of Nevada

DEDICATION

This work is dedicated to Sister Mary Damian, my eighth grade teacher, who encouraged my interest in science and was a friend for many years.

J.A.R.

ACKNOWLEDGEMENTS

I would like to acknowledge and thank those who contributed to this dissertation. I am grateful to my advisor Dr. James Huntzicker who provided guidance during the course of this study and to Drs. John Watson and Jitandra Shah who were always willing to discuss various aspects of the project.

I would like to thank Fred Thone who supplied machining advice during the construction of the sampling equipment.

I am especially grateful to Sylvia Edgerton for collaborating with me in source sampling of residential wood burning emissions. Her able handling of the logistics of source sampling encouragement facilitated the gathering of the large amount of source data collected in this research.

The Hillsboro School District provided space for setting up a ambient sampling station in Hillsboro. The opportunity to sample a variety of residential stoves and fireplaces was provided by: Mary K. Lind, Jon Orloff, Rick DeCesar, Barbara Ryall, Mary Mayfield-Gambill, Aslam Khalil and Marc Feldesman who allowed me to sample from their chimneys.

I would like to thank John Core of the Oregon Department of Environmental Quality who provided the copy of the CMB program used in this research and who provided valuable insight into the art of doing CMB analyses. I would also like to thank Rick DeCesar for his insights into CMB analysis.

I would like to acknowledge Dr. John Cooper and NEA Laboratories who did a large part of the XRF analyses used in this study. I would

also like to thank Edie Taylor and Carol Hendrickson for typing figure captions.

I would like to thank Dr. Marc Feldesman of Portland State University for his advice and support in managing my computer.

I would also like to thank my wife, Judy, for her encouragement.

This project was partially supported by U. S. EPA grant (#R810090-01-0).

TABLE OF CONTENTS

LIST OF TABLES

LIST OF FIGURES

ABSTRACT

This research has determined the mass and composition distribution as a function of particle size for wood burning stove and fireplace aerosols. Sampling was done from cooled, diluted smoke plumes to better describe particulate properties as they exist in the atmosphere. The particulate composition variability noted in previous research was controlled by restricting sampling to hot burning (damper open combustion) and cool burning (air starved damper closed combustion). Size distributed traffic and residential oil burner aerosols were also sampled. Samples were collected behind a series of single stage impactors. Special emphasis was placed on the determination of organic and elemental carbon because these species are major components of combustion aerosols. Corrections were made for organic vapor adsorption on quartz fiber sampling filters.

Hot burning RWC particles were black, had a unimodal size distribution and contained from 20 to 60% carbon (primarily elemental carbon) and high levels of trace elements (K, S, Cl). In contrast, cool burning RWC particles were tan, had a bimodal size distribution, and contained from 55 to 65% carbon (almost entirely organic carbon) and only minute amounts of trace elements.

RWC composition data were used in CMB modeling of residential area aerosol samples by: (1) using a composite RWC composition profile adjusted for the proportion of damper-open and closed burning as determined by surveys; or (2) using both hot and cool RWC profiles together. CMB modeling was used across the fine aerosol (<2.5 m) size range to show the size distribution of combustion generated aerosols. It

was demonstrated that combustion generated organic and elemental carbon distributions, especially for particles <0.3 m, shifted to larger sizes during their atmospheric residence time. This shift can be explained by coagulation. CMB modeling was also used to examine the effects of assuming that RWC particles lose organic carbon during their atmospheric residence time. For winter samples the agreement between organic and elemental carbon values calculated by the model and ambient values was improved by allowing RWC particles to lose from 25 to 65% of their organic carbon loading; however, allowing these losses did not significantly alter source contributions.

CHAPTER ONE: INTRODUCTION

1.1 THE INCREASE IN THE USE OF WOOD AS A RESIDENTIAL SPACE HEATING FUEL

In 1970, when the Clean Air Act became law, no list of major air pollution sources contained residential wood burning. In 1984 Time Magazine (January, 16) reported: "Pollution from home wood stoves is nearing crisis proportions". In Missoula, MT. pregnant women, joggers and the elderly were urged to stay indoors rather than breathe the foul air. In a study of seven sites in Oregon, Washington and Idaho during the winter of 1980 to 1981, wood-burning stoves were found to be responsible for 66 to 84 percent of respirable particulate material (JAPCA, 35:1088). Obviously there have been some changes in the levels of residential wood combustion (RWC) air pollution and in the way it is perceived during the period from 1970 to 1985.

It has been well documented that since the 1973-74 oil embargo the use of wood as a home heating fuel and the associated air pollution has increased dramatically (Bailey et al., 1982a,b; Butcher, 1978; Core et al., 1984; Cummings, 1982; Dalton et al. 1977; DeAngelis et al. 1981; GMA, 1979; Green, 1980; Hatchard and Day, 1979; Howland and Kowalcyzk, 1984; Imhoff et al., 1984; Lipfert and Dungan, 1983; Nero & Assoc., 1984; Otis, 1977; Palmer et al., 1980; Romero et al., 1978; Truesdale et al., 1984). A summary of 20 recent RWC air pollution studies (Nero & Assoc., 1984) (Appendix 1) showed that the average ambient RWC aerosol pollution over the study periods ranged from 6-93 μg/m3 and the 24 hour averages ranged from 24-234 μg/m3. A 1980-81 Forest Service survey

(Nero & Assoc., 1984) showed that residential wood burning occurs in every state and ranges from 11% of households (Florida) to 58% of households (Oregon, Vermont) (Appendix 1). The 28% of households in the nation that burn wood burn an average of 0.76 to 3.9 cords annually. Consumption of fuel wood in 1980-81 was 40.5 million cords in primary homes and another 1.5 million cords in second homes (21.1 million cords burned in stoves, 19.3 million cords burned in fireplaces or fireplace inserts). The EPA has estimated that 10.6 million stoves were in use by the end of 1983 and that the number is increasing by one half to a million units per year (JAPCA, 35:1088).

Increased concern about RWC air pollution has motivated a need to develop and evaluate methodologies that will accurately determine the RWC contribution to urban particulate air pollution. Chemical mass balance (CMB) modeling has been used for this purpose; however, the results obtained to date have had high uncertainties because of the relatively low concentrations and high variability of the primary RWC inorganic tracers (K and Cl). Because carbon often comprises over 50% of wood smoke particles, CMB modeling uncertainty of RWC can be reduced by the accurate determination of RWC organic and elemental carbon. This effort should include source sampling from cooled, diluted plumes and the accounting of organic vapor assorption on sampling filters to insure that particle compositions are representative of particles as they exist in the atmosphere. It should also determine the sources of and limits of RWC particulate composition variability. Finally it should examine whether RWC particulate composition changes during its atmospheric residence time.

1.2 THE AIR POLLUTION ASPECTS OF RESIDENTIAL WOOD BURNING

Per unit heat output RWC generates much more pollution than burning oil or gas. A reasonably small house using wood as its only heating fuel will emit about 45(+150, -30) kilograms particulate material per heating season. In contrast, by using oil or gas heating emissions would be 2.5 and 1 kilograms, respectively.

Both organic and elemental carbon particles are formed by the burning of carbon in incomplete combustion processes such as RWC (Sexton et al., 1984). Combustion-generated aerosols can vary from particles that are 90% organic carbon to particles that are 90% elemental carbon (Mast et al. 1984; Wolff, 1981). These aerosols contribute mainly to the fine fraction of particulate pollution (<2.5 μm diameter) (Wolff et al., 1982). They pollute both outdoor and indoor air (Sexton et al., 1984a,b)

The group of compounds that comprise the organic carbon fraction of combustion aerosol particles are determined by the fuel type, the combustion process, and the combustion parameters such as: fuel residence time in the combustion zone, temperature, turbulence, and combustion air availability. Hundreds of organic compounds have been isolated from wood smoke aerosol (Alfheim et al. 1984a,b; Boubel et al., 1981; Cooke et al. 1982; DeAngelis et al., 1981; Lipari, 1984). These form the basis of the health concerns associated with wood smoke inhalation.

The elemental carbon in combustion aerosol particles (sometimes called soot, non-volatile carbon, black carbon, non-extractable carbon or free carbon) is black, with an amorphous or graphitic structure

(Ogren and Charlson, 1983; Wolff, 1981b). Most combustion-generated aerosols which contain a significant amount of elemental carbon are composed of clusters of small spherical particles or chains of spherical particles (Dasch, 1982; Howard, et al., 1982; Lahaye and Prado, 1974). Elemental carbon forms the basic structure of the spheres, while organic compounds are deposited on the surface and in the pores of the elemental carbon structure (Fitch and Smith, 1979).

The organic compounds associated with RWC aerosol particles have been found to be irritating, toxic, mutagenic, carcinogenic and co-carcinogenic chemical species (Alfheim, et al., 1984a, b, c; Carlson, 1982; Carnow, 1978; Carnow and Meir, 1973; Cooper, 1980; Cooke et al. 1982; Daisey, 1980; DeAngelis et al., 1981; 1984; Hubble et al., 1982; Kamens et al., 1984a, b, 1985; Kelsey, et al. 1982; Lewtas et al., 1982; Mast, et al., 1984; Peters, 1982; Ramdahl et al., 1982, 1984; Smith, 1983; Smith et al., 1984; Thomson, et al., 1985). These organic compounds include aliphatics consisting of C_8 to C_{27} alkanes and alkenes, ketones, aromatics and polycyclic organic material (Hubble, et al., 1982). Benzo(a)pyrene, a known carcinogen which has caused tumors in hamsters, mice, rats and rabbits, has often been found in wood smoke aerosols. Imhoff et al. (1982) have shown that many of the mutagenic and carcinogenic species associated with wood smoke aerosols were also found in the vapor phase downwind of a community noted for a large amount of residential wood heating. Rudling and Ahling (1982) demonstrated that there is an almost linear relationship between wood burning carbon monoxide emission per mass of wood burned and mutagenicity of solvent extractions of wood burning emissions.

Studies of school children and adults in Missoula, Montana, where wood smoke contributes over half of wintertime aerosol pollution, associated chronic obstructive pulmonary disease and significant lung dysfunction with wood smoke air pollution (Cannon, 1984).

RWC aerosol particles also cause visibility degradation both because they are in the size range where particles effectively scatter light and because they contain black elemental carbon which absorbs light (Bergstrom et al., 1982; Groblicki et al., 1981, Kowalczyk et al., 1982a, b; Packham and Vines, 1978; Patterson and Wagman, 1977; Rosen et al., 1980; Shah, 1981; Shah et al., 1984; Stevens, 1983; Wolff et al., 1981a).

RWC aerosol particles can participate in atmospheric chemistry by causing or promoting gas to particle conversion such as the conversion of SO_2 to particulate sulfates (Chang et al., 1982). In addition, Kamens et al. (1984b, 1985) have shown that the direct acting mutagenicity of wood smoke extracts increased after particles interacted with ambient NOX and/or ozone both under dark and daylight conditions while indirect acting mutagenicity decreased under bright sunlight conditions.

1.4 THE COMPOSITION OF RWC AEROSOL PARTICLES

Both the composition and emission rates of RWC aerosol particles are highly variable and are strongly dependent on combustion parameters. The variability of emission rates is illustrated by the fact that emission rates for both stoves and fireplaces span the range of 1-70 gram particulate material emitted per kg of wood burned

(Butcher and Buckley, 1977; Butcher and Sorenson, 1979; Butcher and Ellenbecker, 1981; Hall and DeAngelis, 1980; Rudling and Ahling, 1981; Stiles, 1983; Kowalczyk et al., 1982; Sandborn and Blanchet, 1982; Barnett and Shea, 1982). RWC aerosols contain large amounts of organic and sometimes large amounts of elemental carbon along with significant amounts of potassium, chlorine, sulfur, aluminum, iron, phosphorous, silicon, lead, zinc and rubidium (Dasch, 1982; DeCesar and Cooper, 1982; Stiles, 1983; Watson, 1979). While there is a large body of literature presenting RWC emission factor data, very little information about wood smoke composition is available, especially as it exists in cooled, diluted smoke plumes, i.e., during its atmospheric residence time. There are some data giving trace elemental composition of forest slash burning aerosols (Hester, 1979). The major concern in determining the composition of RWC aerosols has been with the species that compose the organic carbon fraction of these aerosols (Alfheim, et al., 1984a,b; DeAngelis, et al.,1981; Kamens, et al., 1984; Hubble, et al., 1982; Jahnson, 1961). These data have not been demonstrated to be useful for CMB modeling. Watson (1979) measured trace elements in a few samples of fireplace burning and choked-off wood stove burning (Table 1.1); however, no information about fuel types or burn conditions was given. DeCesar and Cooper (1981) reported carbon and trace element data (Table 1.1) for residential wood combustion source sampling. These data were obtained with a modified dichotomous virtual impactor fitted with an EPA Method 5 probe. Stiles (1983) reported wood stove trace elemental compositions for samples collected from a dilution tunnel where flue gas was diluted nine to one with clean air (Table 1.1). None

Table 1.1

Composition of Residential Wood Smoke Fine Aerosol

(% of mass)

	DeCesar	Stiles	Watson	
	Woodstove		Fireplace	Woodstove
OC	47.5±13.8	33.4±13	45.9±5.5	49.1±4.9
EC	12.8±8.4	7.4±7	12.9±5.2	8.3±0.8
Al	0.021±NR		0.024±.018	0.018±.002
Cl	0.509±0.03	1.7±3	0.61±.057	0.094±.0049
Ca	0.067±NR		0.055±.007	0.037±.002
Fe	<		0.002±.0003	0.0035±.0007
K	0.086±0.01	12.5±11	0.53±.11	0.053±.04
Mn	<		0.002±.001	0.012±.015
Si	<		0.024±.02	<0.005
S	0.182±0.02	3.3±3	0.37±.034	0.28±.46
Zn	0.037±NR		0.12±.16	<0.01

< Below detection limit

NR Not reported

of these studies, which measured RWC aerosol particle carbon composition, accounted for vapor carbon adsorption on sampling filters. Therefore they tend to overestimate organic carbon composition.

1.5 A SURVEY OF WOOD SMOKE SIZE DISTRIBUTION DATA

Dasch (1982) obtained size distribution data for wood burning aerosols from a free standing fireplace. Using impactor sampling she found that 83-90% of the aerosol mass passed a 0.56 μm cut-point impactor. Only a few percent of the aerosol was found above 2.5 μm. The aerosol was shown to have a mass median diameter of 0.17 μm by using an electrical aerosol analyzer.

Kamens et. al. (1983), using an electrical aerosol analyzer (EAA) and an optical particle counter (OPC), showed that most wood smoke particles fell in the 0.04-0.3 μm size range although sometimes significant particulate volume appeared in the 0.422-0.750 μm size range. They also showed that high burn rates produced more small sized particles than lower burn rates and that aging wood smoke over 4 hours produced a sharp decline in particles in the 0.04-0.133 μm size range and some decrease in particles around 0.133 μm. The fact that OPC volume did not decrease as rapidly as EAA volume suggested that the shifting of both number and volume distributions to larger particle sizes with aging was caused by coagulation. Bell et al. (1984) showed that RWC particle volume distributions determined with an EAA for high burn rate particles had a mode at about 0.08 μm and a slightly lesser mode at about 0.15 μm, while low burn rate particles had a single mode at about 0.2 μm.

Radke et. al. (1978) examined forest fire plumes, by aerial sampling, for several prescribed forest fire burns in Washington State. They used an EAA and OPC mounted in an aircraft. The first fire sampled was a vigorously burning slash fire which was described as closely resembling a wild fire. Its plume reached an altitude of 1800 meters. The volume size distribution for this wood smoke aerosol was monomodal with essentially no particles greater than 1.5 μm in diameter nor smaller than 0.07 μm. The mode of the distribution was about 0.3 μm. The second fire sampled was much cooler burning than the first. Its plume was more diffuse and only rose to an altitude of 600 meters. Particles sampled from this plume had a bimodal distribution, with one mode occurring at 0.18 μm and one at 0.9 μm. Essentially no particles had diameters smaller than 0.07 μm nor greater than 1.5 μm. The mass median diameter was about 0.4 μm. The most interesting feature for this cool burning aerosol was that it was bimodal and that about 40% of the aerosol mass was between 0.6 and 1.5 μm. This bimodal distribution might have resulted because organic vapors condensed both on nuclei that were generated in the flame and on particles that had previously existed in the combustion air.

Hester (1979) obtained an extensive series of aerosol samples from forest slash and grass field burning plumes. He found that an average of 81% of slash burning aerosol was less than 2.2 μm in diameter. Similar samples of grass burn aerosols were 71 to 80% below 2.2 μm.

1.6 MEASUREMENT OF AMBIENT LEVELS RWC AIR POLLUTION

The methods used to estimate the impact of RWC can be divided into

four main types: dispersion modeling, source inventory, receptor modeling (Watson,1979; Cooper and Watson, 1980; Kowalczyk et al., 1978; Miller et al., 1972) and use of radioisotope tracers (carbon-14) (Cooper et al., 1979; Currie, 1982). Of these methods source inventory and dispersion modeling are not very useful because of the difficulty in determining source locations, strengths and strength variations over time for all RWC sources.

The Portland Aerosol Characterization Study (PACS) (Cooper et al. 1979b) was one of the first studies to use CMB methods to estimate the contribution of biomass burning to ambient particulate levels. The category biomass (vegetative material) was used because it was not clear that sources such as residential wood burning, slash burning, grass burning or backyard burning could be distinguished from one another. In the PACS study Watson (1979) recognized that the quantification of various biomass burning sources was difficult because they do not have any exclusive elemental tracers and because their source composition profiles were highly variable.

CMB analysis has been described by many authors (Gordon, 1980; Dzubay, 1980; Friedlander, 1973; DeCesar and Cooper, 1982; Kowalczyk et al., 1978; Watson, 1979; Watson et al., 1984). In this model the aerosol at a receptor is assumed to be a linear combination of an assumed group of sources. This is expressed by equation 2.1

$$C_i = \sum_{j=1}^{n} A_{ij} S_j \qquad 1.1$$

where C_i is the concentration of the ith chemical species at the

receptor, A_{ij} is the concentration of ith species in the aerosol from the jth source. S_j is the mass contribution of the j source at the receptor, and n = number of sources. An equation of this form is written for each chemical species measured giving a series of simultaneous equations, which if there are at least as many species as there are sources can be solved for the mass contributions from each source. Because there are usually more species then there are significant sources, the system is over-determined. Solving the system of equations given by Eq. 1.1 can be done in two ways: ordinary least squares or effective variance (Watson, 1979). In the ordinary least squares solution it is assumed that the composition of the sources is known exactly and that only the analytical uncertainty of ambient aerosol composition needs to be considered. The weight given to any tracer species is inversely proportional to the analytical error associated with that species. In the effective variance solution both the ambient aerosol and the source compositions are considered to have uncertainties. Both compositions at least have similar analytical errors. In addition the source compositions can also have uncertainties due to process variability. This is a major factor contributing to RWC particulate emissions uncertainty.

In CMB modeling when a pollution source consists of many individual sources with widely different compositions contributing to the group average, the uncertainty of source composition profile used for CMB modeling should be the standard error of source measurements using an adequately large group of source composition measurements that includes the range of process variations in proportion to their

frequency of occurrence, i.e. the uncertainty used should be the standard deviation of the group composite composition rather than the standard deviation of the sample group. The usual practice of using the standard deviation of a small group of samples is not correct.

A further problem with chemical mass balance models occurs when sources exist which have similar chemical composition profiles (multicollinearity) (Henry, 1982). The reduction of source and ambient uncertainties can slightly reduce multicollinearity effects, but sources with very similar composition profiles (e.g., wood-stove emissions, fireplace emissions, slash burning or backyard brush burning emissions) might not be resolvable by CMB modeling. A mathematical procedure (singular value decomposition) can be used to determine the limit of the accuracy to which sources having similar chemical composition profiles can be distinguished for a given set of sources and uncertainties (Henry, 1984).

The critical assumptions in CMB modeling are that a unique set of identifying properties, usually mass fractions of elemental tracer species for each source of interest, exists and that these properties are preserved during the atmospheric residence time of the aerosol particles. For CMB modeling to be effective, the source composition profiles used must represent aerosol particle compositions from these sources as they exist at the receptor. To meet this requirement the composition profiles of the particles leaving the receptor are at least necessary. Source sampling using EPA Method 5 does not meet this requirement because it interrupts the condensation and coagulation processes occurring as combustion generated particles cool in the

organic vapor rich atmosphere on the stack. For combustion sources, sampling plumes that are cooled and diluted by ambient air more realistically determine composition for particles as they exist in the atmosphere (Gordon, 1980). For combustion-generated particles which contain a significant amount of carbon, the quantification of both organic and elemental carbon can improve CMB modeling results (Hering et al., 1985). This is especially true for sources such as RWC which contain no unique tracer species and in most cases only have very low levels of elemental tracer species. For these sources the ratio of organic to elemental carbon may be relatively unique and the carbonaceous content might be much less variable than that of elemental tracer species.

One final critical point in the determination of the carbon composition of highly carbonaceous aerosol particles is the correct speciation between organic and elemental carbon. The dividing line between organic carbon and elemental carbon is not clearly defined and may not have a precise definition, but in practice is determined by the analytical procedures that attempt to make this separation.

There is today no agreement on the most effective analytical method to determine aerosol particle organic and elemental carbon composition (Stevens, 1982; Cadle and Groblicki, 1982, 1984; Japar et al., 1984). An adjunct to this research has been an effort to improve the thermo-optical carbon analysis procedure (Appendix 2).

1.7 GOALS OF THIS RESEARCH

1. Determine the composition and size distribution of RWC aerosol particles sampled from cooled diluted plumes.

2. Show that the explanation of carbon in residential area aerosol samples using CMB modeling can be improved by using RWC source composition profiles determined by source sampling from plumes that have been cooled and diluted by ambient air.

3. Show that RWC emissions can be represented in CMB modeling by two distinct composition profiles, cool burning and hot burning, and that this procedure improves the explanation of carbon and trace element species.

CHAPTER TWO: EXPERIMENTAL METHODS

2.1 THE SAMPLING SYSTEM

This chapter describes the construction of the sampling system, the experimental protocol and the aerosol particle composition analysis. The same sampling system was used to collect both source and ambient aerosol samples at a series of points over the particle size ranges spanned by the sources. The sources examined were residential stove and fireplace wood combustion, residential oil burning, and vehicular aerosols collected from a highway tunnel. Almost all of the aerosol particles from these sources had aerodynamic diameters less than 2.5 μm. The sampling system consisted of a set of single stage impactors which sampled aerosol from a common plenum. Impactors were designed with cut points at 10, 2.5, 1.2, 0.6, 0.3 and 0.1 μm (Marple et al. 1974a,b, 1975). Samples consisted of particles that passed the impactors. Impactor samplers were used in various combinations. Often impactor sets included a sampler run without an impactor to sample "total" aerosol. The 0.1 μm impactor was preceded by a 0.6 μm impactor to preclean the sampled airstream.

The specific chemical compositions measured were carbon composition, expressed as organic and elemental carbon and trace element composition. Carbon was measured by using the thermo-optical carbon analysis system developed at Oregon Graduate Center (OGC). Trace elemental composition was measured by x-ray fluorescence analysis (XRF).

2.1.1 THE DETERMINATION OF ORGANIC VAPOR ADSORPTION

An important sampling artifact that occurs when sampling carbonaceous aerosols is organic vapor adsorption on to the glass or quartz fiber sampling media (Schwartz et al.,1981; VanVaeck et al.,1984). Unless a correction is made for this artifact a variable addition to the measured organic carbon component of aerosol particles results because during carbon analysis adsorbed vapor carbon cannot be distinguished from particulate organic carbon. Organic vapor adsorption can contribute up to 30 to 40% of the total organic carbon deposited on an aerosol sampling filter.

This artifact has been noted by Duce (1978), Stevens et al. (1980), Cadle et al. (1983), and McDow (1986). Cadle et al. showed that the adsorbed carbon was not CO2, but was likely to be a mixture of organic compounds that can exist in the vapor phase at ambient temperatures. They also noted that field blanks adsorbed about 28% as much organic vapor as sampling filters, i.e. organic vapor adsorption occurs by diffusion for filters that are not actually used for sampling. Further evidence that the adsorbed artifact material was organic carbon was obtained by noting that filters loaded only with adsorbed carbon turned dark on heating due to the pyrolytic conversion of organic carbon to elemental carbon.

In this research the magnitude of this artifact was determined by measuring the organic vapor adsorption on quartz fiber filters (backup filters) that were located behind Teflon filters when aerosols were being sampled by the Teflon filters. In this arrangement the Teflon

filter removed aerosol particles from the sampling stream, while the vapor species passed through the Teflon filter and were adsorbed on the quartz fiber filter. Vapor adsorption on Teflon filters was assumed to be negligible or at least much smaller than it was on quartz fiber filters (McDow, 1986). It was found that the collection of organic vapor on backup filters was independent of the impactor behind which they were used. Therefore usually only one back-up filter behind a Teflon filter and one behind a quartz fiber filter were used per sampling experiment. The quartz fiber backup filter used behind a quartz fiber front filter determined the organic vapor collection efficiency on quartz fiber filters.

2.1.2 FILTER MEDIA

Aerosol samples were collected on quartz fiber filters for carbon analysis and on Teflon filters for XRF analysis. The collection of particles on filters satisfies the requirement of both carbon and XRF analysis that particulate material must be uniformly distributed over a surface which has low blank levels for the species being measured. For XRF analysis Teflon filters also satisfy the requirement that the aerosol particles were uniformly collected on filter surfaces rather than deposited within the filter medium.

For carbon sampling quartz fiber filters were preferable to glass fiber filters because they can be heated to higher temperatures than glass fiber filters to reduce carbon blank levels prior to sampling and to insure that all the deposited carbon was removed from the filter during analysis. It was noted in the analysis of a diesel emission

sample collected on a glass fiber filter that even when the filter was heated to near its melting point it was still gray, indicating that some of the elemental carbon in the sample had not been removed by the analysis procedure. Quartz fiber filters were heated to 800°C in a muffle furnace for at least an hour to reduce blank levels. This typically reduced blank levels to 0.5-0.7 μg/cm2. Glass fiber filters also exhibit a change in their light reflecting properties when the filter material approaches its melting point which makes accurate correction for pyrolytic conversion of organic to elemental carbon impossible.

Quartz fiber filters were more fragile than glass fiber filters and therefore required careful handling in order to obtain useful sample mass data. Also some brands of quartz fiber filters tended to adsorb water and retained it even for long equilibration periods at low humidity conditions. Fortunately most brands of quartz fiber filter material equilibrated well over short time periods.

2.1.3 IMPACTOR SAMPLING

For an ideal single stage impactor all particles with aerodynamic diameters larger than some design value (the cut point) are captured by the impactor and all particles with aerodynamic diameters less than the cut-point diameter remain in the flowstream passing the impactor. Aerodynamic diameter is the diameter of a spherical particle with a density of 1 g/cm^3 that will have the same Stokes settling velocity as the actual particle being considered. Real impactors pass some particles

which have diameters greater than the cut-point and capture some which have diameters smaller than the cut-point. Both of these effects occur because ideal impactor design conditions only apply in the central section of the flowstream through the impactor where laminar flow is well defined. At the margins of the flow stream conditions exist which produce non-ideal conditions. Particles larger than the cut-point can also elude capture by bouncing after hitting the impaction plate. Good design keeps these undesirable effects to a minimum.

Samples collected in this research consisted of particles which remained in the flowstream after passing the impactors. Aerosol mass between two impactor cut-point values was determined by subtracting the mass collected behind a given impactor from the mass collected behind the impactor with the next largest cut-point. By using data from a series of impactors in this way the size distribution of particulate mass or the distribution of any other particulate property can be determined. By subtracting the mass collected behind the 2.5 μm impactor from the mass collected by the "total" sampler (no impactor) a measure of the aerosol mass above 2.5 μm was obtained. Since using a "total" sampler did not give information about the upper limit of the aerosol size range a 10 μm impactor was used at times to better define the upper size limits of aerosol samples. This cut-point choice was used because of the present EPA trend to use a 10 μm upper limit cut-point standard for aerosol particle sampling (i.e., PM_{10}).

The sampling system was required to be reasonably portable, rugged and useful in field situations. Figure 2.1 shows a schematic drawing of the system. The sampling plenum was constructed using a 20 cm diameter,

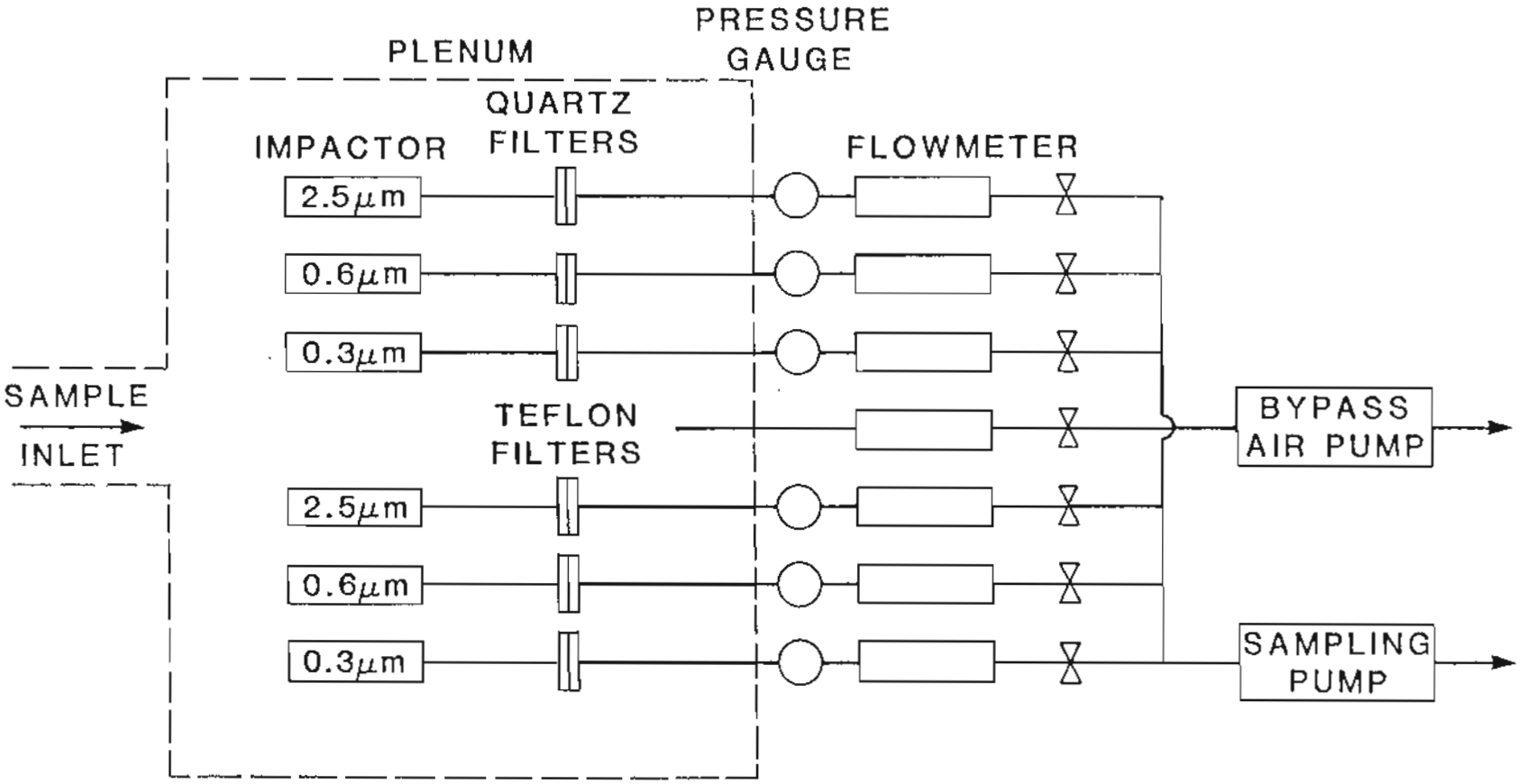

Figure 2.1. Sampling system schematic drawing for sampling size segregated aerosols with single stage impactors. #2 impactor set shown.

2 m long aluminum pipe. Air entering the plenum was moved by two separate pumping systems, the bypass air system and the sampling system. About two-thirds of the air entering the plenum was by-passed. The remaining third was sampled. Even when sampling ambient aerosols for periods of twenty four hours or longer the flow control system was highly stable. Flow settings usually did not vary by more than 0.5 lpm from the set value over these sampling times. This was in large part due to the fact that most of the long ambient sampling runs were done in locations (Portland residential area) where particulate loading was low enough to prevent filters from becoming excessively loaded. In areas where ambient particulate loading was high (Hillsboro) short sampling times were usually used. The residence time of the sampled gas in the plenum was about 0.6 min. The entry section of the plenum consisted of a 5 cm diameter flexible metal tube. This tube could be used directly as an inlet or attached to other inlet extension tubes, i.e., for sampling stoves and fireplaces while leaving the sampling system on the ground a 6 m, 7.5 cm diameter aluminum extension tube was used to reach up into the plume coming from a chimney. Residence time in the extension tube was 15 seconds. Aerosol losses to the tube walls by diffusion for 0.1 μm diameter particles were calculated to be about 2%. For sampling the Earthstove the sampling system was moved onto the roof because the wood stove chimney was located so that the long sampling pipe was not useful.

The sampling assemblies shown in Figure 2.2 were mounted in the far end of the plenum away from the plenum inlet. Flow straighteners, 30 cm long and 4 cm in diameter were mounted ahead of each sampling assembly. These insured that a symmetrical laminar flow field entered each

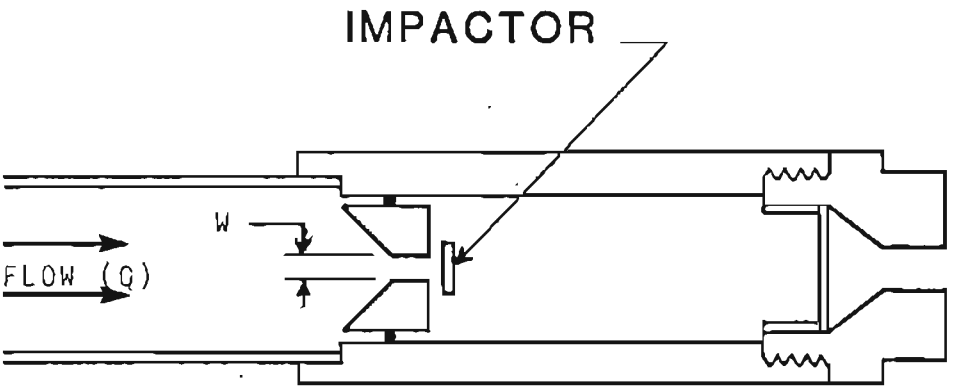

$$D_{p50} = f(W,Q) \qquad \text{(a)}$$

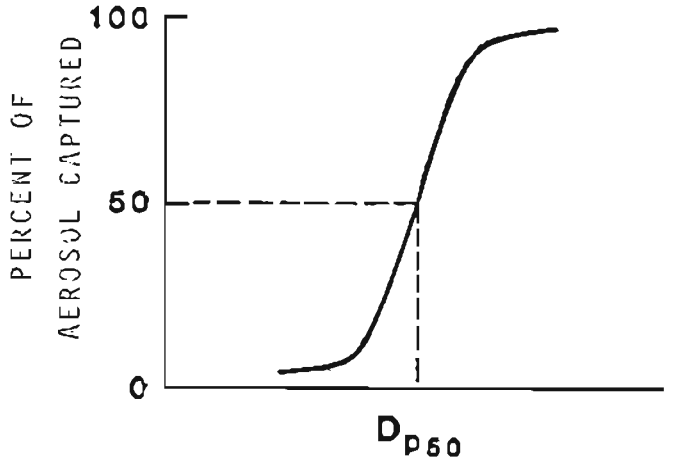

(b)

Figure 2.2. (a) Impactor assembly schematic drawing.
(b) Impactor performance curve.

impactor. Flow conditions were such that the air entering the flow straighteners was isokinetically sampled. The bypass flow system insured that air in the plenum was well mixed and that all of the impactors were sampling the same aerosol. Each impactor was mounted in a sampling assembly as shown in Figure 2.2. A 12 cm tube separated the impactor exit plane from the filter collection surface to insure that the aerosol was uniformly distributed in the flow stream after going through the impactor and would be uniformly deposited on the filter. The filter holders were screwed into the sampling assemblies. Teflon tape was wrapped around the screw threads to prevent air leakage around the threads.

A statistical analysis of 38 aerosol mass sample pairs, where one member of the pair was collected on Teflon and the other member was collected on quartz, showed no significant differences at the 95% confidence level. The largest relative mass differences usually occurred for small sample masses where random mass errors, such as losing a small piece of filter material, were comparable to the mass of material sampled. An occasional problem which occurred when quartz backup filters were used was that filter mass might transfer between the front and back filters. This error was correctable when a series of backup filters were used and the weight change of all filters used in the experiment was measured.

Impactors could easily be removed from the sampling assembly for cleaning and regreasing between test runs. All impaction stages, except the 0.1 μm impactor stage, were coated with Apiezon vacuum grease to decrease particle bounce (Cheng and Yeh, 1979; Esmen et al.,1978).

diameter it was not necessary to grease the impaction stages. On the other hand Hering (1978) found it useful to use oil impregnated, fritted glass impaction surfaces for the stages with cut-points in the region of 0.1 μm for a low pressure impactor when calibrating with latex spheres. This difference is probably explained by differences in adhesion and bounce characteristics between latex spheres and traffic aerosols. For most particles sampled in this research, especially those from cool RWC which were largely composed of heavy tarry liquid, it would be expected that they remain attached to the impaction plate. The 0.1 μm cut-point

Berner and Lurzer (1980) found that for traffic aerosols <0.7 μm diameter it was not necessary to grease the impaction stages. On the other hand Hering (1978) found it useful to use oil impregnated, fritted glass impaction surfaces for the stages with cut-points in the region of 0.1 μm for a low pressure impactor when calibrating with latex spheres. This difference is probably explained by differences in adhesion and bounce characteristics between latex spheres and traffic aerosols. For most particles sampled in this research, especially those from cool RWC which were largely composed of heavy tarry liquid, it would be expected that they remain attached to the impaction plate. The 0.1 μm cut-point impactor used an oiled fritted glass stage (Ace Glass, porosity E, 30 mm. diameter, catalog #7176-31) which was noted by Hering (1978) to be especially effective at reducing particle bounce. High vacuum oil (Santovac, vapor pressure = 4×10^{-10} torr.) was used to oil the stage to reduce particle bounce.

2.1.4 DESIGN, CONSTRUCTION AND CALIBRATION OF THE IMPACTORS

Impactors segregate particles by interaction of viscous and inertial forces. Figure 2.2 shows a schematic drawing of an impactor. The jet increases the velocity of the flow stream and the particles within it so that particles which are acted upon by larger inertial forces than viscous drag forces, i.e., particles whose aerodynamic diameters are larger than the impactor cut-point, will impact on the impaction plate. Particles for which viscous drag forces are higher than inertial forces will remain in the flow stream. The impactor cut-point

is defined as that particle diameter for which 50% of the particles are caught by the impactor and 50% are passed. In a well designed impactor, particles which are not very much larger than the cut-point will be 100% captured by the impaction plate and particles which are not very much smaller than the cut-point will be 100% passed.

Impactor performance can be described in terms of Stokes number (Marple et. al., 1974) as shown by eq. 2.1.

$$Stk_{50} = \frac{CV(D_{p,50})^2}{9\mu W} \qquad 2.1$$

Dp = particle aerodynamic diameter

V = jet velocity

W = jet diameter

C = Cunningham slip correction factor

μ = absolute viscosity of air

Table 2.1 gives a summary of the impactor design parameters. The flow parameters in Table 2.1 were computed by treating air as an incompressible fluid. This assumption begins to weaken for the 0.3 and 0.1 μm impactors. For these impactors there was a non-negligible pressure drop across the jet. Therefore in contrast to impactors operating essentially with atmospheric pressure on both sides of the jet, for these impactors, particles with smaller aerodynamic diameters

Table 2.1

Impactor Design Parameters

Cut-point	W	n	V	P2/P1	Re	QT
µm.	mm		cm/sec			lpm
2.5	3.15	1	1755	1.00	3625	8.3
1.2	1.97	1	4500	0.99	5809	8.3
0.6	1.30	1	10430	0.94	8891	8.3
0.3	0.60	4	15700	0.89	6177	10.7
0.1	0.15	20	19300	0.78	1898	4.1

W = jet diameter

n = number of jets

P1 = pressure upstream of the jet

P2 = pressure downstream of the jet

RE = Reynolds number

QT = total flow through all the impactor jets

than the cut-point can impact if the impactor was operated at the design flows given in Table 2.1. This occurs because the lower than atmospheric pressure downstream of the jet decreases viscous drag forces in this region and thus decreases the forces that would turn the direction of motion of particles to allow them to remain in the flow stream. To adjust for this effect the impactor jet velocity and consequently the flow through the impactor must be reduced. Reducing the jet velocity decreases the inertial forces while not changing the viscous drag forces. Experimental data from Kuhlmey et al. (1981), who designed an etched hole 0.1 μm impactor, were used to determine the required flow corrections. This was done by using the experimental data to determine the relationship between the pressure behind the impactor and the square root of the Stokes number at the impactor 50% cut-point. The square root of the Stokes number is a decreasing linear function of the pressure behind the impactor. An iterative solution of eq. 2.1 using the experimentally determined flow rate and pressure behind the impactor was used to determine the flow rate necessary to achieve the desired cut-point. For the 0.3 μm impactor the flow required was 9.3 lpm at a pressure of 58.2 cm Hg. For the 0.1 impactor the flow required was 3.0 lpm at 56 cm Hg.

The 2.5 and 1.2 μm impactors were calibrated by using $(NH4)_2SO4$ aerosol particles produced by a Berglund-Liu Monodisperse Aerosol Generator (Model 3050). This instrument has a vibrating orifice which generates a stream of uniform sized droplets. The droplets have a predetermined solution concentration of $(NH4)_2SO4$ and form uniform sized particles as the solution evaporates from the droplets. Particle

concentration in the flow stream was measured by using a Royco (Model #3050) optical particle counter. This instrument counts particles in the size range from about 0.4 μm to 10 μm.

To calibrate the 2.5 and 0.6 μm impactors a monodisperse test aerosol was generated for each impactor with an aerodynamic diameter near impactor cut-point. The flow of this aerosol through the impactor was then varied about the impactor design flow. This flow variation calibration procedure allows impactor performance to be determined by using one monodisperse aerosol rather than using a series of monodisperse aerosols that would span the impactor cut-point. Aerosol particle concentrations in the flow stream ahead and behind the impactor were measured. The difference between these concentrations measured the particles captured by the impactor. In sampling use the flow rate through the impactor remains constant and the size of particles passing through the impactor varies.

To calibrate the 0.3 and 0.6 μm impactors 0.481 and 0.714 μm latex spheres were used, respectively as the calibration aerosol particles. The 0.481 μm particles where used to allow the use of the Royco particle counter. Therefore for the 0.3 μm impactor calibration lower than Table 3.2 design flows were used to scan the flow region where the cut-point for the impactor would occur at 0.481 μm. This procedure did not examine the behavior of the impactor at its design flow but it did show that the impactor operated according to theory. Figures 2.3-2.6 show that the 2.5, 1.2, 0.6 and 0.3 μm impactors, perform as theory predicts, i.e., the 50% cut point occurred at a value of the square root of the Stokes number in the vicinity of 0.475 and shape of the curves approximated a

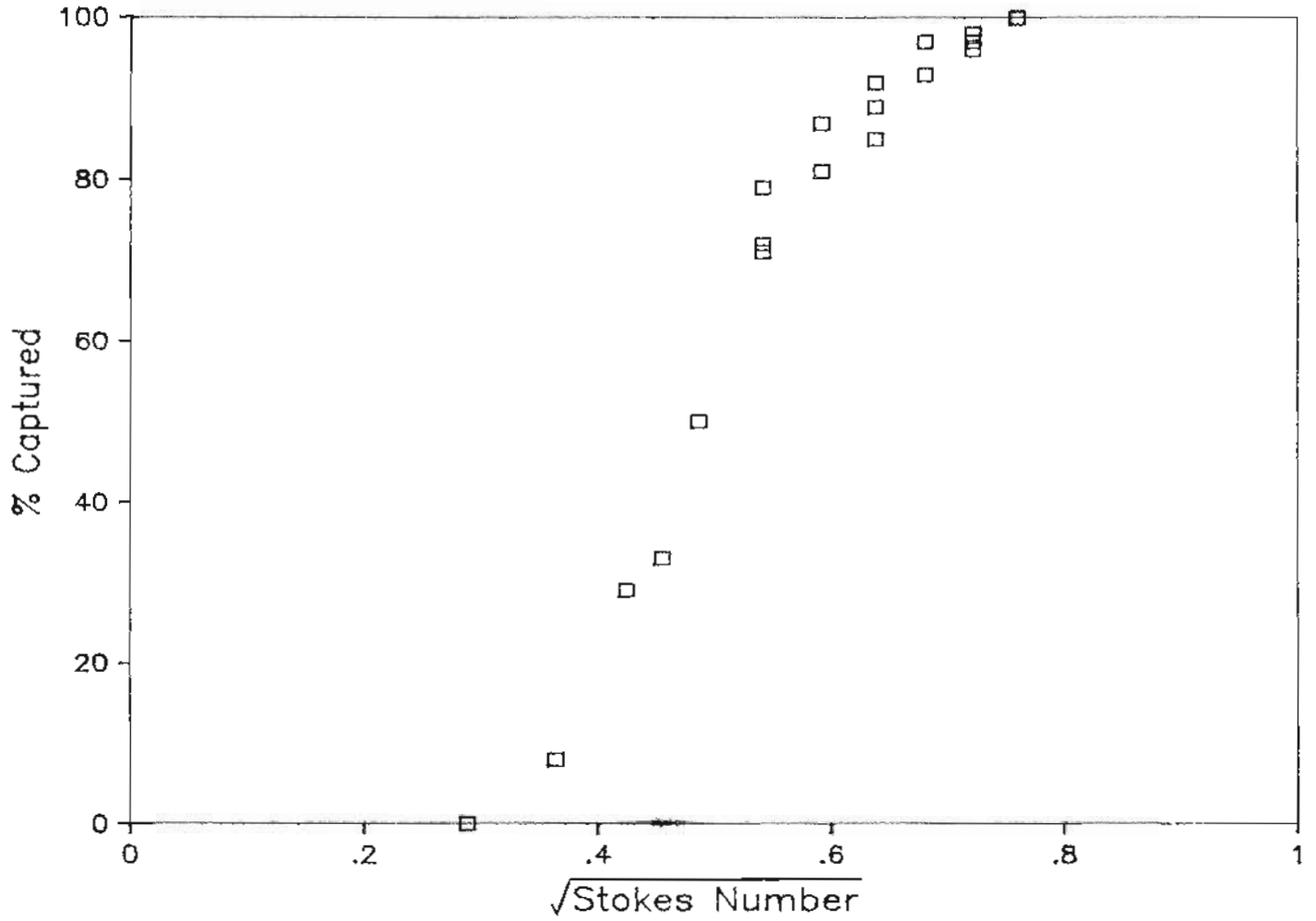

Figure 2.3. 2.5 μm impactor performance calibration.
Aerosol = 2.25 μm $(NH_4)_2SO_4$ particles.

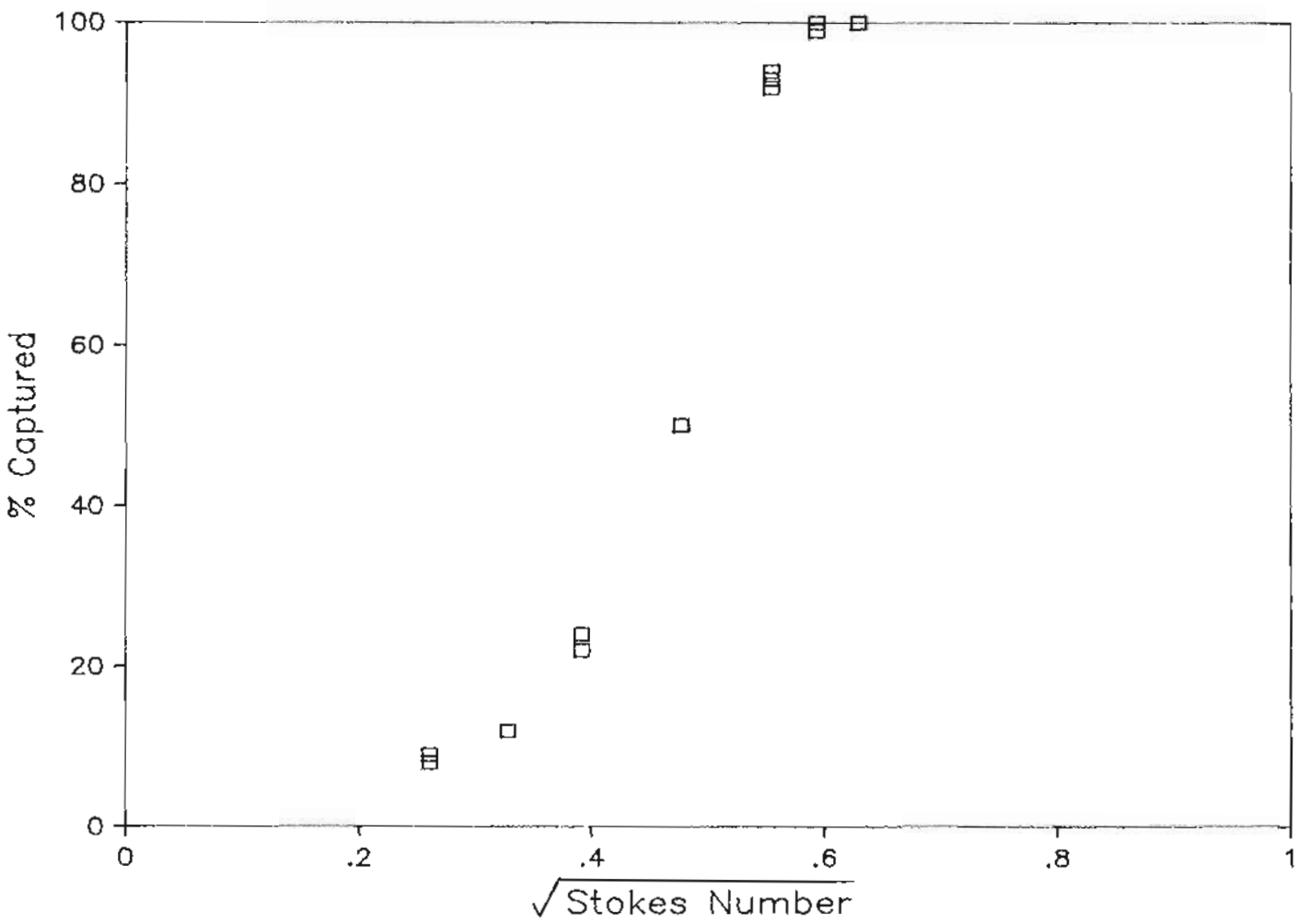

Figure 2.4. 1.2 μm impactor performance calibration. Aerosol = 1.31 μm $(NH_4)_2SO_4$ particles.

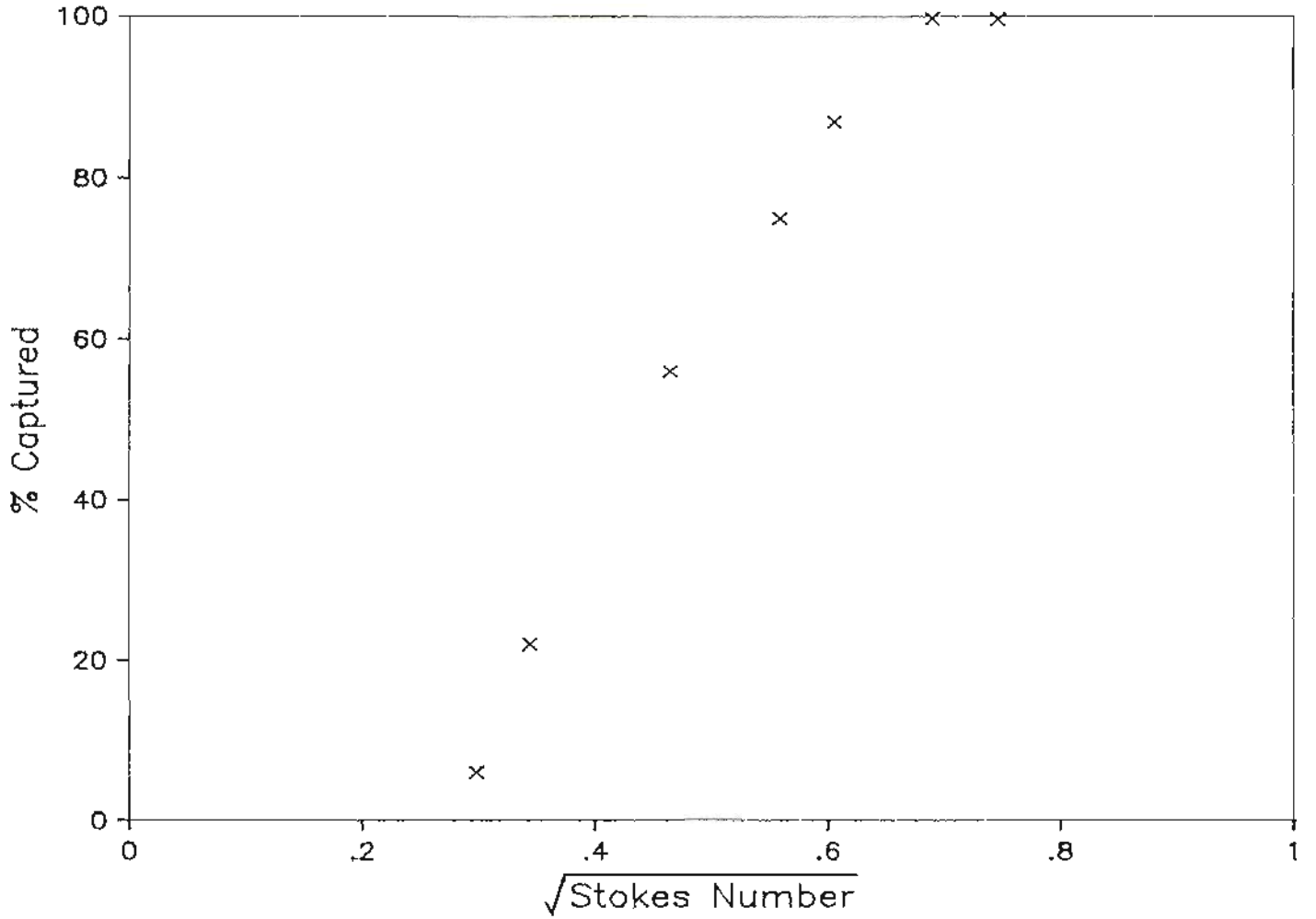

Figure 2.5. 0.6 μm impactor performance calibration.
Aerosol = 0.7 μm latex particles.

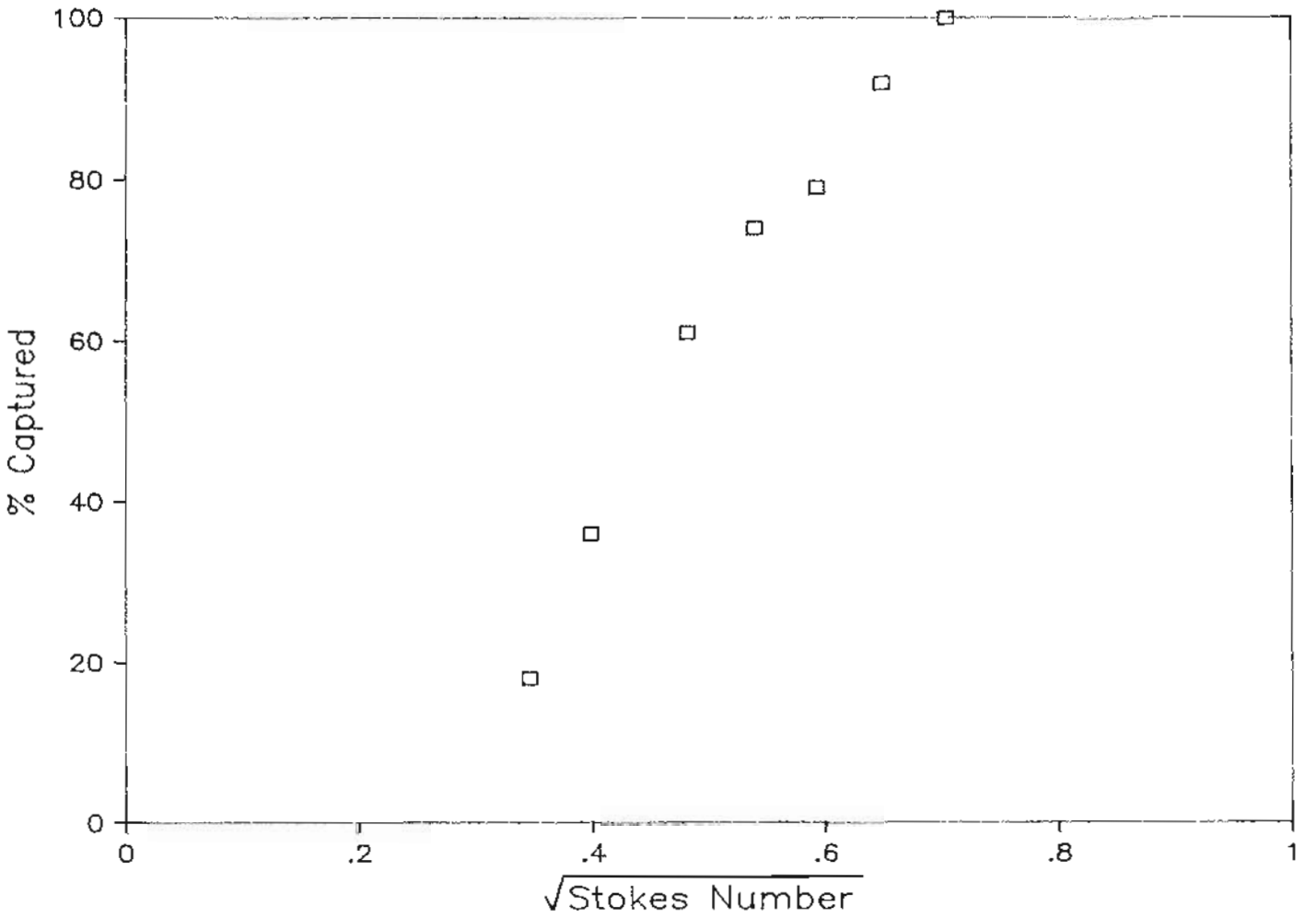

Figure 2.6. 0.3 μm impactor performance calibration.
Aerosol = 0.481 μm latex particles.

step function. Figures 2.3 to 2.6 also show qualitatively that particle bounce was not excessive because particles not too much greater than the cut-point size were essentially 100% captured. Since these calibration curves look similar to curves in the literature their performance can be assumed to be typical.

Calibration of the 0.1 μm impactor was difficult because an effective means of measuring the concentration of 0.1 μm latex spheres in an aerosol or deposited on a filter was not available. An electrical aerosol analyzer would have been useful. Some attempts were made to count aerosols deposited on a Nuclepore filter using scanning electron microscopy. While test aerosol particles could be seen in micrographs their image quality was not well enough defined for reliable counting.

2.2 SOURCE SAMPLING

2.2.1 WOOD STOVE HOT AND COOL BURNING TESTS

The literature which describes measurements of RWC emission factors (Butcher and Buckley, 1977; Butcher, 1978; Butcher and Ellenbecker, 1982; Cooke et al. 1982; Hubble et al., 1982; Kowalczyk et al., 1982a; Peters et al., 1982; Sandborn and Blanchet, 1982; Rudling and Ahling, 1982) and that which describes RWC particulate composition (Watson,1979; Dasch, 1982; DeCesar and Cooper, 1982; and Stiles, 1983) demonstrate large data variability due to variable combustion conditions. The strategy of this research was to determine wood smoke composition at the limits of the combustion conditions that were available for RWC, i.e.

hot burning and cool burning, rather then examine wood smoke composition for a great variety of burn conditions. Hot burning was defined as flaming, turbulent combustion with an ample supply of air. Cool burning was defined as air-starved combustion with or without smoky orange flames. These limits were found to encompass fireplace burning and forestry slash burning as well. This strategy reduced data variation to a minimum.

Typically residential wood burning consists of damper open or partially open operation during start-up and during times of high heat demand and damper closed or mostly closed operation during the majority of the stove operating time, especially during sleeping hours. Discussions with many stove owners have established that especially those who burn their stoves continuously were concerned about not letting the fire go out at night and thus used large fuel loads and burned with the damper closed. A feature of air-tight stoves that is promoted in advertising is that they can be filled with a large fuel load and will run unattended for many hours.

Wood burning tests were conducted mainly with a common box type, air-tight stove (Earthstove) installed in a residence. The fire was started with kindling wood and 2-4 pieces of well-seasoned split logs. Hot burning was established when two to four split logs were burned with the damper open on a bed of glowing coals such that the combustion was flaming and turbulent. To establish hot burning conditions, it was necessary to limit the fuel loading so that the amount of wood surface available for burning was not too large for the amount of air being supplied by the draft system. If a large amount of wood is loaded into a

stove and especially if the wood piece size is small, then the amount of wood surface available for burning will be too large for the available draft. This can cause air-starved combustion to occur even with the damper fully open. This type of combustion can be flaming and have reasonably high flue gas temperatures, but the plume will be very smoky. Hot burning, as defined here, also required that the plume was essentially invisible. Although there was some variability in hot burn conditions, they were always very different from cool burn conditions.

Cool burn conditions were established by burning with the damper closed. This type of burning was always marked by a very visible blue-gray plume. For the Earthstove there was enough air leakage into the stove such that air-starved combustion was possible with the damper closed. For some stoves tested the fire would go out if the damper was completely closed so that it was necessary to leave the damper slightly open during cool burning.

Tests were run on both hardwood and softwood. The most commonly used softwood in the sampling area was Douglas fir. This was used for all softwood burns. Two types of hardwood, alder and oak, were used. No significant differences were noted between alder and oak RWC emission compositions. Since RWC emission compostion depends so strongly on burn conditions, which were not highly controllable with the experimental procedures used, it was not possible to determine significant emission composition differences due to wood type. Wood moisture was also not examined as an experimental variable. Survey data has shown most wood burners use seasoned wood (Cummings, 1982). All wood burned was well-seasoned and could be assumed to have a moisture content of 10-20%. This

was verified by measurements made on one occasion which showed wood moisture to be 12-15%.

Sampling was started after the stove had burned for 30 minutes with the damper open. Wood was added as needed to maintain an approximately constant (1/4 full) fuel load in the stove. These tests simulated wood stoves in constant heat output operation. After a ten minute wait following the addition of wood, sampling was conducted for about 20 minutes. This permitted enough aerosol mass to be collected for accurate mass determination and yet not too much to reduce flow through filters or to overload the carbon analyzer. In a typical sampling run the sampler was located on the roof near the chimney, and the inlet of the sampling line was directed into the plume at about 1-3 m from the chimney. Usually during sampling there was enough wind so that the plume traveled essentially horizontally from the chimney. Measurement of CO2 concentrations in the flue gas and in the sampled, diluted flue gas showed that the flue gas had been diluted by a factor of 50 to 100 by the ambient air. No account was taken of aerosols that were in ambient air since the mass loading of the ambient air was usually about 20 μg/m3 and the mass loading of the diluted flue gas was almost always more than 1000 μg/m3 and usually in the range of 5000 to 10,000 μg/m3. The transition from hot burning to cool burning was accomplished by closing the damper and waiting 10 minutes to establish steady state conditions.

2.2.2 OTHER STOVE TESTS

Tests similar to the Earthstove test were run on three other stoves

and a fireplace insert that were installed in private residences. In all of these tests the sampling equipment remained on the ground and a 6 m. long, 7.5 cm diameter aluminum tube was used to sample the flue gas at a point 1-3 meters from the chimney.

2.2.3 FIREPLACE TESTS

Source sampling tests were conducted on three different fireplaces with one of these being sampled twice. Both softwood and hardwood tests were run. The fire was started with paper and kindling wood, and then three or four pieces of split wood were added. Sampling was started when flaming combustion was well-established. Unlike stove tests fireplace burning allowed little control over burn temperature although the size of the fire could be controlled by the amount of fuel supplied. Usually the amounts of wood used in fireplace tests was similar to that used in stove tests. It was necessary to have a sufficiently large fire to heat the chimney so that an adequate draft was established. Sampling was conducted for twenty minutes. For all tests the 6 m. extension tube was used to reach the plume.

2.2.4 RESIDENTIAL OIL BURNING FURNACE TEST

The oil burning furnace tested was a 45 year old low pressure oil furnace installed in a residence. The unit was reputed to be highly efficient, ran with very little odor and was probably typical of furnaces in older residential areas. Only one unit was tested since the characterization of oil furnace emissions was not a major objective of

this research. A sampling period of one hour was necessary to acquire a suitable amount of particulate material.

2.2.5 AUTOMOTIVE TUNNEL TEST

Motor vehicle emission aerosol was sampled from a port in the ceiling of a one way, two lane, heavily traveled highway tunnel. The port was located 100 m. from the entrance (East) end of the tunnel. The tunnel was 270 m. long and had a slight uphill grade. Traffic through the tunnel was mixed auto and truck traffic and traveled at about 50 mph. Ventilation to the tunnel was provided by natural drafts and was sufficient to maintain relatively low particulate loadings (23-39 μg/m3).

2.2.6 DIESEL AUTOMOBILE TEST

Three test runs were made were made on a 1973, Mercedes 300D diesel automobile, and samples were collected on quartz fiber, glass fiber, and Teflon filter material. Samples were taken from the exhaust plume, about 2 m. from the tail pipe exit. The engine was warm and running at an idle. Five minute sampling times provided a large amount of sample. A similar test run on a 1981 Subaru gasoline engine automobile for one hour provided no visible deposit and no measurable carbon deposit.

2.2.7 SLASH BURNING DATA FOR FLAMING AND SMOLDERING BURNS

A small set of flaming and smoldering forest slash burn aerosol samples were obtained from the Oregon Department of Environmental Quality. These samples were collected, after the combustion aerosol had been cooled and diluted by the atmosphere, by suspending a sampler on a cable over a slash burn area. The samples were analyzed for organic and elemental carbon to examine their similarity with hot and cool burn residential wood smoke. These data showed similar characteristics to hot and cool RWC burning and will be discussed in Chapter 6.

2.3. AMBIENT SAMPLING

2.3.1 PORTLAND RESIDENTIAL AREA AMBIENT SAMPLING

Ambient aerosol sampling was done in a southwest residential area of Portland. The sampling site was about 5 km from downtown Portland and was within 1/2 km of several major highways. It was at a higher altitude than most of the surrounding area to the north, east and south. During the winter about 10% of houses emitted visible blue-gray smoke plumes typical of wood burning.

2.3.2 HILLSBORO AMBIENT SAMPLING

Hillsboro is a city of 30,000 population located about 30 km west of Portland. It is mainly a residential area of lower and middle income residents. Fuel wood is readily available, and residential wood burning

is very common. Many wood smoke plumes were visible during the heating season. The area has no significant industrial aerosol pollution sources. Transportation, residential wood burning and distillate oil burning were the major sources of fine aerosol pollution.

2.4 AEROSOL ANALYSIS

2.4.1 GRAVIMETRIC DATA

All aerosol mass data were determined by using a Cahn Model 25 Electrobalance. This balance, which had a digital readout, was operated on the 200 mg scale so that mass data could be read to the nearest 0.01 mg. Greater precision could be obtained by using counter weights, but the general inaccuracies associated with filter weighing did not justify the additional effort required. Filters usually weighed in the range of 60 to 100 mg and aerosol mass weights ranged from less than a milligram to several milligrams. The scale was housed in a constant humidity (relative humidity = 15-20%) clean air chamber where the air was supplied by a Aadco Model 737 High Volume Pure Air Generator which supplied air with less than 5 ppb of hydrocarbons and less than 300 ppb of carbon dioxide. Filters were stored in this chamber prior to weighing. After sampling the filters were returned to the chamber and allowed to equilibrate with the chamber atmosphere before being weighed. The time period for equilibration was determined by noting how long it took a field blank to equilibrate to its initial weight. Usually one hour was sufficient. Glass fiber and Teflon field blank filters would

equilibrate very closely to their original weight. Pallflex QAOT quartz fiber field blank filters; however, tenaciously held sorbed water and would not equilibrate to their initial weight even after over 24 hour equilibration periods. They were not useful for precision weighing. Pallflex QAST, Microfiltration and Gelman quartz fiber filters were found to equilibrate well and were used for most of the research program.

2.4.2 CARBON ANALYSIS

2.4.2.1 DESCRIPTION AND OPERATION OF THE THERMO-OPTICAL CARBON ANALYSIS SYSTEM

The carbon analysis system used was a unique thermal oxidation system developed at the Oregon Graduate Center (Johnson et al., 1981; Huntzicker et al., 1982). This system differs from other thermal oxidation systems because it corrects for the pyrolytic conversion of organic carbon to elemental carbon (charring) during the analysis process. The pyrolytic conversion correction was made by continuously monitoring the filter reflectance during the analysis process. As the organic analysis progresses, the filter becomes darker as organic carbon is pyrolytically converted to elemental carbon. When O_2 is introduced into the carrier gas stream elemental carbon was oxidized and the filter becomes lighter. The correction for pyrolytic conversion of organic carbon to elemental carbon was taken to be the amount of elemental carbon oxidation necessary to return the filter reflectance to its

initial value, i.e., before pyrolytic conversion of organic to elemental carbon occurred.

Figure 2.7 shows a schematic diagram of the thermo-optical carbon analysis system. The system consists of temperature controlled ovens, flow controllers, a flame ionization detector (FID), a pyrolysis correction system, and a data processing system all automatically controlled by a Commodore-64 computer.

The sample oven and the MnO_2 oven were constructed from a single quartz tube. These ovens had separate heaters, each controlled by a temperature controller. The temperature in the sample oven was under computer control and could be programmed as a function of time. The temperatures in the MnO_2 oven (1000°C) and the methanator (500°C) were maintained at a constant values.

The pyrolytic conversion correction system consisted of an optical quality quartz rod going through the center of the MnO_2 oven which conducted light from a He/Ne laser into the sample oven to illuminate the sample surface. Reflected laser light from the sample was conducted back down the quartz rod to a photodetector. A narrow bandpass interference filter ahead of the photodetector discriminated against oven glow. Light was conducted from the laser to the quartz rod and from the quartz rod to the photodetector by a fiber optic light pipe. Gas flow to the oven was controlled by (1) a system of manually set rotameters and precision valves, and (2) three multi-port power driven Carle chromatography valves under control of the computer. The carrier gas stream was composed of three components: the main helium stream, a 10% O_2, 90% He stream and a stream of He equal in flow rate to the 10%

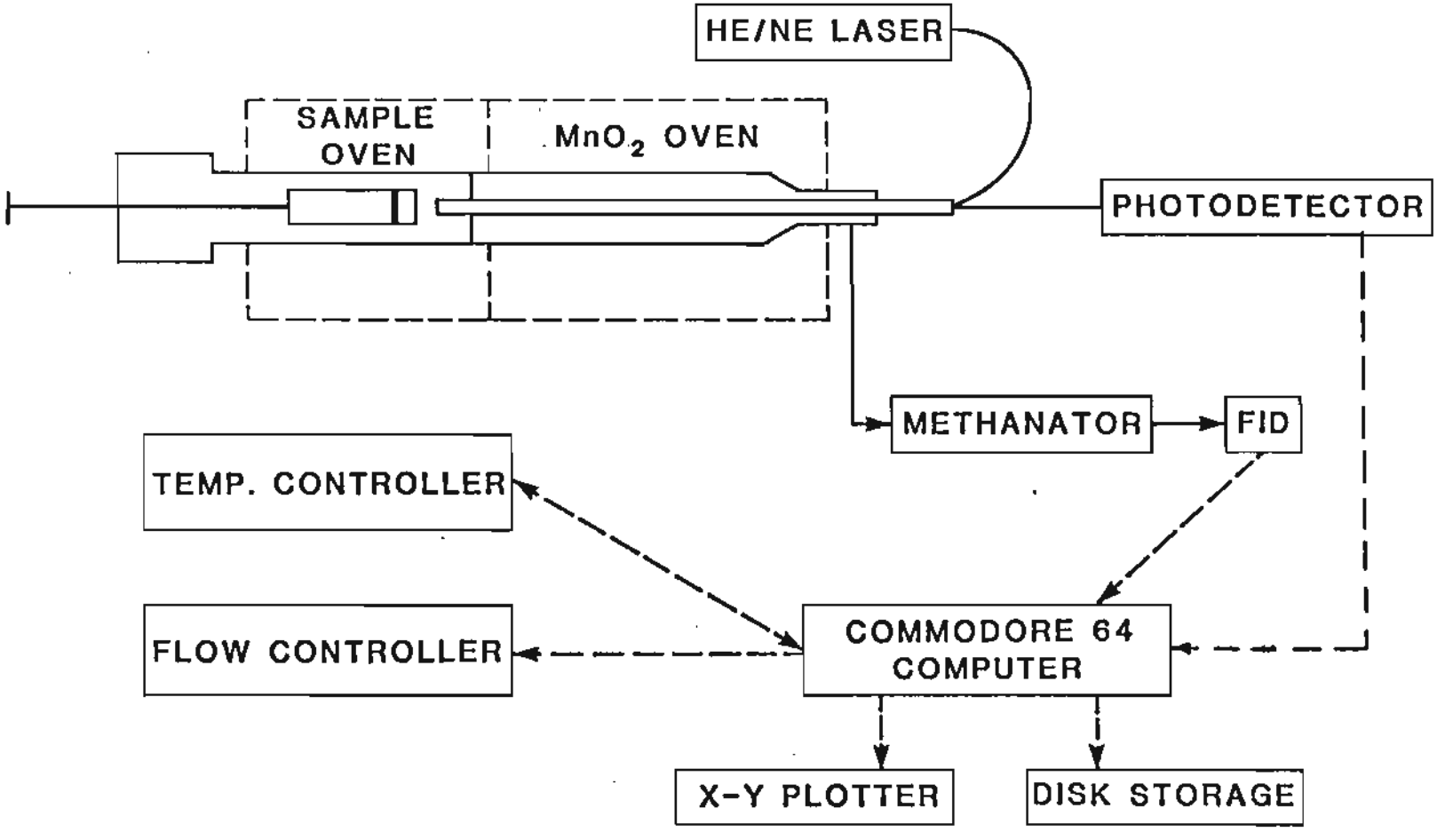

Figure 2.7. Thermo-optical carbon analysis system

O_2, 90% He stream. The two minor streams were switched back and forth into the main stream to provide either a pure helium or a He/O_2 atmosphere in the oven. Other gas streams were hydrogen and air to operate the FID and calibration gas. A 1 ml loop and a Carle valve were used to inject CH_4 into the carrier stream upstream of the oven during each sample analysis for the purpose of calibration. A backflow stream (10% of the initial carrier stream) exited the left (external end) of the oven to purge ambient air that remained when the oven had been open up. The backflow stream rejoined the carrier stream just ahead of the FID so that all the calibration gas carried by the backflow stream was always measured by the FID.

Carbon analysis of an aerosol sample was begun by placing one or more filter disks (usually 4 with area of 0.25 cm^2 each) into a quartz boat which was slid into the temperature-controlled oven at a precise time after the computer-controlled analysis program was started. The sample was heated in an atmosphere of He at several temperature steps, usually 300, 450 and 650°C to vaporize organic carbon. The step heating program was used to minimize the pyrolytic conversion of organic carbon to elemental carbon. Then the atmosphere in the sample heating oven was changed to 1-2% O_2/98% helium to oxidize elemental carbon. The carbon vaporized from the sample traveled with the carrier gas stream through the MnO_2 oven. Here all carbon species were oxidized into CO_2. Following this the stream went through the methanator which consisted of a heated bed of nickel catalyst on powdered firebrick. Here the CO_2 was converted to methane. These various conversions were required because the FID has a very high sensitivity to methane and varying sensitivities to many of

the carbon species than have been found in atmospheric aerosol particles. The output signal from the FID, which was proportional to the carbon concentration in the carrier stream, was integrated by the computer to generate aerosol carbon concentration data. Besides controlling the system during analysis, the computer also generated a graph of FID output, photodetector output and oven temperature and printed these data to disk storage and to a plotter.

Figure 2.8 shows the thermo-optical carbon analysis system output for a cool burn RWC aerosol and Figure 2.9 shows the output for a hot burn RWC aerosol. The bottom curve shows the FID output, the middle curve shows the photodetector output and the top curve shows the oven temperature all as a function of time. The photodetector signal starts at an initial value and decreases as organic material on the filter is pyrolytically converted (by charring) to elemental carbon. When O_2 is introduced, the filter becomes lighter and eventually white as all the elemental carbon is removed by oxidation. Also as O_2 is introduced the FID output increases as elemental carbon is removed from the sample. A horizontal line drawn from the initial point on the laser output line again intersects the laser output line where the laser output equals it's initial output. A vertical line drawn down from this point intersects the FID output curve at the split-point between organic and elemental carbon. All carbon (integrated area under the FID output curve) to the left of this point is assumed to be original organic carbon, and all carbon to the right of this point is assumed to be original elemental carbon. The carbon represented by the area under the FID output curve from the position under the point where the laser

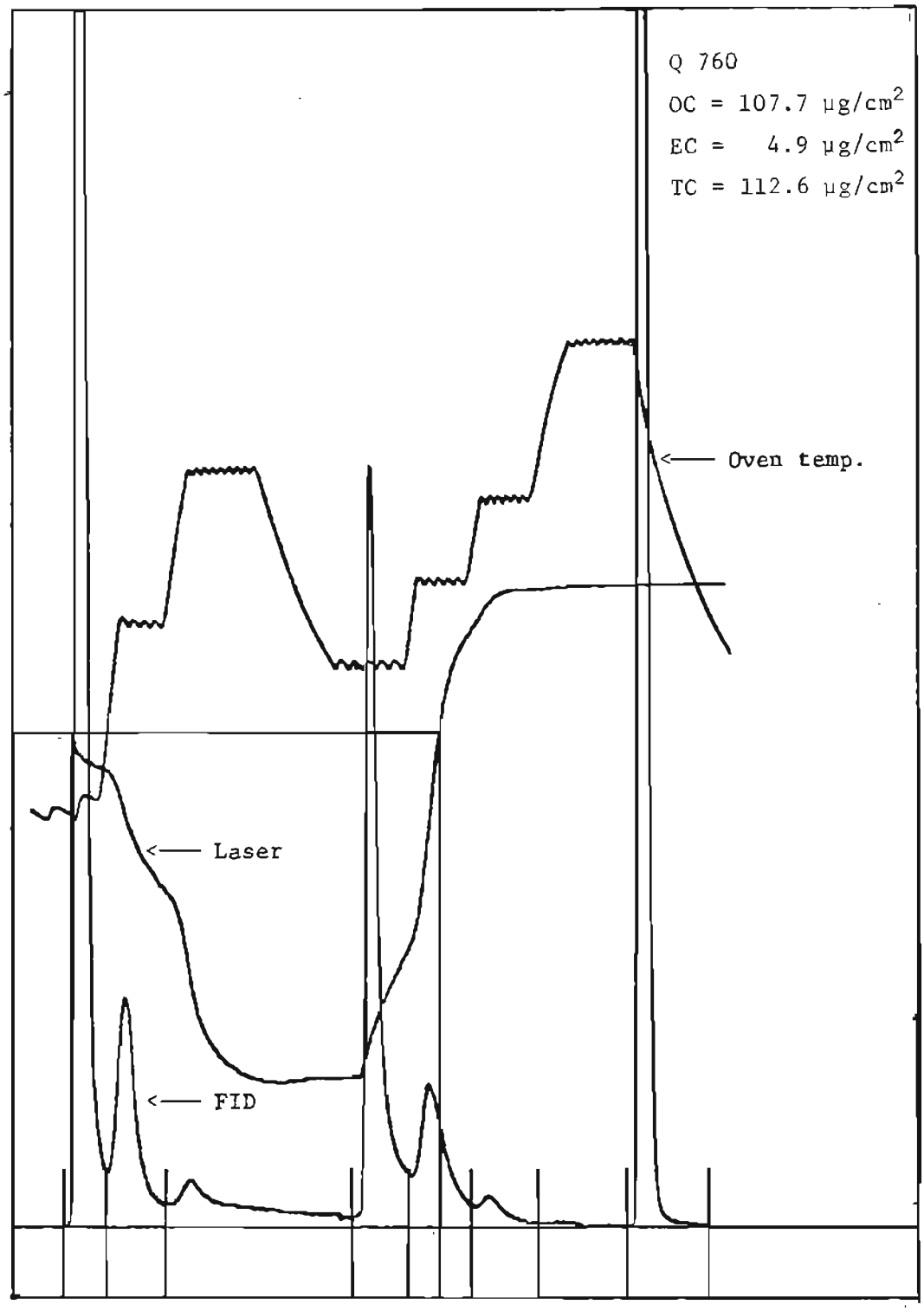

Figure 2.8. Typical thermo-optical carbon analyzer output for cool burn wood stove emissions.

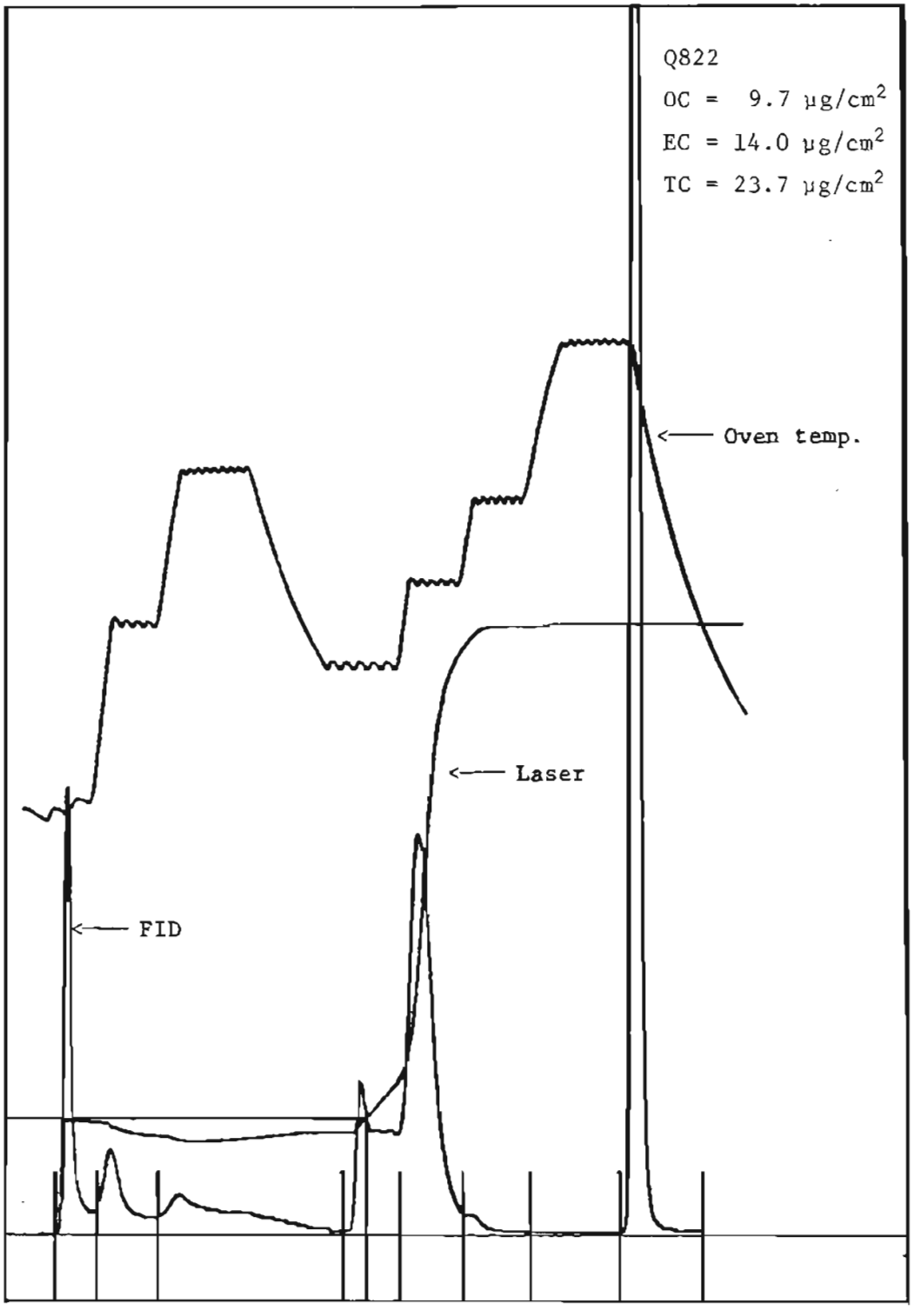

Figure 2.9. Typical thermo-optical carbon analyzer output for hot burn wood stove emissions.

signal starts increasing when O_2 was introduced to the split point is original organic carbon that was pyrolytically converted to elemental carbon. This amount of carbon would have been wrongly classified if the pyrolysis correction was not made. Figure 2.8 shows that for a cool burn RWC aerosol a large amount of organic carbon was removed from the sample by the initial heating and that the amount of pyrolytic conversion was a large fraction of the total amount of carbon measured. This measured amount of elemental carbon was an upper limit estimate of elemental carbon because the laser light is absorbed both by the black elemental carbon and the colored (tan) organic matter. For cool burn particulate material the possible presence of elemental carbon might be indicated by a gray cast over the tan color of the material. For samples of this type solvent extraction and reanalysis by thermo-optical carbon analysis indicated that real original elemental carbon was about 1% rather than the 5% indicated by the first analysis. Figure 2.9 shows that for a hot burn RWC sample the filter was very black to begin with (indicated by the low initial laser value). The laser signal shows very little evidence of pyrolysis and the indicated amount of organic carbon that was pyrolytically converted to elemental carbon was a small fraction of the total carbon measured. Fifty-nine percent of the carbon in this sample was elemental carbon.

2.4.2.2 MODIFICATIONS OF THE THERMO-OPTICAL CARBON ANALYSIS SYSTEM

Prior to beginning the analytical phase of this work, the carbon analyzer was redesigned and rebuilt. The modifications incorporated are

described in Appendix 2. This new instrument and the improvements incorporated in it contributed to the quality of carbon data obtained in this research.

2.4.2.3 CARBON ANALYSIS SYSTEM VALIDATION

The objective of the thermo-optical carbon analysis system was to accurately determine the total, organic and elemental carbon in any aerosol sample. The determination of total carbon required only that all of the carbon was removed from the sample, delivered to the FID detection system in the form of methane and that this methane was correctly measured. Organic and elemental carbon determination required that the split point between organic and elemental carbon be correctly determined.

The accuracies of all carbon determinations depend on the accuracy with which carbon species are removed from the sample, converted to CO_2, converted to CH_4, delivered to the FID, converted to an electrical signal and the accuracy with which this signal is integrated and calibrated to determine the amount of carbon species. The major source of uncertainty in this process results from uncertainties in calibration. In the thermo-optical carbon analysis system an internal standard was supplied during every analysis. It consisted of an injection of a known amount of methane into the carrier stream and measuring the instrument response. The source of uncertainty in this process results from uncertainty in the determination of the mass of methane injected. This uncertainty in turn results from three sources:

uncertainty in the volume of the calibration gas loop and the associated attachment lines; uncertainty in the methane concentration of the commercially supplied calibration gas; and uncertainty resulting from variations in ambient atmospheric pressure which determines the gas pressure in the calibration loop. The accuracy of the loop volume was specified by the manufacturer to be ±1-2%. The loop volume includes the actual loop volume, the internal valve volume and the volume of 1 inch lengths of the attaching lines. Uncertainty in the methane concentration of the calibration gas was according to the manufacturer ±3-5%. Uncertainty due to atmospheric pressure variations are less than ±1%. Therefore the total uncertainty of the calibration gas injections was less than ±6%. Precision was about 2%.

Primary calibrations of the system were done with external sugar (sucrose) and potassium hydrogen phthalate standards. Solutions were made up to contain a known mass of standard per unit volume of solution. Primary calibrations were done by analyzing a known volume of calibration solution on a clean filter. Repeated primary calibrations have been done with a standard deviation of 5%. Results of replicate analysis of a large data set have indicated that standard error in precision for total carbon analysis was 6.2%.

The system has demonstrated the ability to analyze the carbon in substances that contained only organic carbon, i.e. sugar and a variety of other organics as essentially 100% organic carbon. Carbon blacks which were almost 100% elemental carbon were analyzed as at least 98% elemental carbon. These demonstrations verify that the system can correctly characterize pure organic or elemental carbon substances.

The system's ability to correctly determine the split between organic and elemental carbon in substances that contain both organic and elemental carbon, such as aerosol particulate material, has not been rigorously determined. This determination even from a theoretical viewpoint requires the specification of a temperature (split-point temperature, usually 650°C) such that substances which do not volatilize in a non-oxidizing atmosphere below this temperature will not be categorized as organic carbon. Substances that volatilize or oxidize in an oxidizing atmosphere at higher temperatures than split-point temperature will be defined as elemental carbon even though they may not have a pure graphitic carbon composition. This is necessary because the boundary between organic and elemental carbon is not clearly defined in terms of those species that compose real ambient aerosol particulate material. The goal of organic/elemental particulate carbon analysis is to make a distinction between organic and elemental carbon in source aerosol particles and then to make this same distinction when these particles are found in mixtures of particles from many sources in the atmosphere. This requires for all aerosols and mixtures of aerosols both that organic carbon which is pyrolytically converted into elemental carbon is correctly classified as organic carbon and that no original elemental carbon is classified as organic carbon.

To date only one experiment has been done which demonstrated under particular circumstances that thermo-optical carbon analysis can correctly determine the split point between organic and elemental carbon. In this experiment an analysis was begun on a known amount of sugar. Just before the time when oxygen was normally introduced into the

carrier stream, the analysis was stopped. At this point a known amount of carbon had been removed from the sample and the remaining carbon had been pyrolytically converted to elemental carbon. Thus the amount of elemental carbon in the sample was known. A known amount of sugar was then added to the sample and the sample was then reanalyzed as a new sample. For this new sample where both the organic and elemental carbon components were known the analysis produced the expected organic and elemental carbon values. This experiment supports the hypotheses that for non-colored organic carbon species the thermo-optical carbon analysis system can correctly make the organic/elemental carbon split.

A totally rigorous examination of the split point question would require the examination of a variety of aerosol organic and elemental carbon combinations where the split point is known. The difficulty with this approach is that for real aerosols the split between organic and elemental carbon is not known *a priori* and in fact cannot be accurately determined.

2.4.3 X-RAY FLUORESCENCE ANALYSIS (XRF)

Trace elemental analyses of source and ambient filters were done using XRF (Giaque,1974). This method was useful to identify up to 32 trace elemental species in aerosols. It required no sample preparation and was non-destructive. Some of the XRF analyses were done using the Oregon Graduate Center Ortec TEFA instrument; however, majority of the analyses were done by NEA Laboratories using an Ortec TEFA-3 instrument.

CHAPTER THREE: SOURCE DATA

3.1 DATA ANALYSIS

This chapter presents aerosol particle mass, carbon (organic, elemental and total) and trace elemental composition data as functions of aerosol size for emissions from residential wood combustion (RWC), automotive transportation (measured in a highway tunnel), residential oil combustion and a diesel automobile. These source data are necessary for CMB modeling and will be used in CMB analyses of some Portland and Hillsboro size distributed ambient aerosol samples (Chapter 5). Before presenting aerosol data, the sampling artifact of organic vapor adsorption on quartz fiber filters will be discussed.

3.1.1 ORGANIC VAPOR ADSORPTION ON QUARTZ FIBER FILTERS

Section 2.1.1 explained that vapor organic species can adsorb onto quartz fiber filter material during both source and ambient aerosol sampling. During carbon analysis this adsorbed organic vapor cannot be distinguished from the particulate organic carbon, and thus it adds a positive increment to particulate organic carbon values. Organic vapor adsorption was found to be a significant contribution to organic carbon loading on all quartz fiber filters sampled in this research.

Table 3.1 shows examples of the differences obtained in carbon mass fractions by correcting or not correcting for organic vapor adsorption. The first column in Table 3.1 gives the cut-point of the impactor behind which the aerosol was sampled. The second column (OC) gives the sum of particulate organic carbon and adsorbed organic vapor on the filter. The

Table 3.1

Effect of Vapor Carbon Correction on Residential Wood Smoke Aerosol Composition

Cut Pt. µm.	OC µg/cm²	VOC µg/cm²	With Correction OC/M %	With Correction TC/M %	Without Correction OC/M %	Without Correction TC/M %
0.3	8.3	4.8	13	53	31	72
0.6	9.6	4.8	15	57	29	71
2.5	9.7	4.8	20	60	29	74
0.3	30.6	5.2	51	56	61	67
0.6	32.8	5.2	49	54	58	64
2.5	49.4	5.2	54	59	60	65
0.3	127.7	6.4	57	59	60	62
0.6	106.2	6.4	54	57	58	60
2.5	189.0	6.4	54	56	55	58

OC = organic carbon (particulate and vapor organic carbon)

VOC = adsorbed organic vapor

TC = total carbon

M = aerosol mass

third column (VOC) gives the organic vapor that was adsorbed on the particle collecting quartz fiber filter as determined by a quartz fiber filter sampled behind a Teflon filter.

The correction was done by subtracting the organic carbon loading ($\mu g/cm^2$) that was obtained on a quartz fiber filter sampled behind a Teflon filter from the organic carbon loading on aerosol sampling filters. The quartz fiber filter run behind a Teflon filter was assumed to have the same adsorbed vapor loading as quartz fiber filters sampling aerosols, but of course no aerosol loading because the particles were removed from the sampled gas stream by the Teflon filter. Although Teflon filters adsorb much less organic vapor than quartz fiber filters some organic vapor adsorption on Teflon filters has been measured (McDow, 1986). Therefore the organic vapor correction made by the method described must be viewed as a lower limit for organic vapor adsorption on quartz fiber aerosol sampling filters.

Table 3.1 shows three groups of samples: lightly loaded, moderately loaded, and heavily loaded. The amount of adsorbed organic vapor increased only slightly as particulate loading increased by an order of magnitude. Sampling times for these data sets were the same. The first data set came from a hot burning wood stove test where both the particulate loading and organic vapor loading in the flue gas were low. The second and third data sets came from damper-closed wood smoke sampling tests which had successively higher organic vapor and particulate loadings. Organic vapor adsorption was not a function of impactor cut-point as long as the flow rate through each impactor was the same. The effect of organic vapor correction is shown by comparing

the fourth and sixth or fifth and seventh columns. The effect of organic vapor adsorption on particulate carbon composition can be observed by comparing the three data sets. The first data set, where the organic carbon loading on the filter was very low, shows that the error effect was most severe with light organic carbon loadings. For this case a factor of two difference occurs. For the heaviest loaded filters the adsorbed vapor correction accounts for differences of about 5%.

Table 3.1 shows that neglecting to account for organic vapor adsorption can result in over estimating carbon mass fraction values both in source and ambient aerosol composition data, especially for data based on small samples. These errors can exceed 40% of the total carbon loading on a filter. In this research the magnitude of organic vapor adsorption has been determined for all samples and subtracted from the sample's measured organic carbon loading.

Figures 3.1 and 3.2 show adsorbed organic vapor as a percent of total organic carbon loading (adsorption ratio) plotted as a function of total carbon deposited per unit area on quartz fiber filters for hot and cool wood stove burning, respectively. These figures show that the adsorption ratio decreases sharply as total carbon loading increases indicating that vapor adsorption was non-linear, i.e., adsorption was high on clean filters but approached a saturation value as filter loading increased.

Up to this point all organic vapor adsorption data presented have been collected from aerosol sampling experiments that were run at the same flow velocity through the sampling filter (20 cm/sec). McDow (1986) has shown that organic vapor adsorption was a function of flowstream

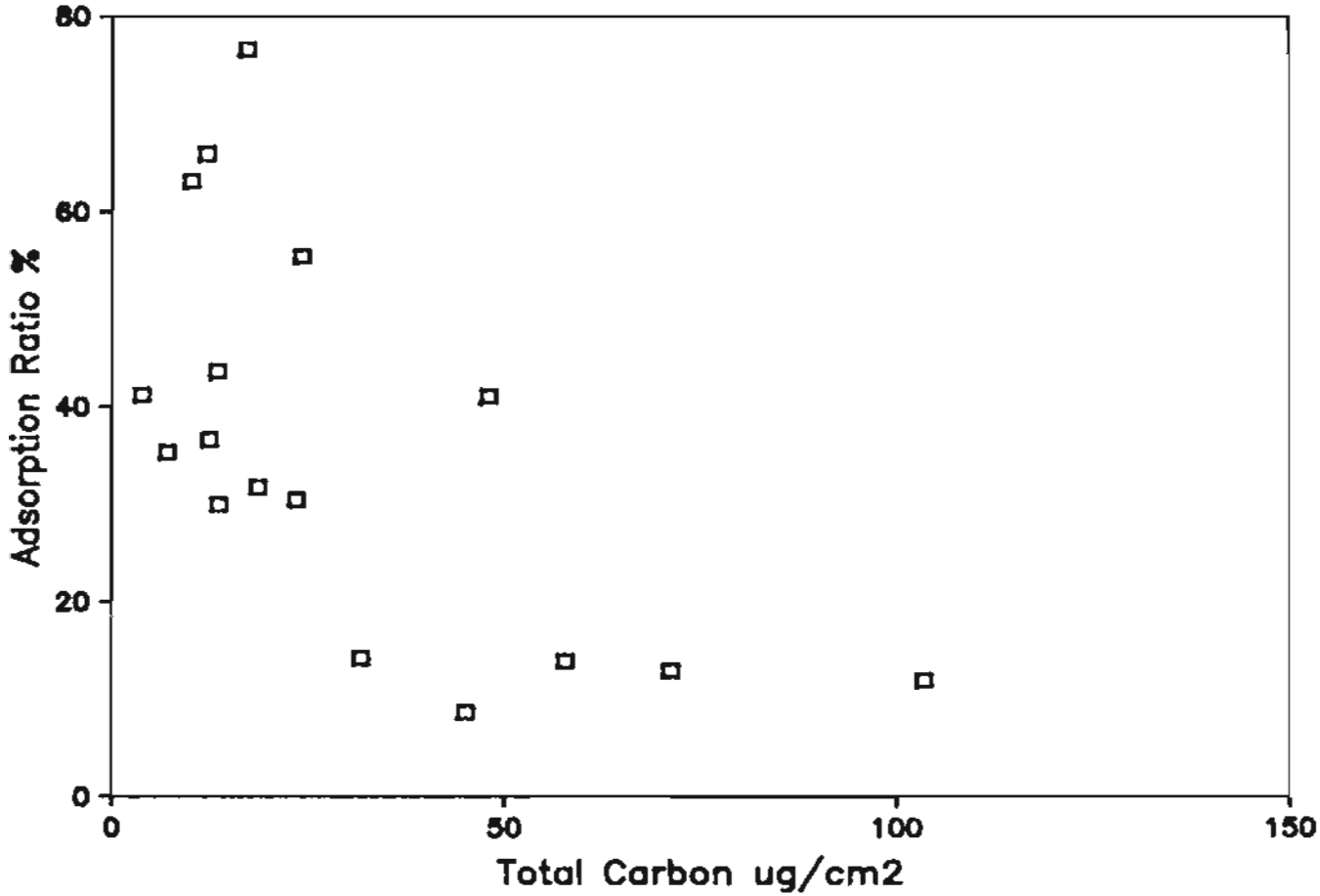

Figure 3.1. Vapor carbon adsorption on quartz fiber filters during sampling of hot burning wood stove emissions. Adsorption ratio = adsorbed OC/total OC.

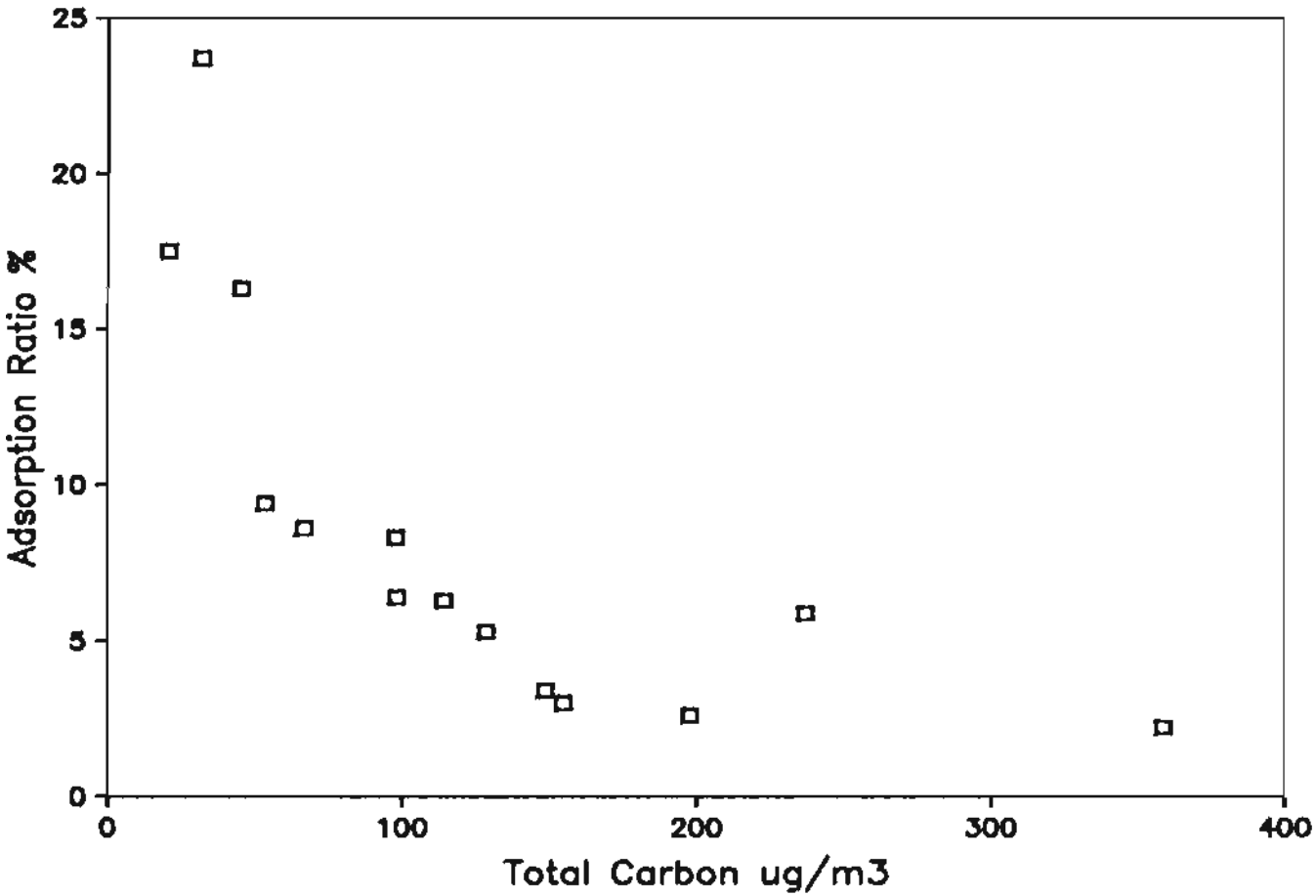

Figure 3.2. Vapor carbon adsorption on quartz fiber filters during sampling of cool burning wood stove emissions. Adsorption ratio = adsorbed OC/total OC.

velocity through the sampling filter. Since the filters sampled behind the 0.1 μm impactor were run at a sampling velocity of 7 cm/sec, organic vapor adsorption data were also determined at this lower sampling velocity. These data show that, comparing 7 cm/sec and 20 cm/sec sampling velocities, organic vapor adsorption on quartz fiber filters was 53±13% (N=12) as great for sampling behind quartz fiber filters and 49±11% (N=19) as great for sampling behind Teflon filters.

For source samples, organic vapor loadings on quartz fiber filters behind Teflon filters had a maximum range of 1 to 9 $\mu g/cm^2$, but most of the organic vapor loading data were in the range of 4 to 7 $\mu g/cm^2$. Total aerosol carbon plus adsorbed organic vapor loadings for all source tests ranged from 3.7 to 359 $\mu g/cm^2$, Longer sampling times or sampling from gas streams that had high organic vapor concentrations appeared to result in higher adsorbed organic vapor loadings. Average organic vapor adsorption was 6.8±2.4 $\mu g/cm^2$ for cool wood stove burning samples and 4.4±1.8 $\mu g/cm^2$ for hot wood stove burning samples. Since the sampling times were the same for hot and cool burning tests, the higher adsorption loadings noted for cool burn samples probably resulted because cool burn flue gases were richer in organic vapor than hot burn flue gases. Cool burning appears to be mainly a destructive distillation process which produces large amounts of organic vapors that escape the combustion zone because temperature, combustion air supply and turbulence are too low to convert these vapors to CO_2, CO. or EC particles. In contrast during hot burning the temperature, combustion air supply and turbulence are high enough to convert most of the organic vapors produced to CO_2, CO, or EC. EC particles are produced in a

reducing atmosphere and will be subsequently burned to CO or CO_2 if they enter an oxidizing atmosphere that is sufficiently hot.

The carbon composition of hot and cool burn aerosols gives evidence of the organic vapor concentrations in the respective flue gases. The carbon concentration in hot burn aerosol particles was usually greater than 50% elemental carbon and in some cases was as high as 80% elemental carbon. Elemental carbon must be generated in flames. Therefore these particles could either acquire their complement of organic carbon within flames or by condensation as they cooled in the flue gas. But since the organic carbon fraction of hot burn aerosols was low, these particles did not acquire any appreciable organic carbon during their residence time in the flue gas. Therefore there must not have been much organic vapor available in the flue gas to allow organic vapor condensation on these particles, i.e. organic vapor concentrations in hot burn flue gases must have been low. In contrast the carbon content of cool burn aerosols was usually more than 90% organic. These aerosols were probably formed primarily by condensational growth on existing particles in organic vapor rich flue gas atmospheres.

For fireplace samples average adsorbed organic vapor was 7.7±2 $\mu g/cm^2$. This value was similar to the value obtained for cool burning wood stoves. The composition of fireplace emissions also tended to be similar to cool burning wood stove emissions.

For residential oil furnace samples organic vapor adsorption was 4.3±1 $\mu g/cm^2$. This rather low value resulted even though the sampling time for this source was three times as long (one hour) as for wood stove sampling. This indicates, similarly to hot RWC flue gases, that

very low adsorbable organic vapor concentrations existed in residential oil burning flue gases.

For tunnel samples organic vapor adsorption on quartz fiber filters was 7.1±0.6 $\mu g/cm^2$. For ambient samples from a Portland residential area the organic vapor loading was 6.4±1.5 $\mu g/cm^2$. Similar values were obtained (for 20 minute sampling times) for cool burning wood stove and fireplace source sampling. These similar values indicate that either for source sampling for short periods of time in high organic vapor atmospheres or for long sampling times in lower organic vapor atmospheres, adsorbed organic vapor on quartz filters will approach a saturation value. Generally organic vapor adsorption increased with increasing organic carbon loading on filters and with increasing sampling time.

Some further understanding of organic vapor adsorption can be gained by considering the relationship between organic vapor adsorption on a quartz fiber filter sampling behind a Teflon filter and one sampling behind a quartz fiber filter. In the case of two quartz fiber filters adsorbing organic vapor in series, the second filter adsorbs less organic vapor than the first because the adsorbable vapor in the sampling stream has been depleted by the organic vapor adsorption on the first filter.

Table 3.2 shows the ratios of adsorbed carbon on quartz fiber filters sampled behind quartz fiber filters to the adsorbed carbon on quartz fiber filters sampled behind Teflon filters for the sources studied. Both longer sampling times and richer organic vapor loading in the sampling stream tend to drive the ratio to one.

Table 3.2

Organic Carbon Vapor Adsorption on Quartz Filters

Source	Sampling Time (hrs)	Quartz/Teflon Adsorption Ratio
Cool burning stove	1/3	0.71±0.03**
Hot burning stove	1/3	0.50±0.06
Fireplace	1/3	0.64±0.06
Oil furnace	1	0.34±0.04
Auto tunnel	24	0.68±0.01

* Ratio of the adsorbed vapor carbon of a filter sampled behind a quartz filter to to the adsorbed vapor carbon on a filter sampled behind a Teflon filter.

** Uncertainties are standard error of the mean.

3.1.2 SOURCE AEROSOL DISTRIBUTION AND COMPOSITION DATA

Carbon was the most abundant element composing the source aerosols studied in this research. Therefore accurate carbon composition data, including organic and elemental compositions, along with the usual trace element concentrations can improve the CMB modeling accuracy of these sources. In addition aerosol size distribution information can aid in understanding particle behavior in the atmosphere and it can improve CMB source resolution where sources of very similar composition exist in different parts of the aerosol size range.

Mass, carbon, and trace element size distribution data will be presented. In cases where aerosol carbon or trace elemental composition was not a function of aerosol size, the mass, carbon and trace elemental distributions were very similar. This is a necessary consequence when aerosol composition is independent of aerosol size.

The source EC/TC values will also be presented. For cool burning RWC particles the ratio was about 0.05, while for hot burning RWC particles it was in the range of 0.5 to 0.8. For motor vehicle emission aerosols the ratio was in the range of 0.3 to 0.35. Ambient aerosols which were dominated by a particular source would be expected to have EC/TC ratios near the value for that source.

Aerosol composition data will be given for total aerosols and for aerosols collected behind impactors. For the latter the data represent average properties for aerosols with aerodynamic diameters less than the impactor 50% cut-point.

3.1.2.1 RESIDENTIAL WOOD STOVE AEROSOL DATA

Two sets of data will be presented. The first data set (A) comes from a series of wood stove tests using paired impactors having cut-points at 2.5, 0.6 and 0.3 μm where one impactor in each set sampled on a quartz fiber filter and the other sampled on a Teflon filter. This test series was conducted on an Earthstove. The second data set (B) used a sampling arrangement where samples were collected on quartz fiber filters with no impactor and behind 1.2 and 0.3 μm impactors. Samples were also collected on Teflon filters behind 2.5, 0.6 and 0.1 μm impactors. Data set (B) includes mostly Earthstove tests, but also includes tests on three other stoves and a fireplace insert located in residences. Both data sets show similar RWC aerosol composition data. Differences occurred mainly because of difficulties in reproducing hot burn conditions. It should be noted that composition differences associated with wood type may at least in part have resulted from differences in burn temperature that were a consequence of wood type and thus may not have resulted from differences in wood type *per se*.

The principal parameter which determined the nature of residential wood combustion emissions was burn temperature. This has been noted by other investigators (Ramdahl et al., 1982). When burn temperature is used as a parameter to characterize combustion conditions, it can be viewed as being equivalent to rate of wood burning. In most research where emission factors were measured these factors were determined as a function of wood burn rate, but they could just as well have been given as a function of burn temperature. In this research burn temperature was measured in the stove at the entrance to the flue. Burn temperature was

mainly a function of the availability of combustion air but might have been to a lesser degree also a function of wood type, wood size, wood moisture level and the previous history of the fire.

Hot burn conditions were established when: the stove was hot, the fire was flaming on a bed of glowing coals, the damper was open, and the amount of wood burning was not too large for the available draft. This condition was characterized by bright yellow turbulent flames. For hot burning in the Earthstove the temperature at the entrance of the flue was 600±100°C. During hot burning the smoke plume leaving the chimney was practically invisible because the particles were too small to scatter light efficiently. The particles deposited on filters were black in color and had a mild, acrid smell rather than the strong typical wood smoke smell associated with cool burning particulate matter. Hot burn particles were from 25 to 55% carbon and this carbon was up to 80% elemental carbon.

Cool burning was established by closing the damper. This caused the flames to become smaller, orange and smoky. During cool burning the temperature at the Earthstove flue entrance was 250±50°C. The smoke plume leaving the chimney was very visible and had the blue-gray color typically associated with wood burning. The aerosol mass concentration in cool burn plumes was on the average 4.8 times greater than in hot burn plumes. Cool burn aerosol particles deposited on filters were tan or yellow in color with sometimes a slight gray cast. These particles were composed of from 55 to 65% carbon, and the carbon was almost entirely organic. Because in thermo-optical carbon analysis the tan color of these aerosols was interpreted to some degree as original

elemental carbon, the elemental carbon measurement of tan cool burning aerosol particles was an upper limit to the true elemental carbon content of these particles. To provide a better estimate of the true elemental carbon value, a filter from a cool burn was gently (to minimize removal of particulate elemental carbon) extracted in CH_2Cl_2 to remove most of the tan color (extractable organic carbon). Prior to the extraction the measured elemental carbon content was 6% of total carbon. After the extraction it was about 1% of the initial total carbon. Thus, cool burn aerosol particles actually contain very little elemental carbon; however, some small amount of elemental carbon probably does form in the charcoal burning phase of cool wood combustion. Such elemental carbon particles could serve as condensation nuclei for organic vapor condensation.

Tables 3.3A-B show the mass distributions for set (A) and (B) residential wood smoke aerosols, respectively. Figure 3.3 presents these data graphically for set (A) and Figures 3.4A-D present these data graphically for set (B). Note that in all log distribution graphs like Figures 3.4A-D it is assumed that there are no particles <0.05 μm. It is further assumed that there is negligible particulate material <10 μm so that aerosol collected with no impactor can be treated as if it had been collected behind a 10 μm cut-point impactor. These assumptions are made for the convenience of plotting log distribution graphs and at most only slightly modify the appearance of these graphs. For Table 3.3A the percentages were based on the mass passing the 2.5 μm impactor while for Table 3.3B the percentages were based on the aerosol mass collected without an impactor located ahead of the filter in the sampling stream.

Table 3.3A

Average Wood Stove Aerosol Particle Mass Distribution

(% of aerosol passing 2.5 um impactor)*

	Damper open		Damper closed	
Size um.	Softwood (N=3)	Hardwood (N=2)	Softwood (N=3)	Hardwood (N=2)
<0.3	67±3	48±2	53±1	49±5
0.3-0.6	24±6	39±4	9±5	9±1
0.6-2.5	9±2	13±6	38±5	42±5

Table 3.3B

Average Wood Stove Aerosol Particle Mass Distribution

(% of total aerosol mass)

	Damper open		Damper Closed	
Size µm.	Softwood (N=6)	Hardwood (N=8)	Softwood (N=7)	Hardwood (N=7)
<0.1	24±5	19±3	28±5	20±6
0.1-0.3	25±6	30±8	14±5	11±4
0.3-0.6	20±6	30±4	6±3	7±3
0.6-1.2	15±6	9±2	37±7	42±4
1.2-2.5	10±7	3±2	10±5	13±6
>2.5	6±2	9±3	5±2	7±2

* Uncertainties are standard errors of the mean.

N = Number of tests

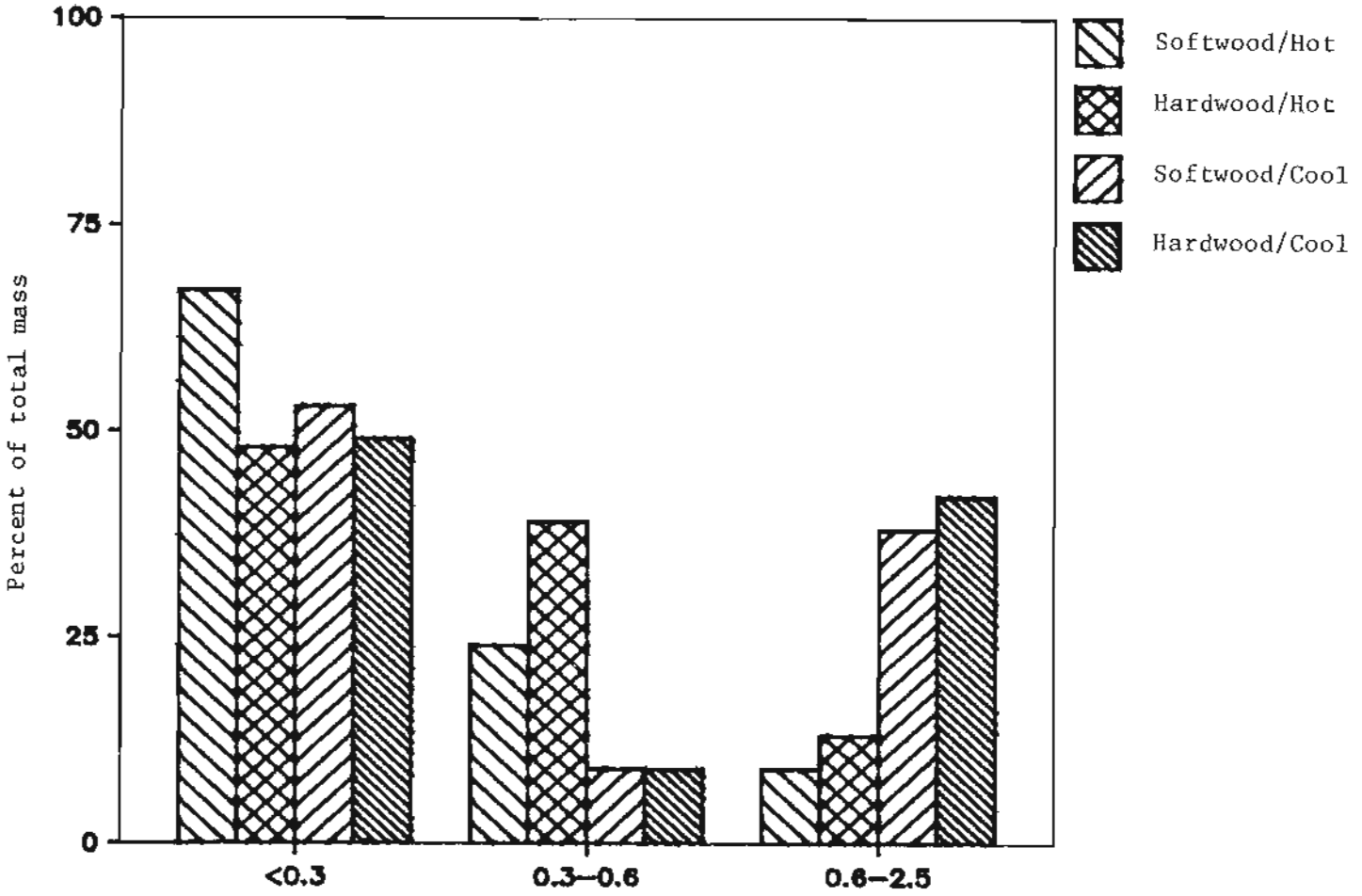

Figure 3.3. Average wood stove aerosol particulate mass distribution.

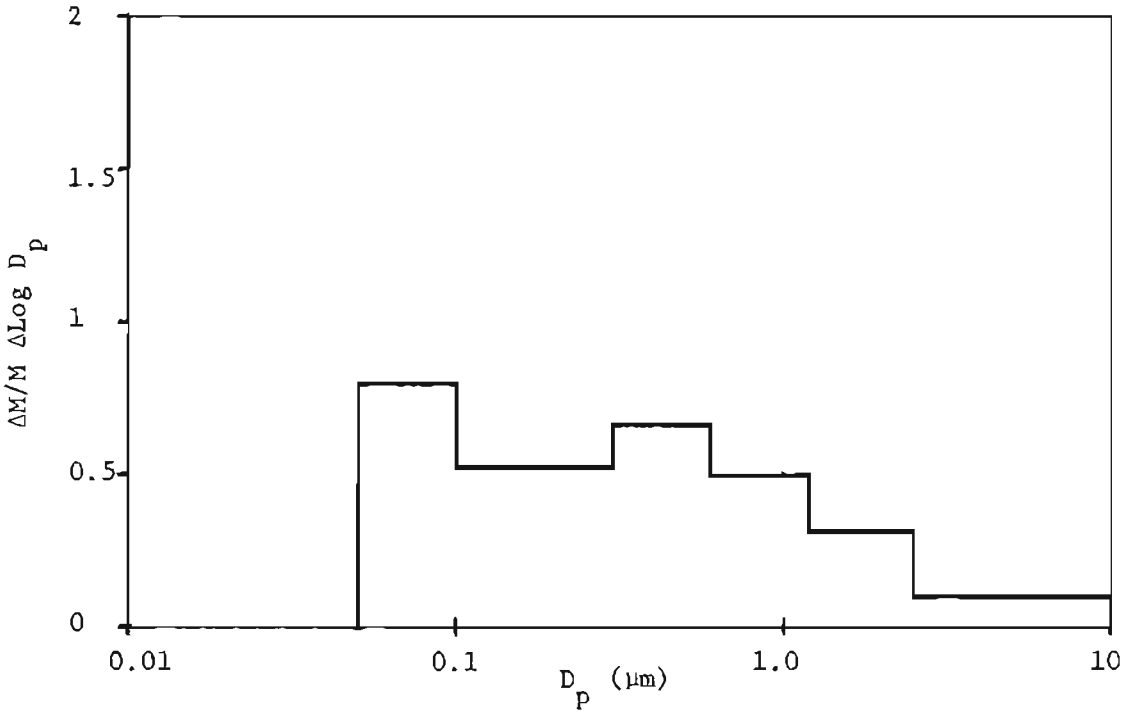

Figure 3.4A. Size distribution of aerosol mass in woodstove soft wood hot burning emissions.

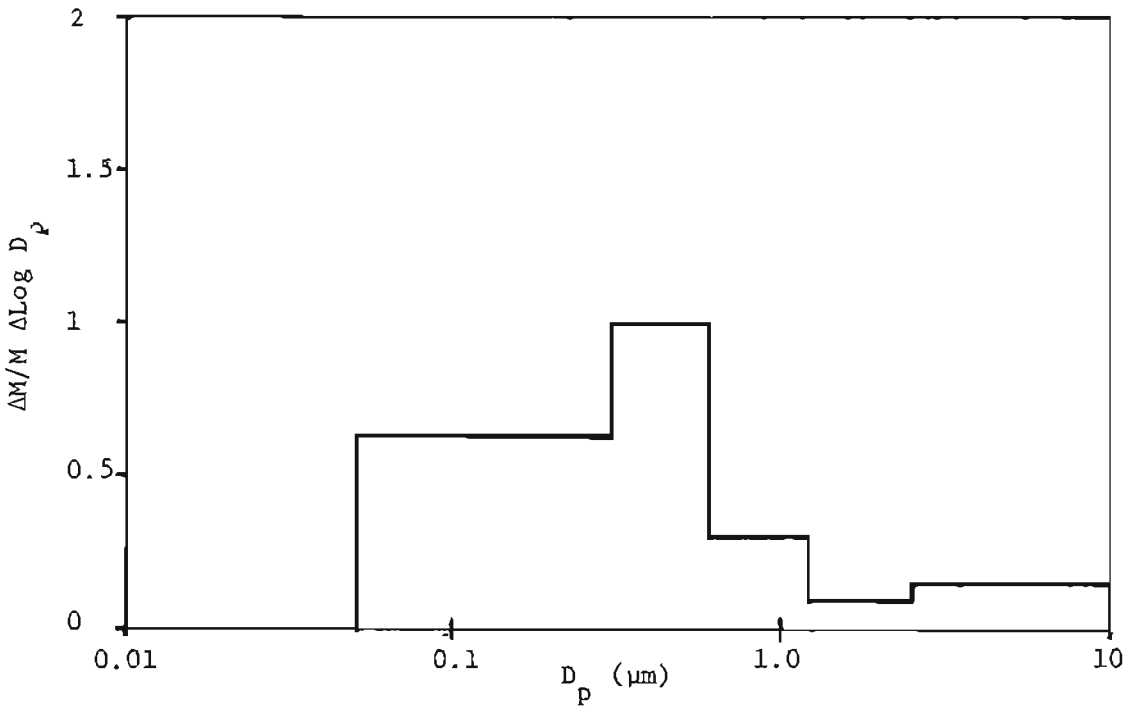

Figure 3.4B. Size distribution of aerosol mass in woodstove hard wood hot burning emissions

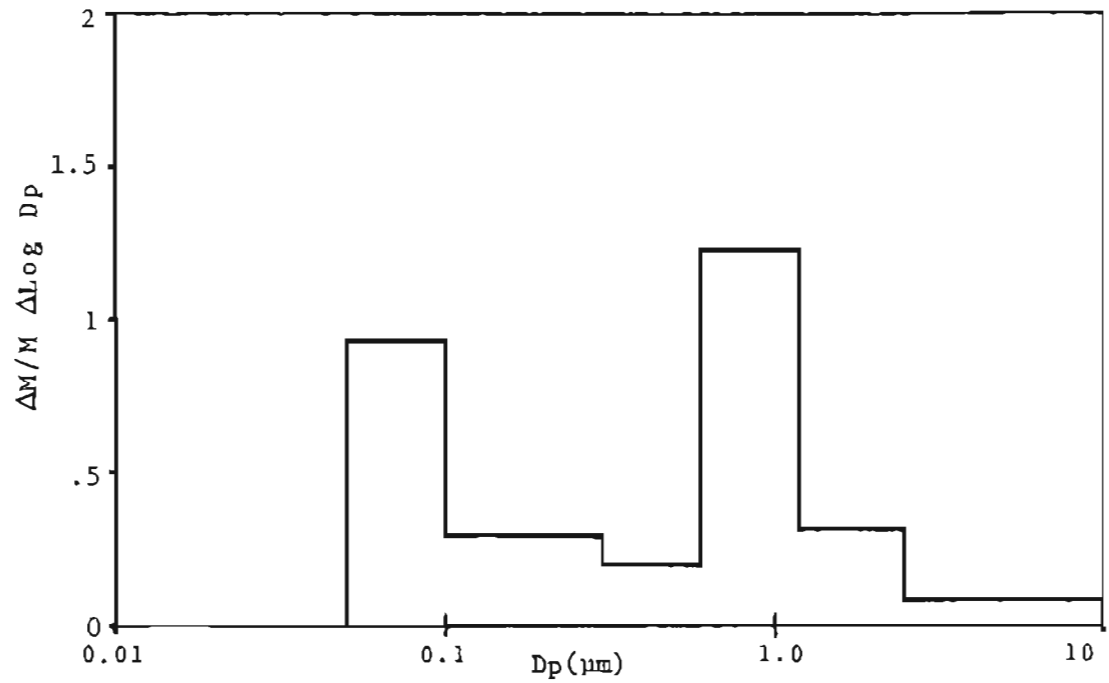

Figure 3.4C. Size distribution of aerosol mass for wood stove soft wood cool burning emissions.

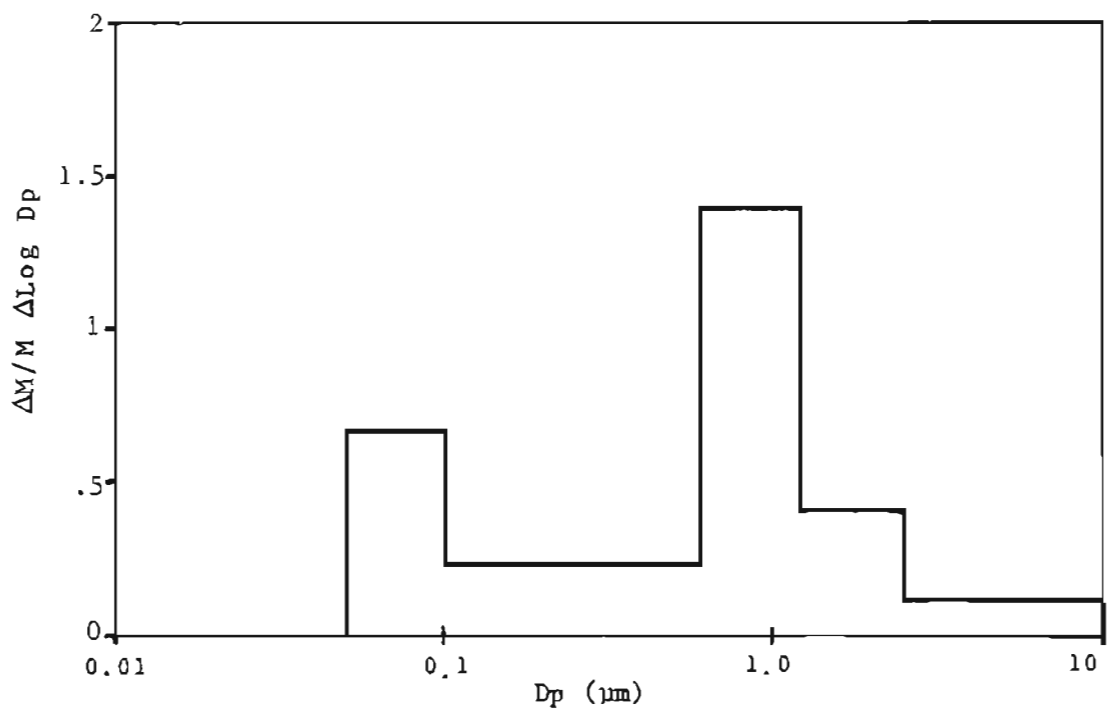

Figure 3.4D. Size distribution of aerosol mass for wood stove hard wood cool burning emissions.

Since about 10% of the aerosol mass is shown by Table 3.3B to have diameters greater than 2.5 μm, the values in Table 3.3A will be slightly higher than comparable values in Table 3.3B. For hot burning the aerosol mass distribution was unimodal with 50% or more of the mass in particles smaller than 0.3 μm. For cool burning the mass distribution was significantly different from hot burning in that it was bimodal. Similarly to hot burning up to 50% of the mass was concentrated in particles smaller than 0.3 μm, but almost 50% of the remaining mass was found between 0.6 and 1.2 μm. Very little mass was found between 0.3 and 0.6 μm. This type of aerosol distribution was also found by Radke et al. (1978) for aerosols sampled by aircraft from slow (cool) burning forest slash. This study also found that aerosols from a fast burning (hot) slash burn had a single mode below 0.3 μm. Kamens et al., (1983) also mention occasional significant particulate volumes in the 0.42-0.75 μm size ranges (measured by an electrical aerosol analyzer) but do not attribute a cause to this result.

The existence of a bimodal distribution, as mentioned in chapter 2, probably involves heterogeneous condensation on nuclei that were generated by combustion and on aerosol particles already present in the combustion air. In cool burning, gases leaving the combustion zone were very rich in condensable organic vapors. As these gases cooled, organic vapors condensed on all available particles. Since particles generated in flames had diameters much less than 0.1 μm while ambient aerosols usually had a mode about 0.2-0.3 μm diameter, particles forming by condensational growth on these two different sized particle populations would form a bimodally distributed aerosol. The fact that the bimodal

aerosol particle distribution effect occurs only in cool burning flue gases where the concentrations of condensable vapors were high, and did not occur in hot burn flue gases where the concentrations of condensable vapors were low, supports the hypothesis that the effect involves condensation mechanisms.

Hot burning and cool burning are essentially different processes which occur on either end of the range of RWC combustion possibilities. In hot burning large bright flames produce comparatively large amounts of elemental carbon. If temperature, oxidizer concentration and turbulence is high enough as in commercial hog fuel boilers even the elemental carbon particles produced in the flames will be oxidized to CO and CO_2. Usually this is not the case for RWC. Cool burning is mainly a pyrolysis process where wood is changed into vapor organics and charcoal. The burning of the charcoal might be the main process which produces elemental carbon particles in cool burning.

Wood type did not have a large effect on the mass distribution. Hardwood burning aerosol mass was not as concentrated in the very smallest particle size range as was softwood aerosol mass, but usually it had more mass in the next to the smallest size range. This effect occurred for both hot and cool burning.

Tables 3.4A and Figures 3.5A-D show hot and cool burning residential wood stove aerosol particle carbon distributions from set (A) experiments as a function of particle diameter for organic, elemental and total carbon. The percentages in Table 3.4A are based on the carbon passing the 2.5 μm impactor. Table 3.4B and Figures 3.6A-D show carbon distributions for set (B) data. The percentages in Table

Table 3.4A

Average Wood Stove Aerosol Carbon Distribution

(% carbon passing 2.5 μm. impactor)

Size (μm)	Damper open		Damper Closed	
	Softwood (N=3)	Hardwood (N=2)	Softwood (N=3)	Hardwood (N=2)
	Organic Carbon			
<0.3	70±9	46±10	52±1	58±1
0.3-0.6	18±10	39±1	5±3	3±1
0.6-2.5	12±6	15±10	43±3	39±1
	Elemental Carbon			
<0.3	67±3	49±4	51±6	61±21
0.3-0.6	25±3	42±1	18±1	16±13
0.6-2.5	8±1	9±4	31±5	23±8
	Total Carbon			
<0.3	65±2	50±6	53±1	58±1
0.3-0.6	24±4	40±0	5±3	4±2
0.6-2.5	11±4	10±6	42±3	38±1

Uncertainties are standard errors of the mean.

N = Number of tests

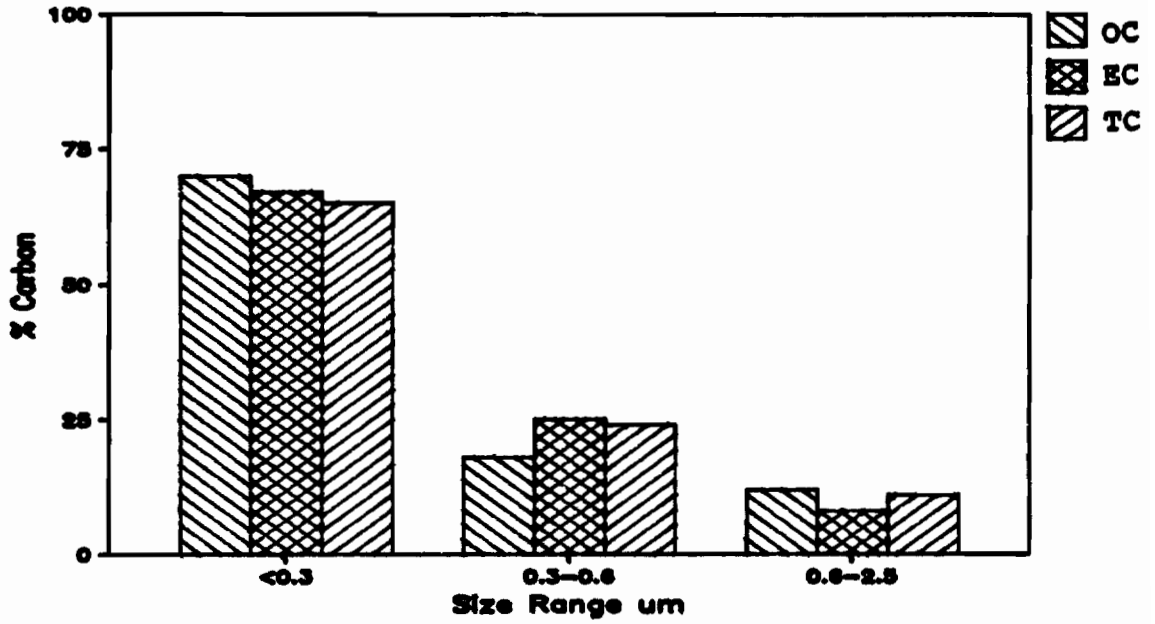

Figure 3.5A. Size distribution of carbonaceous aerosol in woodstove softwood hot burning emissions.

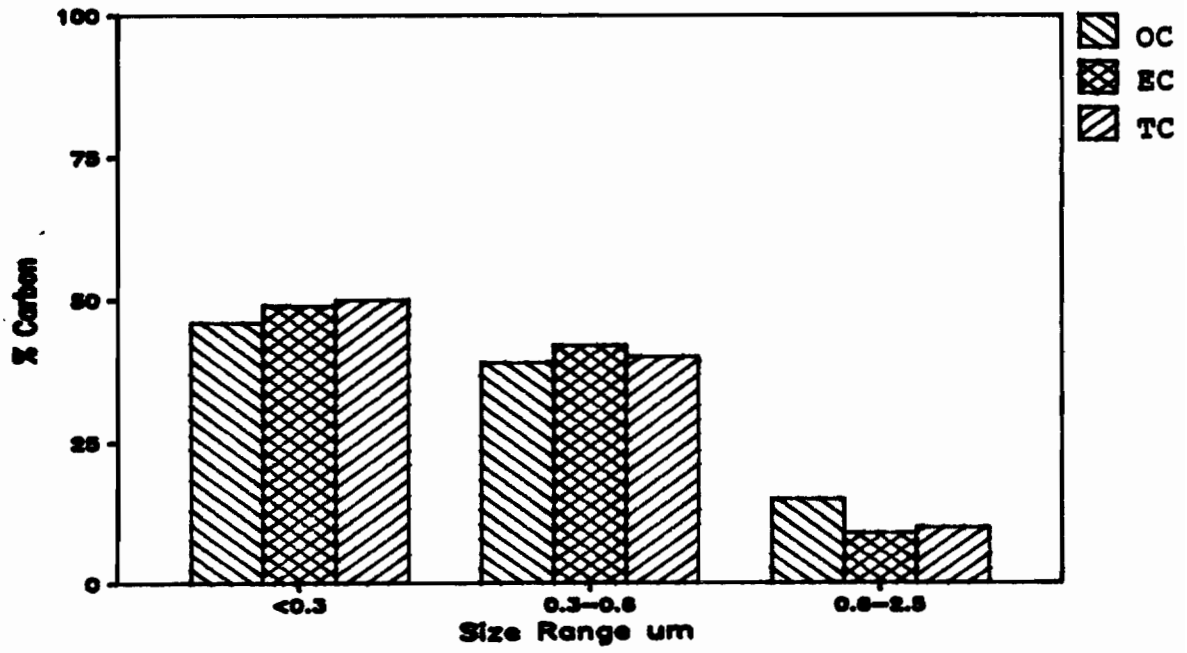

Figure 3.5B. Size distribution of carbonaceous aerosol in woodstove hardwood hot burning emissions.

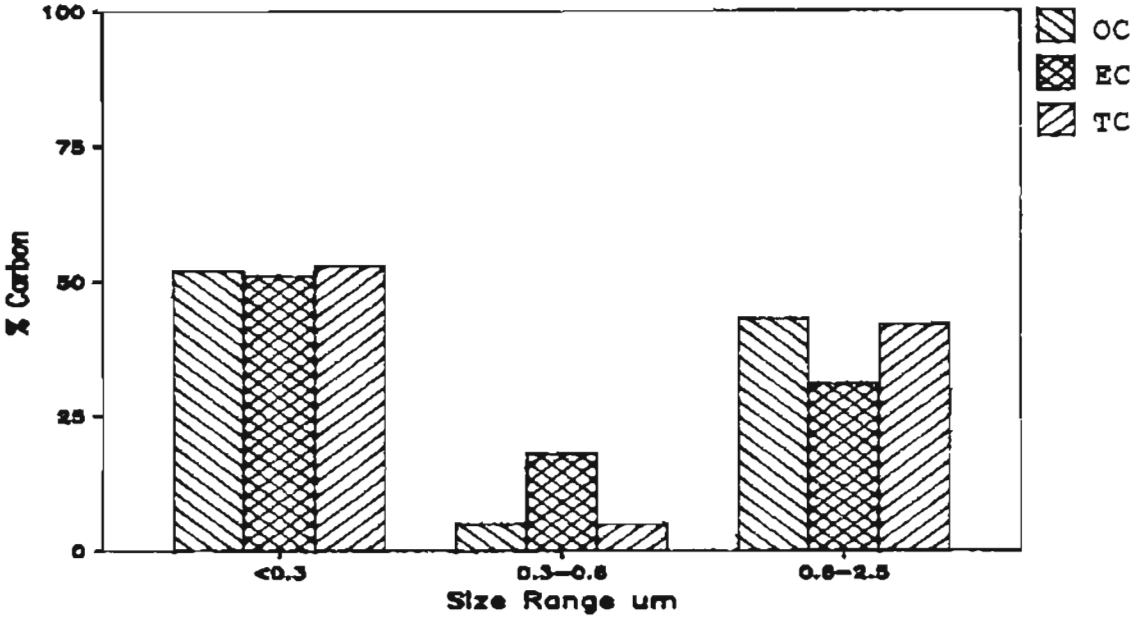

Figure 3.5C. Size distribution of carbonaceous aerosol in wood stove softwood cool burning emissions.

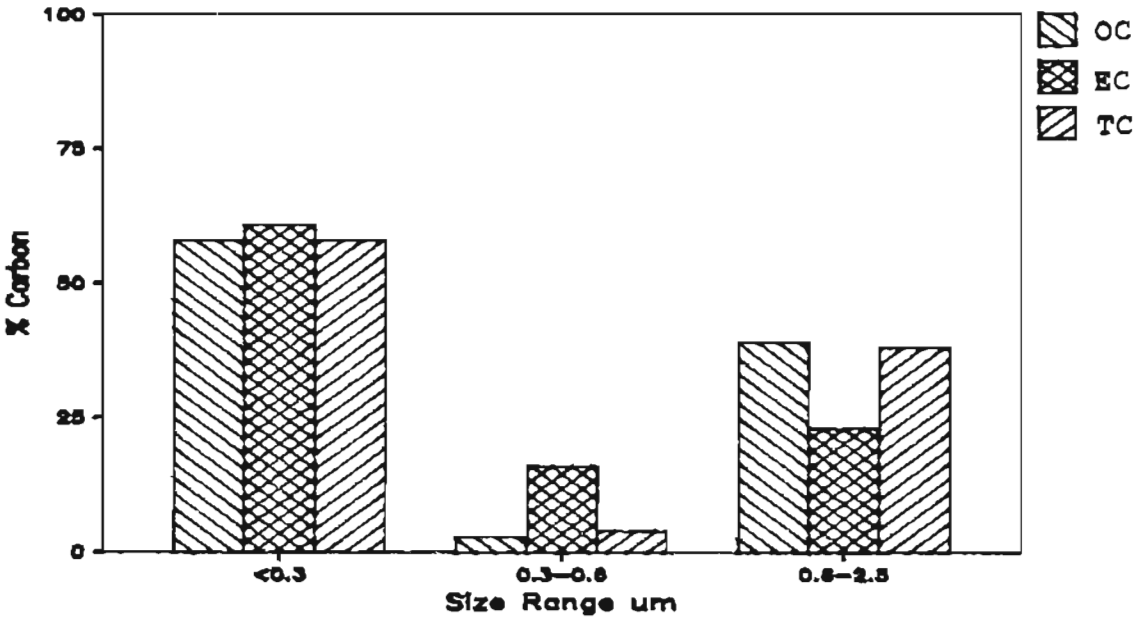

Figure 3.5D. Size distribution of carbonaceous aerosol in wood stove hardwood cool burning emissions.

Table 3.4B

Average Wood Stove Aerosol Carbon Distribution

(% of carbon in the total aerosol)

Size μm	Damper open		Damper Closed	
	Softwood (N=6)	Hardwood (N=7)	Softwood (n=7)	Hardwood (N=7)
Organic Carbon				
<0.3	36±11	48±9	33±6	32±
0.3-1.2	40±10	44±8	50±7	54±6
>1.2	24±6	8±3	17±6	14±5
Elemental Carbon				
<0.3	41±5	41±7	46±7	51±11
0.3-1.2	42±7	55±6	36±7	39±9
>1.2	17±2	4±2	18±6	10±5
Total Carbon				
<0.3	40±6	44±7	32±5	34±8
0.3-1.2	42±7	51±6	54±5	53±6
>1.2	18±2	5±2	14±5	13±5

Uncertainties are standard errors of the mean.

N = Number of tests

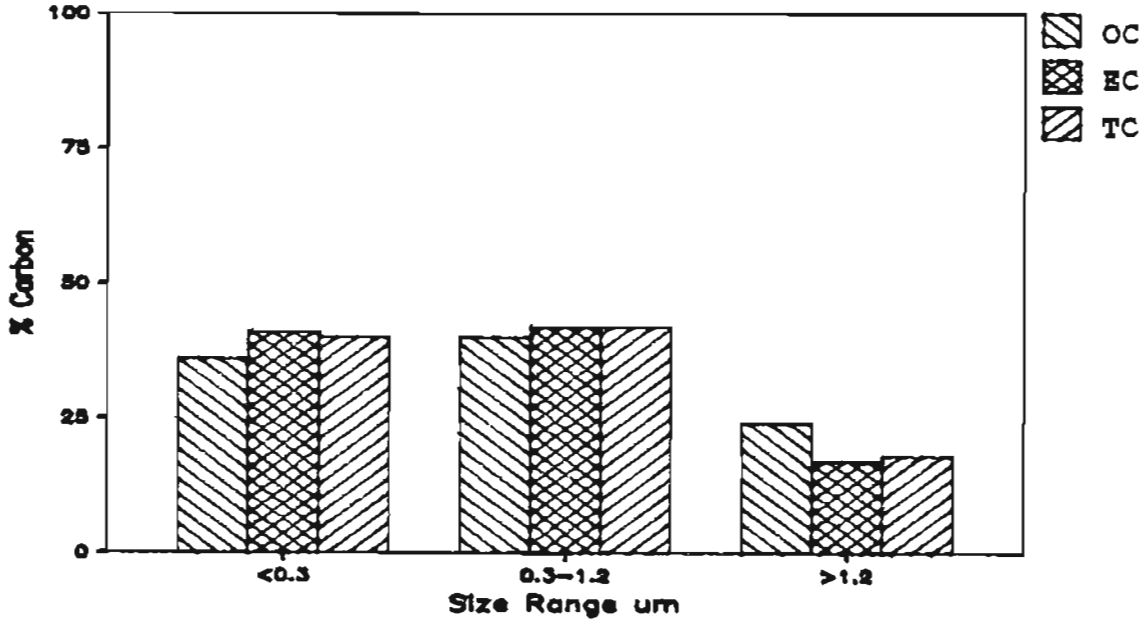

Figure 3.6A. Size distribution of carbonaceous aerosol in wood stove softwood hot burning emissions.

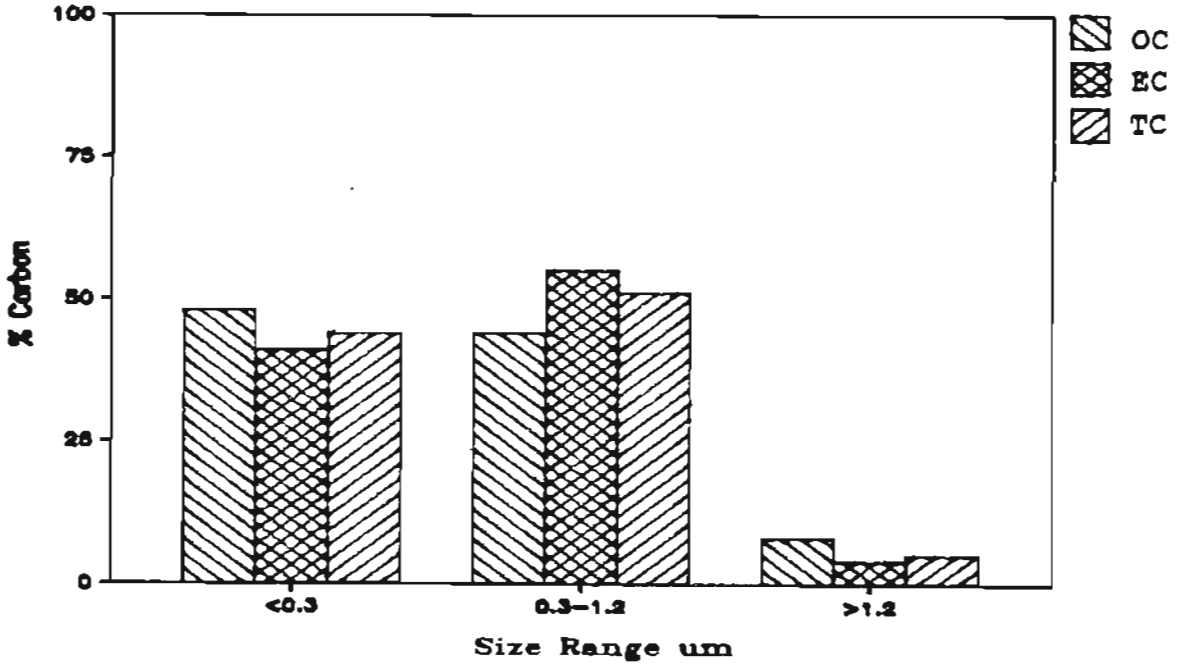

Figure 3.6B. Size distribution of carbonaceous aerosol in wood stove hardwood hot burning emissions.

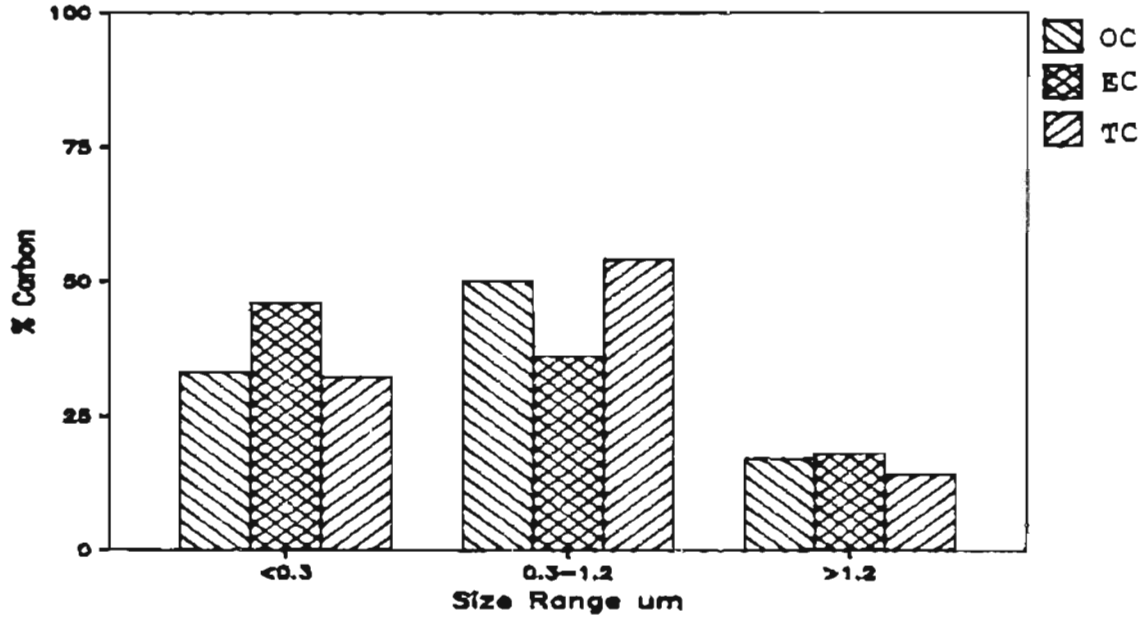

Figure 3.6C. Size distribution of carbonaceous aerosol in wood stove softwood cool burning emissions.

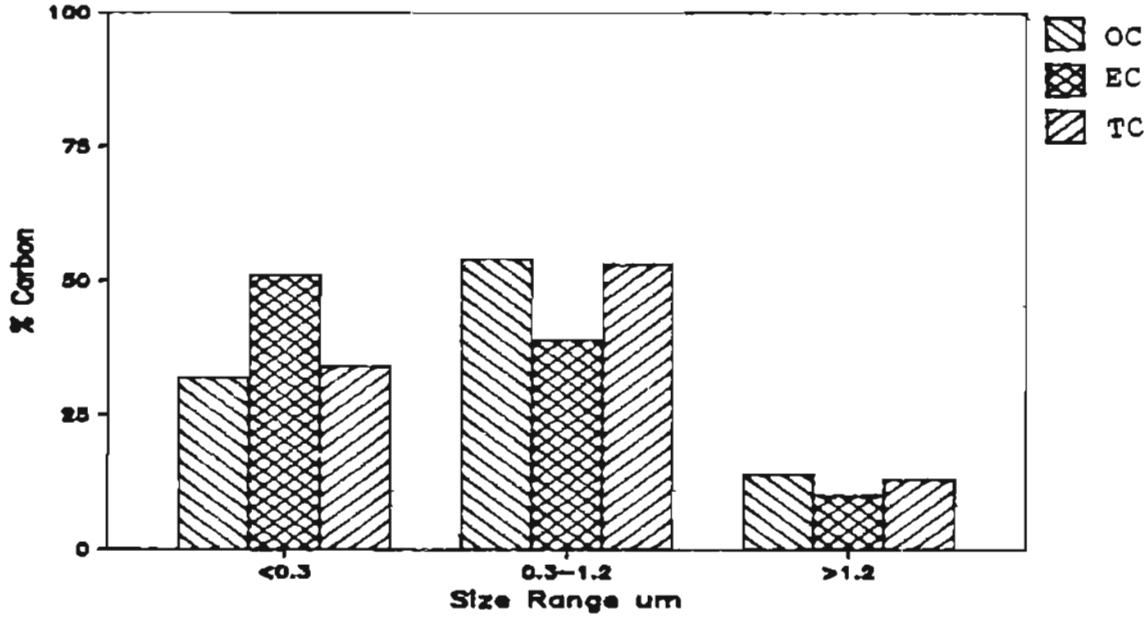

Figure 3.6D. Size distribution of carbonaceous aerosol in wood stove hardwood cool burning emissions.

3.4B are based on the carbon in the total aerosol collected without an impactor in the sampling stream. Therefore, compared to Table 3.4B the values in Table 3.4A will be slightly higher due to the difference in percentage base. The format used in Figures 3.4A-D is such that the area under the graphs is proportional to the amount of carbon within the size range considered. Both carbon and mass distributions were unimodal for hot burn wood stove aerosol particles and bimodal for cool burn particles. Because the composition of wood stove aerosol particles does not change significantly as a function of particle size (See Tables 3.6A-B) the distributions of aerosol particle mass, carbon and trace elements were essentially the same.

Table 3.4A shows that for hot burn aerosols only about 10% of the total carbon was associated with particles >0.6 μm. For cool burn aerosols about 40% of aerosol carbon was associated with particles >0.6 μm. Table 3.4B generally agrees with Table 3.4A, although it does show that 18% of total carbon for softwood hot burn aerosols was associated with particles >1.2 μm. Distributions for organic and elemental carbon were very similar to total carbon distributions. Table 3.4B does not emphasize the bimodal nature of cool burn aerosols. This table alone would give the impression that hot and cool burn aerosols have similar carbon distributions.

Figures 3.7A-C and 3.8A-C show a subset of set B for hot and cool burning respectively. Samples in this subset were all collected on quartz filters (rather than three filters collected on quartz and three on Teflon) so that they can be used to generate the detailed OC, EC, and TC distributions shown in the figures. Comparing Figures 3.7A and 3.8A

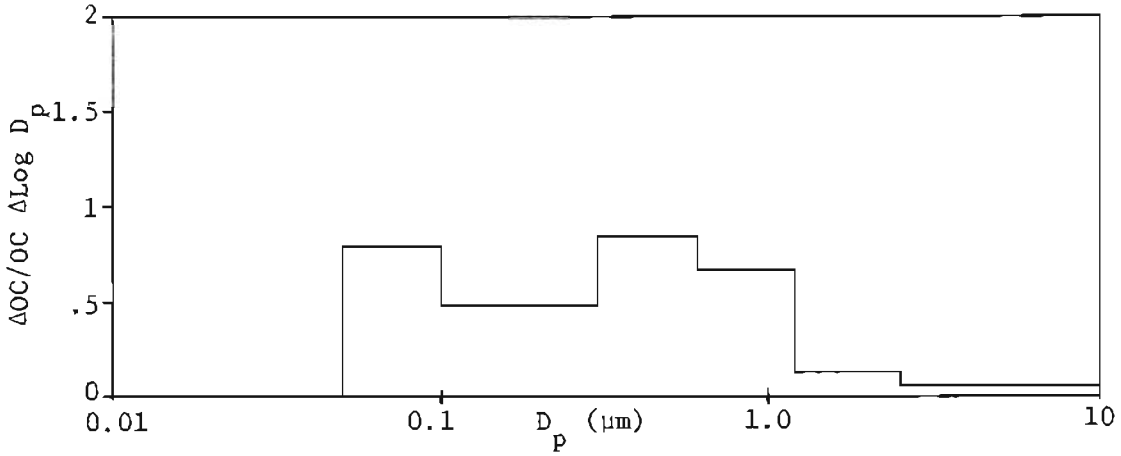

Figure 3.7A. Size distribution of organic carbon in hot burning wood stove emissions.

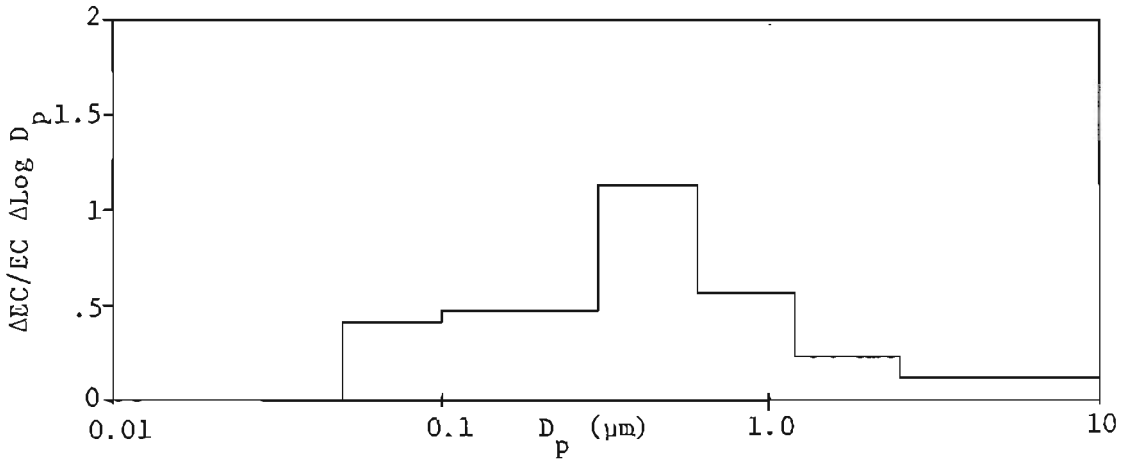

Figure 3.7B. Size distribution of elemental carbon in hot burning wood stove emissions.

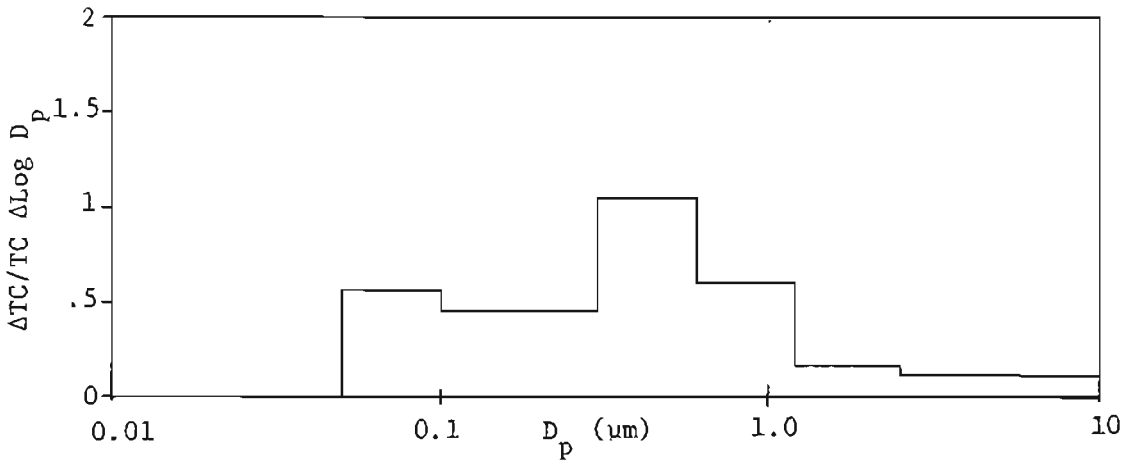

Figure 3.7C. Size distribution of total carbon in hot burning wood stove emissions.

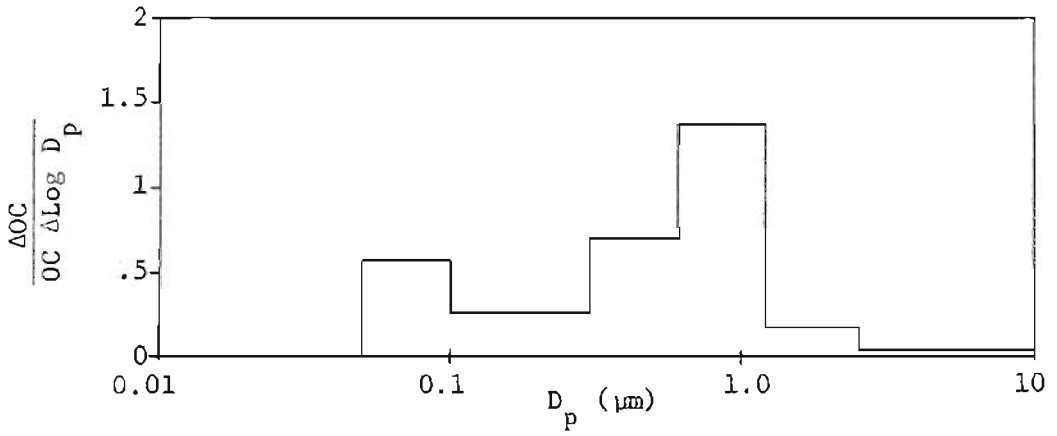

Figure 3.8A. Size distribution of organic carbon in cool burning wood stove emissions (N = 4).

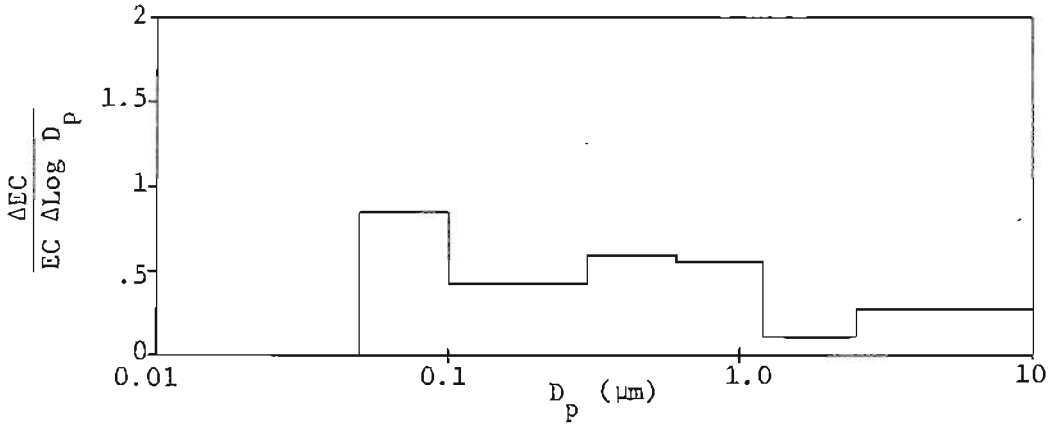

Figure 3.8B. Size distribution of elemental carbon in cool burning wood stove emissions (N = 4).

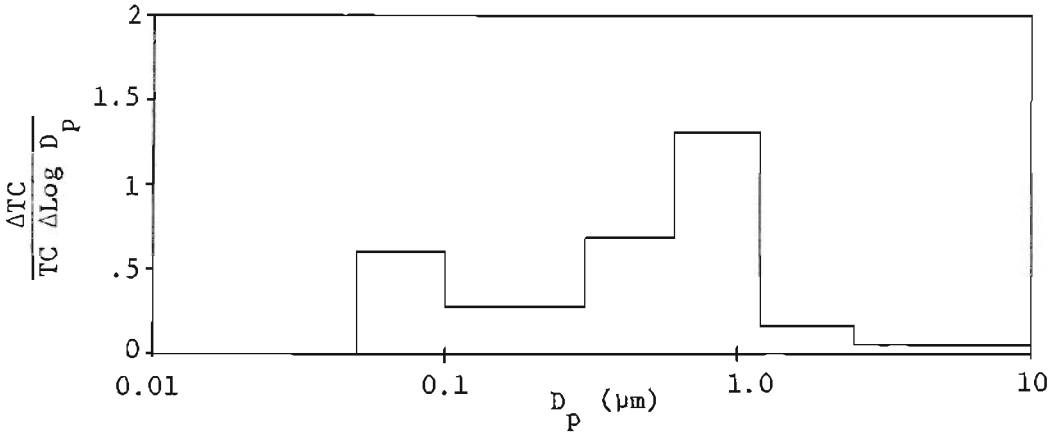

Figure 3.8C. Size distribution of total carbon in cool burning wood stove emissions (N = 4).

shows that about 1/4 to 1/3 of the OC in the 0.05-0.1, 0.1-0.3, and 0.3 to 0.6 μm size ranges for hot burning appeared in the 0.6-1.2 μm. size range for cool burning, i.e., for hot burning OC is more associated with smaller particles. Making the same comparison of EC distributions (Figures 3.7B and 3.8B) shows that almost 1/2 of the EC in the 0.3-0.6 μm size range for hot burning was shifted to the 0.05-0.1 μm size range for cool burning.

Tables 3.5A-B show trace elemental distributions for hot burn stove aerosol particles for data sets (A) and (B), respectively. Figures 3.9A-B show trace elemental distributions for these data graphically. For the same reason as for mass and carbon distributions the percentage values in Table 3.5A are slightly higher than those in Table 3.5B. Tables 3.5A-B and Figures 3.9A-B pool hot burn data for softwood and hardwood. This was done because the differences between softwood and hardwood data were not statistically significant. Trace elements were all approximately distributed in the same manner as mass and carbon distributions. Cool burn trace elemental distributions are not shown because trace elemental concentrations in cool burn aerosols were so small that distribution trends were usually overwhelmed by XRF errors.

Tables 3.6A-B show organic, elemental and total carbon compositions of stove RWC aerosol particles generated by burning softwood and hardwood under hot and cool burn conditions. Both these tables show that the distribution between organic and elemental carbon was very different for hot burn and cool burn particles. Hot burn particles had very high EC/TC values, while cool burn particles had very low EC/TC values. Values of EC/TC greater than 0.8 were recorded in some hot burns. The

Table 3.5A

Average Wood Stove Aerosol Trace Element Distributions *

Damper open (N=5)			
Size (μm)	<0.3	0.3-0.6	0.6-2.5
Al	56±3	30±5	14±5
Cl	50±4	38±2	12±6
K	50±3	37±2	13±4
Fe	46±16	40±10	14±6
P	42±3	42±3	16±3
Rb	46±3	19±5	35±6
S	49±3	35±5	16±6
Zn	52±4	37±4	11±5

Table 3.5B

Average Wood Stove Aerosol Trace Element Distributions*

Damper open				
Size (μm)	<0.1	0.1-0.6	0.6-2.5	N
Cl	5±2	77±2	18±3	8
K	11±1	78±1	10±2	8
P	1±1	76±3	23±3	4
Rb	0	80	19	1
Zn	9±2	75±-3	16±-3	7

* Softwood and hardwood data are pooled.

Uncertainties are standard errors of the mean.

N = Number of tests

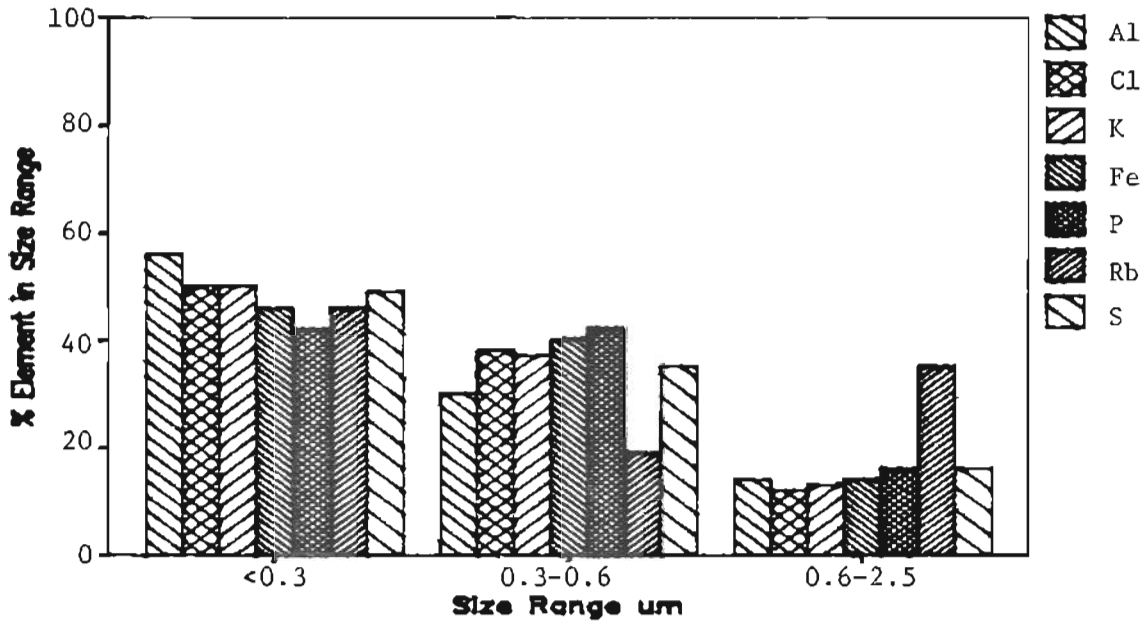

Figure 3.9A. Size distribution of aerosol trace elements in hot burning stove emissions.

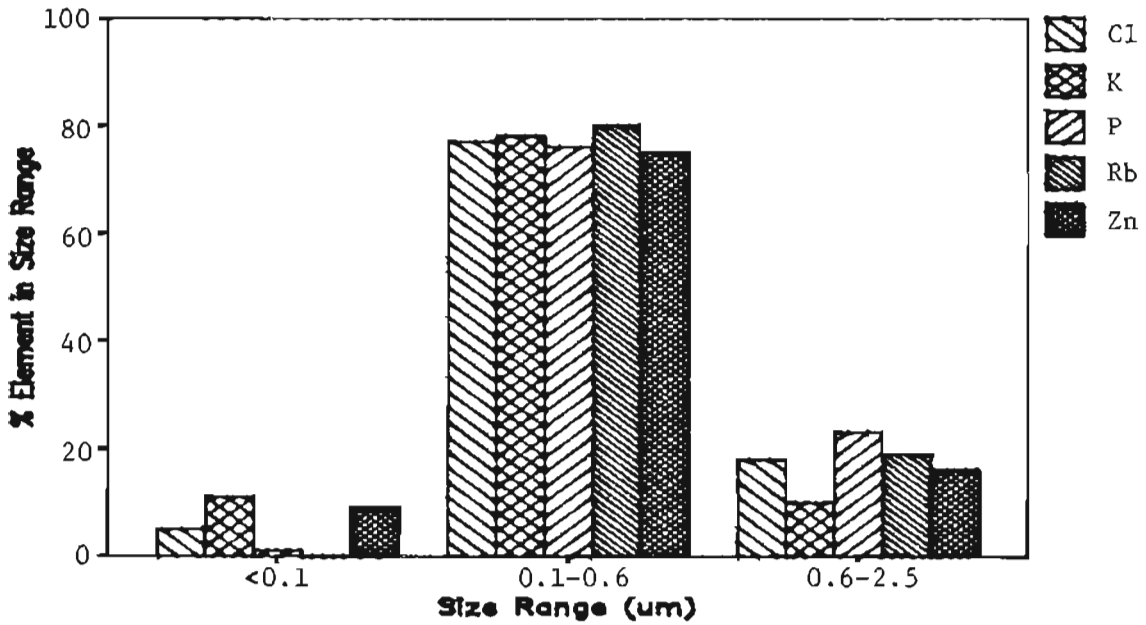

Figure 3.9B. Size distribution of aerosol trace elements in hot burning stove emissions.

Table 3.6A

Average Wood Stove Aerosol Carbon Composition (% Mass)

Size (μm)	EC/TC	OC/M	EC/M	TC/M
Fir	Damper Open (Hot)		N = 4	
<0.3	63±11	13±2	25±9	38±8
<0.6	72±5	10±2	28±8	38±10
<2.5	73±3	10±3	29±9	39±11
Hardwood	Damper Open (Hot)		N = 2	
<0.3	54±34	28±20	29±17	57±4
<0.6	54±33	27±19	31±18	58±1
<2.5	53±32	26±18	29±17	55±0
Fir	Damper Closed (Cool)		N = 3	
<0.3	7±2	56±2	4±1	60±2
<0.6	7±2	55±3	4±1	59±3
<2.5	6±1	55±1	4±1	59±1
Hardwood	Damper Closed (Cool)		N = 2	
<0.3	5±0	59±1	3±0	62±1
<0.6	7±1	56±1	4±1	60±2
<2.5	6±2	51±5	3±1	54±6

Uncertainties are standard errors of the mean.

N = Number of tests

Table 3.6B

Average Wood Stove Aerosol Carbon Composition (% Mass)

Size (μm)	EC/TC	OC/M	EC/M	TC/M
Fir	Damper Open (Hot) N = 7			
<0.3	67±8	16±5	30±5	46±4
<1.2	66±7	20±4	38±5	58±4
Total	68±8	20±5	38±5	58±6
Hardwood	Damper Open (Hot) N = 8			
<0.3	52±8	13±4	15±5	28±5
<1.2	56±6	15±5	17±4	32±6
Total	55±7	14±4	16±4	30±5
Fir	Damper Closed (Cool) N = 7			
<0.3	12±3	41±3	5±1	46±3
<1.2	10±2	50±2	5±1	55±2
Total	9±1	51±1	5±2	56±2
Hardwood	Damper Closed (Cool) N = 9			
<0.3	13±2	45±2	7±1	52±2
<1.2	9±1	56±1	6±1	62±2
Total	8±2	57±2	5±1	62±2

Uncertainties are standard errors of the mean.

N = Number of tests

presence of large amounts of elemental carbon in hot burn aerosol particles made these particles appear black. The 6 to 8% EC/TC values noted for cool burning aerosols were upper limit values due to an artifact of the carbon analysis system. The EC/TC value was a convenient parameter for measuring the intensity of hot burning. Values of EC/TC less than about 8% identify cool burning, while high EC/TC (>55%) values were associated with hot burn conditions and with high trace elemental concentrations in the aerosol. Figure 3.10 shows Cl, K, and S concentrations from data set A, plotted as a function of EC/TC. This figure shows that trace elemental concentrations increased with increasing EC/TC values but that there was considerable variability in the trace elemental concentrations at high values of EC/TC. This variability is related to the particulate TC/M values. For hot burn particles TC/M varied widely because burn temperature and turbulence were not precisely controlled. This variability in hot burn conditions also results in trace element concentration variability. When burning conditions existed which allowed EC to burn than TC/M values decreased while trace elements in the particles become a larger proportion of the remaining particulate mass.

Cool burn aerosol particles had very reproducible carbon compositions over all cool burn tests. TC/M values clustered closely in the range of 56 to 63%. EC/M values clustered in the range of 3 to 7% and OC/M values were generally in the range of 50 to 56%. Hot burn aerosols showed much greater variability in carbon composition. TC/M ranged from 10-60% while OC/M ranged from 7 to 50%, EC/M ranged from 11 to 50%, and EC/TC ranged from 20 to 85%.

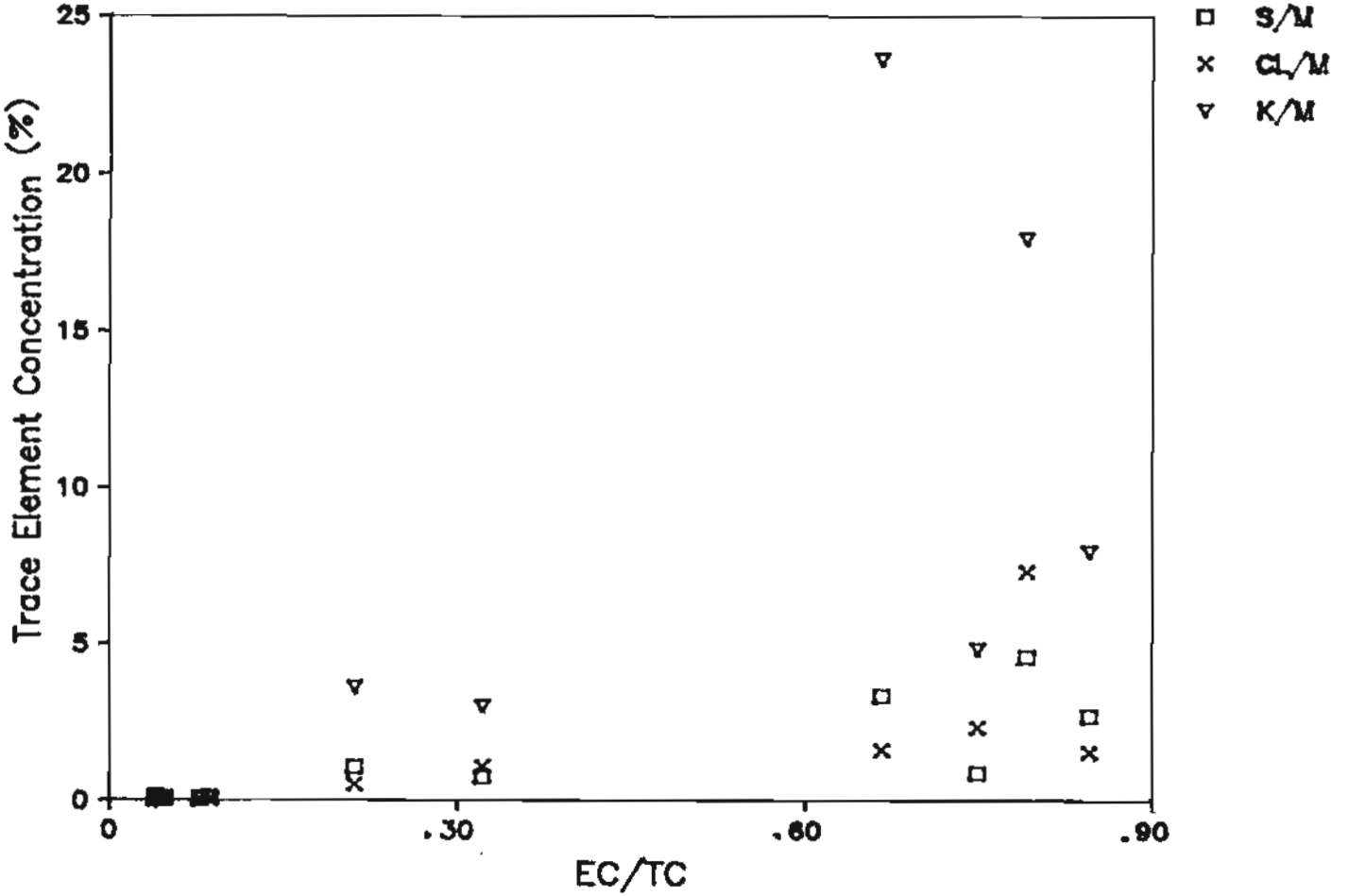

Figure 3.10. The relationship of sulfur, chlorine, and potassium concentrations to EC/TC in residential wood stove emissions.

Comparing hot burn TC/M, values from Table 3.6A shows that the values for hardwood in one table are about equal to the softwood values in the other table and vice versa. This demonstrates that particulate carbon composition is determined by hot burn conditions rather than by wood type. It will also be noted that in Table 3.6A lower TC/M values are associated only with lower OC/M values (EC/M is similar for both hardwood and softwood burns) while in Table 3.6B lower TC/M values are associated both with lower OC/M and EC/M values. For all hot burn tests the plume was essentially invisible while for cool burning the plume was always very visible.

The data of Tables 3.6A-B can be examined to determine how carbon composition varies as a function of particle size. Since the data presented are carbon composition values for aerosol particles passing an impactor (except for total aerosol values in Table 3.6B), they represent average values for aerosols whose diameters were less than the impactor cut-point diameter. Therefore only the <0.3 μm data are representative of a subset of the fine particle size range. The <0.6 μm data results from particles both in the 0.3-0.6 and <0.3 μm size ranges. From mass distribution data it is known that about 50% of RWC aerosol is in the <0.3 μm size range while only 10-20% is in the 0.3-0.6 μm size range. Therefore small composition differences that particles in the 0.3-0.6 μm size range may have compared to those in the <0.3 μm size range are not detectable. When total or <2.5 μm data are compared with <0.3 μm data a comparison is being made between all the aerosol collected and 50% of the aerosol collected. In these cases significant carbon composition differences in particles <0.3 μm and >0.3 μm would be indicated by

differences in OC/M, EC/M and TC/M values in Tables 3.6A-B. Table 3.6A generally does not show such differences. On the other hand Table 3.6B, which is compiled from a much larger data set, consistently shows slightly lower carbon mass fractions for particles <0.3 μm than for total or <1.2 μm particles. Note that total and <1.2 μm values are essentially the same because only a very small percentage of RWC aerosol is >1.2 μm. Table 3.6B shows that the carbon mass fractions of particles <0.3 μm are slightly lower than particles >0.3 μm and that the carbon mass fractions of those particles >0.3 μm are larger than the total or <1.2 μm values shown because these values are diluted by the lower carbon mass fraction values of particles <0.3 μm. Higher carbon mass fraction values on larger particles might result if condensation nuclei were composed of relatively lower organic carbon mass fraction material and then larger particles formed by condensation of organic carbon vapors on these nuclei. Since both Tables 3.6A and B do not show the slightly lower carbon mass fractions for <0.3 μm particles it must be concluded that this effect is produced by some combustion variable that is not always present.

Most of the data indicate that the elemental carbon mass fraction (EC/M) does not vary as a function of particle size. For cool burning, since the elemental carbon values given are upper limit values and the real elemental values are less than these values, the question of elemental carbon variation is not well addressed by these data. For hot burning, both tables show slightly lower EC/M values for particles <0.3 μm for hot burning fir but not for hot burning oak.

The mechanism of soot formation has been recognized for many years

as an extremely complex problem and the nucleation step, i.e., the transition from molecular species where chemical reactions dominate to incipient soot particles where physical processes dominate is the least understood step in the process (Olson and Calcote, 1981). Wood initially consists of long chain polymers. During combustion chemical bonds in these structures are broken, creating a variety of free radicals. These highly reactive species engage in reaction chains, forming other free radicals, and finally more stable chemical species. The chemical species formed in part depend on temperature and oxidant availability. In flaming combustion stable clusters of non-organic molecules and clusters of high molecular weight organic molecules can form. Organic molecular clusters can pyrolyze to elemental carbon. Spherical soot (mainly elemental carbon) particles 30-100 Angstroms in diameter containing 10^7 carbon atoms form in milliseconds in flames (Prado and Lahaye, 1981). As chemical species move away from the hottest regions of a flame their partial pressures can become equal to or greater than corresponding equilibrium pressures of the condensed phases. Heterogeneous condensation can then occur on non-organic, elemental carbon nuclei, and ions. Since nuclei always exist in flames, homogeneous nucleation is not necessary and does not occur. As condensing species move to cooler regions, condensation of inorganic species will go to completion because these species have high vapor pressures. Organic vapors will continue to condense on all particles available, so that particles that were originally mostly inorganic will acquire an organic carbon loading. High molecular weight organic species will condense first. As soon as particles are formed, coagulation of particles will occur to form larger

particles. Particles that were mainly carbon can coagulate with particles that were mainly inorganic so that the cluster particles will tend toward homogeneous compositions. In hot burning flue gases inorganic and elemental carbon particle concentrations will be abundant relative to concentrations of condensable organic vapor. Particles formed will be solid and possibly grease covered. In cool burning flue gases concentrations of inorganic and elemental carbon particles will be low, while concentrations of condensable organic species will be high. Particle growth will thus consist of vapor condensation on particles.

Tables 3.7A-B show the trace elemental compositions of hot and cool burn wood stove aerosol particles captured behind 2.5 μm impactors. Data for other size cuts >0.3 μm are not shown because they were not significantly different from these data, i.e., no significant trace elemental variation was observed for particles >0.3 μm. Particles <0.3 μm usually showed about a 20% increase in trace elemental concentrations compared to larger particles, but there was a high degree of variability associated with these data because the small sample sizes available made both mass determination and XRF analysis difficult. For data set (B) trace elemental data were obtained for aerosols <0.1 μm. These data usually indicated that smaller particles had slightly higher trace elemental concentrations than larger particles but these data also had large uncertainties because of the small masses collected.

These tables show that hot burn wood stove aerosol particles contain large amounts of K, Cl, and S and lesser amounts of Al, Si, P, Zn, Rb, Pb, and Fe, while cool burn particles contain less the 0.03% of all trace elements except K. Obviously burn temperatures were not high

Table 3.7A

Average Wood Stove Aerosol Trace Element Composition

(% of mass)

	Damper open		Damper closed	
	Fir (N=3)	Oak (N=2)	Fir (N=3)	Oak (N=2)
Al	0.37±0.14	0.28±0.13	0.08±0.02	0.04±0.01
Ca	0.27±0.03	0.03±0.02	0.03±0.01	0.02±0.01
Cl	3.4±1.4	1.2±0.6	0.02±0.01	0.02±0.0
Fe	0.04±0.01	0.01±0.0	0.03±0.01	0.01±0.01
K	13.1±4.8	6.3±2.5	0.08±0.04	0.07±0.03
P	0.23±0.07	0.14±0.05	0.02±0.01	0.02±0.01
Pb	0.16±0.04	0.05±0.03	n.d.	n.d.
Rb	0.03±0.01	0.02±0.01	n.d.	n.d.
S	2.6±1.0	2.1±1.0	0.07±0.04	0.04±0.01
Si	0.56±0.12	0.32±0.23	0.02±0.02	0.03±0.01
Zn	0.17±0.03	0.05±0.03	n.d.	n.d.

Uncertainties are standard errors of the mean.

N = Number of tests

Table 3.7B

Average Wood Stove Aerosol Trace Element Composition

(% Of Mass)

	Damper open		Damper closed	
	Softwood	Hardwood	Softwood	Hardwood
	(N=5)	(N=7)	(N=5)	(N=2)
Al	0.29±0.13	0.41±0.23	0.03±0.01	0.03±0.02
Ca	0.41±0.08	0.12±0.08	0.07±0.03	n.d.
Cl	1.9±0.6	3.5±0.91	0.06±0.01	0.04±0.02
Fe	n.d.	0.03±0.01	n.d.	n.d.
K	3.4±1.5	1 8.2±2.9	0.10±0.01	0.40±0.18
P	0.07±0.03	0.23±0.05	0.01±0.01	0.02±0.01
Pb	n.m.	0.09±0.14	n.d.	n.d.
Rb	n.m.	0.06±0.02	n.d.	n.d
S	1.3±0.80	1.3±0.68	0.06±0.01	0.11±0.06
Si	0.39±0.25	0.74±0.09	0.05±0.03	0.10±0.04
Zn	0.28±0.07	0.33±0.07	0.02±0.01	0.0

Uncertainties are standard errors of the mean.

N = Number of tests

enough in cool burning to volatilize inorganic species so that they were available for particle formation. For cool burning these species must remain in the ash. The variation of potassium concentrations spans over two orders of magnitude going from cool burn to hot burn combustion conditions. For cool burn aerosols the concentration of potassium averaged 0.08% and was as high as 0.16% for aerosols sampled toward the end (charcoal burning) of an oak burn test. The differences shown for hot trace elemental compositions by the two tables were due mainly to variability in reproducing hot burn conditions.

3.1.2.2 FIREPLACE AEROSOL DATA

Fireplace aerosol composition data were derived from a series of nine test runs on three different residential fireplaces. Both hardwood and softwood were burned. Fires were built with kindling wood and with three to five pieces of well-aged split logs. Sampling was started after flaming combustion was well established. Aerosol samples were collected in smoke plumes at 1-2 m from the chimney. Data for hard and soft wood burning were pooled because there were no significant differences in particle composition attributable to wood type.

Aerosol average mass distribution for fireplace aerosol particles is shown in Table 3.8 and Figure 3.11. Unlike emission distributions from cool burning wood stoves, which were bimodal and had very little mass in the 0.3-0.6 μm range, fireplace emissions were monomodal with the mode located in the 0.3 to 0.6 μm. range.

Table 3.9 and Figures 3.12 and 3.13A-C show carbon distributions for fireplace aerosols. Figure 3.12 shows the average carbon

Table 3.8

Average Fireplace Aerosol Mass Distribution (N=9)*

(% of total aerosol mass)

Size range (μm)	Mass %
<0.1	13±3
0.1-0.3	29±6
0.3-0.6	35±4
0.6-1.2	14±3
1.2-2.5	4±3
>2.5	5±2

Table 3.9

Average Fireplace Aerosol Carbon Distribution (N=9)*

(% of total)

Size (μm.)	OC	EC	TC
<0.3	43±6	42±8	43±6
0.3-1.2	47±6	49±7	48±6
>1.2	10±3	9±3	9±3

* These data pool hardwood and softwood data from three residential fireplaces.

Uncertainties are standard errors of the mean.

N = Number of tests

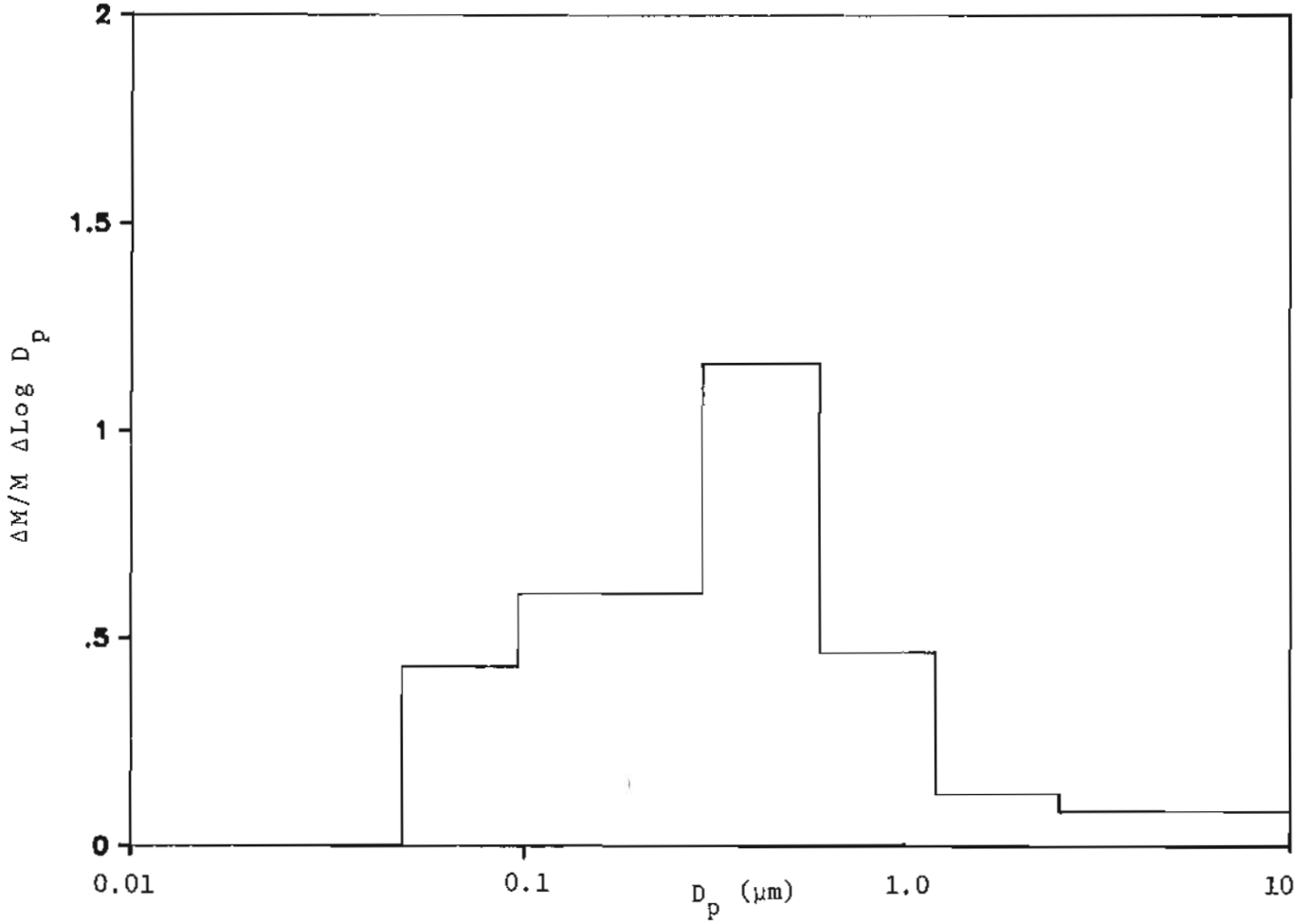

Figure 3.11. Mass distribution of fireplace emissions.

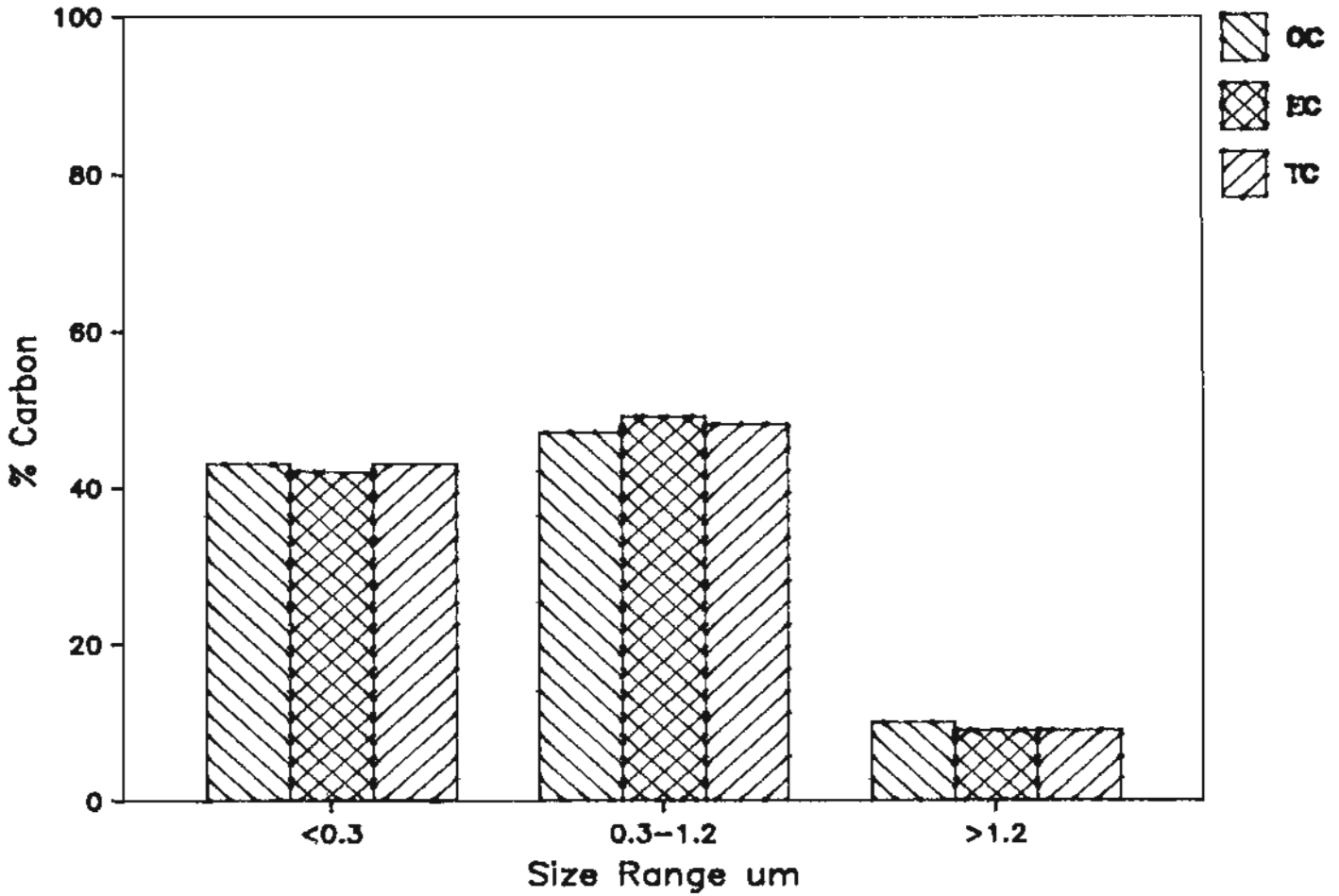

Figure 3.12. Size distribution of carbonaceous aerosol in fireplace emissions (N=9).

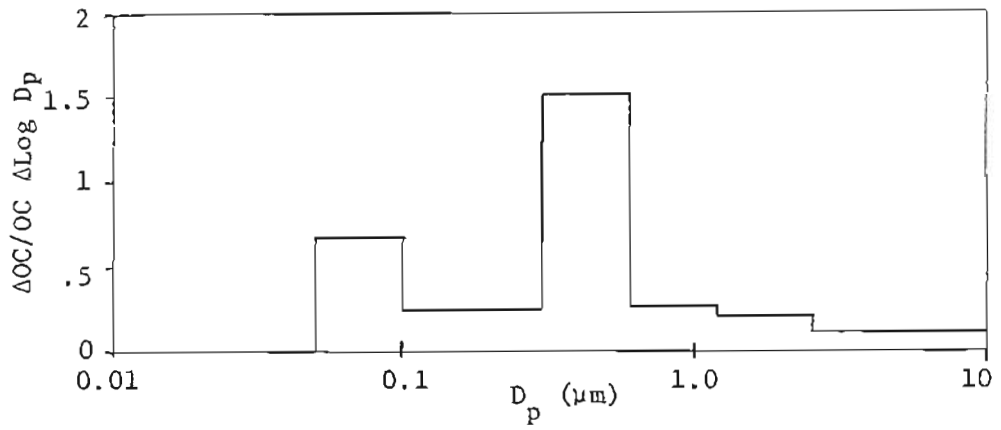

Figure 3.13A. Size distribution of organic carbon in fireplace emissions (N = 2).

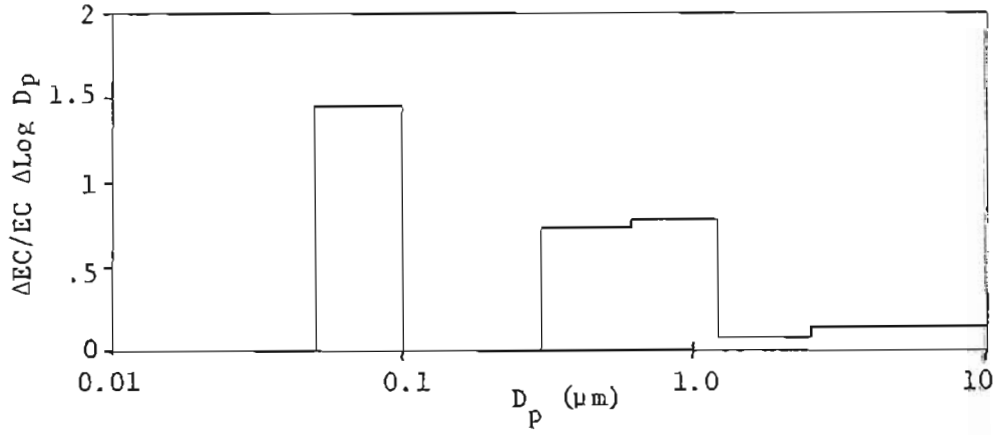

Figure 3.13B. Size distribution of elemental carbon in fireplace emissions (N = 2).

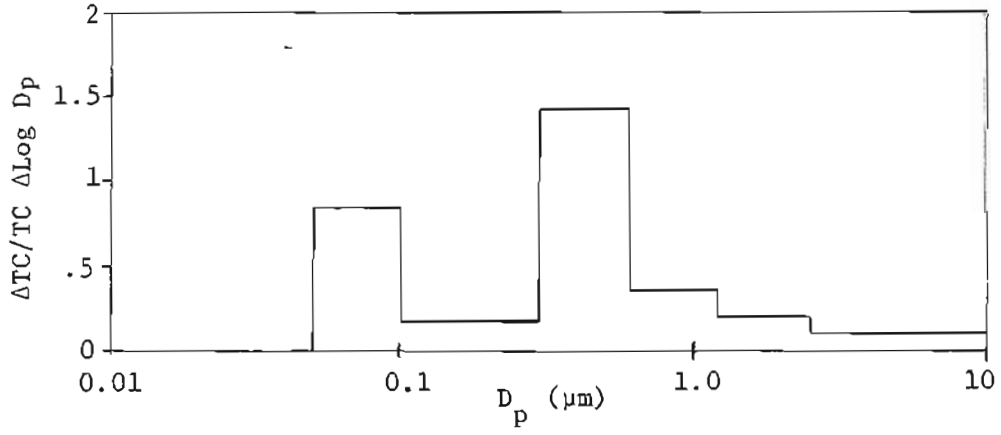

Figure 3.13C. Size distribution of total carbon in fireplace emissions

distribution of all data sets where aerosol samples were collected on quartz fiber filters behind impactors with cut points at 0.3, 0.6, and 2.5 μm. Figures 3.13A-C show carbon distributions for a subset (N = 2) of this group where quartz fiber filters were used for sampling behind all the impactors. These distributions are very similar to the mass distributions for fireplace aerosols shown in Table 3.8 and Figure 3.11. Table 3.10 and Figure 3.14 show trace element distributions for fireplace aerosols. No fireplace trace element data were collected to further resolve the trace element distribution between 0.1 and 0.6 μm.

Tables 3.11 and 3.12 show aerosol carbon and trace element composition, respectively. As noted for wood stove emissions, the aerosol composition was not a significant function of aerosol size for particles >0.1 μm. Reasonably high uncertainties were associated with the trace element data because trace element levels were low and therefore subject to large XRF uncertainties. Table 3.12 shows that fireplace aerosol contained very small amounts of trace element species.

Fireplace aerosol elemental carbon and trace element concentrations were usually slightly higher than the respective values for cool burning wood stove aerosols, even though the flaming combustion that occurs in fireplaces appears to be very similar to that in hot burning wood stoves. Fireplace combustion is certainly not air-starved. However, it does generate aerosols similar to those of wood stove air-starved combustion because of the flame cooling effects caused by the large excess combustion air flows that occur during fireplace combustion. Airtight stoves operate at excess air levels of about 50%, whereas fireplaces operate at excess air levels of up to 2000%. Fireplace

Table 3.10

Average Fireplace Aerosol Trace Elemental Distribution

(% of trace element passing 2.5 um impactor) (N=4)

Size (μm)	0.6-2.5	0.1-0.6	<0.1
Ca	54±22	29±13	17±11
Cl	10±2	84±5	7±6
K	6±4	76±9	19±7
P	13±5	63±13	24±12

Uncertainties are standard errors of the mean.

N = Number of tests

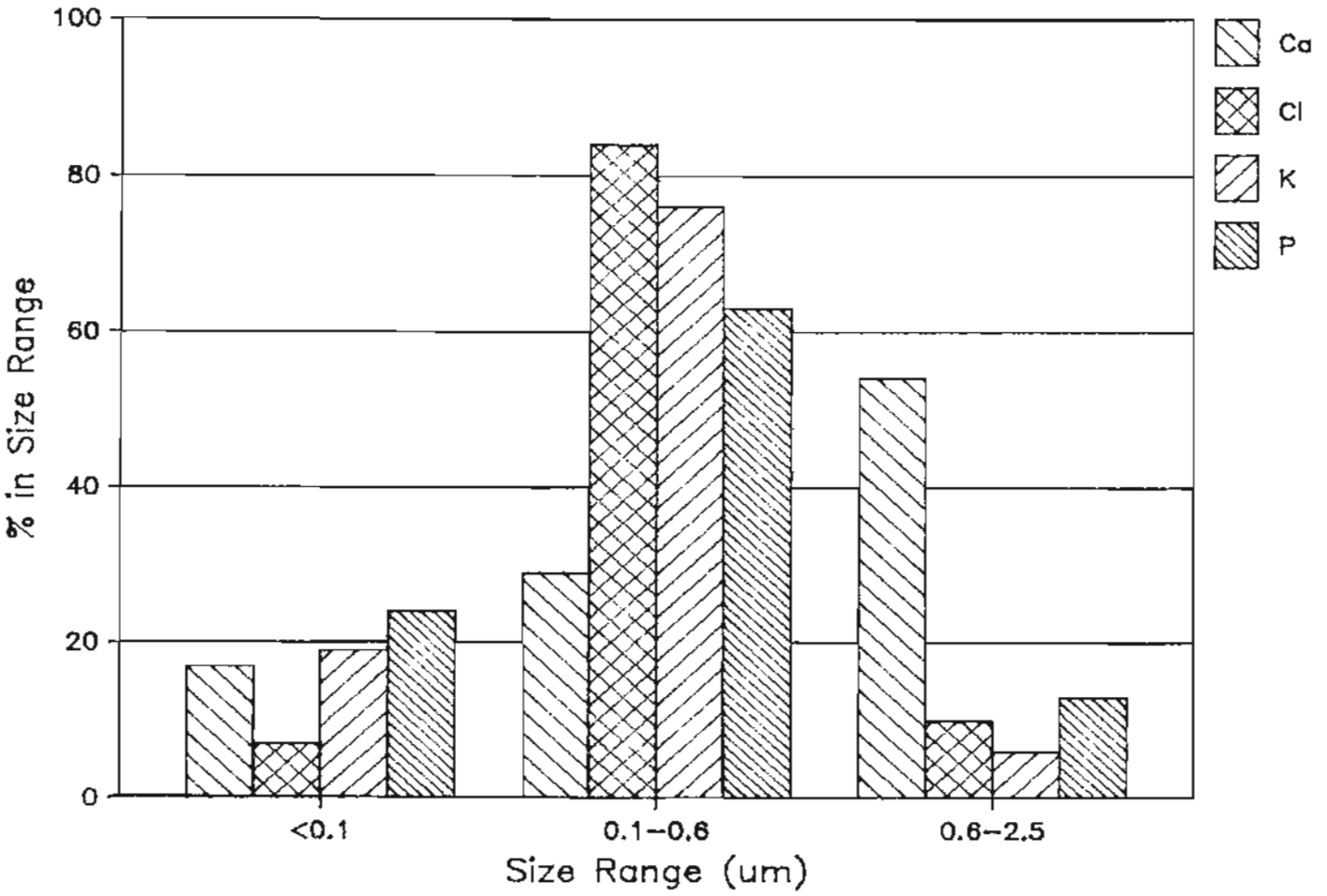

Figure 3.14. Size distribution of trace elements in fireplace particulate emissions.

Table 3.11

Average Fireplace Aerosol Carbon Composition (%)

Size	EC/TC	OC/M	EC/M	TC/M	N
<0.1 (μm)	27±19	44±17	15±10	59±14	2
<0.3	17±12	52±7	9±5	61±6	6
<0.6	12±10	58±10	8±6	66±3	2
<1.2	15±9	51±8	9±6	60±4	7
<2.5	12±9	54±7	7±5	61±2	3
Tot. Aerosol	14±10	52±7	10±6	62±4	7

These data pool data from hardwood and softwood burns in three residential fireplaces

Uncertainties are standard errors of the mean

N = Number of tests

Table 3.12

Average Fireplace Aerosol Trace Element Composition (N=4)

(% mass)

Size (μm.)	<2.5	<0.6	<0.1
Al	0.03±0.01	0.05±0.03	0.08±0.02
Ca	0.06±0.03	0.14±0.12	0.10±0.07
Cl	0.86±0.40	0.63±0.33	0.26±0.23
K	0.56±0.28	0.70±0.33	0.37±0.10
P	0.03±0.01	0.03±0.01	0.07±0.02
Pb	0.04±0.04	0.05±0.04	0.01±0.01
S	0.17±0.06	0.18±0.07	0.23±0.06
Si	0.09±0.04	0.10±0.05	0.18±0.10
Zn	0.02±0.01	0.05±0.03	0.04±0.02

Note: These data pool hardwood and soft wood burns in three residential fireplaces and are percentages of mass.

Uncertainties are standard errors of the mean.

N = Number of tests

combustion also differs from stove combustion because in a fireplace the region surrounding the flame is cooler and radiation heat losses from the flames are higher than they would be in a stove where the stove structure reduces radiation heat losses from the combustion region.

Fireplace EC/TC values ranged from 7 to 20%. Since the aerosols were gray in color these percentages, unlike the case for cool burning wood stove aerosols, probably do represent real elemental carbon. When the EC/TC value for fireplace aerosols was near 7% the trace elemental compositions were very similar to cool burning wood stove aerosol particles. High levels of EC production do not occur in fireplace flames because the high flame temperatures and reducing conditions necessary for EC production are only minimally available. Prado and Layaye (1981) noted that EC production, a process of OC to EC conversion, was a function of residence time in the high temperature regions of a flame. It seems that the very high amounts of excess air in fireplace combustion causes sufficient flame cooling so that the organic carbon produced in the reducing regions of the flames remains in the form of OC rather than being pyrolyzed to elemental carbon.

3.1.2.3 RESIDENTIAL OIL FURNACE AEROSOL DATA

The oil furnace aerosol data were collected from three test runs on a 46 year old low pressure furnace. Table 3.13 and Figure 3.15 show that most of the aerosol mass was associated with particles <2.5 μm and that more than half of it was associated with particles <0.3 μm. Figures 3.16A-B show the organic and elemental carbon distributions for this aerosol as measured by one test. Table 3.14 shows that the aerosol was

Table 3.13

Average Residential Oil Furnace Aerosol Mass Distribution (N=3)

Size Range (μm)	% of Total Mass
<0.3	51±5
0.3-0.6	23±6
0.6-1.2	10±6
1.2-2.5	6±3
>2.5	10±1

Uncertainties are standard errors of the mean.

Table 3.14

Average Residential Oil Furnace Aerosol Carbon Composition (% of total carbon) (N=2)

Size Range (μm)	EC/TC	OC/M	EC/M	TC/M
<0.3	51	18	12	30
<0.6	36	16	13	29
<1.2	48	11	11	22
<2.5	53	11	12	23
<10	39	14	10	24
total aerosol	42	14	10	24

N = Number of tests

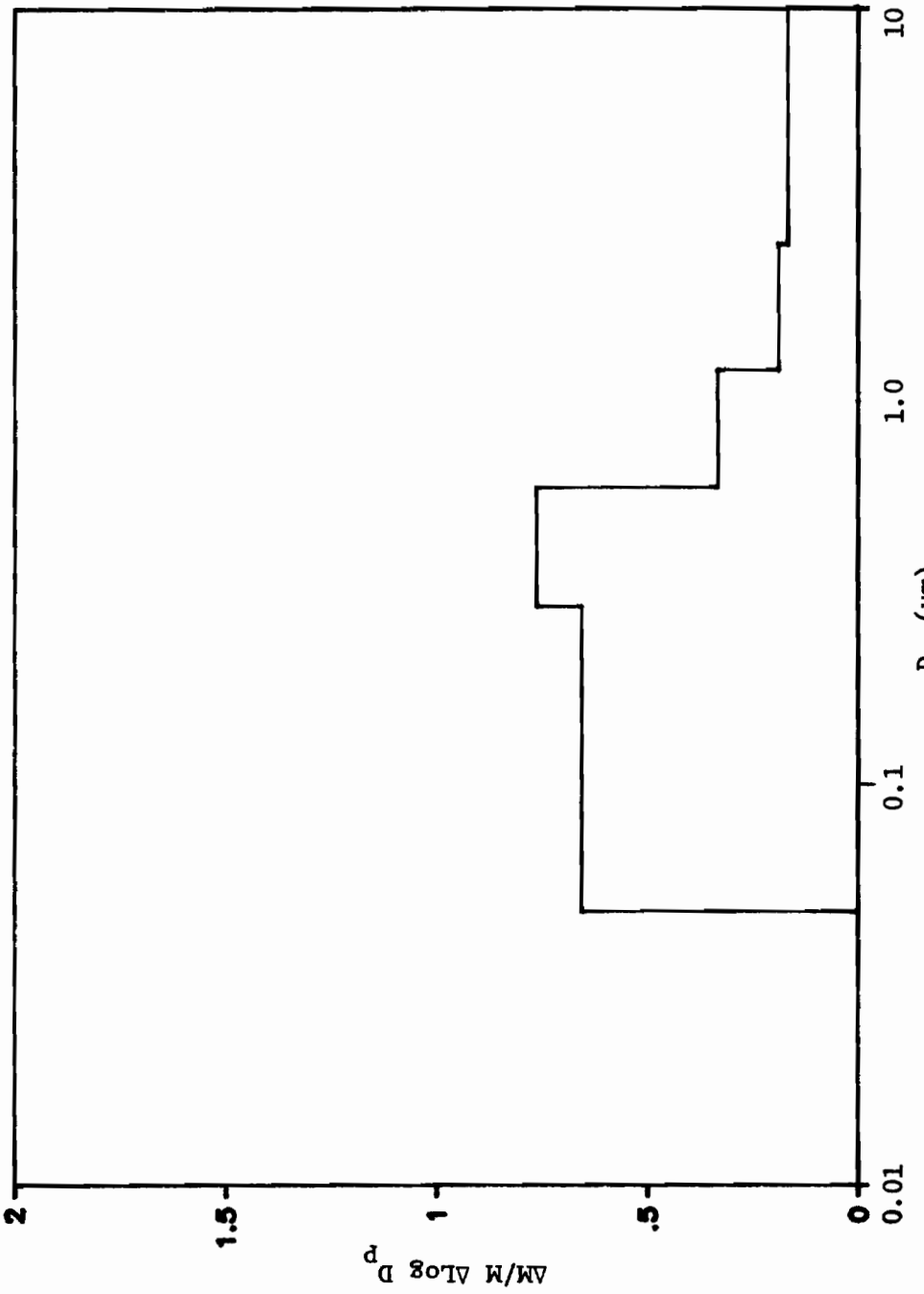

Figure 3.15. Average mass distribution for residential oil furnace emissions (N=3).

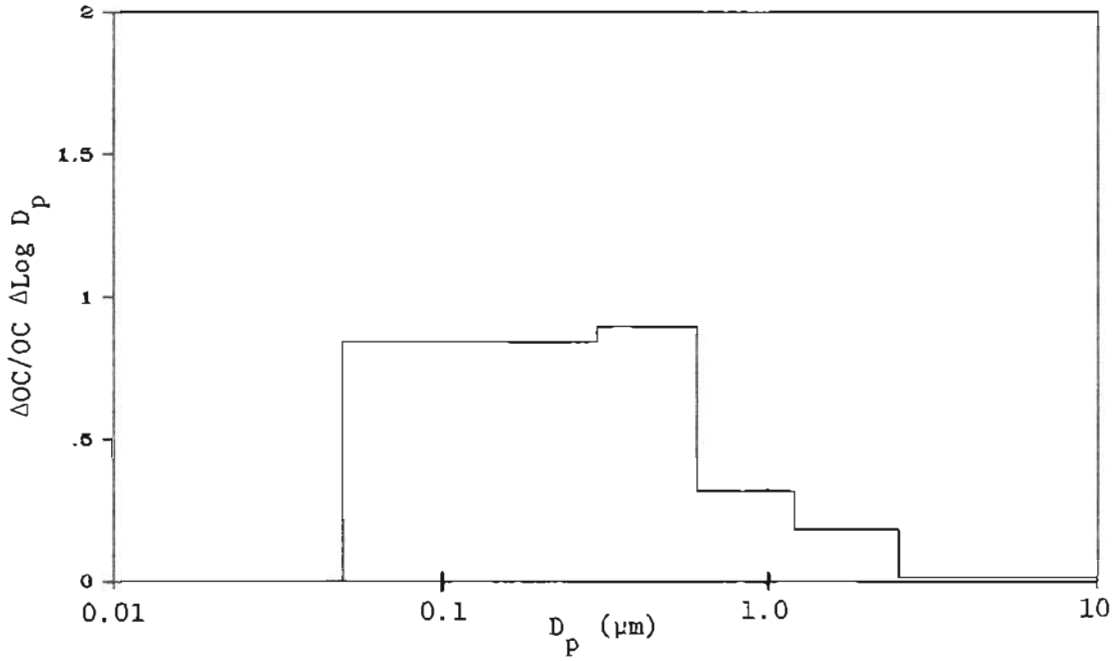

Figure 3.16A. Size distribution of organic carbon in residential oil furnace emissions.

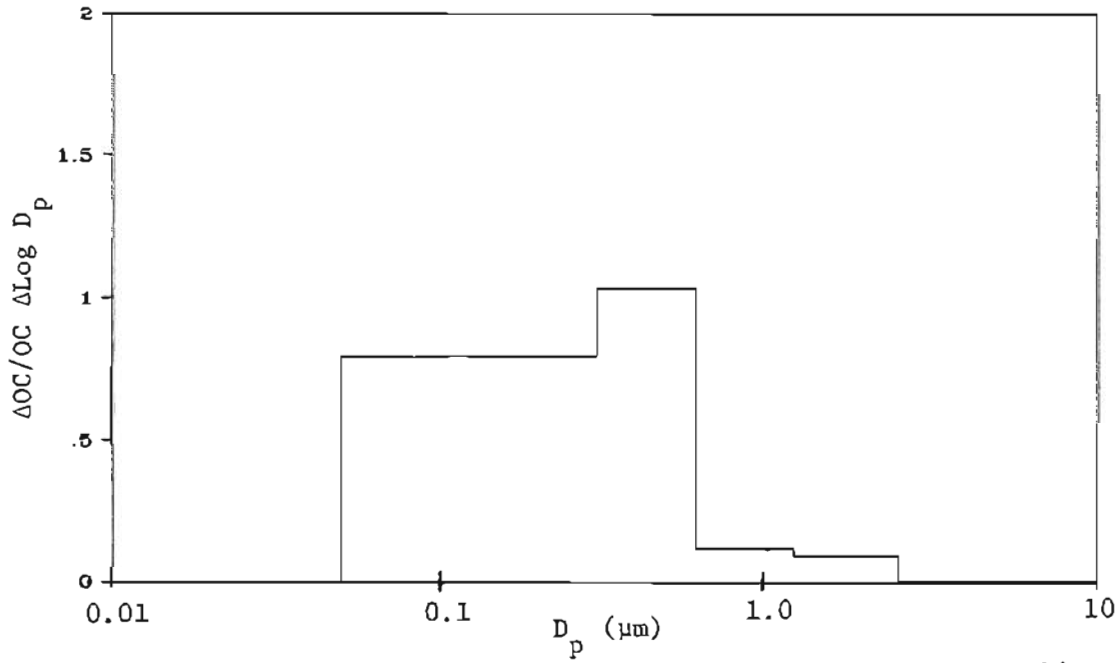

Figure 3.16B. Size distribution of elemental carbon in residential oil furnace emissions.

about 25% carbon and that almost half of the carbon was in the form of elemental carbon. Table 3.15 shows that the aerosol contained very low concentrations of trace elemental species except for sulfur which composed about 12% of the aerosol mass. These oil furnace source composition data are reasonably similar to the distillate oil composition data given in the EPA Source Library (Core, et al., 1984).

3.1.2.4 MOTOR VEHICLE (AUTOMOTIVE TUNNEL) AEROSOL DATA

Motor vehicle aerosols were sampled on three weekdays and one weekend in August from the 270 m long route 26 west highway tunnel located on the west side of downtown Portland. Sampling was done from a port in the roof of the west directed traffic tunnel about 100 m from the tunnel entrance. Tunnel traffic was a mix of automobiles and trucks and traveled about 50 mph up a slight incline. Total suspended particulate loadings were 26.5, 36.6, and 25.2 μg/m3 for weekdays and 38.8 μg/m3 for the weekend. These low aerosol mass concentrations were due to the clean natural drafts which ventilated the tunnel. Table 3.16 and Figure 3.17 show the average mass distribution for tunnel aerosols. The same assumptions (that there is negligible mass <0.05 μm and >10 μm) as have been previously made in log distribution graphs have been made in Figure 3.17. On this graph significant mass might be found beyond both the end points used so that end sections shown will be somewhat different from the actual log distribution. The aerosol was log normally distributed with 27% of the aerosol mass above 2.5 μm and 30% below 0.3 μm. This distribution was similar to that obtained by Pierson, (1980).

Table 3.17 and Figure 3.18 give the carbon size distribution for

Table 3.15

Average Residential Oil Furnace Aerosol Particle

Trace Element Compositon (% of total aerosol mass) (N=2)

Size (μm)	<10	<2.5	<1.2	<0.6	<0.3
Al	0.56	0.59	0.48	0.42	0.43
As	0.01	0.02	0.02	0.02	0.03
Fe	0.09	0.04	0.04	0.03	0.03
K	0.04	0.02	0.00	0.00	0.02
P	0.32	0.38	0.31	0.36	0.27
Pb	0.06	0.03	0.00	0.03	0.00
S	12	14	12	12	12
Se	0.01	0.01	0.00	0.01	0.01
Si	0.79	0.75	0.42	0.62	0.42
Zn	0.05	0.05	0.05	0.05	0.05

N = Number of tests

Table 3.16

Motor Vehicle Aerosol Average Mass Distribution

(% of Total Aerosol Mass) (N=4)

Size (μm.)	
<0.1	12.9±4.5
0.1-0.3	17.6±3.9
0.3-0.6	13.7±3.6
0.6-1.2	14.2±2.6
1.2-2.5	14.8±3.7
>2.5	26.8±3.5

Table 3.17

Motor Vehicle Aerosol Average Carbon Distribution

(% of Total Aerosol Carbon) (N=3)

Size (μm.)	OC	EC	TC
<0.3	47±1	49±9	48±5
0.3-1.2	20±3	24±12	23±7
>1.2	33±2	24±6	29±2

Uncertainties are standard errors of the mean.

N = Number of Tests

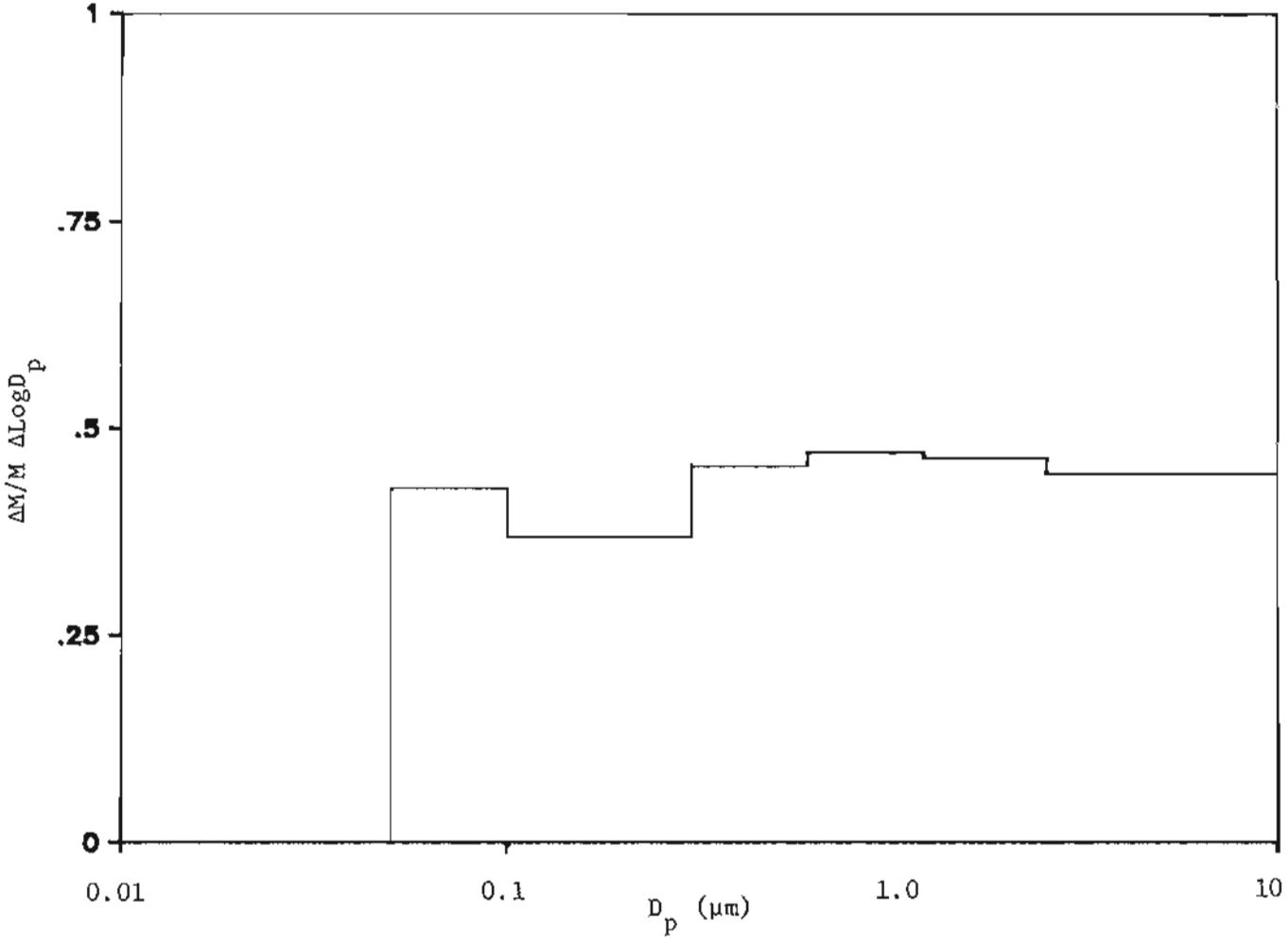

Figure 3.17. Size distribution of aerosol mass in motor vehicle emissions.

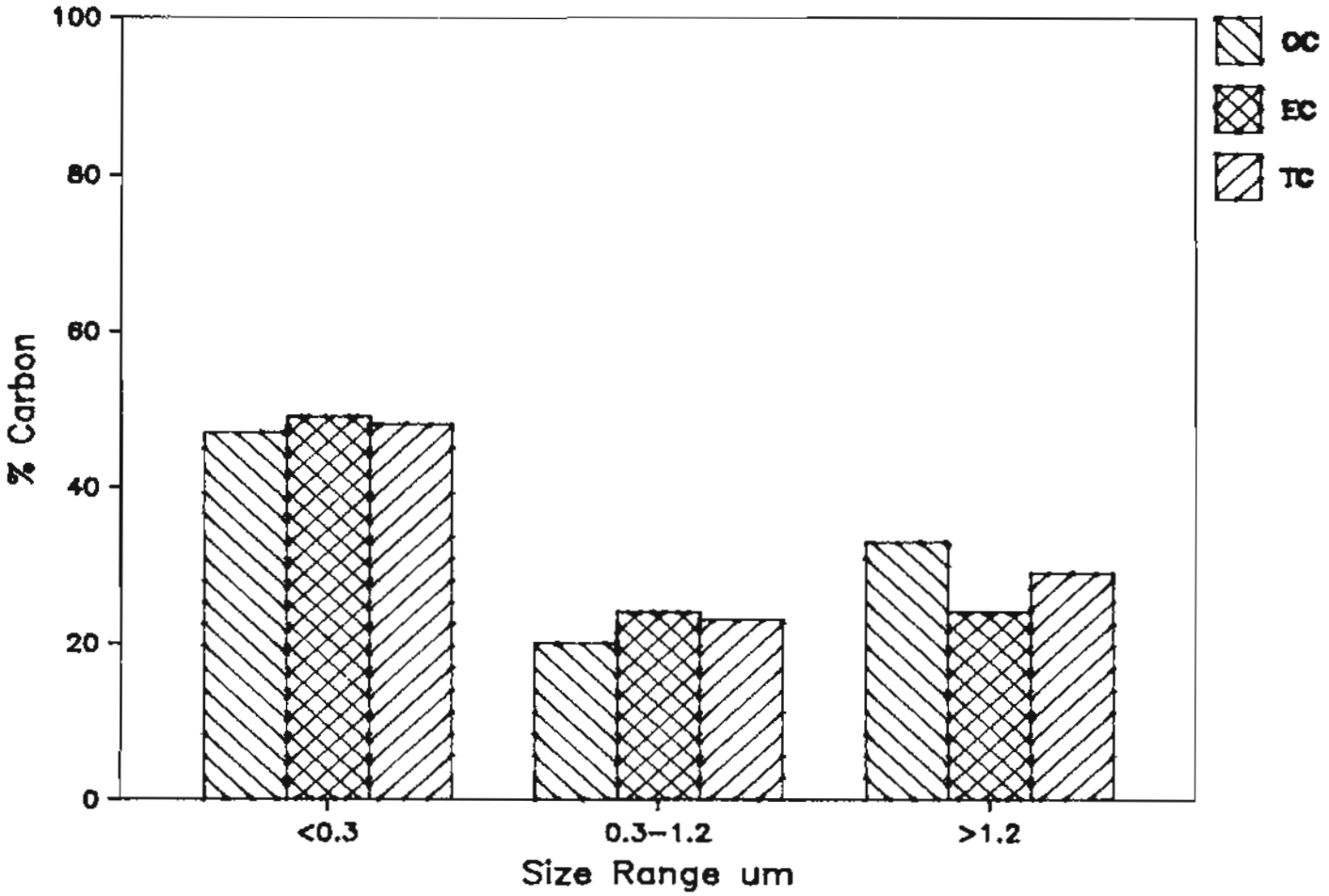

Figure 3.18. Size distribution of carbonaceous aerosols in motor vehicle emissions.

tunnel aerosols. Almost 50% of the aerosol carbon was associated with particles less than 0.3 μm, indicating that carbon was concentrated in finer aerosols. This fine carbon component most likely contained some diesel engine emissions which in fresh aerosols are found mainly below 0.3 μm (Albrechcinski et al., 1984). Results of the present research have shown that 72% of diesel emissions were <0.3 μm and that the remaining emissions were <0.6 μm.

Table 3.18 and Figure 3.19A-B give trace elemental distributions for the tunnel aerosol. The elements Br, Pb, and S which come from automotive emissions were found mainly in the very fine fraction below 0.3 μm. In contrast Ca, Cl, and Fe were mainly associated with coarse aerosols. The Ca can be associated with road wear particles which tend to be coarse. The majority of Cl can be associated with marine aerosols which are coarse, rather than automotive emissions which, as characterized by Pb, are mostly <0.3 μm. The Fe can be associated with vehicle rust particles which are coarse particles.

Tunnel aerosol material was some combination of fresh motor vehicle aerosols, resuspended road dust, and background aerosols. Resuspended road dust is mainly of geological origin, but also contains a vehicle emission component. Vehicle emissions coagulate with soil, roadway and brake wear particles, and rust particles from vehicles to form resuspended road dust. The fraction of resuspended road dust and background aerosol (these sources both contain 0.3% Pb)(Core et al., 1984). contained in the tunnel samples can be estimated by considering the Pb fraction found in the composite of transportation aerosols. By projecting previous years' data (Shah, 1984) to the time when these

Table 3.18

Motor Vehicle Trace Element Distributions

(% of total trace element mass) (N=1)

Size Range (μm)	>2.5	2.5-1.2	1.2-0.6	0.6-0.3	0.3-0.1	<0.1
Br	12	13	12	0	30	33
Ca	64	17	2	4	8	5
Cl	82	9	1	0	0	8
Fe	68	16	0	3	10	3
K	45	27	9	2	0	17
Mn	24	26	14	17	0	19
Pb	12	11	10	0	33	33
S	10	15	22	20	9	24
Zn	37	24	13	5	7	14

N = Number of tests

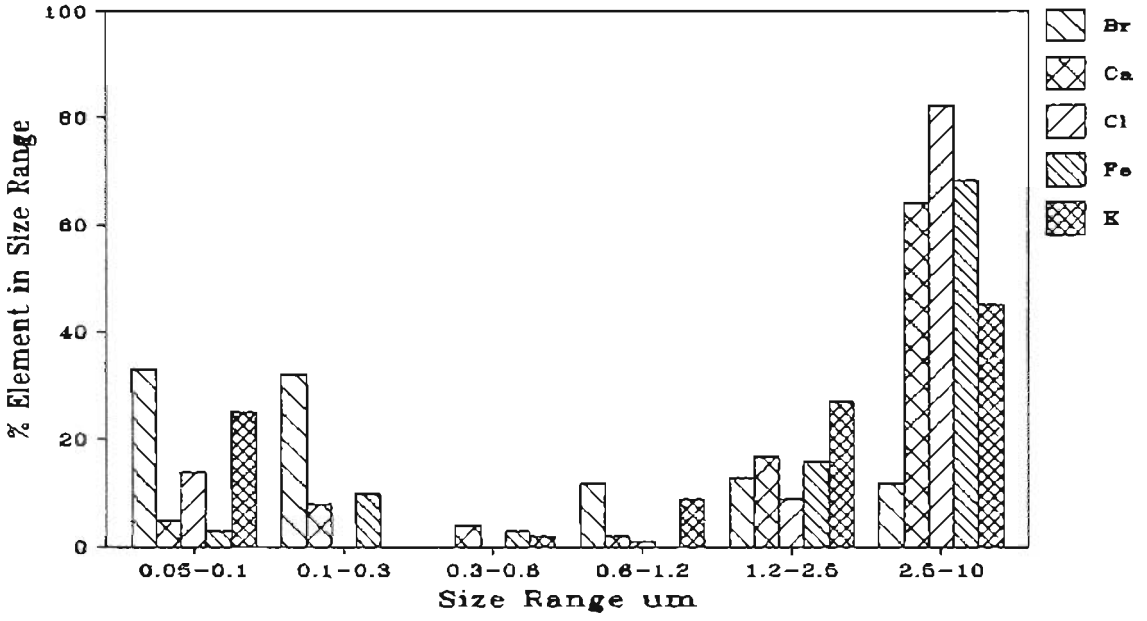

Figure 3.19A. Size distribution of trace elements in motor vehicle emissions.

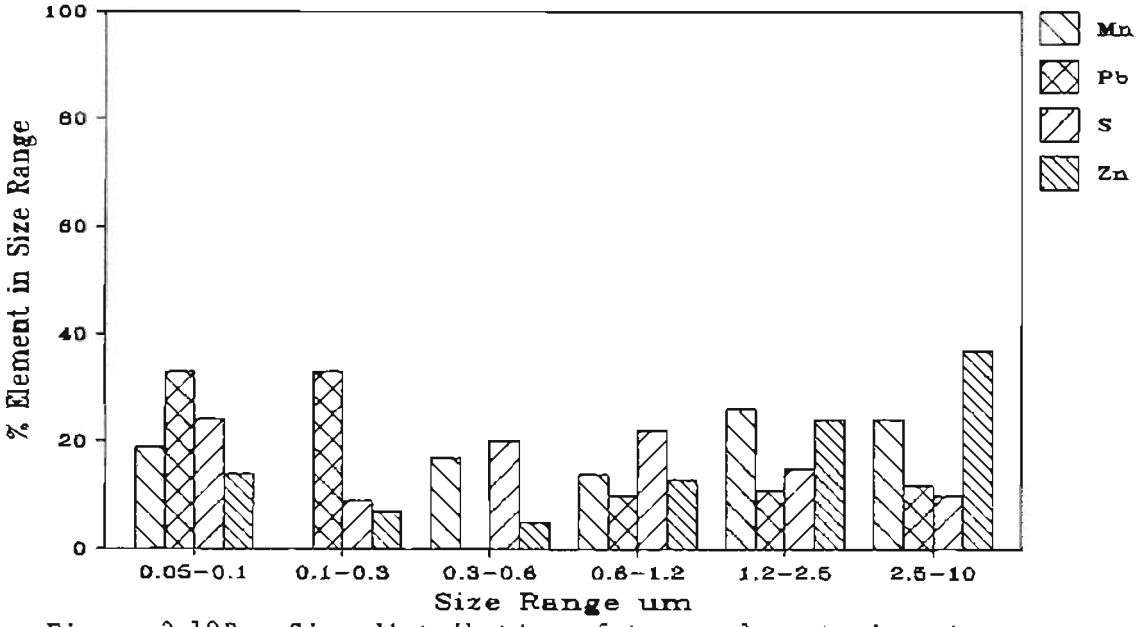

Figure 3.19B. Size distribution of trace elements in motor vehicle emissions.

samples were collected, it was estimated that the Pb concentration in the Portland transportation fine fraction (<2.5 μm) was 5.9%. Since the Pb fraction for the <2.5 μm tunnel samples was 5.5% (Table 3.20) and assuming that automotive aerosols are in fact 5.9% lead the tunnel aerosol <2.5 μm must be diluted with resuspended road dust and background aerosol. Based on Pb concentrations the sum of resuspended road dust and background aerosols cannot exceed 7% in tunnel aerosols.

Average tunnel aerosol carbon composition is given by Table 3.19. The total carbon fraction (TC/M) for fine aerosol (<2.5) was 33% (from 7/18/84 data, appendix 3). This compares well with Watson's, (1979), value of 32.5±24% for leaded auto exhausts; however, the confidence limits of the current data are much tighter. Pierson (1980) determined an average value of TC/M for total aerosol from turnpike tunnels of 68±11%, but he also quotes a value of 43±5% for the Detroit & Canada tunnel. These higher values are probably due to a combination of not correcting for adsorbed organic vapor and possibly a higher fraction of diesel truck traffic. Current fine aerosol carbon percentage values used by the Oregon Department of Environmental Quality for CMB analysis are 39±10% for automobiles with catalysts and 54±13% for general automotive aerosol. Tunnel carbon fraction aerosol values would be lowered by the addition of road dust and raised by the addition of diesel exhaust.

Table 3.19 shows that tunnel aerosol organic and elemental carbon fraction increase as the particle size becomes smaller, except for EC/M values <0.1 μm. This occurs because as tunnel aerosol size becomes smaller the aerosol was more dominated by vehicle emissions and less by non-vehicle emission sources. Vehicle emissions, since they were

Table 3.19

Average Motor Vehicle Aerosol Carbon Composition

(% of total carbon) (N=3)

Size (μm)	EC/TC	OC/M	EC/M	TC/M
<0.1	37	26	15	41
<0.3	50±2	24±1	25±2	49±2
<0.6	56	20	25	45
<1.2	52±4	18±1	20±2	38±2
<2.5	58	14	19	33
Total	50±3	16±1	16±1	32±2

Note: Values with error limits are the averages of three data sets. Values without error limits are from a single data set.

Uncertainties are standard errors of the mean.

N = Number of tests

combustion aerosols, contained proportionately more carbon than the various non-vehicle emission aerosols that contributed to the tunnel aerosol. EC/TC values for tunnel aerosol were independent of aerosol size because they were determined by vehicle emissions and for these emissions EC/TC values were relatively independent of aerosol size.

Table 3.20 shows trace element compositions for tunnel aerosols. Tunnel aerosols were found to have similar trace element compositions to those reported by Ondov et al. (1982). Pierson (1980), measured an average lead fraction value of 5.6±2% for turnpike tunnel aerosols, but measured a value of 11±6 for the Detroit & Canada Tunnel. These values depend mainly on the mix of leaded and non-leaded vehicles in the transportation composite at the time of sampling and on vehicle emissions dilution by background air. Table 3.20 shows that smaller aerosol particles contain proportionately more bromine, lead and sulfur than larger particles. Consequently larger particles in tunnel aerosols must be enriched with other species besides carbon, lead, sulfur, and bromine which are associated with soil and road dust.

3.1.2.5 DIESEL AUTOMOBILE AEROSOL PARTICLE DATA

Three test runs were done on a 1973, 300D Mercedes diesel automobile. One set was sampled on quartz fiber, one on glass and one on Teflon. These tests showed that all the aerosol mass had aerodynamic diameters less than 0.6 μm. The carbon properties for the aerosol were EC/TC = 0.70, OC/M = 0.22, EC/M = 0.50, TC/M = 0.72. Figures 3.20A-C show the OC, EC, and TC distributions for these aerosols. Diesel trace elemental samples were not analyzed.

Table 3.20

Motor Vehicle Aerosol Trace Element Composition (%)

	Total Aerosol	<2.5 μm	<1.2	<0.6	<0.3	<0.1
Al	0.59	0.54±0.1	0.42	0.82±0.01	0.7	----
Br	2.1	2.7±0.3	2.7	3.5±0.3	4.3	6.1±2.0
Ca	1.3	0.49±0.1	0.4	0.52±0.1	0.6	0.66±0
Cl	2.0	0.89±0.4	0.29	0.40±0.1	0.56	----
Fe	2.3	1.0±0.2	0.66	1.0±0.3	1.0	0.57±0.1
K	0.27	0.30±0.1	0.12	0.25±0.1	0.14	----
Mn	0.19	0.15±0.1	0.16	0.14±0.1	0.11	----
Ni	0.01	0.02±0.01	0.02	0.02±0.01	0.03	----
Pb	4.6	5.5±0.6	6.0	7.5±0.6	9.8	15.1±4.8
S	4.2	5.5±0.8	5.3	5.7±0.3	4.3	9.8±2.5
Zn	0.24	0.27±0.1	0.16	0.19±0.1	0.17	0.25±0.1

Data with error limits are the averages of three runs, other data are from a single run. These data are percentages of mass.

Uncertainties are standard errors of the mean.

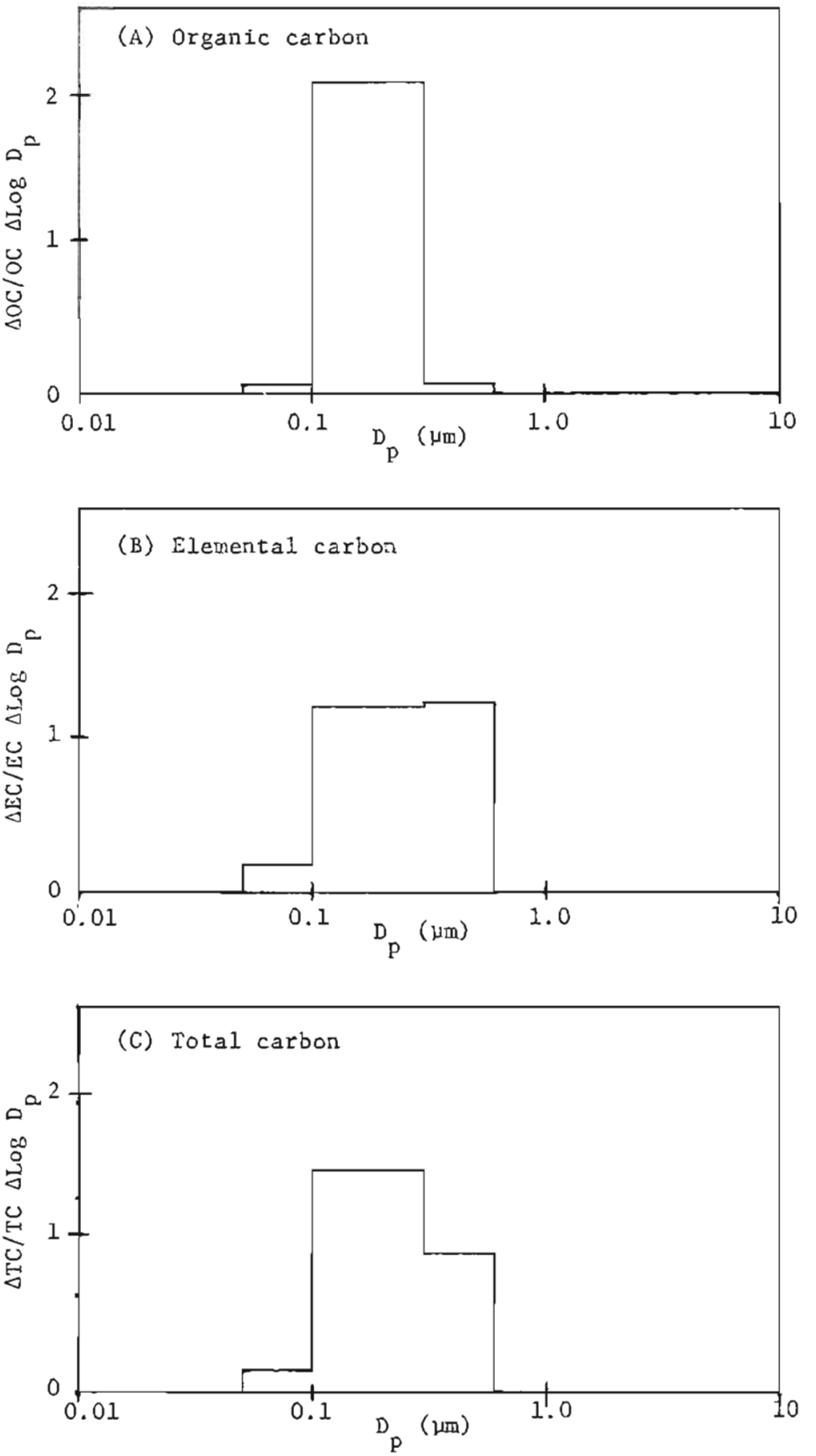

Figure 3.20. Size distribution of carbon in diesel automobile particulate emissions.

CHAPTER FOUR: CARBON IN AMBIENT AEROSOLS

4.1 SIZE DISTRIBUTION OF CARBON IN AMBIENT AEROSOLS

This chapter presents the characteristics of residential area aerosols, with special emphasis on wintertime aerosols which contain a large RWC component. Ambient samples were collected in the same manner as source samples. Samples collected with impactors consisted of aerosol particles that were not captured by the impactors, i.e., particles which had aerodynamic diameters that were less than the impactor cut-points. The impactor sets used were: (#1) no impactor, and a 2.5, 1.2, 0.6, 0.3, and a 0.1 μm impactor; (#2) matched sets (two impactors per set) of 2.5 μm, 0.6, and 0.3 μm impactors; (#3) two 10 μm impactors, and a 2.5, 1.2, 0.6, and a 0.3 μm impactor. When the (#1) impactor set was used, all quartz fiber filters, all Teflon, or alternating quartz fiber filters and Teflon filters were used. For the (#2) impactor set, one member of each set used quartz fiber filters and the other used Teflon filters. For the (#3) impactor set all the impactors used quartz fiber filters except one of the 10 μm impactors which used a Teflon filter. A quartz fiber filter was always run behind at least one Teflon filter to determine vapor carbon adsorption on quartz fiber filters.

4.1.1 CARBON SIZE DISTRIBUTIONS FOR PORTLAND RESIDENTIAL AEROSOL SAMPLES USING IMPACTOR SET #3.

Ambient aerosols were sampled, on February 5, 8, 14, and 20, 1985 in a Southwest Portland residential area using impactor set #3. The

ambient mass loadings for particles passing the 10 μm impactor were 21, 9, 23 and 22 ug/m^3, respectively. These low mass loadings, compared to those typically found in urban areas occurred because Portland's winter rainy weather suppresses resuspension of coarse particles and because the sampling site was located at a higher altitude than the surrounding area which resulted in increased local atmospheric dispersion. These samples were composed mainly of fine aerosol material. Only about 12±10% of the particulate mass that passed the 10 μm impactor was between 2.5 and 10 μm, while 36±7% was less than 0.3 μm. In chapter 5 it will be shown that for these samples the aerosol passing the 10 μm impactor was composed of from 31±54% of RWC emissions.

Figure 4.1A-C and Table 4.1 show the organic, elemental and total carbon distributions of these samples. Usually less than 5% of the organic, elemental and total carbon was associated with particles which had aerodynamic diameters greater than 2.5 μm. About 30% of aerosol carbon was associated with particles less than 0.3 μm and up to 69% with particles in the 0.3-1.2 μm range. Smaller particles contained larger fractions of elemental carbon because they contained increasing proportions of aerosol material from combustion sources.

Figures 4.1A-C show that the carbon distributions were quite similar on a day to day basis. These distributions appear to be dominated by local emissions, i.e., background air was quite clean. The most significant features of these data were that the carbon distributions were monomodal and that the mode of the distribution was always between 0.3 and 0.6 μm. This distribution differed from what would be expected for aerosols dominated by RWC emissions under the

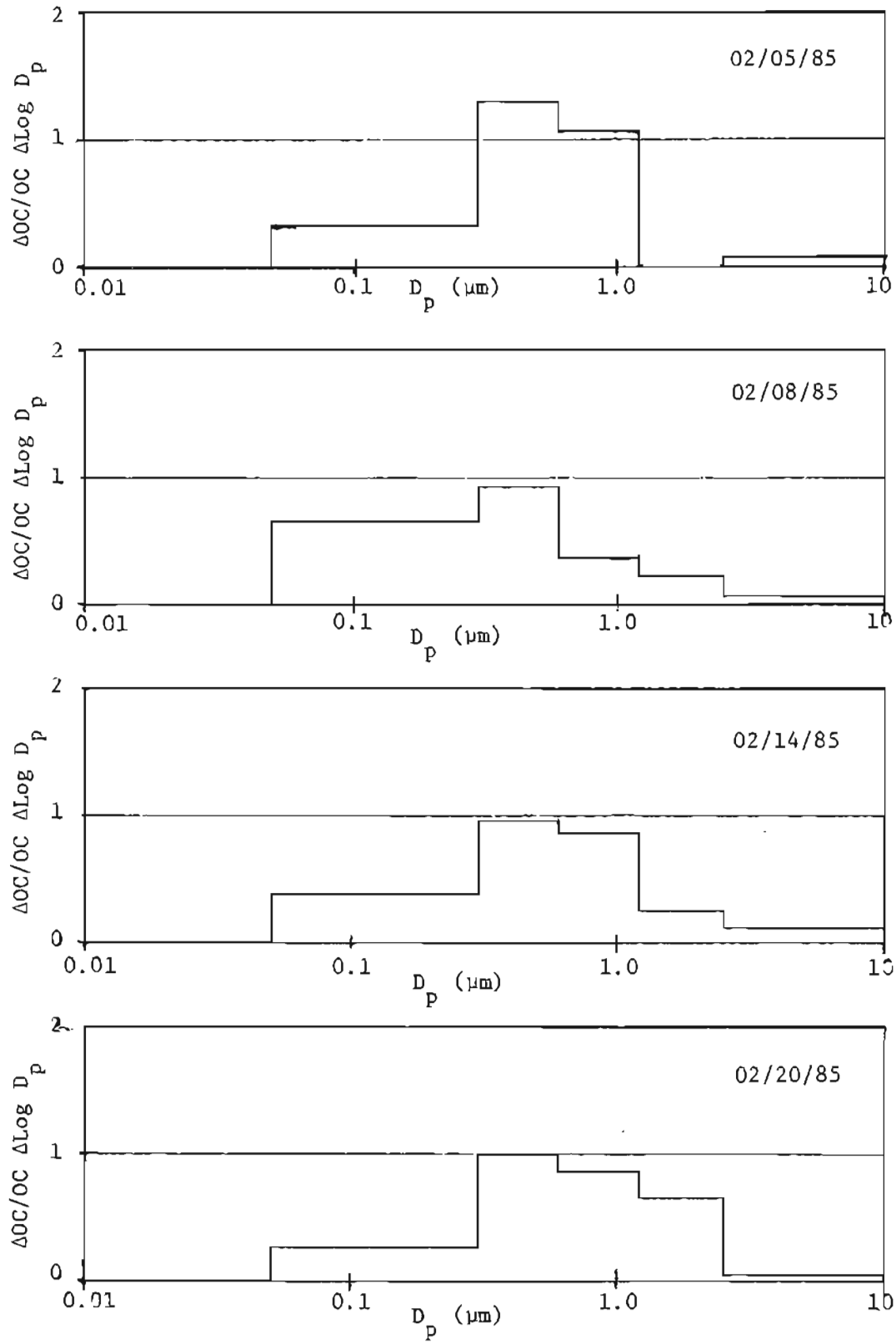

Figure 4.1A. Size distribution of particulate organic carbon in SW Portland residential area ambient aerosols.

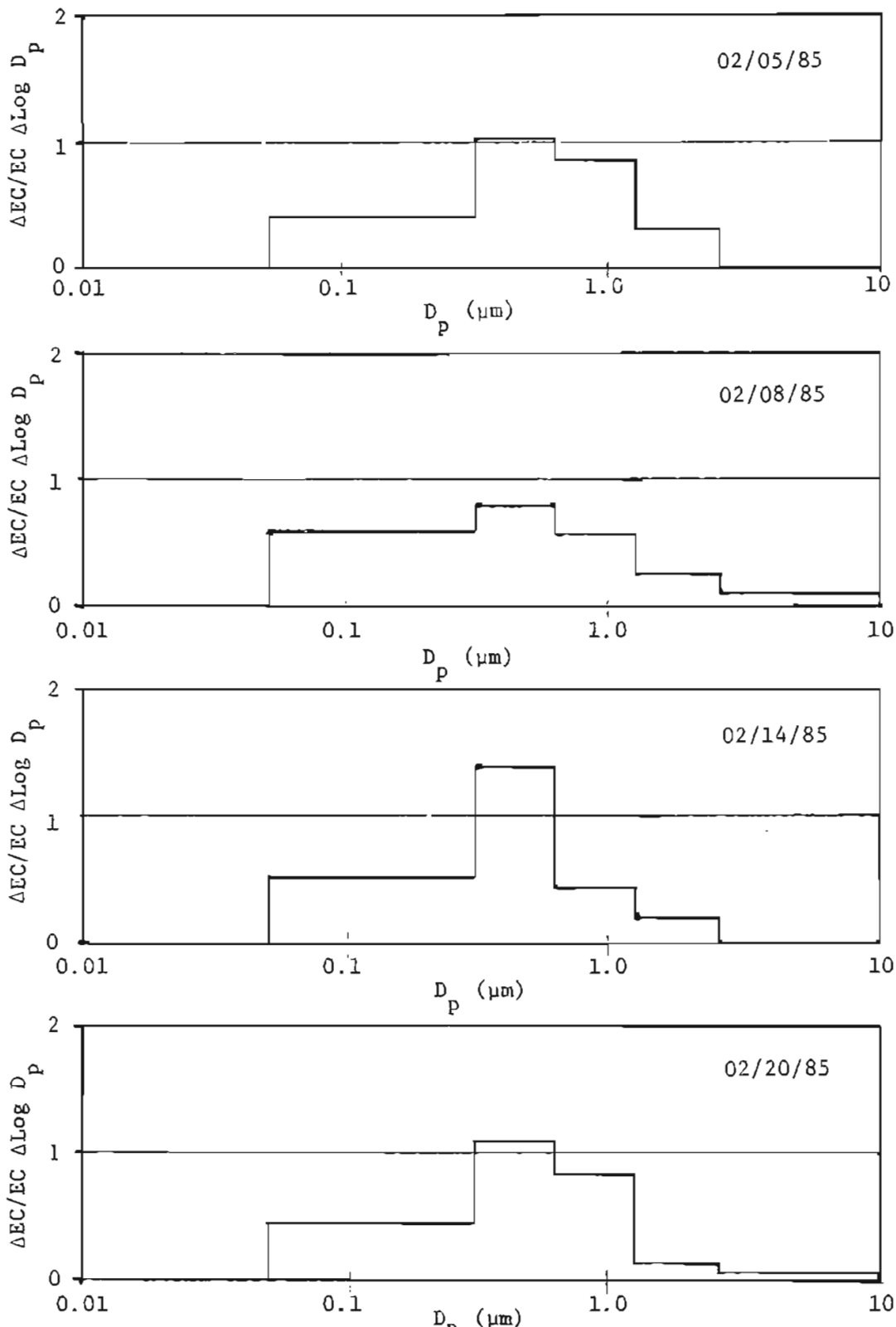

Figure 4.1B. Size distribution of particulate elemental carbon in SW Portland residential area ambient aerosols (Feb. 1985).

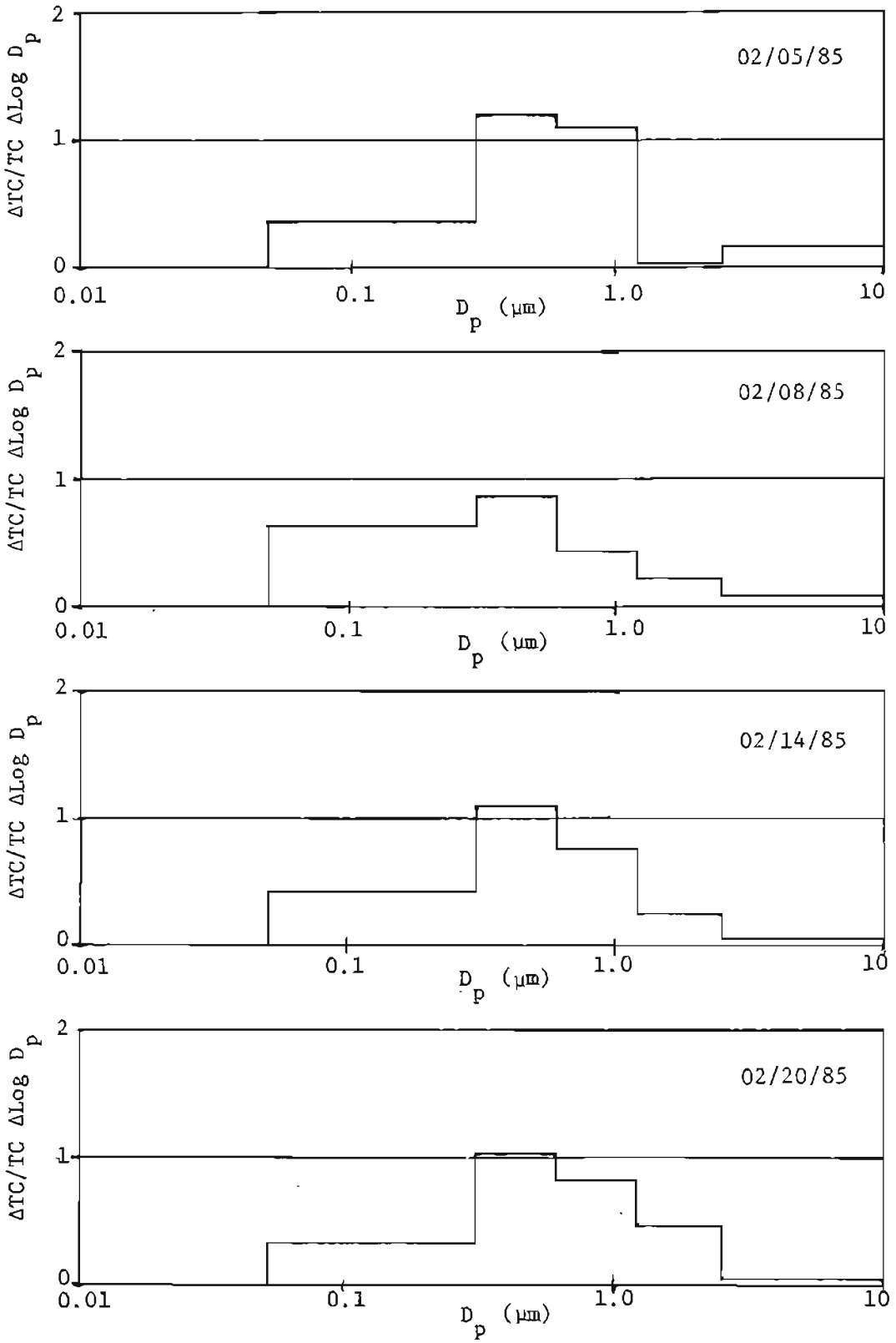

Figure 4.1C. Size distribution of particulate total carbon in SW Portland residential area ambient aerosols (February 1985).

Table 4.1

Wintertime Ambient Aerosol Carbon Size Distributions in SW Portland (% of Carbon Passed by 10 μm. Impactor)

Date:	2/5/85	2/8/85	2/14/85	2/20/85
Size Range (μm)	Organic Carbon			
<0.3	25	51	30	21
0.3-0.6	39	28	30	30
0.6-1.2	33	11	27	26
1.2-2.5	2	7	10	21
2.5-10	1	4	3	3
	Elemental Carbon			
<0.3	32	46	38	35
0.3-0.6	31	24	42	33
0.6-1.2	35	17	13	25
1.2-2.5	1	8	4	4
2.5-10.0	1	6	3	3
	Total carbon			
<0.3	28	49	33	26
0.3-0.6	36	26	33	31
0.6-1.2	33	13	23	25
1.2-2.5	1	7	8	15
2.5-10.0	1	5	3	3

assumption that these emissions came from stoves and that they maintained their emitted distribution during their atmospheric residence time. The composite RWC stove emission carbon distribution from both hot and cool burning (assuming that in the sampling area stove burning was 25% hot burning and 75% cool burning) was expected to be bimodal with one mode between 0.6 and 1.2 μm and the other below 0.3 μm (see Table 5.5). This distribution occurs because for the given stove usage pattern over 90% RWC stove emissions came from cool burning which generates a bimodal emission distribution. The ambient carbon distributions measured could have resulted from either or both of the following causes: (1) size shifting of wood stove aerosol carbon particles during their atmospheric residence time or (2) a significant contribution to the ambient aerosol from fireplace burning which does have a mode in the 0.3 to 0.6 μm size range.

Mechanisms will now be considered which could transport wood stove particulate material from above and below the 0.3 to 0.6 μm size range into this range during the particulate atmospheric residence time. Particulate mass can be moved from below 0.3 μm into the 0.3 to 0.6 μm size range by coagulation and from above 0.6 μm by evaporation of organic carbon.

Particles which have diameters >0.6 μm can be transformed to particles with diameters <0.6 μm by losing mass due to the evaporation of volatile organic species. Evaporation can occur because the vapor pressures of these species are lower in the ambient atmosphere than in the diluted flue gas where the source measurements were made. The fact that RWC particles collected on a filter, especially those from cool

burning, have an odor indicates that these particles continuously lose vapor carbon. In Chapter 5 it will be demonstrated that the CMB model fit can be improved if wood smoke aerosol was assumed to lose from 25 to 50% of its organic carbon. For particles between 0.6 and 0.76 μm a 50% loss in volume will reduce their diameter to below 0.6 μm causing about 10-15% of the organic carbon above 0.6 μm to shift to below 0.6 μm. Vapor carbon loss by particles larger than 0.6 μm explains only a small amount of the ambient carbon found in the 0.3-0.6 μm size range.

Aerosol mass can also be shifted from the range below 0.3 μm into the range above 0.3 μm by heterogeneous coagulation, i.e., aerosol particles, especially those that are much less than 0.3 μm, will coagulate with particles that are >0.3 μm. When two very small particles coagulate, the resulting particle is still a very small particle, but when very small particles coagulate with larger particles mass is transferred from the size range of the smaller particle to the size range of the larger particle. Since the coagulation rate decreases for larger particles, the coagulation mechanism does not transfer significant mass out of the 0.3 to 0.6 μm size range to larger particle sizes. The mechanisms operating here are the same as those that drive the mode of most urban fine aerosol particle distributions to the vicinity of 0.3 μm.

So far the role of fireplace emissions has not been considered in the carbon distribution of ambient aerosol particles which have a significant RWC contribution. Table 3.8 shows that the mode of fireplace mass emissions was between 0.3 and 0.6 μm and that 35% of the aerosol mass was in this size range. The aerosol particulate carbon distribution

has the same form as mass distribution when aerosol particulate carbon mass fraction is essentially not a function of particle size. Therefore the carbon distribution of fireplace RWC aerosol will be very similar to its mass distribution, i.e., it will have a mode in the 0.3 to 0.6 μm size range. Figure 3.15 shows that for two fireplace tests where all samples were collected on quartz filters that organic and total carbon have a significant mode in the 0.3 to 0.6 μm size range. Portland survey data indicated that 1/3 of wood burned in residences was burned in fireplaces (Cummings, 1982). In addition fireplaces emit about 1.2 times as much aerosol per mass of wood burned as cool burning stoves. If 1/3 of wood was burned in fireplaces and stove burning was composed of 75% cool burning and 25% hot burning then 49% of the total residential wood burning aerosol would be generated by cool burning stoves, 48% by fireplaces and 3% by hot burning stoves. For this stove and fireplace usage the composite emitted total carbon distribution would be 28% in the range 0.6 to 2.5 μm, 21% in the range of 0.3 to 0.6 μm and 50% in the range less than 0.3 μm. Figure 4.2A shows this distribution while Figure 4.2B shows the total carbon distribution that would result from stove burning alone (75% of stoves operated with dampers closed and 25% operated with dampers open). Thus the fireplace contribution to the ambient RWC aerosol can result in a significant contribution of wood burning aerosol into the 0.3-0.6 μm size range. In summary is appears that the ambient RWC aerosol in the 0.3-0.6 μm size range can be explained by a combination of mass transfer by evaporative loss for particles >0.6 μm, mass transfer from below 0.3 μm by heterogeneous coagulation and by a fireplace emission contribution.

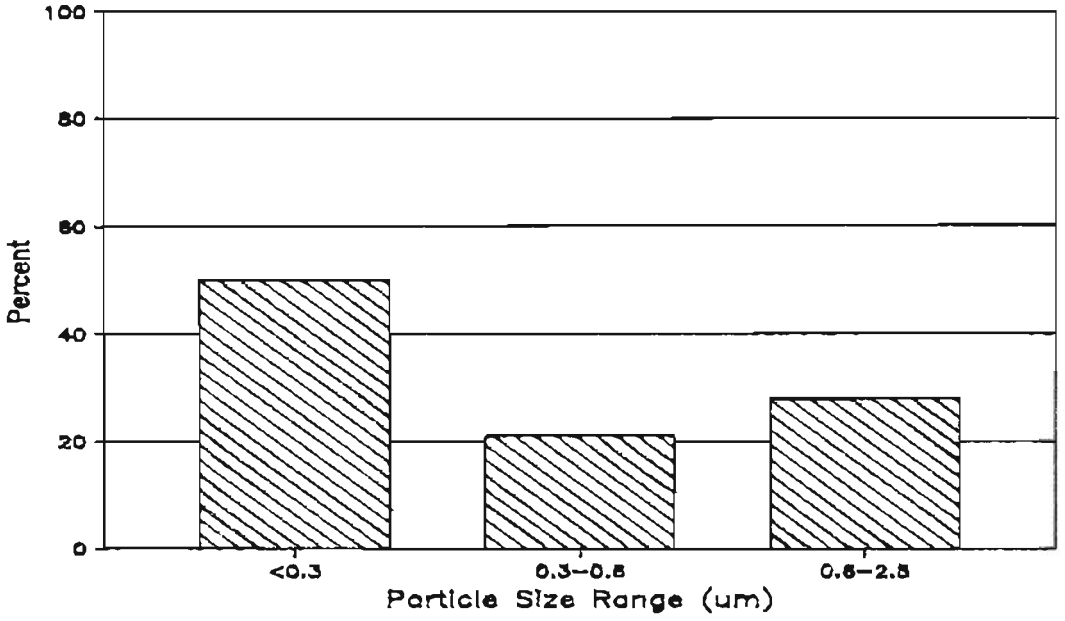

Figure 4.2A. Size distribution of composite total carbon in stove and fireplace RWC particulate emissions.

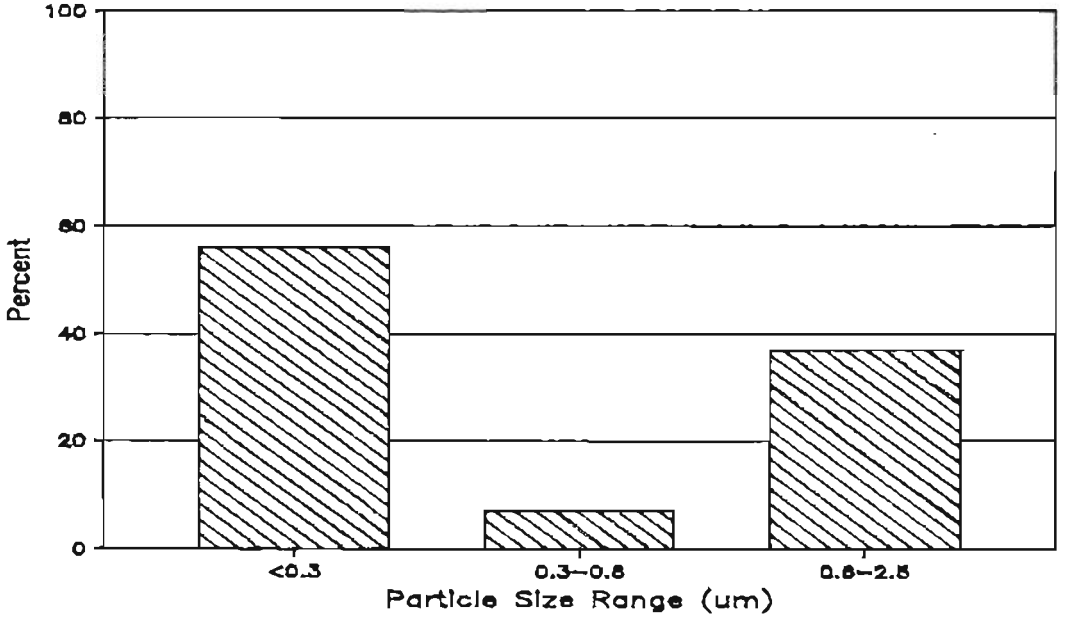

Figure 4.2B. Size distribution of composite total carbon in stove only RWC particulate emissions.

When the RWC composite aerosol particle composition profile, which was developed for hot and cool burning stove RWC, was modified such that 1/3 of wood being burned was assumed to be burned in fireplaces, the resulting composite wood smoke composition profile showed almost no change compared to the original wood stove aerosol particle composition profile. This occurred because the composition of fireplace emissions was very similar to cool burning stove emissions, but its composition was slightly shifted toward the hot burn composition profile. Therefore when CMB analysis was done using the RWC composite or hot and cool burning source composition profiles developed for stoves the resultant RWC contributions to ambient aerosol particle loading can include a significant fraction of fireplace emissions, i.e., the CMB model cannot resolve cool burning stove emissions from fireplace emissions.

4.1.2 SIZE DISTRIBUTION OF CARBON IN PORTLAND RESIDENTIAL AEROSOL SAMPLES COLLECTED USING THE #2 IMPACTOR SET

Figures 4.3A-D show total carbon distributions for Portland residential aerosol samples collected on three days in December 1984, including Christmas Eve, and one day in January 1985. In a later section it will be shown by CMB analysis that the December samples, especially the 12/24/84 sample, had a large residential wood burning component. These samples were collected with set #2 impactors (matched 2.5, 0.6 and 0.3 μm). This impactor set examines only the fine aerosol particles and gives special emphasis to the size range between 0.3 and 0.6 μm. These total carbon distributions showed a very strong mode in the 0.3 to 0.6 μm size range. They were similar, though not quite as detailed, to the

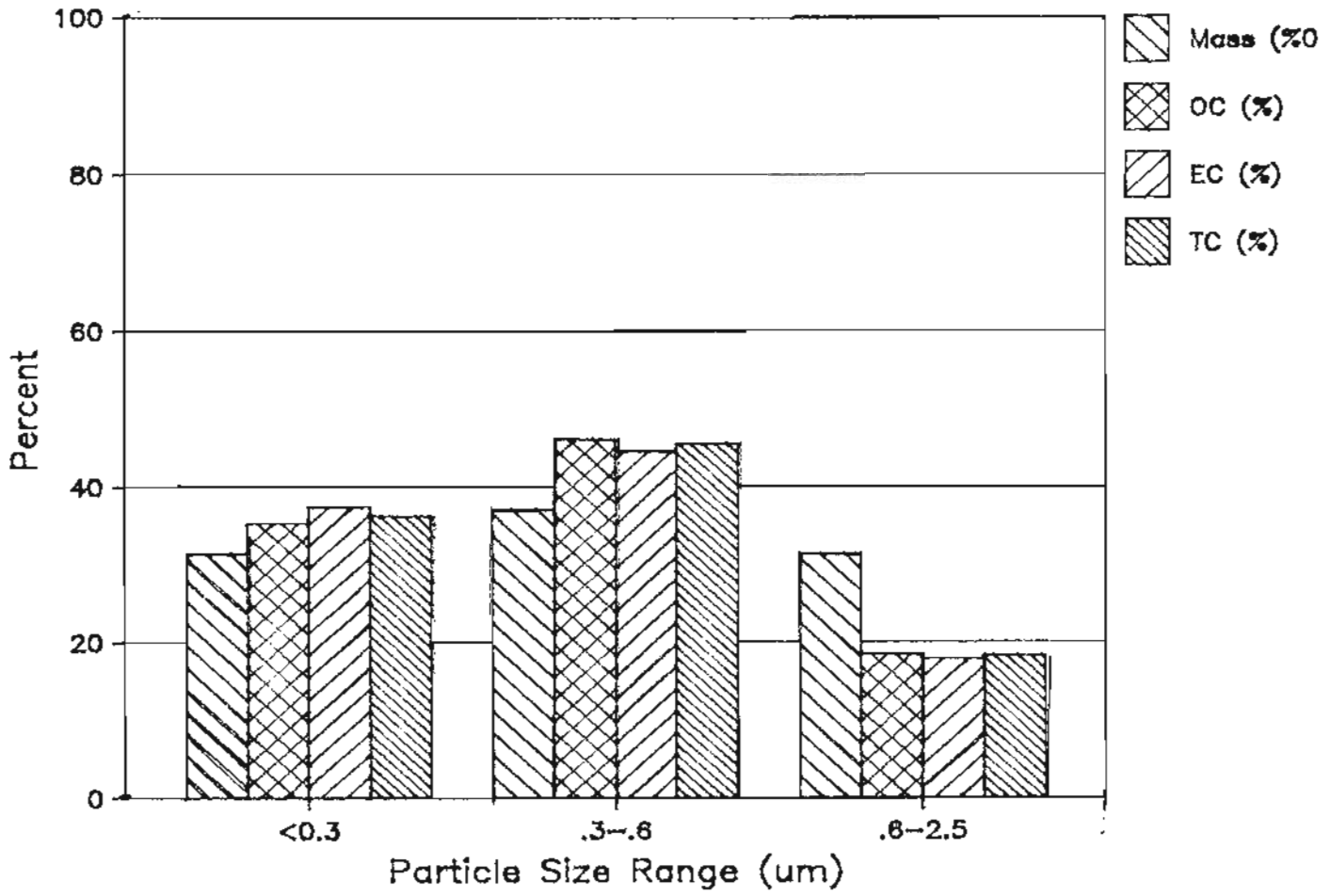

Figure 4.3A Size Distributions of SW Portland
Residential Ambient Aerosol Mass,
OC, EC, and TC (12/8/84)

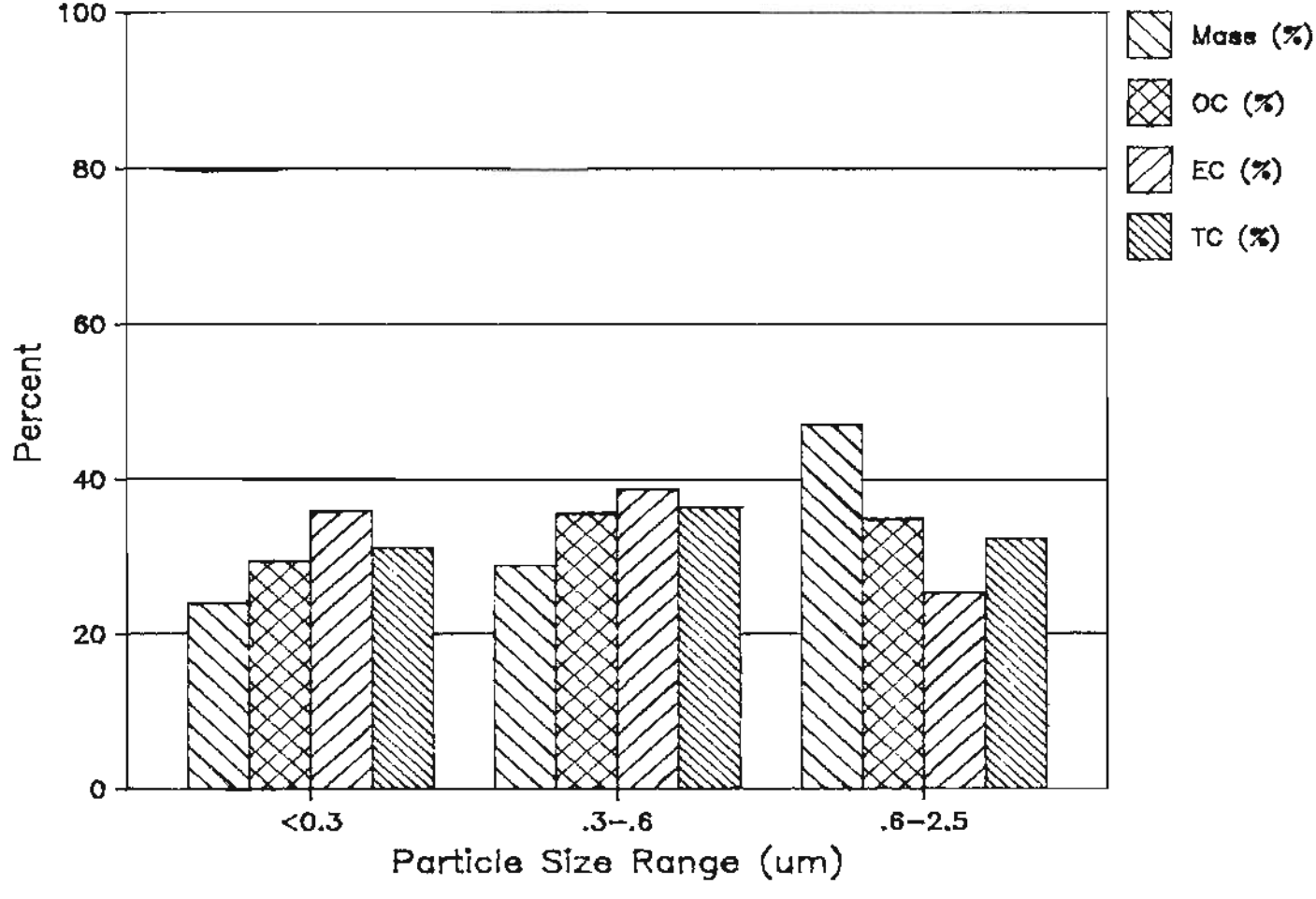

Figure 4.3B Size Distributions of SW Portland Residential Ambient Aerosol Mass, OC, EC, and TC (12/21/84)

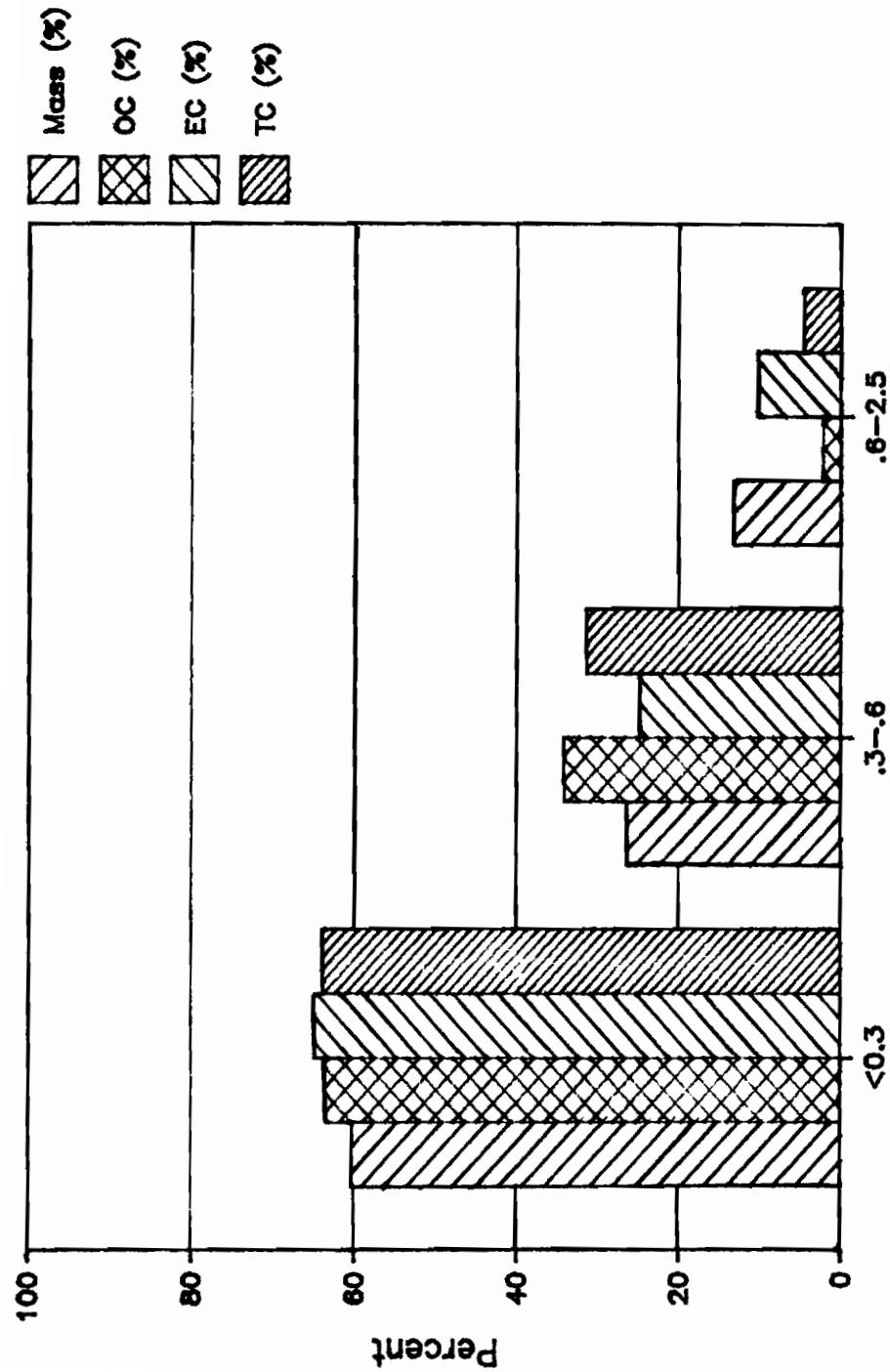

Figure 4.3C Size Distributions of SW Portland Residential Ambient Aerosol Mass, OE, EC, and TC (12/24/84)

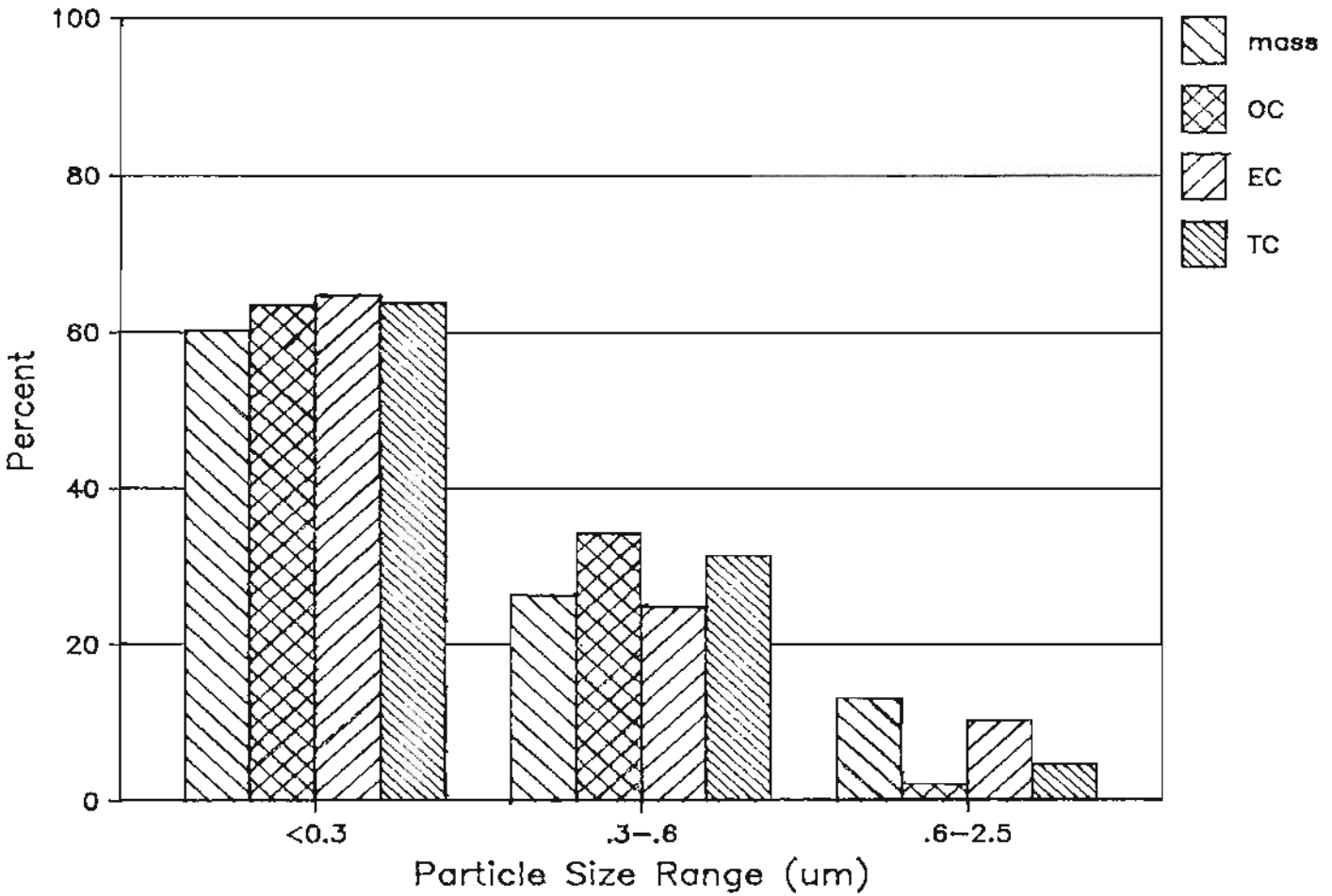

Figure 4.3D. Size distributions of SW Portland residential area ambient aerosol mass, OC, EC, and TC (01/25/85).

carbon distributions shown in Figure 4.1A-C. These carbon distributions, when compared to carbon distributions for cool burning RWC emissions, also show that there is more carbon mass than expected in the 0.3 to 0.6 μm. size range.

Figures 4.3A-B are quite similar showing that carbon was approximately evenly distributed in the three size ranges considered. In contrast Figures 4.3C-D show by far the highest amounts of both mass and carbon in the <0.3 μm size range and very little carbon or mass in the 0.6 to 2.5 μm size range. Carbon size distribution information developed in this research would suggest that the fireplace RWC contribution was relatively larger for the data illustrate by Figures 4.3C-D than it was for Figures 4.3A-C. For all of these data sets there was relatively more mass than carbon in the 0.6 to 2.5 μm size range because larger particles had a larger soil component which contains very little carbon. Elemental carbon was more concentrated in <0.3 and 0.3-0.6 μm size ranges because it was generated in flames as very small particles. Figure 4.3D shows similar mass and elemental carbon distributions as the other figures, but has much larger mass and carbon fractions <0.3 μm. The carbon and mass distribution of this sample indicated that it consisted of mostly fresh RWC aerosol particles, i.e., RWC particles that had not yet coagulated to form larger particles or RWC particles that came primarily from hot combustion.

Because the size distribution of RWC aerosol particles changes during their atmospheric residence time, emission size distribution information was not useful to determine source contributions using receptor modeling techniques.

4.1.3 CARBON SIZE DISTRIBUTIONS FOR PORTLAND RESIDENTIAL AEROSOLS COLLECTED USING THE #1 IMPACTOR SET

Figures 4.4-4.8 show Portland residential ambient aerosol organic, elemental, and total carbon distributions for 9/18/84, 7/26/84, 4/28/84, 3/9/84, and 3/2/84, respectively. These samples were obtained with the #1 impactor set. These distributions, except for Figure 4.5, were similar to the previously discussed winter carbon and mass distributions and were shown by CMB analysis (Chapter 5) to have a significant wood smoke component. Similarly to the previously shown distributions for this site, they show that the mode of the distributions was between 0.3 and 1.2 μm indicating at least that there was a carbon mass shift from below 0.3 μm to above 0.3 μm.

Figure 4.5 shows total carbon and mass distribution for a SW Portland residential area sample collected on 7/28/84 with the #1 impactor set. The total aerosol mass loading for this sample was 36 ug/m^3 and 49% of this mass was greater than 2.5 μm. Only 19% of the mass was in the size range less than 0.3 μm. In contrast to the above winter samples the July sample had a very different total carbon distribution. For the July sample 60% of organic and total carbon was distributed in the size range greater than 1.2 μm, while for wintertime samples 80% of the organic and total carbon was distributed in the size range less than 1.2 μm. For both summer and winter aerosol particles elemental carbon tended to be more associated with small sized aerosol particles.

For the summer sample organic carbon size distribution information provides evidence that the majority of the particulate organic carbon does not come from combustion sources or at least not from the type of

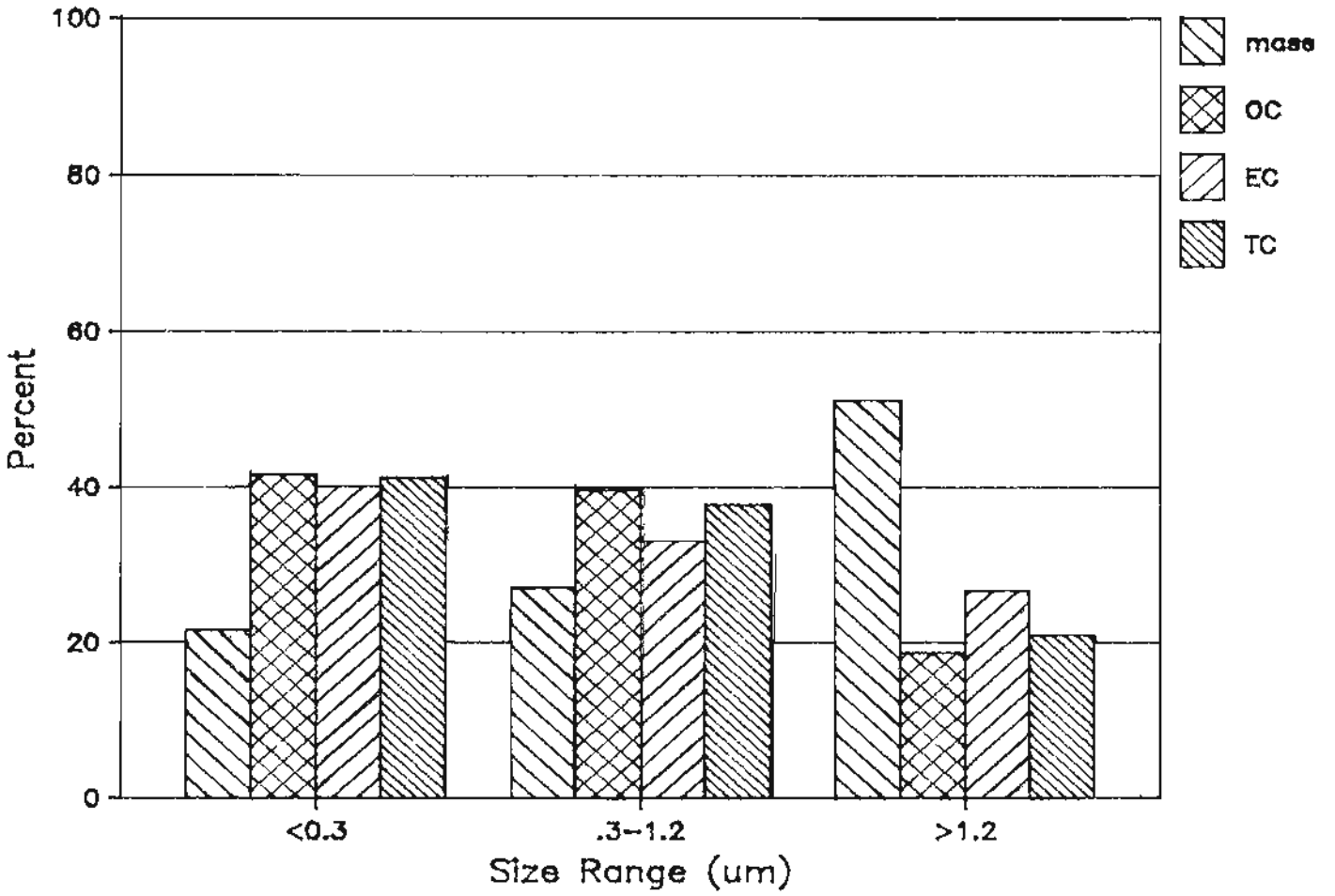

Figure 4.4 Size Distribution of Portland Residential Area Ambient Aerosol Mass, OC, EC, and TC (9/18/84)

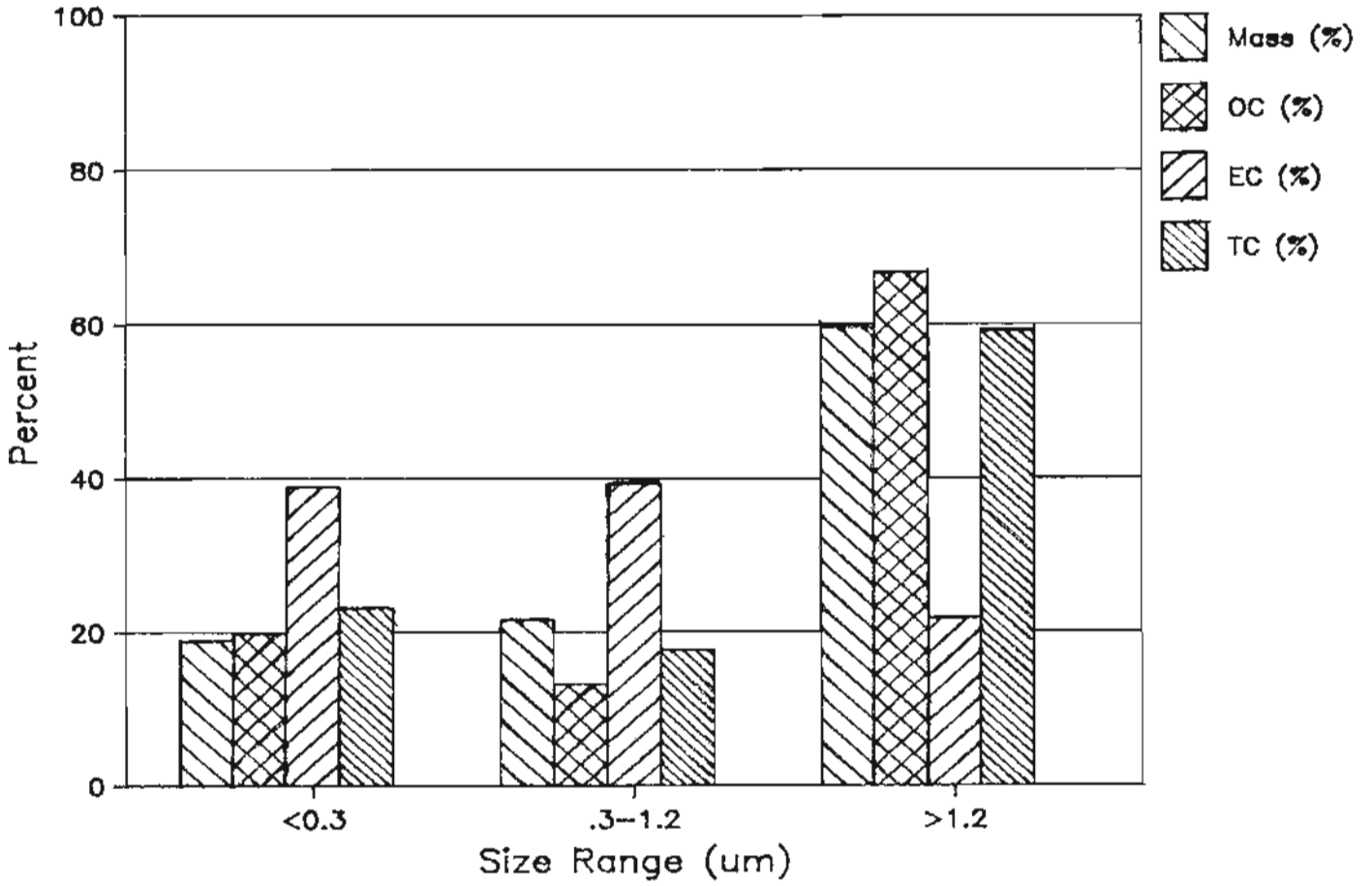

Figure 4.5 Size Distribution of Portland Residential Area Ambient Aerosol Mass, OC, EC and TC (7/26/84)

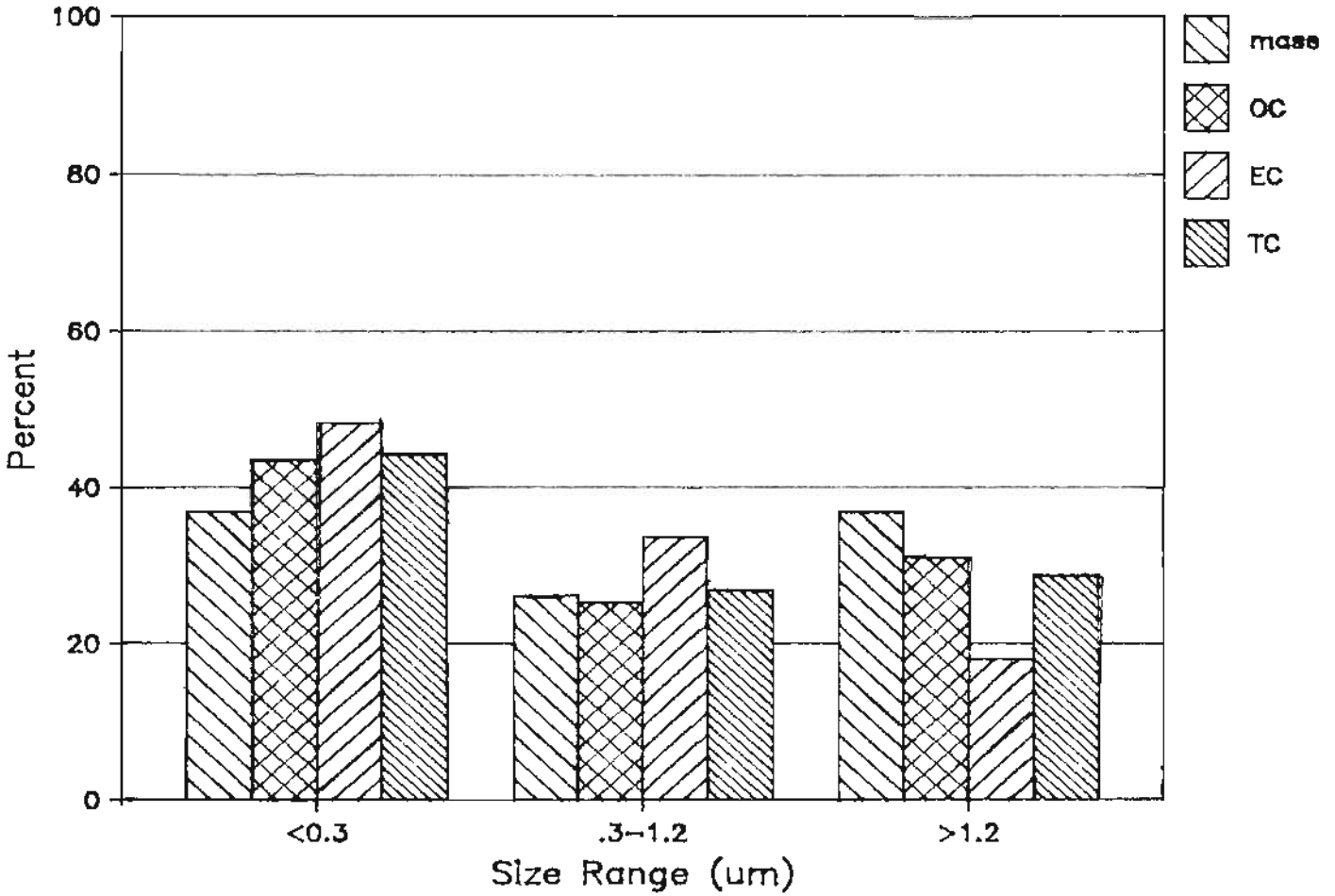

Figure 4.6 Size Distribution of Portland Residential Area Ambient Aerosol Mass, OC, EC, and TC. (4/28/84)

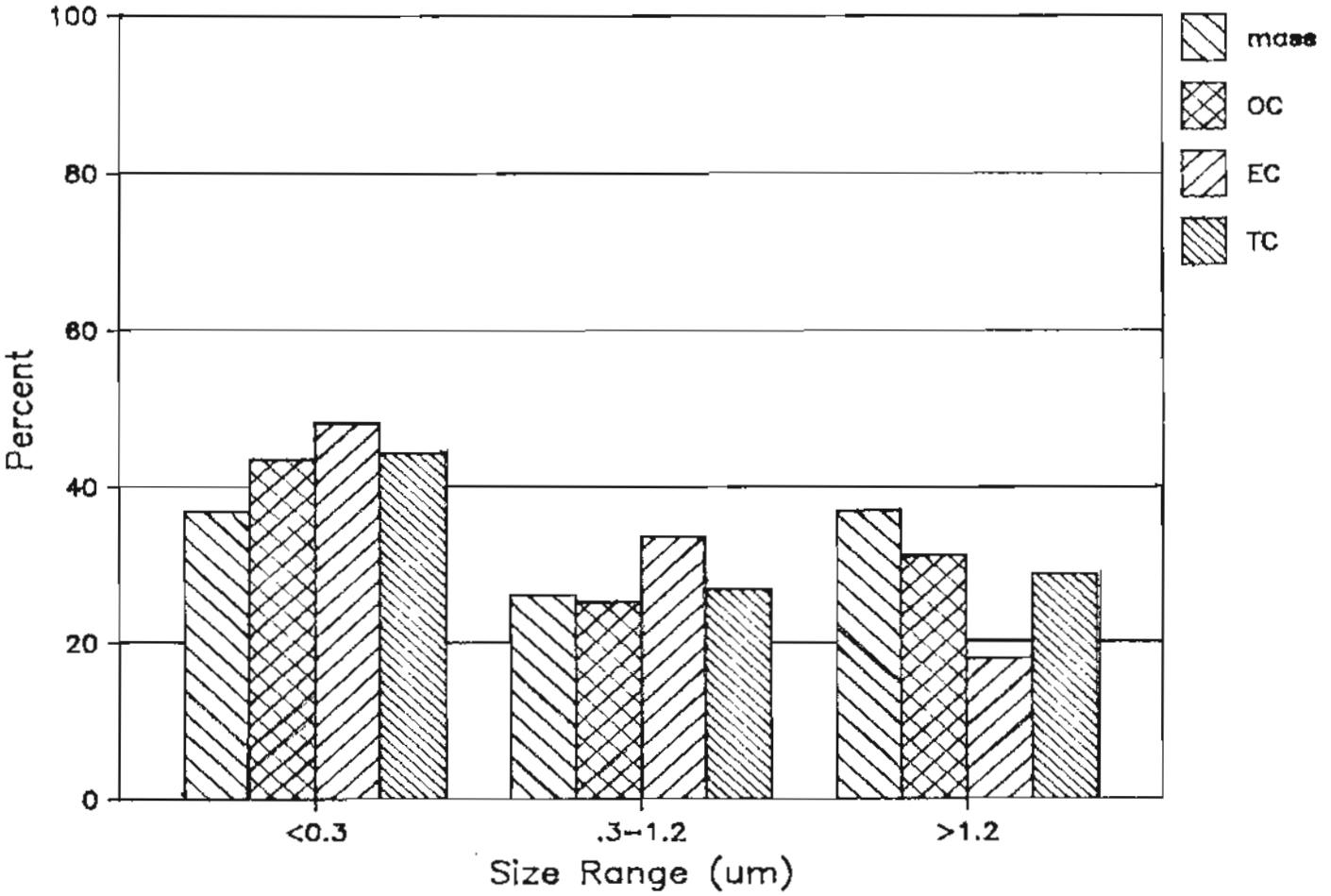

Figure 4.7 Size Distribution of Portland Residential Area Ambient Aerosol Mass, OC, EC, and TC (3/9/84)

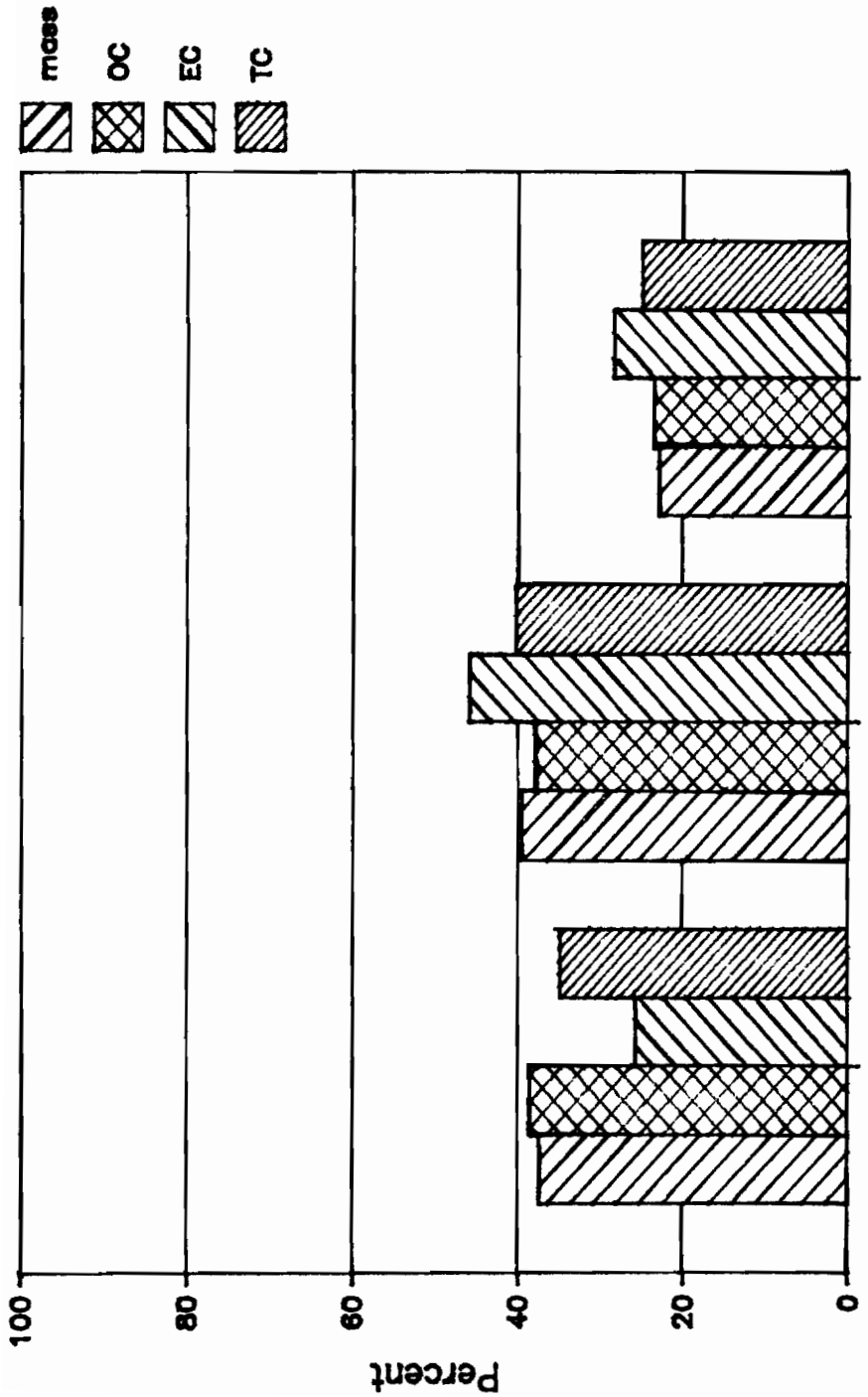

Figure 4.8 Size Distribution of Portland Residential Area Ambient Aerosol Mass, OC, EC, and TC. (3/2/84)

combustion sources typically contributing to wintertime aerosol particle loading. For this sample the coarse mode organic carbon material was probably from plant produced aerosol particles or pollens. CMB analysis, using the composition of raw wood as a surrogate for pollen composition, indicated the presence of a significant amount of coarse raw wood type aerosol particles (see Chapter 5).

Table 4.2 shows the organic, elemental and total carbon distributions for the summertime aerosol sample. A comparison of these data with Table 4.1 data shows that the organic carbon and consequently the total carbon distributions of winter and summer aerosols are very different but the elemental carbon distributions are similar. The similarity of elemental carbon distributions indicates that in both cases the elemental carbon comes from combustion sources.

4.1.4 CARBON DISTRIBUTIONS FOR HILLSBORO RESIDENTIAL AEROSOL PARTICLES COLLECTED WITH IMPACTOR SET #1

Figures 4.9-4.13 show mass and carbon distributions for aerosol particle samples collected in a residential area in Hillsboro, OR. This area was noted for very large contributions of RWC to ambient aerosol particle concentrations. The sample shown in Figure 4.9 consisted of samples collected on quartz fiber filters with no impactor and behind 1.2, and 0.3 μm impactors. The other samples were collected using a sampling set consisting of no impactor and 2.5, 1.2, 0.6, 0.3 and 0.1 μm impactors. The rest of the impactors in the set were used to collect samples on Teflon filters. Figures 4.10-4.13 show mass, and organic, elemental and total carbon distributions for samples collected with the

Table 4.2

Summertime SW Portland Residential Area Aerosol Carbon Size Distribution (% of total aerosol carbon) (7/26/84)

Size Range (μm)	OC	EC	TC
<0.3	20	39	23
0.3-1.2	13	39	18
>1.2	67	22	59

Table 4.3

Average Wintertime Hillsboro Residential Area Aerosol Carbon Size Distribution (% of total aerosol carbon)

Size Range (μm)	OC	EC	TC
	N=7	N=7	N=12
<0.3	36±6	50±5	47±6
0.3-1.2	45±4	35±6	38±5
>1.2	20±4	14±3	15±4

Uncertainties are standard errors of the mean.

N = Number of tests

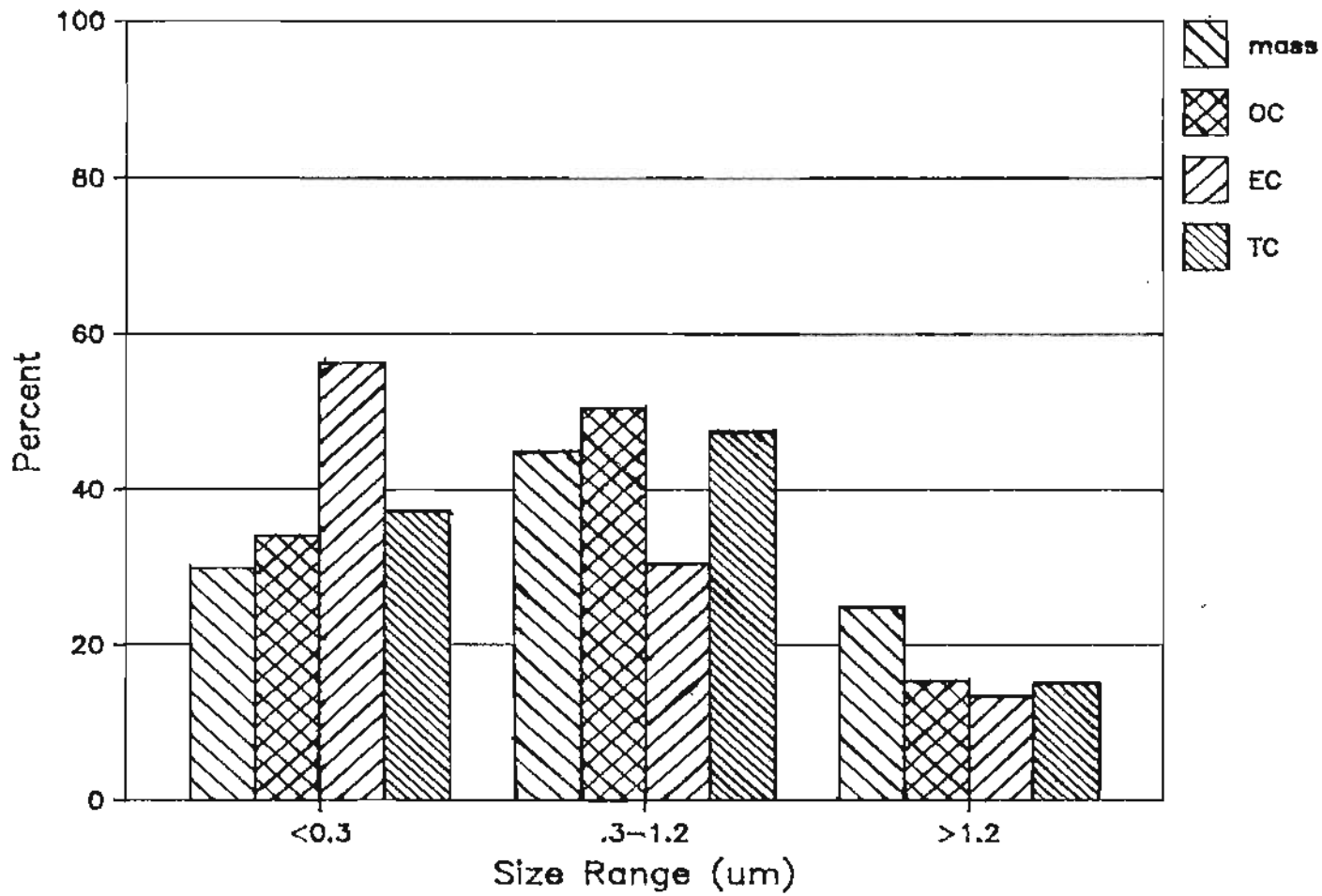

Figure 4.9 Size Distribution of Hillsboro Residential Area Ambient Aerosol Mass, OC, EC, and TC (7/26/84)

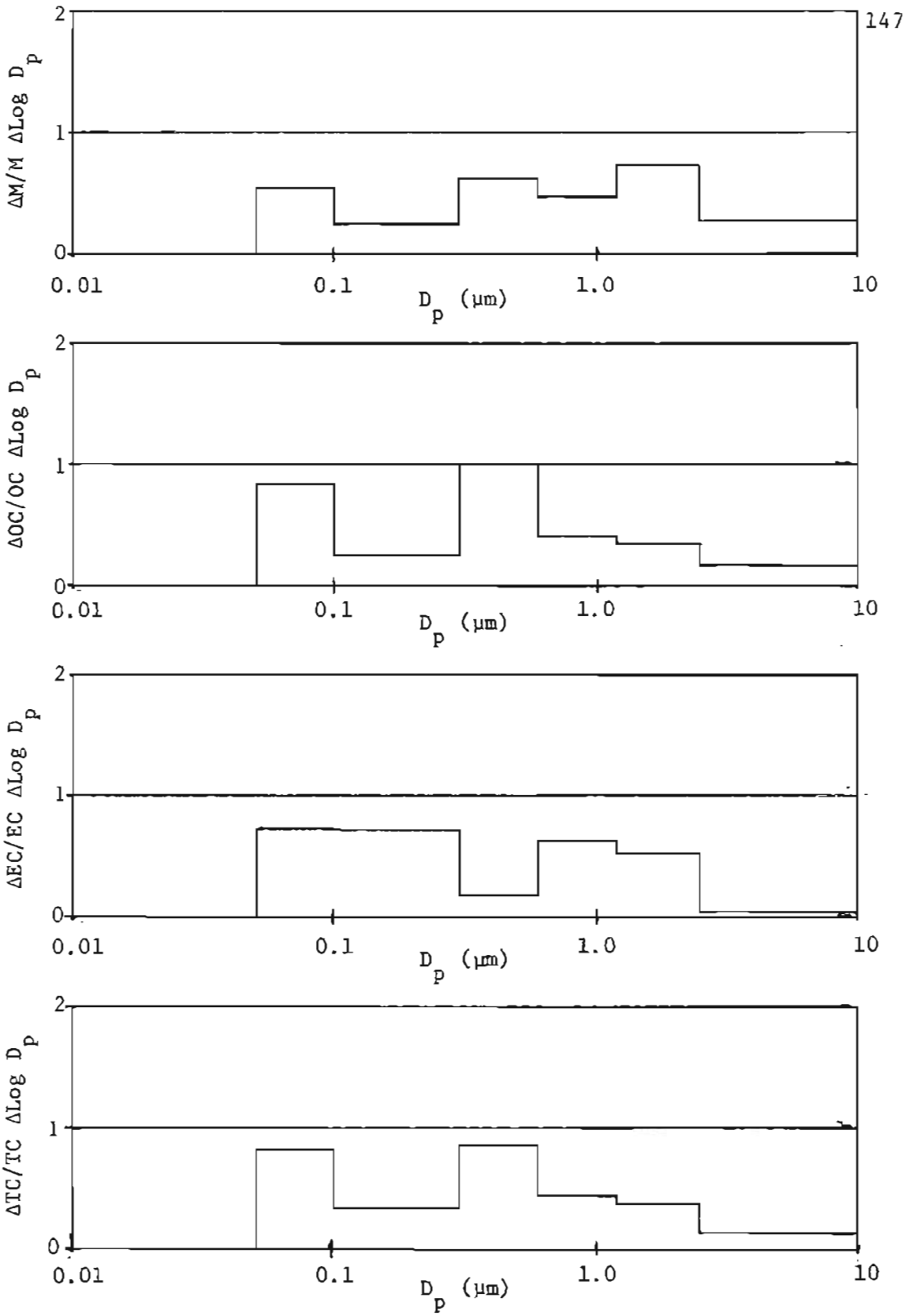

Figure 4.10. Size distribution of Hillsboro residential area ambient aerosol mass, OC, EC, and TC (02/03/84); mass loading = 72 $\mu g/m^3$.

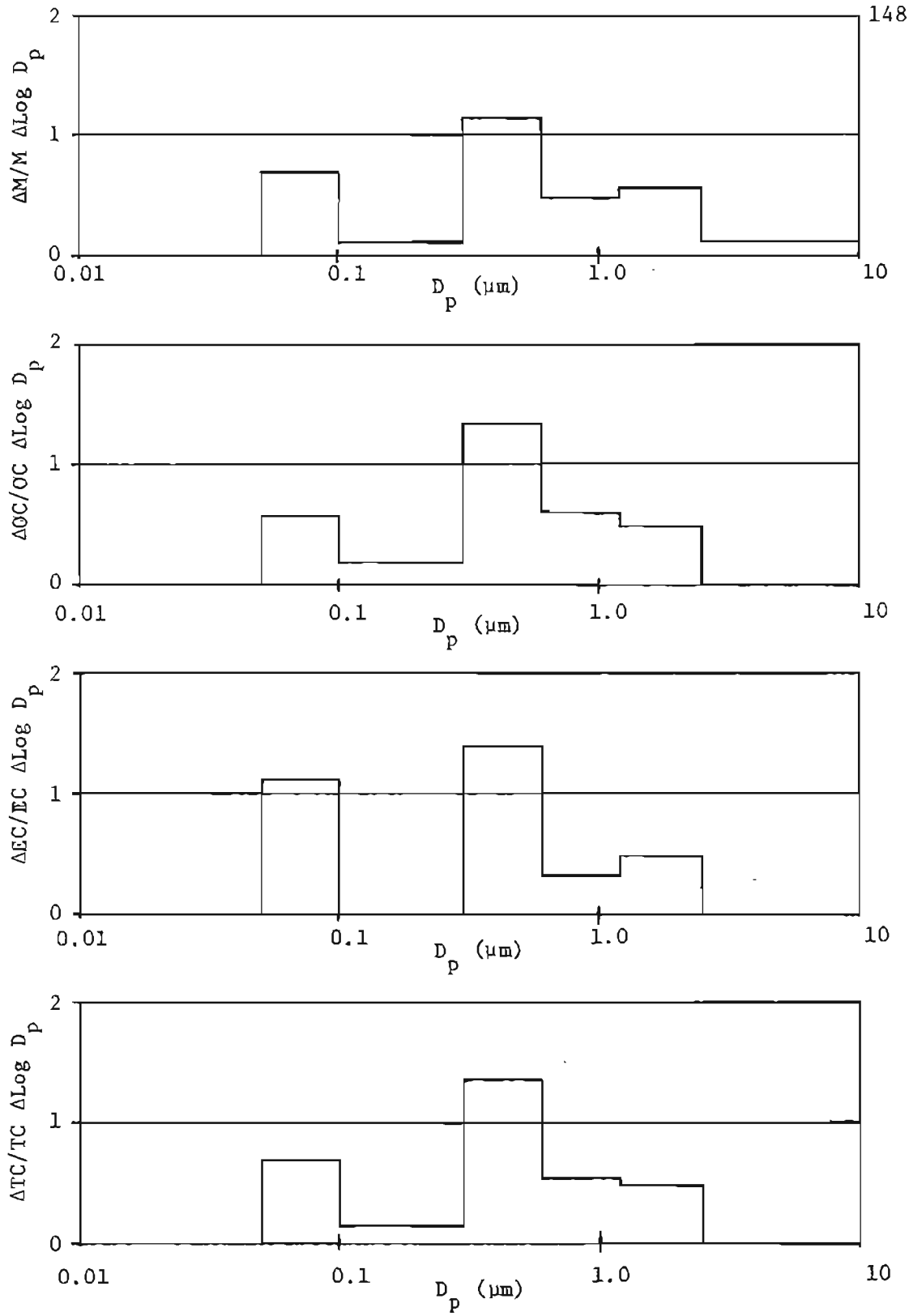

Figure 4.11. Size distribution of Hillsboro residential area ambient aerosol mass, OC, EC, and TC (02/02/84); mass loading = 98 $\mu g/m^3$.

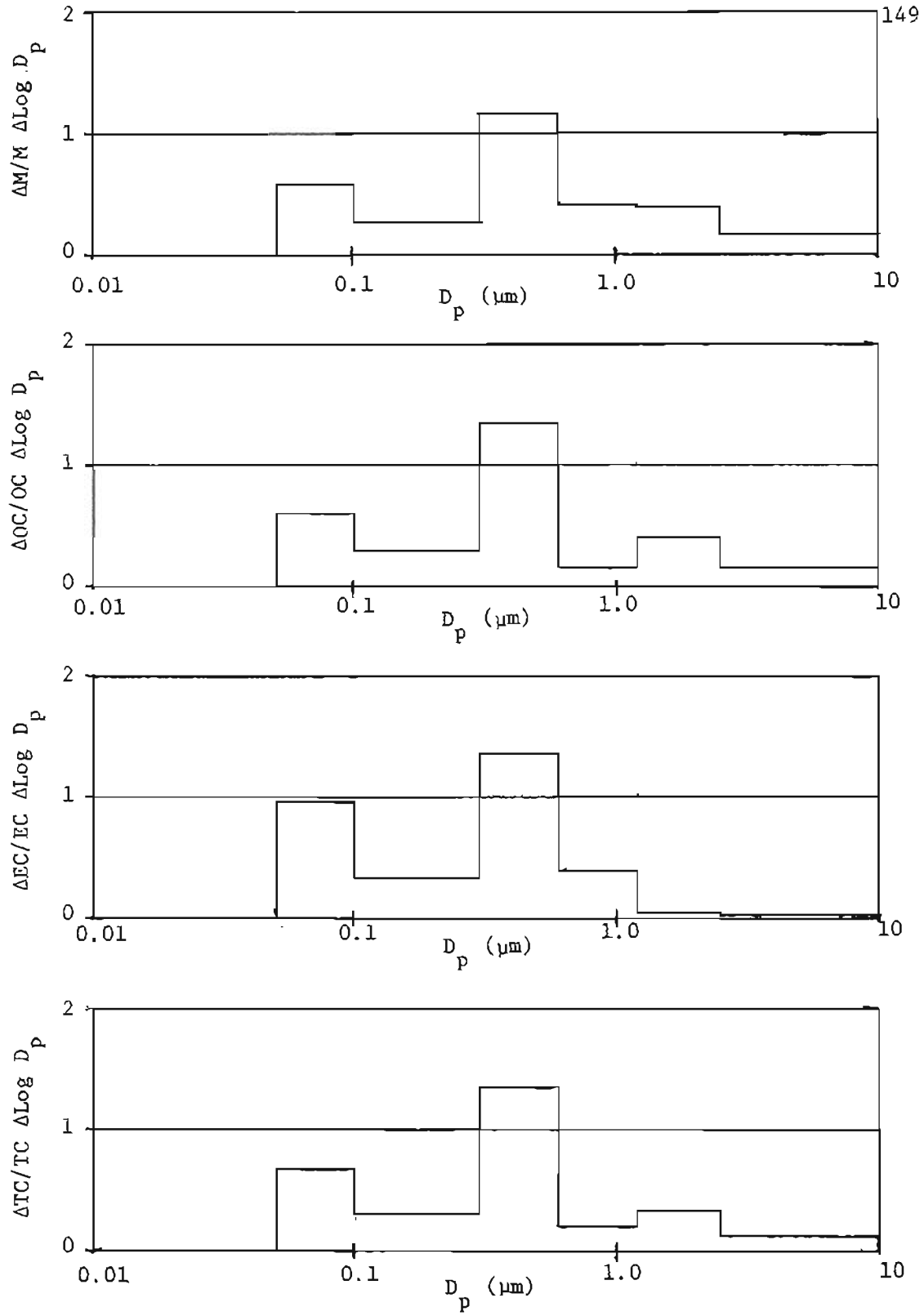

Figure 4.12. Size distribution of Hillsboro residential area ambient aerosol mass, OC, EC, and TC (01/19/84); mass loading = 67 $\mu g/m^3$.

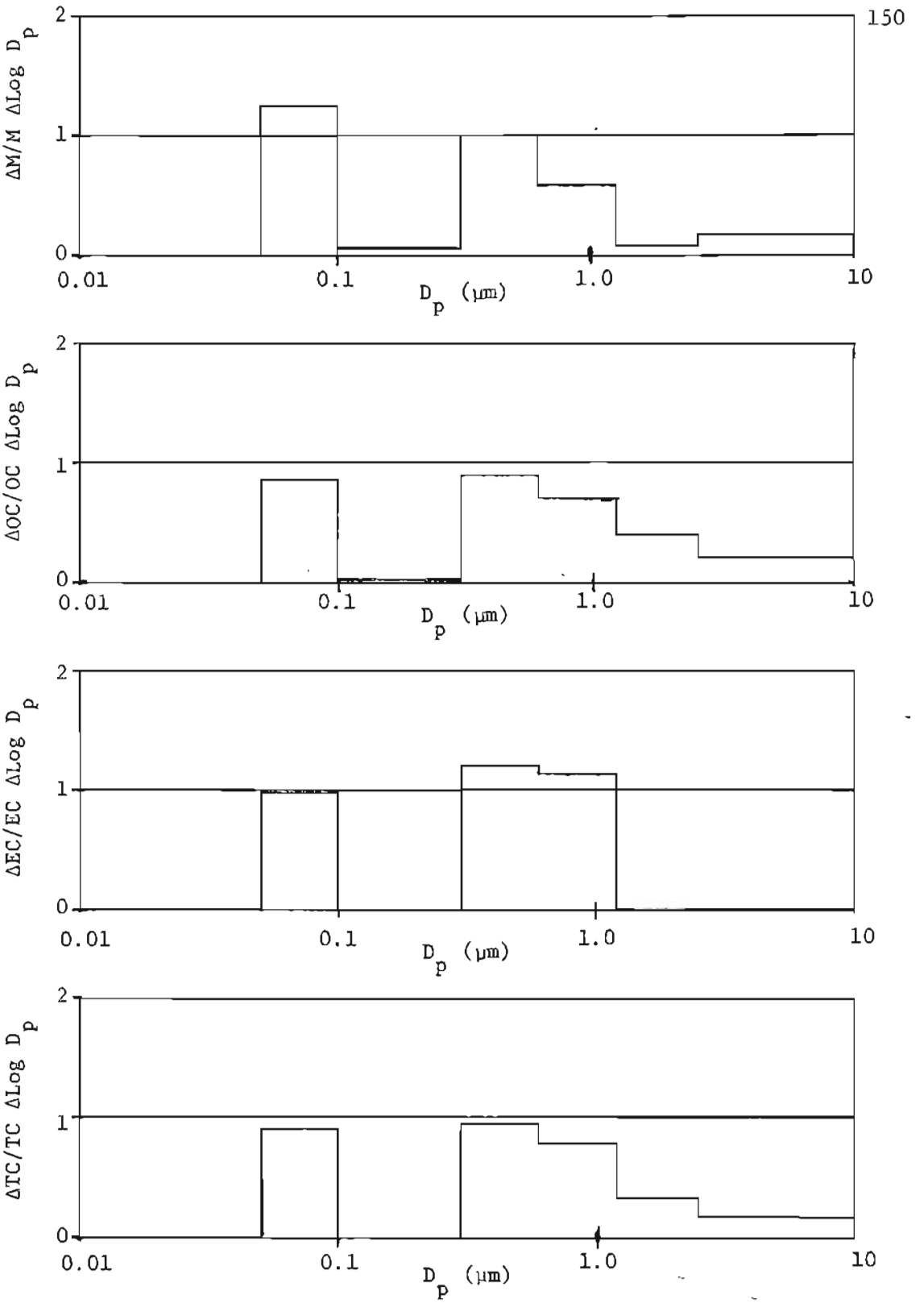

Figure 4.13. Size distribution of Hillsboro residential area ambient aerosol mass, OC, EC, and TC (01/07/84); mass loading = 60 $\mu g/m^3$.

whole sampling set collecting on quartz fiber filters. This allows a detailed determination of the ambient carbon distribution. These figures have many similarities to Figures 4.1A-C in that they have a strong mode between 0.3 and 0.6 μm for OC and also show that elemental carbon is usually more strongly associated with smaller particles. These figures also most often show a mode below 0.1 μm. Whether the Figure 4.1 samples show this mode was not resolved because the 0.1 μm impactor was not used in collecting the Figure 4.1 samples. It is likely that the amount of aerosol material below 0.1 μm would decrease as the aerosol ages and material is transferred to larger aerosol sizes by coagulation.

4.2 CARBON COMPOSITION OF RESIDENTIAL AREA AMBIENT AEROSOLS

This section examines the carbon composition of residential wintertime aerosol particles as a function of particle size and compares their compositions to summertime aerosol particles. Table 4.4 gives the carbon compositions for particle samples collected in a SW Portland residential area during February, 1985. These compositions apply to particles passing the given impactor. The carbon composition values do not change much as a function of particle size. This result occurs because these samples were composed primarily of combustion generated aerosols which were shown by source testing not to change composition significantly as a function of size.

Table 4.5 gives carbon composition data for a group of SW Portland residential area samples. These data show that EC/TC, OC/M, EC/M, and TC/M values range from 17-42%, 13-38%, 4-21%, and 21-55%, respectively. Usually OC/M and EC/M values increased slightly as particle size became

Table 4.4

Wintertime SW Portland Residential Area

Aerosol Carbon Composition (%)

Date	2/5/85	2/8/85	2/14/85	2/20/85
Size (μm)	EC/TC			
<0.3	41	33	34	47
<0.6	35	33	36	41
<1.2	32	35	31	39
<2.5	37	35	31	34
<10.0	35	35	28	34
	OC/M			
<0.3	18	17	23	17
<0.6	23	15	25	25
<1.2	25	17	26	26
<2.5	22	16	27	23
<10.0	23	15	22	19
	EC/M			
<0.3	12	8	12	31
<0.6	12	7	14	43
<1.2	12	9	12	42
<2.5	13	8	12	34
<10.0	13	8	9	29

Table 4.5

SW Portland Residential Area Aerosol Carbon Composition (%)

Size(μm)	EC/TC	OC/M	EC/M	TC/M
Date: 3/2/84			Mass loading = 26 μg/m³	
<0.3	21.2	26.9	7.2	34.1
<1.2	27.4	25.9	9.8	35.7
Total	28.2	26.1	10.5	36.6
Date: 3/5/84			Mass loading = 49 μg/m³	
<1.2	36.7	20.7	13.1	33.8
Total	34.4	23.0	12.1	35.1
Date: 3/9/84			Mass loading = 25 μg/m³	
<0.3	19.5	41.1	10.02	51.3
<1.2	20.7	38.0	9.9	47.9
Total	17.9	34.8	7.6	42.4
Date: 4/28/84			Mass loading = 15 μg/m³	
<0.3	31.4	20.4	9.4	29.8
<1.2	28.9	21.8	8.9	30.7
Total	26.7	16.6	6.1	22.7
Date: 7/26/84			Mass loading = 36 μg/m³	
<0.3	28.6	19.7	7.9	27.6
<1.2	32.5	15.4	7.4	22.8
Total	16.9	18.8	3.8	22.6

Table 4.5 Cont.

SW Portland Residential Area Aerosol Carbon Composition (%)

Size(μm)	EC/TC	OC/M	EC/M	TC/M
Date:	9/18/84		Mass loading = 32 μg/m³	
<0.3	27.8	36.2	13.9	50.1
<1.2	26.5	31.4	11.3	42.7
Total	28.5	18.9	7.5	26.4
Date:	12/8/84		Mass loading = 48 μg/m³	
<0.3	39.0	32.2	20.6	52.8
<0.6	29.8	38.3	16.3	54.6
<2.5	32.4	22.9	11.0	33.9
Date:	12/21/84		Mass loading = 17 μm/m³	
<0.3	42.4	14.3	10.5	24.8
<0.6	41.2	15.1	10.5	25.6
<2.5	41.0	12.7	8.8	21.5
Date:	12/24/84		Mass loading = 44 μg/m³	
<0.3	30.7	34.9	15.5	50.4
<0.6	29.4	35.0	14.6	49.6
<2.5	26.7	27.6	10.0	37.6

smaller. This occurs because the smaller sized particles were more dominated by combustion aerosol particles whereas the larger particles were more dominated by soil particles. The carbon composition differences between large and small ambient aerosol particle samples were not as great as might be expected because increased soil fractions were accompanied by increased amounts of large sized, plant generated particles which like cool burning RWC particles contain about 50% carbon.

Table 4.6 gives average aerosol particle carbon composition data for a group of Hillsboro samples collected during December, 1983 and January, 1984. The carbon content of these samples was significantly higher than for the Portland samples and the EC/TC values were lower. This result was consistent with the larger RWC component in the Hillsboro samples. The Portland EC/TC values were more typical of traffic and distillate oil burning aerosol particles (0.30-0.35). EC/TC values are characteristic of certain sources and have some utility in ambient aerosol source identification.

Table 4.6

Average Carbon Composition of Wintertime Residential Area Ambient Aerosols in Hillsboro (%) (N=8)

Average Mass Loading = 71 $\mu g/m^3$

Size (μm)	EC/TC	OC/M	EC/M	TC/M
<0.3	24±2	40±3	11±1	51±4
<1.2	21±2	40±3	10±1	50±4
Total	20±1	37±4	9±1	46±4

Uncertainties are standard errors of the mean

N = Number of tests

CHAPTER FIVE: CMB ANALYSES OF RWC CONTRIBUTIONS TO RESIDENTIAL AREA AIR POLLUTION

5.1 RESIDENTIAL WOOD COMBUSTION COMPOSITION PROFILES

To obtain accurate RWC source contributions by using CMB modeling the average composition of RWC particulate material emitted by all wood burners in a study area as it arrives at the receptor must be known. This research has shown, by source sampling from cooled diluted plumes, that the composition of RWC particulate emissions spans a range bounded by hot and cool burning particle compositions and that the compositions of hot and cool burning wood smoke particles are very different.

Usually CMB source compositions are determined by measurements at the source. The assumption is made that compositions do not vary over time (as a function of process) or over the atmospheric residence time during which the aerosol travels from the source to the receptor. RWC particulate emissions do not conform to these assumptions because emitted particulate composition depends on stove operation practices of all wood burners in the area being sampled, and the composition of RWC particles can change during its atmospheric residence time. CMB modeling of RWC requires that at least the average burning practices of stove users over the sampling period be known so that an average RWC composition profile can be generated. Since the average burning practices of stove users are usually not available, alternative strategies must be considered. Average RWC composition has been estimated by averaging available data but this has resulted in high particle composition uncertainty (Watson, 1979). Average RWC

composition can also be determined by measuring the composition of the ambient aerosol under circumstances where most of the ambient aerosol comes from RWC (DeCesar and Cooper, 1981). This approach is practical but may conceal non-RWC sources if they are present when the ambient aerosol is assumed to be mostly from RWC.

This research examined two alternative strategies to determine RWC composition profiles. First the average composition profile was estimated by using hot and cool wood burning composition profiles together with wood burning practice data determined by surveys. Second, to circumvent the problem of knowing the wood burning behavior in the study area, separate hot and cool burning composition profiles were used in the same CMB analysis. For simplicity it was assumed that all wood burning could be described as damper open or damper closed stove operation. This research has shown that burning with the damper partially open results in aerosols which are similar to cool burning aerosols. Fireplace burning was not considered as a separate source in CMB analyses because the composition of these emissions was very similar to cool burning stove emissions. CMB results obtained using the above methods were compared with CMB results obtained using the RWC composition profile given in the EPA Receptor Model Source Composition Library (Core et al., 1984).

Wood smoke composition data for damper open and closed softwood and hardwood burning were obtained by averaging all the test data acquired in this research. These profiles are given in Table 5.1. Because these profiles resulted from averaging a large data set of residential stove burn tests they should be reasonably representative

Table 5.1

Residential Wood Stove Aerosol Composition Profiles

(% of mass)

	Damper Open		Damper Closed	
	Softwood	Hardwood	Softwood	Hardwood
	N=8	N=9	N=8	N=4
Al	0.32±0.14	0.48±0.21	0.05±0.01	0.04±0.02
Ca	0.36±0.06	0.10±0.07	0.06±0.02	0.01±0.01
Cl	2.5±1.0	3.0±0.8	0.05± 0.01	0.01±0.01
Fe	0.02±0.01	0.03±0.01	0.01±0.01	0.01±0.01
K	7.0±2.8	15.6±2.8	0.09±0.02	0.24±0.11
P	0.13±0.05	0.21±0.05	0.01±0.01	0.02±0.01
Pb	0.16±0.04	0.08±0.12	nd	nd
Rb	0.03±0.01	0.05±0.02	nd	nd
S	1.3±0.9	1.4±0.7	0.06±0.01	0.08±0.04
Si	0.45±0.21	0.65±0.12	0.04±0.03	0.07±0.03
Zn	0.24±0.06	0.27±0.06	0.01±0.01	nd
OC	17.5±4	16.4±7	52.2±1	55.9±2
EC	34.6±7	18.6±7	4.7±2	4.6±1
TC	51.1±6	35.0±4	56.9±2	60.5±3

Uncertainties are standard errors of the mean.

N = Number of tests

of damper open and closed operation of common box type, air-tight wood stoves.

Some test data (Table 3.6B) showed that carbon concentrations for particles <0.3 μm were slightly less that for particles >0.3 μm. Also elemental concentrations based on particles <0.1 were generally about 20% higher than for particles >0.1 μm; however, because of the small sample masses collected behind the 0.1 μm impactor these data had a large amount of variability.

It is interesting to compare the hot burn compositions in Table 5.1 with the two sets of composition data for wood fired boilers presented in Table 5.2. These data sets had the lowest and highest values of potassium concentration for wood fired boiler data given in the EPA Receptor Model Source Composition Library (Core et al. 1984). These boiler data probably represent an upper limit for trace element concentrations that could be expected from hot wood burning. The highest of these concentrations, except for aluminum, are a factor of two or more higher than the values obtained for hot burning wood stoves in this research.

It should be noted that a small wood boiler contribution to the background aerosol in a residential area can result in an overly large CMB evaluation of RWC aerosols if carbon is not included as a fitting species. Because industrial wood burning furnaces produce very little aerosol carbon compared to RWC, accounting for ambient carbon insures that trace elements from wood boilers are not confused with RWC emissions.

The data in Table 5.1 were used to develop hot and cool burning

Table 5.2

Two Aerosol Composition Profiles for Wood-Fired Boilers (% of mass)*

Al	0.240±0.180	0.130±0.07
Br	0.055±0.300	0.017±
Ca	5.600±4.000	3.0±2.0
Cl	9.500±4.900	13.0±12.0
Cu	0.120±0.060	0.27±
Fe	1.260±0.880	0.30±0.1
K	22.400±11.20	9.0±6.0
Mn	0.520±0.340	0.2±0.1
Ni	0.006±0.004	<
Pb	0.420±0.220	0.03±0.02
S	8.800±2.400	3.0±2.0
Si	0.760±0.370	0.5±0.3
Zn	0.730±0.340	0.3±0.1
OC	------	5.0±4.0
EC	------	4.3±4.0

< Below detection limit

* Core et al., 1984

average composite wood smoke composition profiles for burning 50% softwood and 50% hardwood (Table 5.3). This usage pattern in Portland was determined by Cummings (1982) and confirmed by Fitzgerald (1985). A survey of wood dealers indicated that people who heat with wood prefer hardwood over softwood but that wood type availability was the prime factor which determined the type of wood that was burned. A hot burn profile was also developed for burning 75% softwood and 25% hardwood (Table 5.3). The similarity of 50/50 and 75/25 softwood/hardwood composition profiles and Tables 3.6-3.7 indicate that wood type has at most a minor influence on RWC particulate composition and does not need to be considered in CMB modeling. All CMB modeling in this research used 50/50 softwood/hardwood composition profiles.

It should be noted that the differences between softwood and hardwood hot burn particulate compositions might not be specifically associated with wood type but could result from differences in burn temperature that occurred for the specific soft and hard woods burned. Since burn temperature so strongly dominates smoke composition for RWC, only rigidly controlled laboratory burns can determine the true effects of wood type on particulate composition.

The data in Table 5.3 were used to develop a composite wood smoke composition profile for 25% damper open burning and 75% damper closed burning with a 50% softwood and 50% hardwood wood mix. This profile is presented in Table 5.4. It takes into account that average damper closed burning emits 4.8 (Appendix 3) times more aerosol than damper open burning. Thus if all RWC aerosol is assumed to come from stoves, 7% of the aerosol comes from damper open burning and 93% comes from

Table 5.3

Composite Wood Stove Smoke Composition Profiles

(% of mass)

	50% softwood 50% hardwood		75% softwood 25% hardwood
	Damper open	Damper closed	Damper open
Al	0.40+0.18	0.04+0.01	0.36±0.16
Ca	0.23±0.06	0.03±0.01	0.30±0.06
Cl	2.7±0.9	0.03±0.01	2.6±0.9
Fe	0.02±0.01	0.01±0.01	0.02±0.01
K	11.3±2.8	0.17±0.07	9.1±2.8
P	0.17±0.05	0.02±0.01	0.15±0.05
Pb	0.12±0.08	nd	0.14±0.06
Rb	0.04±0.02	nd	0.04±0.02
S	1.35±0.8	0.07±0.02	1.3±0.8
Si	0.55±0.17	0.05±0.03	0.50±0.19
Zn	0.25±0.06	nd	0.23±0.06
OC	17.0±6.5	54.0±1.5	17.1±2
EC	26.6±7	4.6±1.5	30.6±7
TC	43.6±5	58.6±2.5	47.7±5

Uncertainties are standard errors of the mean.

Table 5.4

Composite Residential Wood Burning Composition Profile

(% of mass)

50% hardwood and 50% softwood burned. 25% hot burn(damper open), 75% cool burn(damper closed)	
Al	0.065±0.022
Ca	0.044±0.014
Cl	0.22±0.07
Fe	0.011±0.010
K	0.95±0.26
P	0.031±0.013
Pb	0.008±0.006
Rb	0.003±0.001
S	0.16±0.08
Si	0.085±0.038
Zn	0.018±0.004
OC	51.4±2
EC	6.1±2
TC	57.5±3

Uncertainties are standard errors of the mean.

damper closed burning. This damper setting pattern was found by Cummings (1982) and has been substantiated by discussions with many wood burners. It should be noted that stoves operating with large fuel loads, even with dampers fully open, can also generate cool burning aerosol because air starved combustion results when the amount of wood surface burning is too large for the amount of combustion air supplied by the draft system. This type of operation was not common because it usually results in excessive heat outputs. For similar reasons the trend toward air starved combustion increases when burning very dry wood as compared to wood with moderate moisture levels. Very dry wood will tend to burn faster than moderately moist wood and thus will demand more combustion air which leads to air-starved combustion and higher emissions when the capacity of draft system is exceeded.

Columns one and two in Table 5.5 give the carbon size distributions for RWC particulate emissions resulting from burning 50% hardwood and 50% softwood in stoves with the damper open and damper closed, respectively. In column three these data are combined, assuming that damper closed burning emits 4.8 times more particulate mass than damper open burning, to estimate the carbon distribution for 75% damper closed burning and 25% damper open burning. Column four shows the carbon distributions expected for 2/3 of wood burned per column three combined with 1/3 of wood burned in fireplaces. It will be noted when RWC emissions are dominated by cool burning emissions there is relatively little aerosol between 0.3 and 0.6 μm. When fireplace emissions are added to the emissions mix the amount of emissions between 0.3 and 0.6 μm is significantly increased.

Table 5.5

The Carbon Size Distribution of RWC Emissions for Various Residential Wood Burning Operating Modes

50% softwood and 50% hardwood				
Size (μm)	Stove Emissions			2/3 Stove 1/3 FP **
	Damper Open	Damper Closed	75% Closed 25% Open *	
	Organic Carbon			
<0.3	57±10	55±1	55±3	51±4
0.3-0.6	29±6	4±2	6±3	18±4
0.6-2.5	14±8	41±2	39±3	31±4
	Elemental Carbon			
<0.3	57±4	56±14	56±14	51±12
0.3-0.6	34±2	17±7	18±7	26±7
0.6-2.5	9±3	27±7	26±7	23±6
	Total Carbon			
<0.3	57±4	55±1	56±1	51±4
0.3-0.6	32±2	5±3	7±3	19±3
0.6-2.5	11±5	40±2	37±2	30±4

*Assumes that 75% of wood is burned in stoves with dampers closed and 25% is burned with dampers open and that closed damper burning produces 4.8 times more aerosol particle mass than open damper burning. (6% of aerosol from hot burning and 94% of aerosol from cool burning.)

**Assumes that 2/3 of wood is burned in stoves (75% dampers closed 25% dampers open) and 1/3 burned in fireplaces (fireplaces emit 5.4 times more aerosol than hot burning stoves)

Table 5.6 gives the composite RWC composition profile for the case where one-third of the wood burned was burned in fireplaces and two-thirds were burned in stoves. This usage pattern was given by Cummings (1982). The composition profile in Table 5.6 is not significantly different from the stove only burning composition profile shown in Table 5.4.

5.2 CHEMICAL MASS BALANCE (CMB) ANALYSIS

The CMB analyses were done on total aerosol samples (i.e. collected with no impactor in the sampling stream) and on samples that were collected behind several different impactor sets. Impactor-collected samples consisted of the particulate material passing the impactors and thus were representative of particles which had aerodynamic diameters less than the impactor cut-points. For size-distributed CMB analyses source composition profiles were used which applied to source aerosols that were collected behind the same impactors as the ambient aerosols. With this procedure the amount of wood smoke aerosol or other source type in each size fraction of the ambient aerosol could be determined. These data show how aerosol mass from various sources was distributed in ambient samples and were useful in making inferences about the stability of carbonaceous aerosols during their atmospheric residence time, about their inhalation characteristics, and about their impact on visibility degradation. This procedure can also facilitate CMB analysis in the case where sources with similar compositions exist in different size ranges.

CMB analyses were done using the composite and separate hot and

Table 5.6

Composite RWC Composition Profile

(% of mass)

50% hardwood and 50% softwood burned. Two thirds burned in stoves, one third in fireplaces. Stoves: 25% damper open and 75% damper closed.	
Al	0.05±0.02
Ca	0.05±0.02
Cl	0.51±0.22
Fe	0.01±0.01
K	0.69±0.25
P	0.03±0.01
Pb	0.02±0.02
Rb	0.001±.001
S	0.16±0.06
Si	0.08±0.04
Zn	0.02±0.01
OC	51.4±4
EC	7.8±4
TC	58.2±3

Uncertainties are standard errors of the mean.

cool burning RWC source composition profiles (Tables 5.3 and 5.4).

The accuracy of CMB results has not been independently determined. This can strictly only be done by making measurements of known source contributions in a controlled ambient situation. Confidence in CMB results can be strengthened by comparisons with concurrent carbon-14 measurements. Since neither of these methods were available the validity of CMB results was assessed by noting the overall goodness of fit measured by chi-squared (X^2) and noting the fit of individual tracer species. Since RWC smoke particles are over 50% carbon it is especially important that total carbon (TC) is well fit by CMB modeling. If organic (OC) and elemental carbon (EC) are also well fit, then confidence in the model results is further improved.

During their atmospheric residence RWC particles can undergo processes which change their mass and composition distribution as a function of size. Particles can coagulate to shift size distributions toward larger particle sizes. Particles can also lose mass by evaporation of volatile species or they can gain mass by condensation of vapor species or by gas to particle chemical reactions. Any gain or loss of particle mass changes the mass based concentrations of all species comprising the particle. This in turn creates a difference between particle composition profiles determined at the source (those used in CMB analysis) and those arriving at a receptor. Such changes can cause errors in CMB-determined source contributions. This research examined the effect on CMB results of assuming that RWC particles lose organic carbon by evaporation during the atmospheric residence time.

Ambient particulate organic and elemental carbon size

distributions were compared with expected distributions which were computed by using CMB source contributions together with measured source emission distributions. These comparisons were useful to examine the behavior of combustion generated particles in the atmosphere.

These CMB analyses are intended to show the utility of improved source characterization data and to demonstrate the use of chemical mass balance methods on size-distributed data.

5.3 APPLICATIONS OF SOURCE COMPOSITION DATA TO CMB ANALYSIS

CMB analyses were done on a Columbia PC computer (IBM compatible) using version 2.2 of the CMB program developed by Watson (1985) for the Oregon Department of Environmental Quality (DEQ). Emission composition profiles for composite RWC particles, hot and cool burning RWC particles, residential oil furnace aerosol and vehicular transportation (tunnel) developed in this research were used. Note the tunnel source will be labeled "motor vehicle" in CMB results. Other necessary source profiles, (i.e., road dust, soil, distillate oil combustion, residual oil combustion, heavy duty diesel, Kraft recovery boiler, and sea salt) were those currently used by the Oregon DEQ. Many of these profiles and the RWC profile currently used by the DEQ are given by Core et al. (1984).

In all CMB analyses OC and EC were used as fitting species rather than only using TC. This, in effect, incorporates more information about the sources and the ambient aerosol into the CMB analysis. It therefore should make CMB results more valid. The differences in source contributions obtained by using either OC and EC or TC alone were not

evaluated. Neither mass and nor TC were used as fitting species; however, the fits of these species were useful indicators of goodness of fit. It is reasonable to expect that the ratios of CMB-computed TC and mass values to measured TC and mass values, respectively should be slightly less than one since every source that actually contributes to the ambient aerosol might not have been included in the analysis.

5.3.1 ANALYSIS OF PORTLAND RESIDENTIAL AEROSOLS PASSING A 10 μm CUT-POINT IMPACTOR

Several wintertime (February 1985) ambient aerosol samples were collected using impactor set #1 (two 10 μm impactors and a 2.5, 1.2. 0.6 and 0.3 μm impactor) in a Southwest Portland residential area. One 10 μm impactor collected a sample on Teflon while the other impactors collected samples on quartz fiber filters. Samples collected on Teflon were analyzed for trace element species and samples collected on quartz fiber filters were analyzed for carbon. The mass loadings passing the 10 μm impactor were 21, 9, 23 and 22 μg/m3, for February 5, 8, 14 and 20, respectively. These low ambient mass loadings occurred because the sampling location was at a higher altitude than the surrounding area and because the winter rains suppressed the resuspension of soil dust and removed coarse particles from the air. Summertime samples at this site did have the expected coarse mode component. The mass percentages above 2.5 μm were 0, 0, 24, and 17% for the February 5th, 8th, 14th and 20th samples, respectively. No more than 4% of the carbon was above 2.5 μm. Thus these samples were composed mainly of fine mode aerosol and the carbon would be expected to come from combustion sources.

Major sources contributing to these samples were determined by CMB analyses. The source contributions, in percentages of measured aerosol mass, are shown in Tables 5.7A-D. For each date the first column (Normal) shows results obtained using the RWC composite composition profile (W/S Comp). "Normal" refers to CMB analyses that use RWC composition profiles that do not include OC loss by particles during their atmospheric residence time. The normal analysis shows that residential wood smoke component ranged from 22 to 38% of aerosol particulate mass. The second largest pollution source, distillate oil burning emissions, ranged from 24 to 34%. The third largest source, the sum of road dust and motor vehicle emissions ranged from 12 to 29%. The road dust source was assumed to be mainly geological material while the motor vehicle source was assumed to be mainly automotive emissions. The road dust and motor vehicle sources were always resolvable by the CMB analysis. Figure 5.1 shows the contributions of the sources used in CMB modeling to these samples. This figure shows that the source distribution was very similar on a day to day basis. This distribution is probably typical for winter residential aerosol where RWC is a significant pollution source. Mass was not used as a fitting species in the CMB analyses. Therefore since usually more than 80% of the aerosol mass was accounted for it can be assumed that no major aerosol sources have been neglected.

Note that in this group of CMB analyses residential oil burning was represented by the "distillate oil" composition profile given in the EPA Receptor Source Composition Library, (Core et al., 1984). For other CMB analyses the "oil furnace" composition profile determined in

TABLE 5.7A

Comparisons of CMB Analyses Using Various Wood Smoke Composition Profiles

Site: SW Portland Residential Area 2/5/85 Size: 10 μm.			Mass loading = 21 μg/m³	
	Normal	-25% *	-50% *	-65% *
W/S Comp(%)	37.5±7.6	40.8±8.4	45.2±9.6	48.2±10.7
Road dust(%)	7.9±1.5	7.8±1.5	7.7±1.5	7.7±1.5
Motor Veh.(%)	6.1±1.1	6.1±1.1	6.1±1.1	6.1±1.1
Dist oil(%)	30.4±6.9	29.6±6.9	28.7±6.9	28.5±7.0
X^2	1.817	1.423	1.206	1.293
DF	10	10	10	10
OC Ratio**	1.18±0.10	1.11±0.09	1.00±0.08	0.89±0.07
EC Ratio**	0.64±0.11	0.68±0.12	0.73±0.15	0.79±0.17
TC Ratio**	0.99±0.12	0.96±0.11	0.91±0.10	0.85±0.10
K Ratio**	0.73±0.20	0.87±0.25	1.07±0.37	1.25±0.48
Mass calc(%)	82.0±8.2	84.2±8.4	87.7±8.7	90.4±9.0

Uncertainties are standard errors.

* For CMB analysis organic carbon is decreased by the percentage shown for the RWC sources.

** Ratio of CMB calculated/measured

DF = Degrees of freedom

TABLE 5.7B

Comparisons of CMB Analyses Using Various Wood Smoke Composition Profiles

Site: SW Portland Residential Area 2/8/85 Size: 10 μm.			Mass loading = 9 μg/m³	
	Normal	-25% *	-50% *	-65% *
W/S Comp(%)	22.3±5.7	24.7±6.3	28.0±7.4	30.8±8.4
Road dust(%)	5.4±1.0	5.3±1.0	5.2±1.0	5.1±1.0
Motor Veh.(%)	6.9±1.5	7.1±1.5	6.9±1.5	6.8±1.5
Sea salt(%)	3.9±1.3	3.8±1.3	3.6±1.2	3.5±1.2
Dist oil(%)	33.8±8.5	33.7±8.4	34.1±8.6	35.3±8.8
X^2	1.706	1.311	0.991	0.949
DF	7	7	7	7
OC Ratio**	1.16±0.13	1.13±0.12	1.06±0.12	0.98±0.12
EC Ratio**	0.83±0.15	0.86±0.16	0.93±0.18	1.00±0.21
TC Ratio**	1.04±0.17	1.03±0.16	1.00±0.17	0.98±0.17
K Ratio**	0.63±0.14	0.74±0.18	0.90±0.26	1.03±0.33
Mass calc(%)	72.3±7.2	74.4±7.4	77.8±7.7	80.8±8.1

Uncertainties are standard errors.

* For CMB analysis organic carbon is decreased by the percentage shown for the RWC sources.

** Ratio of CMB calculated/measured

DF = Degrees of freedom

TABLE 5.7C

Comparisons of CMB Analyses Using Various Wood Smoke Composition Profiles

Site: Portland Residential Area 2/14/85 Size: 10 μm. Mass loading = 23 μg/m³				
	Normal	-25% *	-50% *	-65% *
W/S Comp(%)	31.6+6.7	34.0±7.3	37.1±8.5	38.8±9.5
Road dust(%)	9.8±1.6	9.6±1.6	9.5±1.6	9.5±1.6
Motor Veh.(%)	4.2±0.9	4.2±0.9	4.1±0.9	4.1±0.9
Sea salt(%)	5.4±1.5	5.2±1.5	5.1±1.4	4.9±1.4
Dist oil(%)	33.7±7.4	33.5±7.5	33.8±7.6	34.6±7.8
X^2	0.987	0.724	0.679	0.881
DF	7	7	7	7
OC Ratio**	1.11±0.10	1.06±0.10	0.96±0.09	0.86±0.09
EC Ratio**	0.89±0.18	0.94±0.19	1.01±0.23	1.09±0.26
TC Ratio**	1.05±0.15	1.02±0.14	0.97±0.14	0.92±0.14
K Ratio**	0.80±0.19	0.91±0.24	1.08±0.33	1.21±0.41
Mass calc(%)	84.6±8.5	86.6±8.7	89.7±9.0	91.9±9.2

Uncertainties are standard deviations.

* For CMB analysis organic carbon is decreased by the percentage shown for the RWC sources.

** Ratio of CMB calculated/measured

DF = Degrees of freedom

TABLE 5.7D

Comparisons of CMB Analyses Using Various Wood Smoke

Composition Profiles

Site: Portland Residential Area 2/20/85 Size: 10 μm. Mass loading = 22 μg/m³				
	Normal	-25% *	-50% *	-65% *
W/S Comp(%)	22.5±5.9	24.3±6.3	25.4±7.0	25.6±7.4
Road dust(%)	18.8±2.9	18.4±2.9	18.0±2.8	17.9±2.8
Motor Veh.(%)	10.2±1.7	10.2±1.7	10.2±1.7	10.1±1.7
Sea salt(%)	1.6±0.6	1.6±0.6	1.5±0.5	1.5±0.5
Dist oil(%)	36.6±8.4	36.7±8.3	37.7±8.5	39.1±8.7
X^2	0.759	0.462	0.272	0.277
DF	8	8	8	8
OC Ratio**	1.17±0.14	1.13±0.12	1.04±0.13	0.95±0.13
EC Ratio**	0.90±0.16	0.94±0.17	0.99±0.19	1.04±0.20
TC Ratio**	1.08±0.17	1.06±0.17	1.02±0.17	0.98±0.17
K Ratio**	0.78±0.17	0.86±0.20	0.96±0.24	1.02±0.27
Mass calc(%)	89.8±9.0	91.2±9.1	92.8±9.3	86.2±8.6

Uncertainties are standard deviations.

* For CMB analysis organic carbon is decreased by the percentage shown for the RWC sources.

** Ratio of CMB calculated/measured

DF = Degrees of freedom

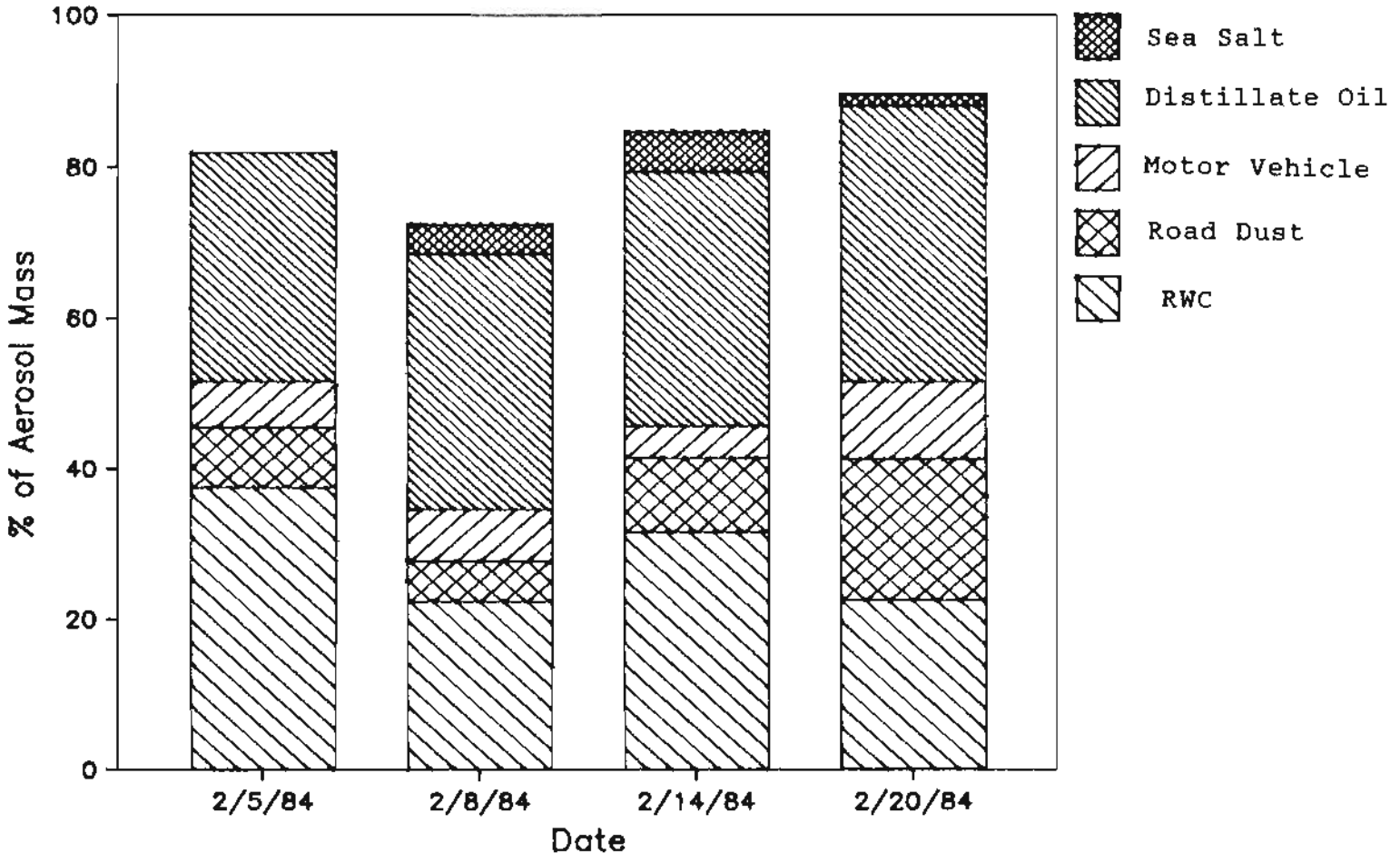

Figure 5.1. CMB source contributions to <10 μm southwest Portland residential area aerosol samples where RWC emissions were characterized by the RWC composite composition profile.

this research was used. These profiles are quite similar but may reflect differences due to oil burning in different types of furnaces. Usually one or the other of the profiles resulted in a better source fit in CMB analyses and was thus used even though either of the profiles would have given a satisfactory fit.

The OC, EC, TC, and K ratio values given in Tables 5.7A-D are the calculated to measured ratios of the various chemical species. When the CMB model fits the measured data well, these values will be close to 1.0.

It will be noted in Tables 5.7A-D that in the column labeled "normal" the EC ratio is less than 1.0 and the OC ratio is greater than 1.0. It will be shown that this discrepancy can be reduced by decreasing the organic carbon content of the RWC profile in CMB analysis. This is equivalent to assuming that RWC particles lose organic carbon during their atmospheric residence time. The point of this exercise is to examine the effect on CMB modeling results if organic carbon loss is assumed to occur from RWC particles during their atmospheric residence time rather than to prove that this loss does occur.

While it is conceivable that RWC particles could either gain or lose organic carbon during their atmospheric residence time physical arguments can be presented to support the concept that RWC particles lose organic mass. RWC particles, especially those generated by cool burning, are mainly composed of organic carbon. They form in the flue gas where organic vapor concentrations are high. When these particles enter the atmosphere they enter an environment where the concentration

of the condensable species is less than it was in the flue gas. As a result organic species can evaporate from particles causing both a loss of organic carbon and a loss of particle mass. The fact that RWC particles have an odor indicates that organic carbon loss occurs.

Columns two, three, and four of Table 5.7A-D repeat the CMB analysis using RWC composite composition profiles recalculated assuming that 25, 50% and 65%, respectively, of RWC organic carbon has been lost. Figures 5.2A-D show how the OC ratio, EC ratio, and K ratio change as a function of OC loss. Starting at low OC loss values the OC ratio decreased while the K ratio and the EC ratio increased for increasing values of OC loss. For these samples the OC ratio and the EC ratio and usually the K ratio (in all figures except 5.2A) approach a common value near one at some value of OC loss. This OC loss value occurred at the minimum value of X^2 indicating that this was the solution which best fit the sample data, i.e., the probability of obtaining the observed values was maximized (Watson, 1979). Since the fit of a group of sources that are really contributing to an ambient sample must improve as the composition of these sources used in CMB modeling approaches the true values that exist at the receptor the fact that the OC, EC and K ratio values approached one at the same point where X^2 was a minimum can be taken as evidence that RWC particles have lost the percentage of OC corresponding to this point. For this group of samples the OC loss values ranged 40 to 65%. Van Vaeck et al., (1984) noted that losses as high as 70% can occur for some organic compounds when particle samples collected on filters were exposed to a high flow rate stream of nitrogen. Since about 50% of RWC particles

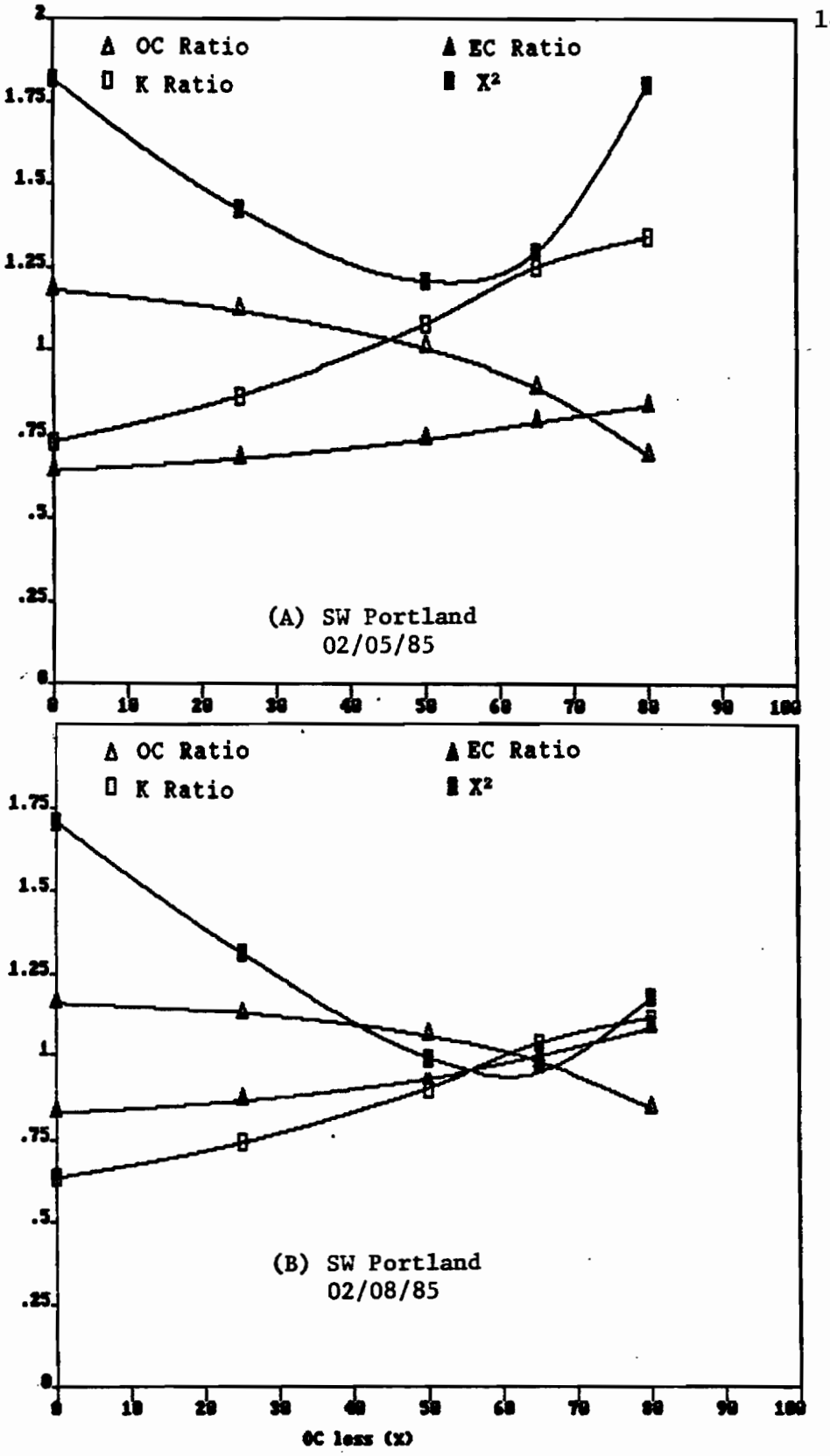

Figure 5.2. The variation of CMB model outputs as a function of RWC composite source OC loss.

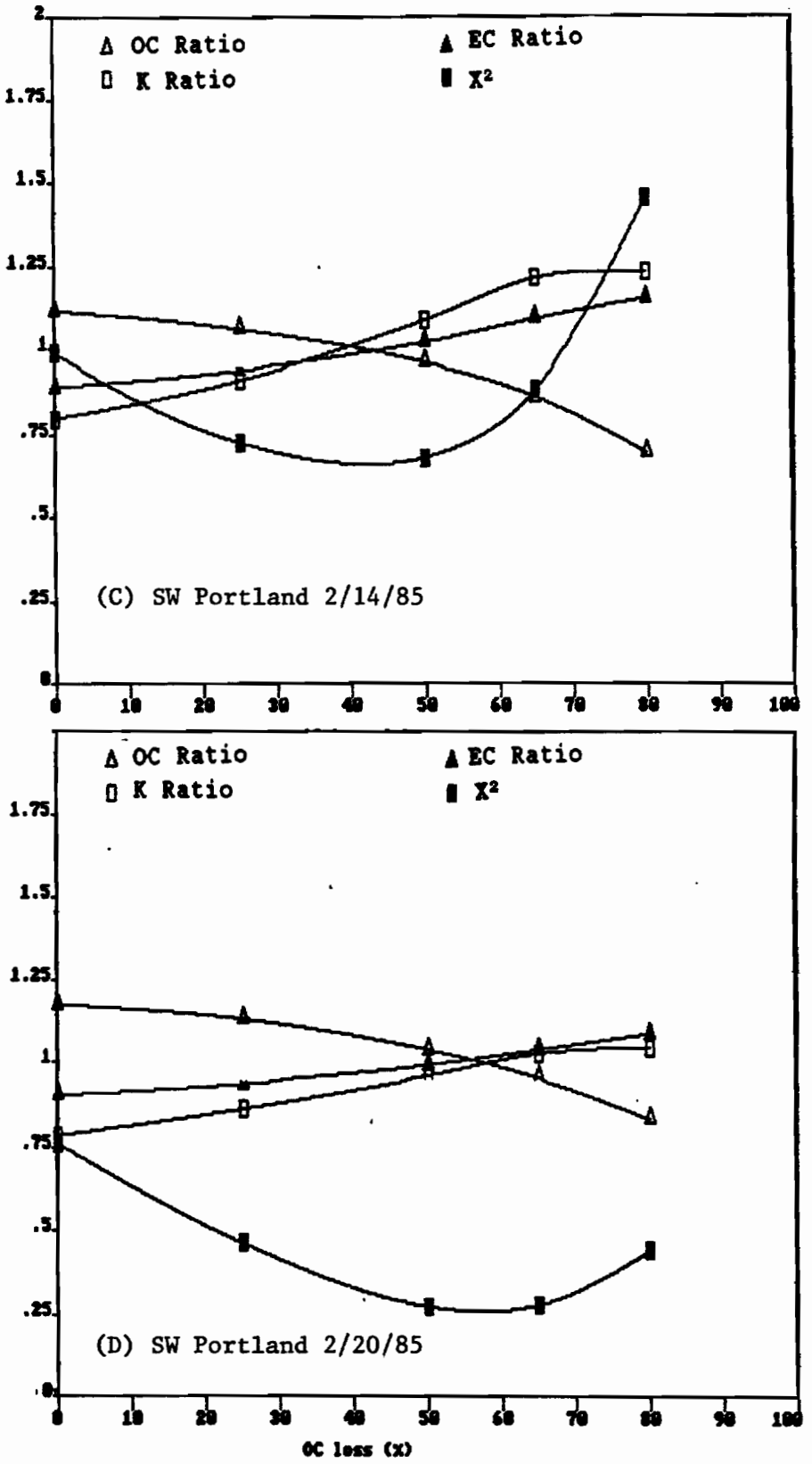

Figure 5.2 The Variation Of CMB Model Outputs
As A Function of RWC Composite Source OC Loss

were <0.3 μm, evaporation from these particles would be increased by the Kelvin effect. It should also be noted that over 90% of RWC particles result from cool burning and that these particles are composed of over 50% organic carbon species some of which might be reasonably volatile (in comparison to hot burn particles which have high molecular weight organics coating an elemental carbon surface).

The reasons to expect the OC, EC and K ratios to approach one will now be examined. Consider the case where OC, EC and K are found only in the sources that are used in the CMB model; i.e., they are not found in unknown sources contributing to the sample. Then if the source profiles represent the sources as they exist at the receptor the model will correctly fit the known sources within the uncertainty limits. All the OC, EC, and K would be accounted for and the OC ratio, EC ratio, and K ratio values will approach one, i.e., the computed value for these species would equal the measured value. This will also occur for an actual sample if all the major emitters of carbon and potassium are included in the CMB solution and negligible amounts of these species are contributed by unknown sources. Ratios of calculated to measured species values will only be different from one if species concentrations in known sources are misspecified, the analysis of the ambient sample is in error, sources that do not exist in the sample are used in the CMB analysis, or if significant unknown sources contribute to the sample.

Figures 5.3A-D show that the various source contributions calculated by the CMB model did not change greatly as a function of RWC particle OC loss. The RWC source contribution was largest at the OC

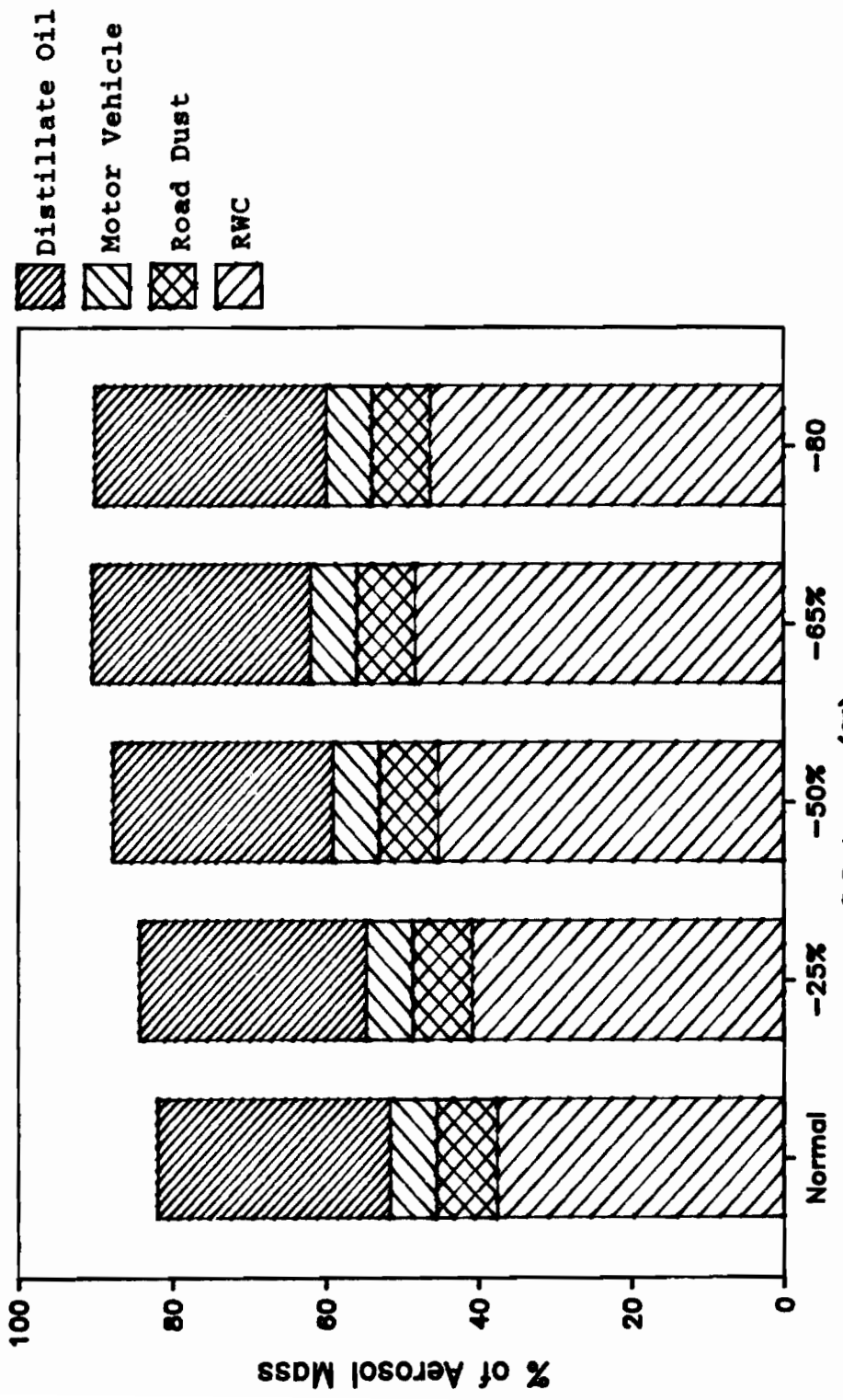

Figure 5.3A. CMB source contributions as a function of RWC composite source OC loss (southwest Portland, 2/5/85).

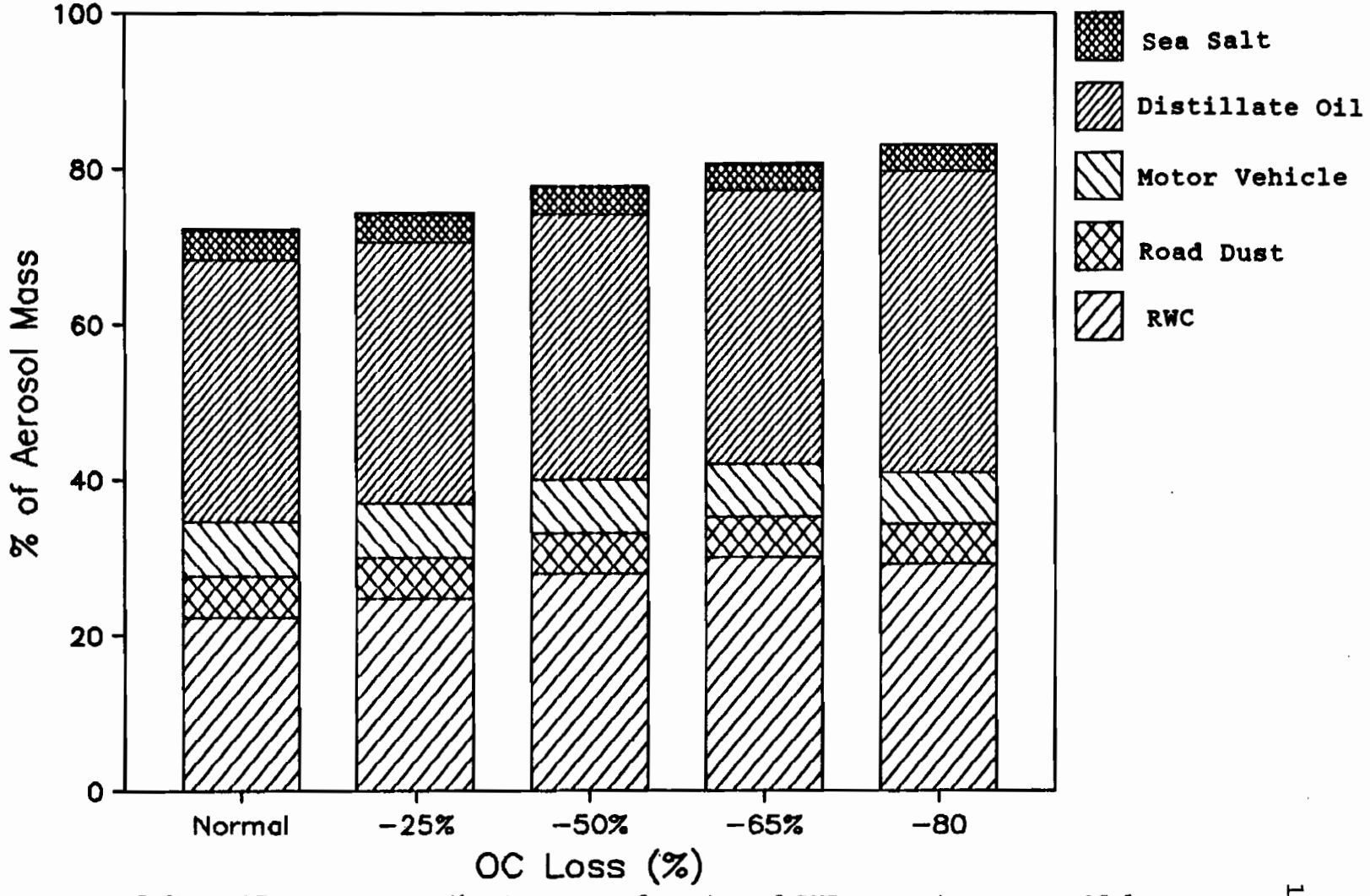

Figure 5.3B. CMB source contributions as a function of RWC composite source OC loss (SW Portland, 02/08/85).

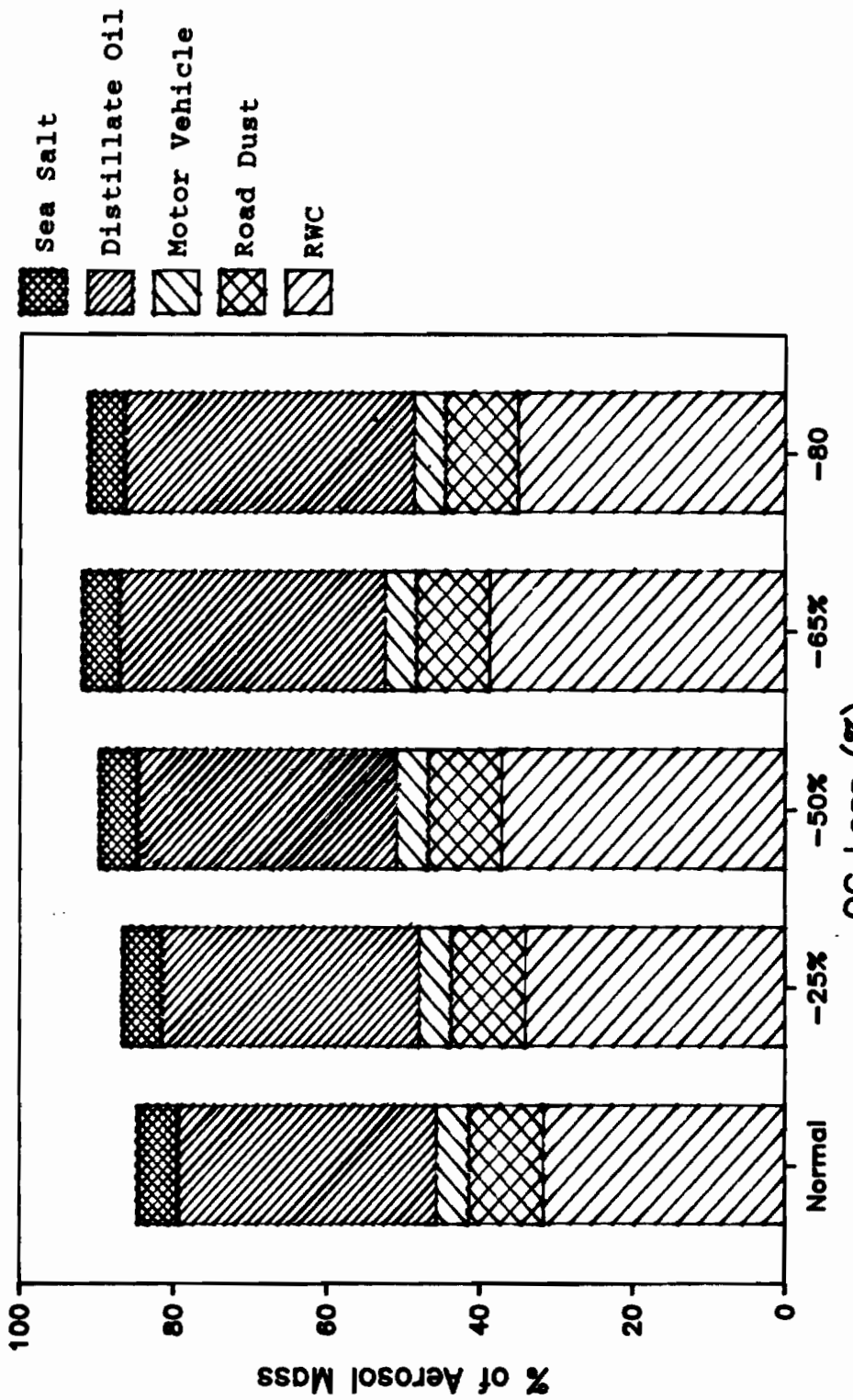

Figure 5.3C. CMB source contributions as a function of RWC composite source OC loss (southwest Portland, 2/14/85).

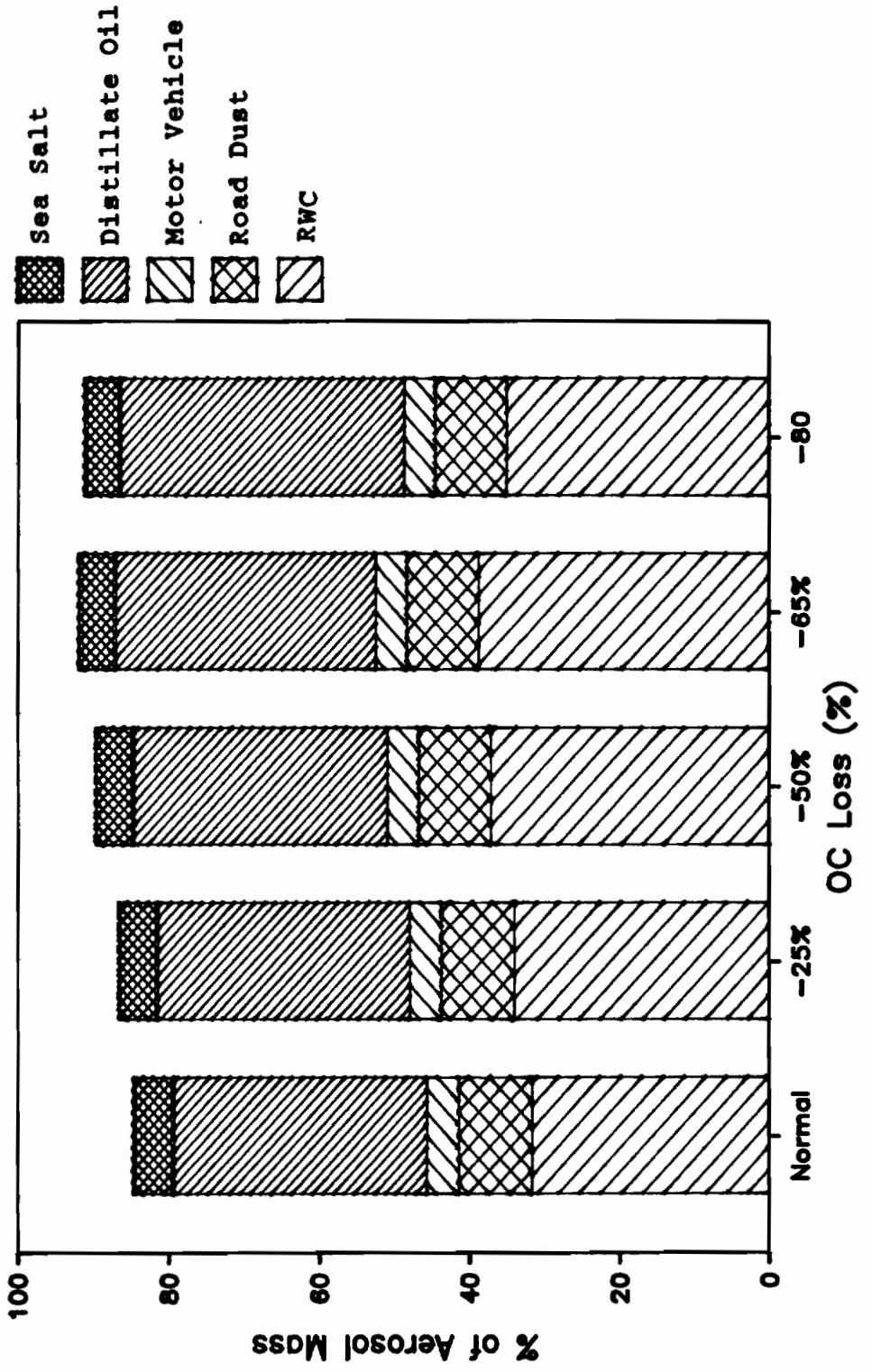

Figure 5.3D CMB Source Contribution As A Function of RCW Composite Source OC Loss (SW Portland, 2/20/85)

loss corresponding to the minimum X^2. In order to balance carbon, the other large carbon source, distillate oil combustion, was a minimum at this OC loss value. Road dust and motor vehicle contributions were almost unaffected by changes in RWC vapor carbon loss. Organic vapor loss for distillate oil burning and motor vehicle aerosol particles was not considered because particles from these sources were products of high temperature, turbulent combustion and were expected have small organic vapor loss potential. From the perspective of the CMB model the OC and EC ratio discrepancy could be reduced by assuming that the distillate oil burning particles had lost organic mass; however, the percentage loss amounts would have to be almost twice as large to accomplish the same effect as assuming that the RWC profile loses organic carbon because oil burning particles contain about half the organic carbon. Assuming that motor vehicle aerosols lose organic carbon would have essentially no effect because these aerosols contribute such a small fraction to the aerosol samples considered. The points to note are that RWC OC losses reduce or eliminate the OC and RC ratio discrepancy and that even large OC loses can be allowed without significantly affecting CMB model results. Therefore neglecting RWC OC loss will not introduce a large error into CMB results.

The CMB solutions using the composite RWC composition profile were constrained by the fact that the mix of hot and cool burning was specified. Tables 5.8A-D show CMB analyses for the case where the composite RWC composition profile was replaced by separate hot and cool burning RWC profiles. In these solutions the constraint of a specified hot and cool burn mix was removed. Table 5.3 shows that the

Table 5.8A

Comparisons of CMB Analyses Using Hot/Cool Composition Profiles

Site: SW Portland Residential Area Size: 10 μm			Mass loading = 21μg/m³	
Date:	2/5/85			
	Hot/Cool	-25% *	-50% *	-65%
Hot burn(%)	4.3±1.2	4.0±1.2	3.6±1.1	3.1±1.0
Cool burn(%)	28.3±7.4	33.8±8.6	44.0±10.8	56.7±13.6
Road Dust(%)	7.7±1.5	7.7±1.5	7.7±1.5	7.7±1.5
Motor Veh.(%)	6.0±1.1	6.0±1.1	6.1±1.1	6.1±1.1
Dist. Oil(%)	31.0±7.1	30.1±7.0	29.1±6.9	27.3±6.7
X^2	1.632	1.528	1.337	1.190
DF	9	9	9	9
Mass calc.(%)	77.4±7.7	81.7±8.2	90.5±9.0	100.9±10.0
OC Ratio**	1.04±0.09	1.05±0.08	1.05±0.08	1.04±0.07
EC Ratio**	0.66±0.09	0.69±0.08	0.75±0.13	0.82±0.16
TC Ratio**	0.91±0.11	0.92±0.11	0.94±0.10	0.96±0.10
K Ratio**	1.01±0.28	1.02±0.28	1.02±.27	1.03±0.27

Uncertainties are standard deviations.

* For CMB analysis organic carbon is decreased by percentage shown for RWC and tunnel sources.

** Ratio of CMB calculated/measured.

DF = Degrees of freedom

Table 5.8B

Comparisons of CMB Analyses Using Hot/Cool Composition Profiles

Site: SW Portland Residential Area Size: 10 μm			Mass loading = 9 μg/m³	
Date:	2/8/85			
	Normal	- 25% *	- 50% *	- 65% *
Hot burn(%)	3.5±1.2	3.3±1.1	3.0±1.1	2.6±1.0
Cool burn(%)	13.8±6.0	16.6±7.0	22.0±9.0	28.8±11.5
Road Dust(%)	5.2±1.0	5.2±1.0	5.2±1.0	5.1±1.0
Motor Veh.(%)	6.7±1.5	6.7±1.5	6.8±1.5	6.8±1.5
Sea Salt(%)	3.4±1.2	3.4±1.2	3.5±1.2	3.5±1.2
Dist. Oil(%)	37.9±9.1	37.3±9.1	36.0±9.3	34.6±9.5
X^2	1.120	1.111	1.102	1.099
DF	6	6	6	6
Mass calc.(%)	70.5±7.0	72.4±7.2	76.4±7.6	81.5±8.1
OC Ratio**	1.00±0.13	1.01±0.13	1.00±0.12	1.00±0.12
EC Ratio**	0.91±0.17	0.92±0.17	0.95±0.17	0.99±0.19
TC Ratio**	0.97±0.18	0.98±0.18	0.98±0.17	1.00±0.16
K Ratio**	1.02±0.27	1.02±0.28	1.01±0.27	1.00±0.25

Uncertainties are standard deviations.

* For CMB analysis organic carbon is decreased by percentage shown for RWC and tunnel sources.

** Ratio of CMB calculated/measured.

DF = Degrees of freedom

Table 5.8C

Comparisons of CMB Analyses Using Hot/Cool Composition Profiles

Site: SW Portland Residential Area Size: 10 μm			Mass loading = 23 μg/m³	
Date:		2/14/85		
	Normal	- 25% *	-50% *	- 65% *
Hot burn(%)	3.5±1.1	3.2±1.0	2.7±1.0	2.3±0.9
Cool burn(%)	24.2±7.0	28.6±8.1	36.9±10.2	46.5±12.7
Road Dust(%)	9.6±1.6	9.6±1.6	9.6±1.6	9.6±1.6
Motor Veh.(%)	4.1±0.9	4.1±0.9	4.2±0.9	4.2±0.9
Sea Salt(%)	5.0±1.4	5.1±1.4	5.2±1.5	5.2±1.5
Dist. Oil(%)	35.2±7.6	34.4±7.6	33.0±7.6	31.8±7.7
X^2	0.779	0.768	0.777	0.834
DF	6	6	6	6
Mass calc.(%)	81.6±8.1	84.9±8.4	91.5±9.1	99.6±9.6
OC Ratio**	1.01±0.17	1.01±0.09	1.00±0.09	0.98±0.09
EC Ratio**	0.93±0.17	0.95±0.18	1.01±0.20	1.09±0.24
TC Ratio**	0.99±0.14	0.99±0.14	1.00±0.14	1.02±0.13
K Ratio**	1.01±0.24	1.01±0.24	1.00±0.23	0.99±0.22

Uncertainties are standard deviations.

* For CMB analysis organic carbon is decreased by percentage shown for RWC and tunnel sources.

** Ratio of CMB calculated/measured

DF = Degrees of freedom

Table 5.8D

Comparisons of CMB Analyses Using Hot/Cool Composition Profiles

Site: SW Portland Residential Area Size: 10 μm			Mass loading = 22 μg/m³	
Date:	2/20/85			
	Normal	-25% *	-50% *	-65% *
Hot burn(%)	2.9±0.9	2.7±0.9	2.4±0.8	2.2±0.8
Cool burn(%)	13.2±6.7	15.7±7.8	20.6±9.9	26.2±12.6
Road Dust(%)	17.9±2.8	17.9±2.9	17.9±2.8	17.9±2.8
Motor Veh.(%)	10.0±1.7	10.0±1.7	10.1±1.7	10.1±1.7
Sea Salt(%)	1.5±0.6	1.5±0.6	1.5±0.6	1.5±0.6
Dist. Oil(%)	40.5±9.2	39.9±9.2	38.9±9.3	37.9±9.5
X^2	0.298	0.294	0.293	0.305
DF	7	7	7	7
Mass calc.(%)	86.0±8.6	87.8±8.8	91.4±9.1	96.0±9.6
OC Ratio**	1.00±0.13	1.00±0.13	1.00±0.13	0.99±0.12
EC Ratio**	0.96±0.18	0.97±0.18	1.00±0.18	1.04±0.19
TC Ratio**	0.99±0.18	0.99±0.17	1.00±0.17	1.00±0.17
K Ratio**	1.00±0.23	1.00±0.23	1.00±0.22	0.99±0.21

Uncertainties are standard deviations.

* For CMB analysis organic carbon is decreased by percentage shown for RWC and tunnel sources.

** Ratio of CMB calculated/measured.

DF = Degrees of freedom

compositions of these two sources are very different. Their use together introduces no multicollinarity instability into the CMB solution. The degree to which sources are multicollinear can be examined by using the singular value decomposition feature of the CMB program (Henry, 1982).

Column one of Tables 5.8A-D shows that the hot wood stove aerosol fraction of total wood stove aerosol ranges from 3 to 5% of the measured aerosol mass or from 15 to 24% of the total RWC contribution. Survey data (Cummings, 1982) have indicated that 19% of wood stoves were operated with dampers fully open, 44% partially open, and 25% barely open or closed. For the case of 25% hot burning and 75% cool burning 7% of the wood smoke aerosol would be expected to be contributed by hot burning. Test data in this research indicated that only operation with the damper fully open and with fuel loads that were 25% or less of stove capacity produced hot burn aerosols. Aerosols resulting from damper partially open operation had compositions very similar to aerosols from damper closed stove operation (cool burn aerosols) except that trace element concentrations for these aerosols were slightly higher than for cool burn aerosols. The presence of a large number of stoves operating with dampers partially open would have the same effect on ambient aerosol composition as a slight increase in the number of hot burning stoves. Thus somewhat more that 7% of RWC aerosols would be expected to be contributed by hot burning and the rest by cool burning. The fact that CMB analysis indicated that 15-24% of RWC aerosol was from hot burning is not unreasonable. It will be shown below that when organic carbon loss was incorporated into hot and

cool burn CMB analyses that the percentage of hot burning calculated approaches 7%.

CMB solutions which used the hot/cool RWC profile always showed lower RWC contributions than solutions which used the composite profile; however, the differences were not greater than the one standard deviation. The hot/cool solutions also had lower X^2 values than the composite solutions. The contributions of other sources were not significantly different when either the composite or hot/cool profiles were used.

In general, based on OC, EC, and K ratio values, normal CMB solutions which used the hot/cool RWC composition profiles accounted better for carbon and trace element species than solutions which used the composite RWC composition profile. The closer the source profiles used in CMB modeling approach the compositions of aerosol sources as they actually exist at the receptor the better the model can fit the ambient data. This can be achieved either by allowing organic carbon loss when the RWC composite source profile is used or by using hot and cool RWC profiles even without allowing organic carbon loss and of course most effectively achieved by using both procedures at once.

Columns 2-4 in Tables 5.8A-D give the CMB results obtained by including 25, 50, and 65% organic carbon loss hot/cool RWC source composition profiles. Figures 5.4A-D like Figures 5.2A-D show OC, EC, and K ratio values and X^2 values as a function of organic carbon loss. These figures show that using hot and cool RWC source profiles in CMB modeling usually caused OC, EC and K ratio values to be close to one over the organic carbon loss range of 0 to about 50%. Also except for

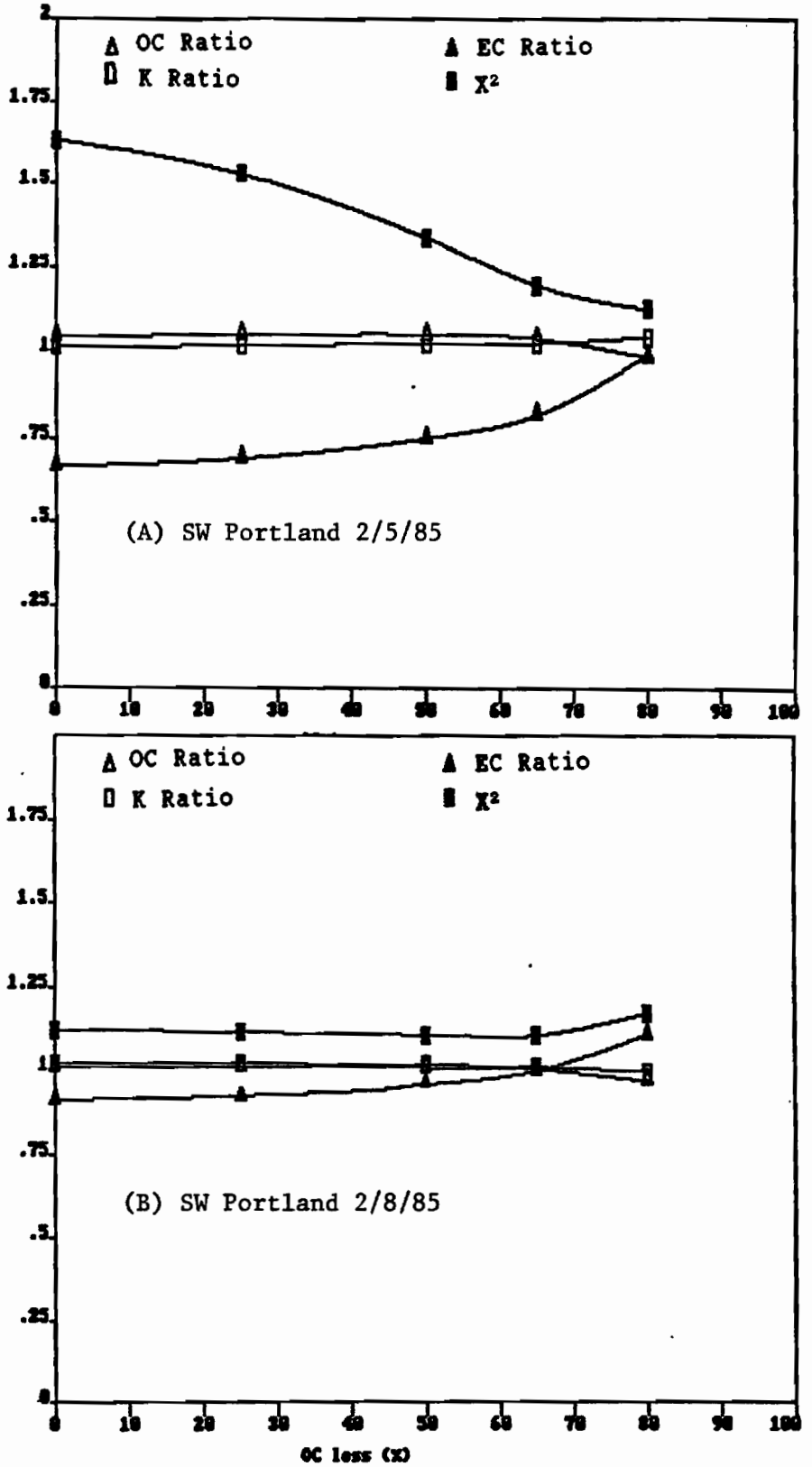

Figure 5.4 The Variation of CMB Model Outputs As A Function of RWC Hot/Cool Source OC Loss

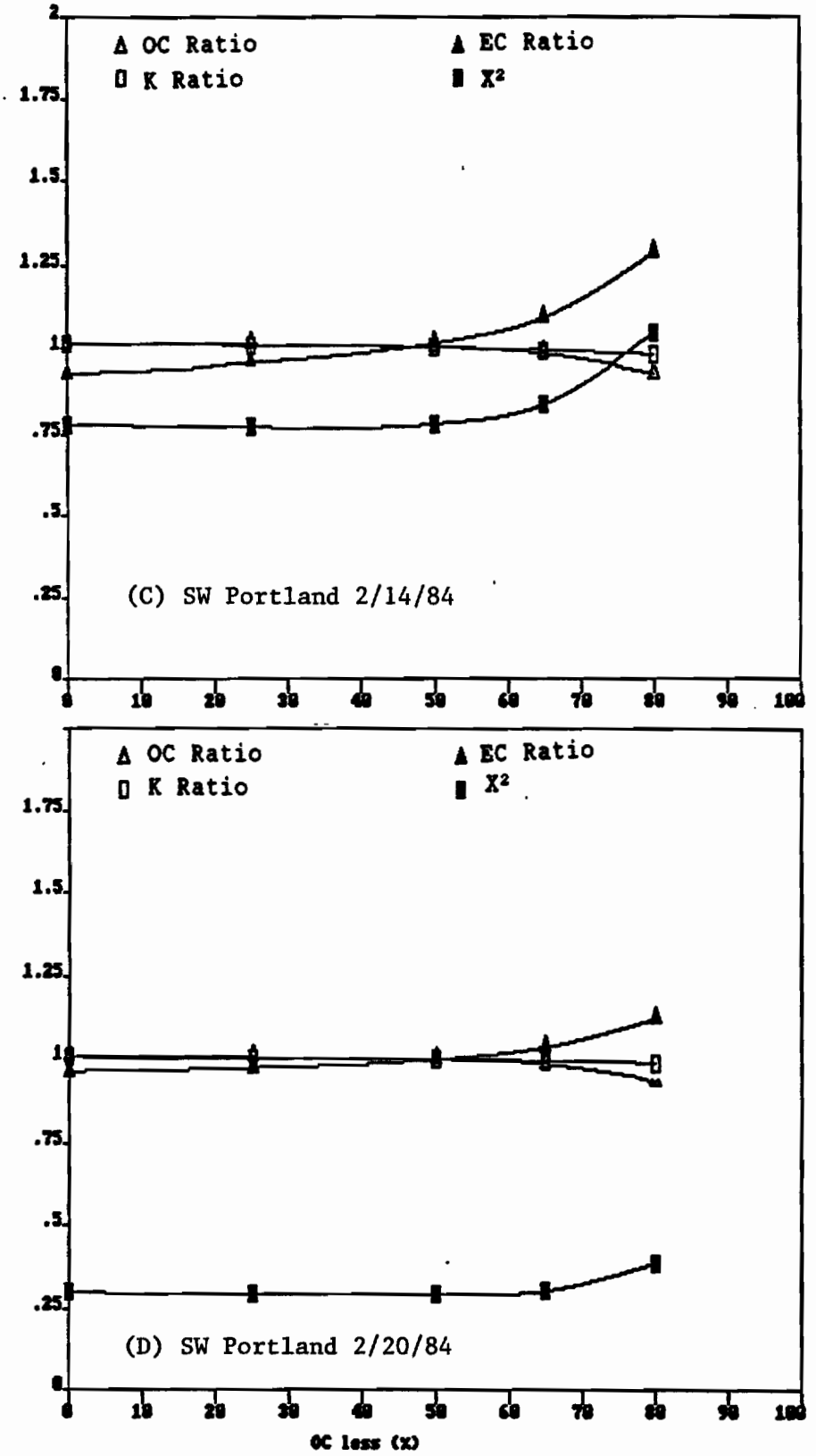

Figure 5.4 The Variation of CMB Model Outputs
As A Function of RWC Hot/Cool Source OC Loss

Figure 5.4A X^2 maintained a constant minimum value up to about 50% and then increased at higher OC loss values. Unlike Figures 5.2A-D Figures 5.4A-D do not indicate an OC loss value where the CMB solution is optimized even though they show that OC, EC, and K ratio values do have a common value near one in the range of 50 to 70% organic carbon loss and that at higher carbon loss values X^2 values increase. Figure 5.4A shows a X^2 minimum at about 70% OC loss. Figures 5.2B-D indicate that OC loss values as high as about 50% can exist before the model fit starts to degrade. When hot/cool RWC composition profiles are used, CMB modeling results do not indicate that OC loss does occur but they do not indicate that it doesn't occur either. The concept of RWC carbon loss should not be viewed as evidence that RWC particles loose organic carbon but during their atmospheric residence time but rather that such losses are possible without causing major perturbations in CMB results.

Figures 5.5A-D show the distribution of source contributions as a function of organic carbon loss. These figures show that the cool burn contribution computed by the CMB model increased quite dramatically with increasing organic carbon loss. These figures also show that at organic carbon loss values greater than the value at which the OC and EC ratio values were equal (where the value of X^2 starts increasing as shown by Figures 5.5A-D) the total source contributions given by CMB modeling can exceed 100% of the measured aerosol. The organic carbon loss value at which the sum of the CMB source contributions exceeds 100% provides an upper limit to the organic carbon loss values that can be considered possible.

Table 5.9 shows CMB results (Wstove) for the four February 1985

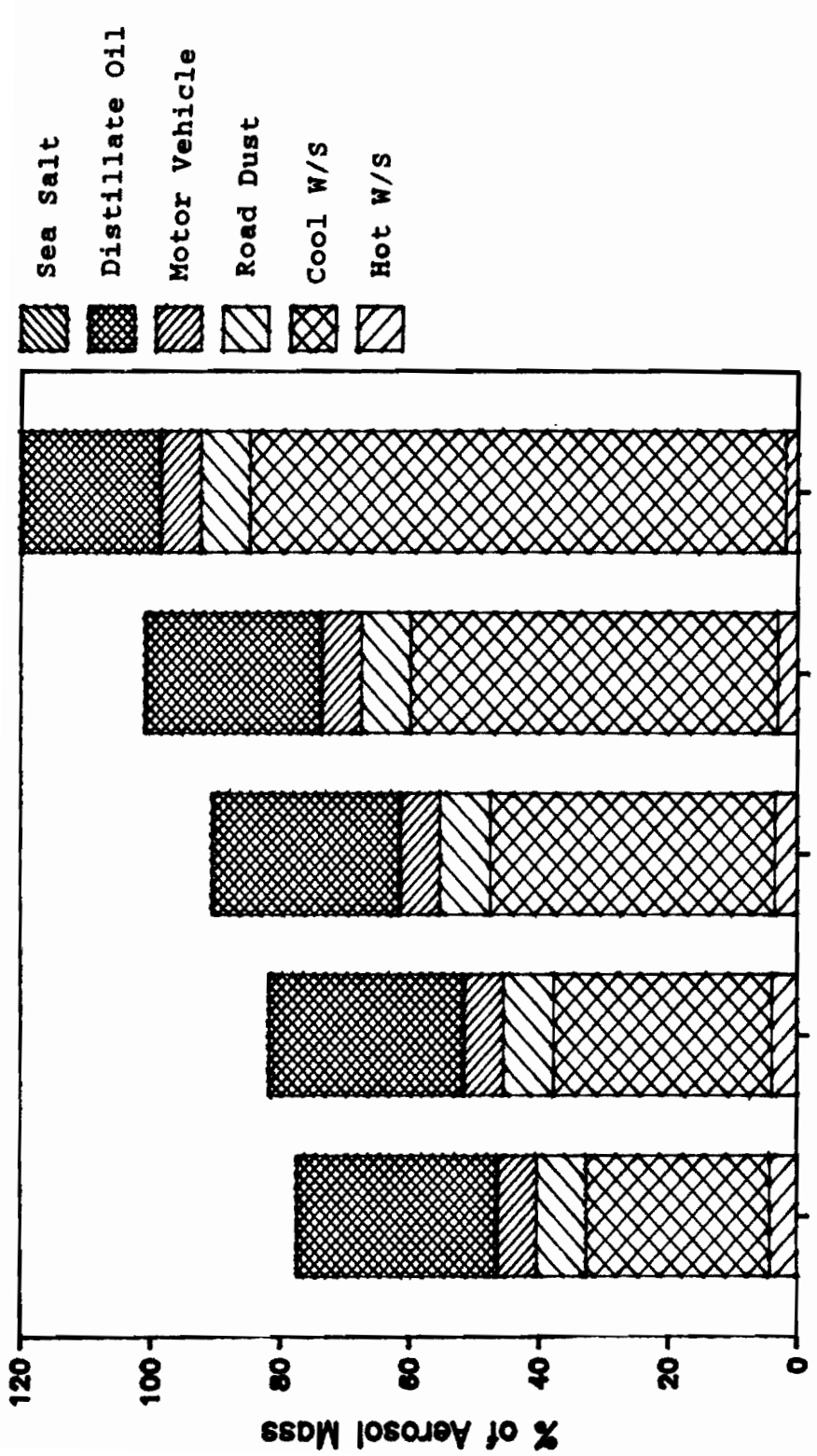

Figure 5.5A. CMB source contributions as a function of RWC hot/cool source OC loss (southwest Portland, 2/5/85).

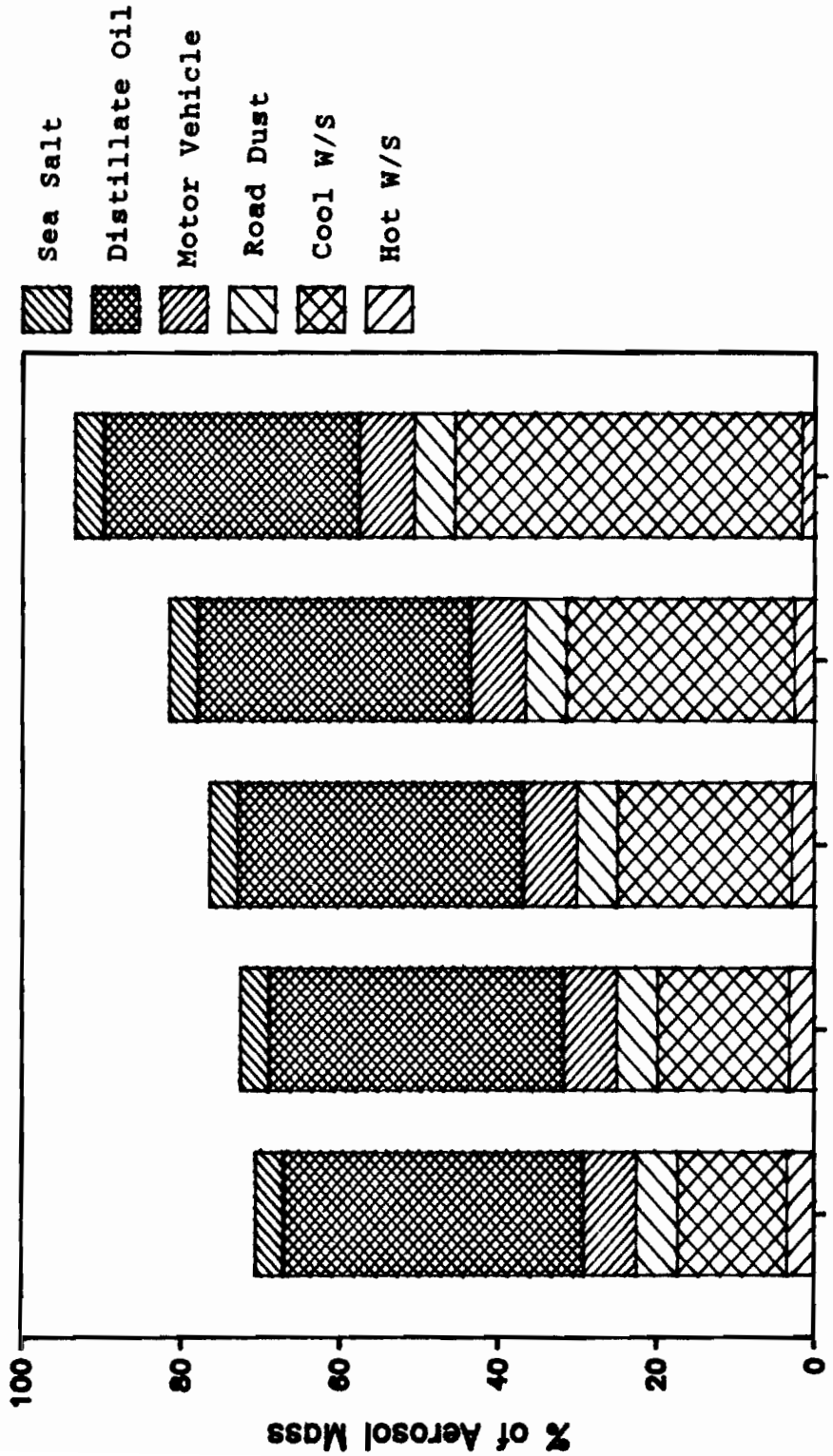

Figure 5.5B. CMB source contributions as a function of RWC hot/cool OC loss (SW Portland, 02/08/85).

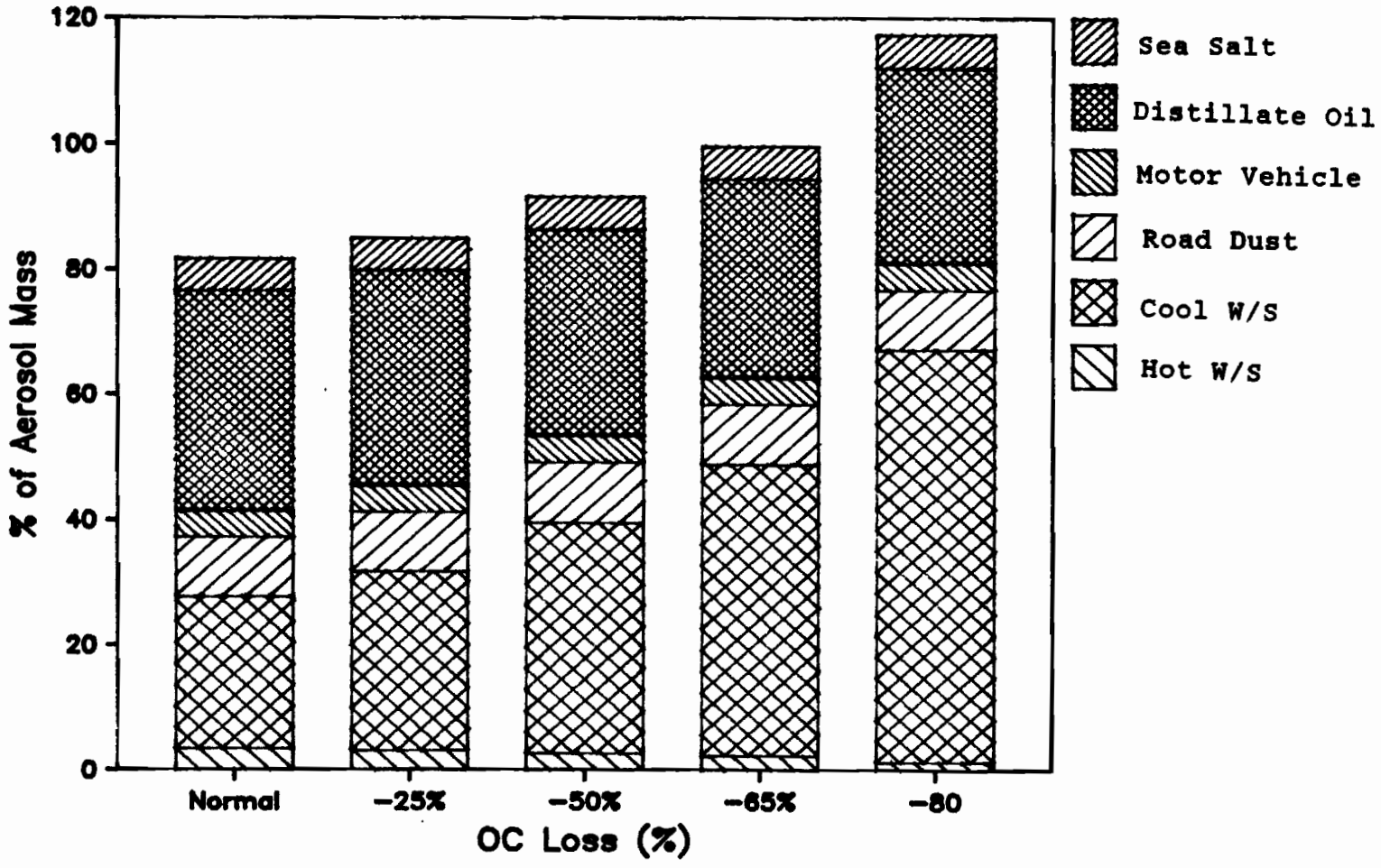

Figure 5.5C CMB Source Contributions As A Function of RWC Hot/Cool OC Loss (SW Portland 2/14/85)

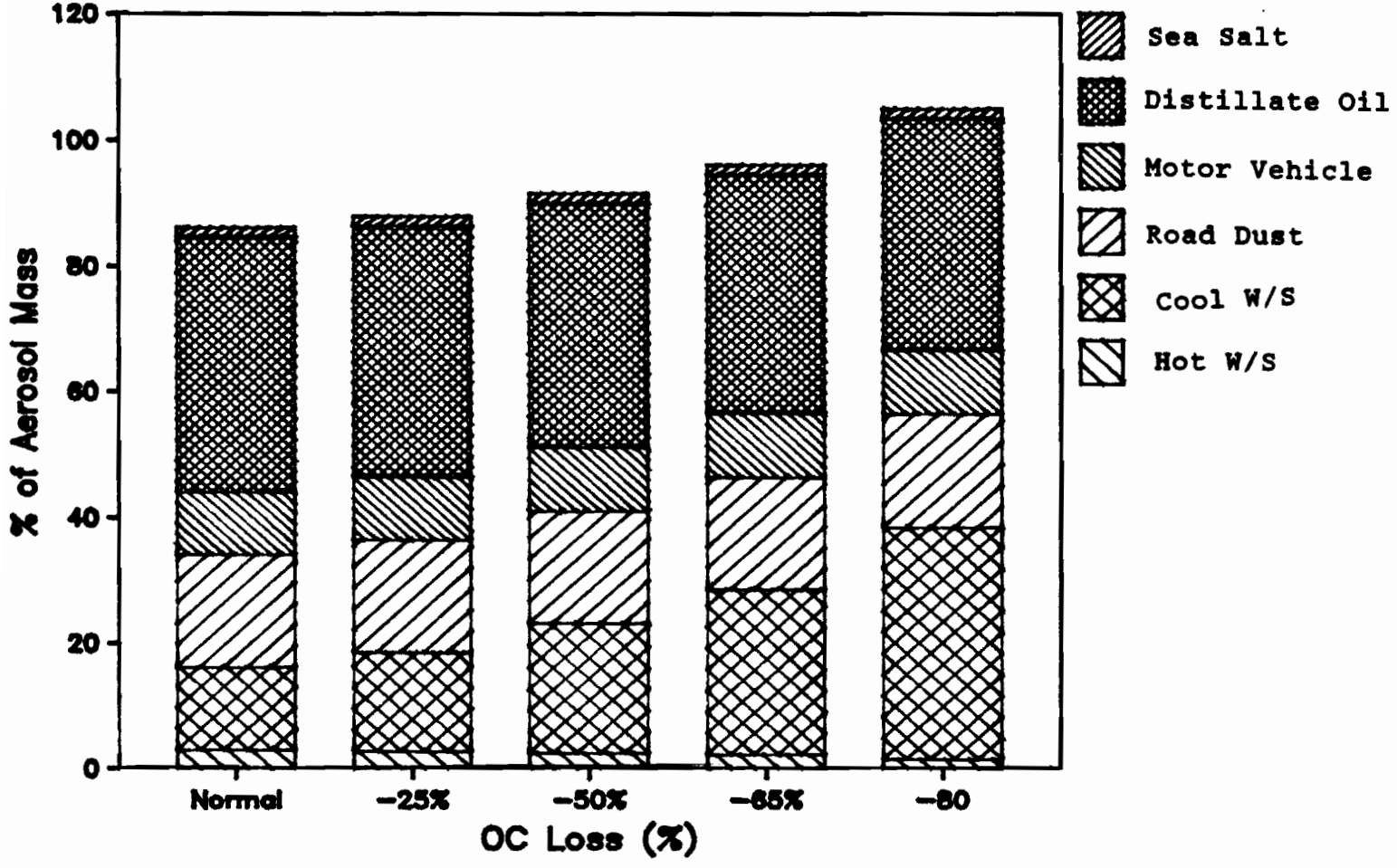

Figure 5.5D CMB Source Contributions As A Function of RWC Hot/Cool OC Loss, (SW Portland, 2/20/85)

TABLE 5.9

CMB Analyses Using the EPA Wood Smoke Composition Profile

Site: Portland Residential Area Size: 10 μm.				
	2/5/85	2/8/85	2/14/85	2/20/85
WStove(%)	51.5±10.4	33.6±8.4	42.3±8.7	32.3±5.9
Road dust(%)	8.2±1.5	5.5±1.0	9.9±1.6	18.8±2.9
Motor Veh.(%)	6.3±1.2	7.1±1.5	4.2±0.9	10.4±1.8
Sea salt(%)	-----	3.7±1.2	5.2±1.5	1.5±0.5
Dist oil(%)	22.3±6.1	29.8±9.0	31.8±7.8	34.1±8.9
X^2	1.760	1.451	0.961	0.663
DF	10	7	7	8
OC Ratio**	1.33±0.51	1.37±0.47	1.27±0.43	1.34±0.41
EC Ratio**	0.89±0.46	1.07±0.46	1.24±0.65	1.14±0.44
TC Ratio**	1.17±0.26	1.26±0.28	1.26±0.28	1.27±0.26
K Ratio**	0.87±0.11	0.78±0.09	0.90±0.11	0.89±0.13
Mass calc(%)	88.3±8.8	79.7±7.9	93.4±9.3	97.0±9.7

Uncertainties are standard deviations.

The "Wstove" source used the EPA RWC composition profile.

* For CMB analysis organic carbon is decreased by the percentage shown for the RWC sources.

** Ratio of CMB calculated/measured

DF = Degrees of freedom

Portland residential area samples using the EPA RWC composition profile. These results are quite similar to those given by Table 5.7A-D except that the Table 5.7 solutions more effectively fit carbon data especially if the 50% organic vapor loss solutions are used in the comparison. Since the EPA RWC profile has a high similarity with ambient aged RWC particles it is valid to make the comparison with the composite 50% loss solution, i.e., the EPA RWC source profile represents wood smoke particles which have lost some organic carbon during their atmospheric residence time.

Table 5.10 compares CMB computed RWC source contributions using RWC normal and 25 and 50% organic carbon loss composition profiles with RWC contributions computed by using the EPA RWC source profile. For this group of samples the EPA RWC source profile resulted in higher RWC contributions in all cases, though the difference was less as the organic carbon loss value increased. The hot-cool composition profiles always yielded the lowest RWC contribution. Other source contributions were similar. Note that the differences were minimized by making the comparison using RWC contributions computed with RWC composition profiles which included a 50% organic carbon loss. This is not surprising because the EPA RWC composition profile was chosen from available source data by its similarity to an ambient aerosol which was expected to be composed almost exclusively of wood smoke. If wood smoke particles loose organic carbon during their ambient residence time such an aerosol would be composed of particles that had lost some of their organic carbon.

It should not be expected that using the RWC composite or the hot

TABLE 5.10

Comparison of RWC Contributions Obtained by Using

Different RWC Composition Profiles in CMB Modeling

	Normal	-25%	-50%	EPA
2/5/85				
Composite(%)	37.5±7.7	40.8±8.4	45.2±9.6	51.5±10.4
Hot-Cool(%)	32.6±7.5	37.8±8.7	47.6±10.8	
Hot/Total(%)	13.2	10.6	7.6	
2/8/85				
Composite(%)	22.3±5.7	24.7±6.3	28.0±7.4	33.6±8.4
Hot-Cool(%)	17.3±6.2	19.9±7.1	25.0±9.0	
Hot/Total(%)	20.2	16.6	12.0	
2/14/85				
Composite(%)	31.6±6.7	34.0±7.4	37.1±7.6	42.3±8.7
Hot-Cool(%)	27.7±7.1	31.8±7.1	39.6±10.2	
Hot/Total(%)	12.6	10.1	6.8	
2/20/85				
Composite(%)	22.5±5.9	24.3±6.3	25.4±7.0	32.3±7.3
Hot-Cool(%)	16.1±6.8	18.4±7.8	23.0±9.9	
Hot/Total(%)	18.0	14.7	10.4	

Uncertainties are standard deviations.

For Composite and Hot-Cool percentages are percent of aerosol mass

Hot/Total(%) is the percentage that the hot burn CMB contribution is of the total RWC contribution

and cool profiles in CMB analysis will always result in lower RWC contributions than using the EPA source profile. The differences in RWC source contributions that result from using different RWC composition profiles depend on how well the composition profiles characterize ambient aerosols. A practical approach might be to consider that the true RWC contribution lies between the values given by using the various profiles. On the other hand since carbon usually comprises over 50% of wood burning emissions and it can be analytically well quantified the CMB analysis which best accounts for carbon can be considered most valid if no unknown sources of aerosol carbon exist.

X^2 values obtained using the EPA profile were similar to those obtained using the composite RWC profile developed in this research but the total carbon and usually OC and EC were not as well fit by this solution. This is shown by examining OC, EC, and TC ratio values.

Table 5.10 also gives the percentage of the total RWC contribution that was contributed by hot burning (Hot/Total(%)). This percentage decreases for increasing organic carbon loss and was near 7% for CMB solutions which used hot and cool RWC profiles which allowed a 50% organic carbon loss. According to survey data and the relative emission strengths of hot and cool RWC burning about 7% of emissions would be expected to be contributed by hot burning. This result is consistent with previously presented evidence which indicated organic carbon loss in the area of 50% was reasonable for these samples.

The points illustrated by the CMB analyses shown in Tables 5.7A-D and 5.8A-D are: (1) hot and cool burning profiles can be resolved as separate sources by the CMB model and they more effectively account for

trace elements and carbon than using the composite profile; (2) the RWC contributions calculated by using the RWC composite composition profile were similar to the sum of the hot and cool burn contributions; (3) the contributions of non-RWC sources were not affected by using different RWC composition profiles; (4) allowing up to 50% organic carbon loss in RWC composition profiles may improved CMB solutions and does not result in major changes in any source contributions; and, (5) road dust and motor vehicle emissions could be resolved as separate sources.

5.3.2 COMPARISON OF AMBIENT AND CALCULATED PARTICULATE CARBON SIZE DISTRIBUTIONS FOR SW PORTLAND 10 μm SAMPLES

The atmospheric stability of combustion generated OC and EC size distributions was examined by comparing ambient OC and EC distributions with calculated distributions for these sources determined from CMB results and emission size distributions. The combustion sources considered were RWC, residential oil burning, and motor vehicles. Road dust was not included because its size distribution was not known, its contribution to ambient aerosol was low, and its carbon content (OC ~ 11%, EC ~1%) was low. Calculated OC and EC distributions were determined by taking OC and EC source contributions computed by the CMB model and distributing them according to the measured emission distribution for the respective sources. For RWC emissions it was assumed that 2/3 of the wood burned were burned in stoves and 1/3 was burned in fireplaces and that 75% of the wood burned in stoves was burned in the cool burning mode while 25% was burned in the hot burning mode.

The computation was done by multiplying CMB-determined source contributions ($\mu g/m^3$) by the appropriate OC/M and EC/M values to obtain the OC and EC contributions for each source to the 10-2.5, 2.5-0.6, 0.6-.03, and <0.3 μm size ranges. These contributions for normal CMB solutions were added for each size range to give the calculated data column in Tables 5.11A-B. These tables show both the ambient and calculated OC and EC distributions for February 1985 SW Portland samples. The data are shown graphically in Figures 5.6A-D. The form of the distributions was similar for all the samples even though the magnitude of the source contributions was different for different samples. The OC distributions were dominated by RWC emissions while the EC distributions were dominated by distillate oil burning emissions. Except for the 2/5/84 sample the CMB sources accounted for almost all the measured OC and EC, i.e., the calculated and ambient OC or EC distributions contain the same amount of OC and EC, respectively. For the 2/5/84 sample there seems to be a large unknown EC contribution to the 0.6-2.5 μm size range.

The CMB derived and ambient distributions are reasonably similar but do show some differences which can be explained by considering aerosol processes which can occur in the atmosphere. Comparing ambient and calculated distributions shows that for OC (except for the 2/8/85 sample) and to a lesser degree for EC the calculated carbon value in the size range <0.3 μm was larger than the ambient carbon value in this size range and the calculated carbon values in the size ranges >0.3 μm were less than the ambient carbon values. These results can be explained by considering that particulate mass shifting from below 0.3

Table 5.11A

Comparison of Calculated and Ambient Organic Carbon Over the Sampled Size Range (μg/m³)

Size Range μm.	Calculated	Ambient
Date: 2/5/85.		
<0.3	2.19	1.22
0.3-0.6	1.03	1.87
0.6-1.2	1.07	1.65
1.2-2.5	0.34	0.08
2.5-10	0.23	0.08
Date: 2/8/85		
<0.3	0.79	0.77
0.3-0.6	0.35	0.42
0.6-1.2	0.27	0.26
1.2-2.5	0.11	0.10
2.5-10	0.07	0.06
Date: 2/14/85		
<0.3	2.74	1.81
0.3-0.6	1.28	1.77
0.6-1.2	1.20	2.15
1.2-2.5	0.40	0.57
2.5-10	0.25	0.21
Date: 2/20/85		
<0.3	2.00	0.89
0.3-0.6	0.87	1.29
0.6-1.2	0.58	2.03
1.2-2.5	0.27	0.91
2.5-10	0.18	0.12

Table 5.11B

Comparison of Calculated and Ambient Elemental Carbon Over the Sampled Size Range (μg/m³)

Size Range μm.	Calculated	Ambient
Date: 2/5/85.		
<0.3	0.94	0.85
0.3-0.6	0.47	0.81
0.6-1.2	0.16	0.93
1.2-2.5	0.07	0.03
2.5-10	0.06	0.03
Date: 2/8/85		
<0.3	0.42	0.38
0.3-0.6	0.21	0.19
0.6-1.2	0.06	0.20
1.2-2.5	0.03	0.05
2.5-10	0.02	0.05
Date: 2/14/85		
<0.3	1.25	0.94
0.3-0.6	0.62	1.05
0.6-1.2	0.18	0.42
1.2-2.5	0.08	0.10
2.5-10	0.06	0.07
Date: 2/20/85		
<0.3	1.17	0.79
0.3-0.6	0.56	0.74
0.6-2.5	0.15	0.63
1.2-2.5	0.09	0.08
2.5-10	0.08	0.07

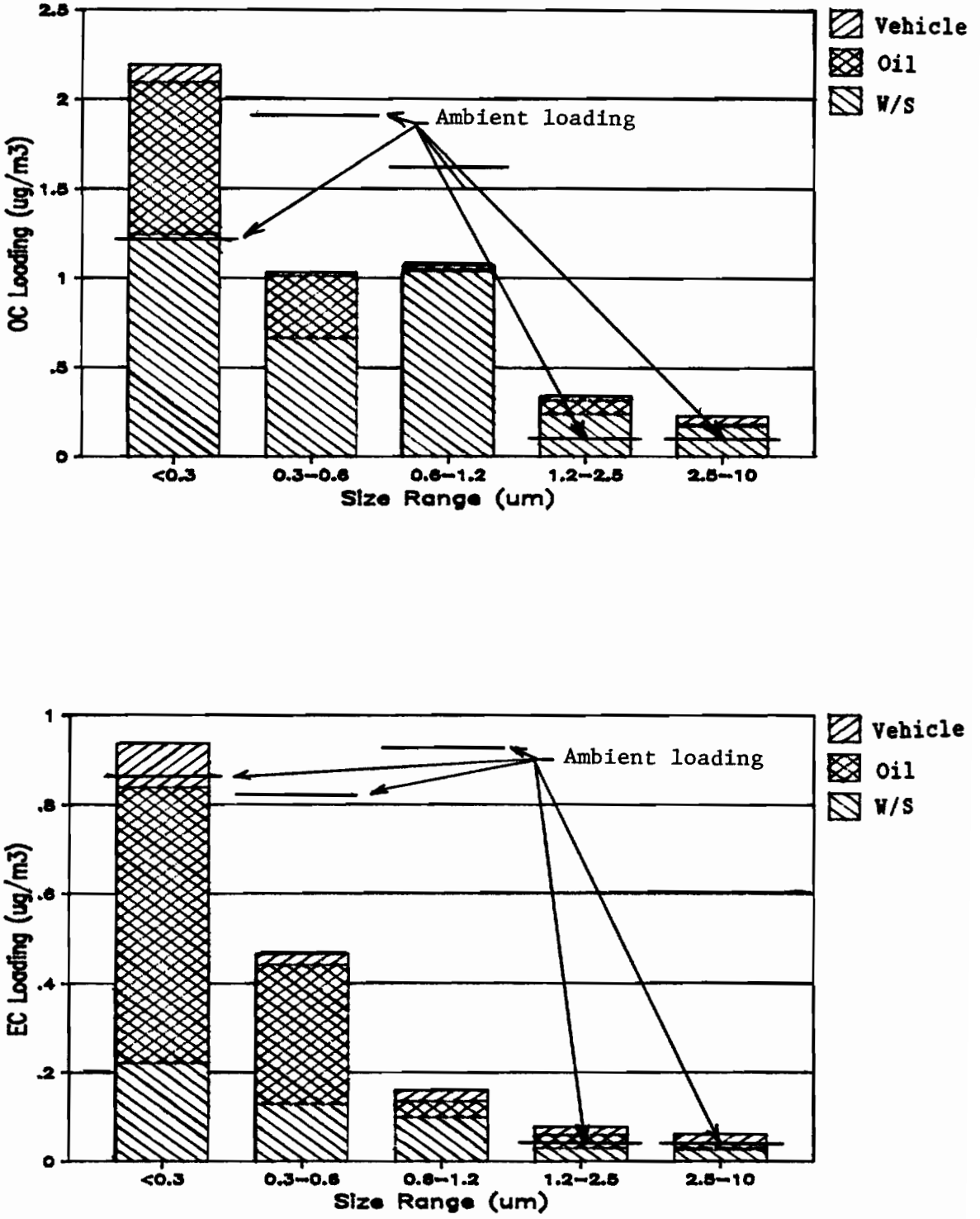

Figure 5.6A. A comparison of ambient organic and elemental carbon loadings with organic and elemental source contributions computed using the CMB model (histogram) (Portland residential area, 02/05/85).

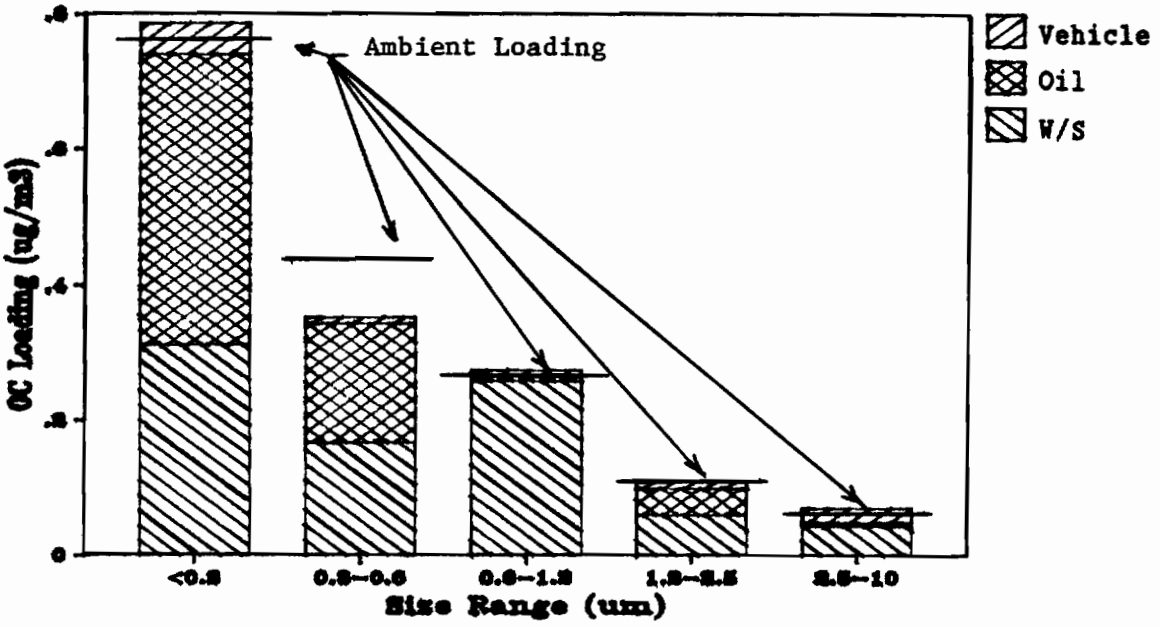

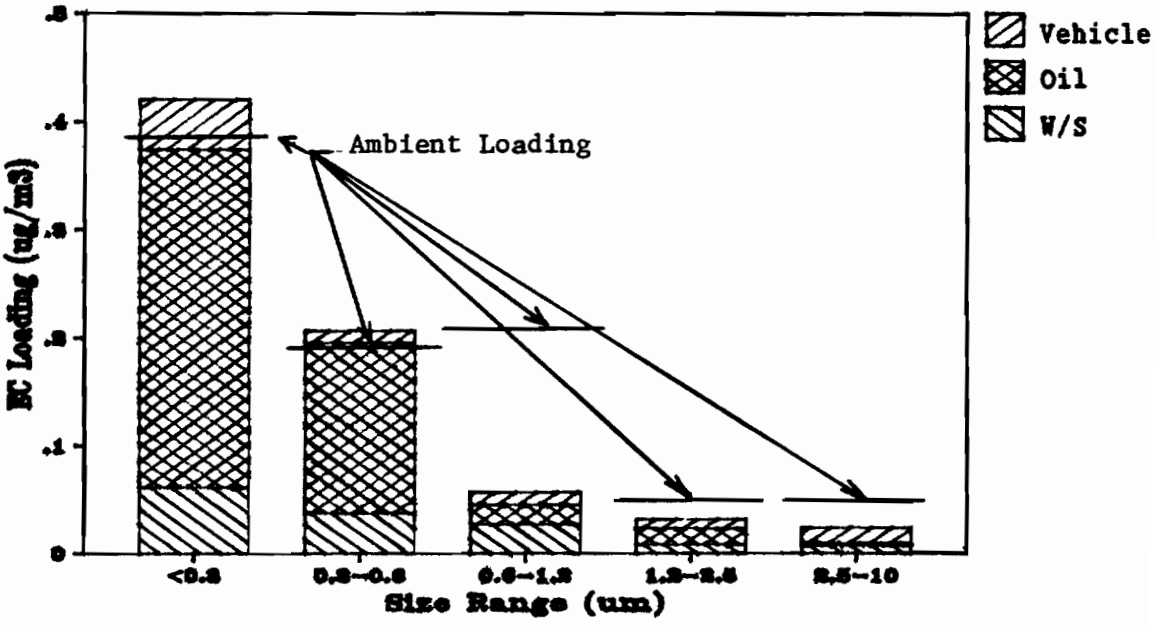

Figure 5.6B. A comparison of ambient organic and elemental carbon loadings with organic and elemental source contributions computed using the CMB model (histogram) (Portland residential area, 02/08/85).

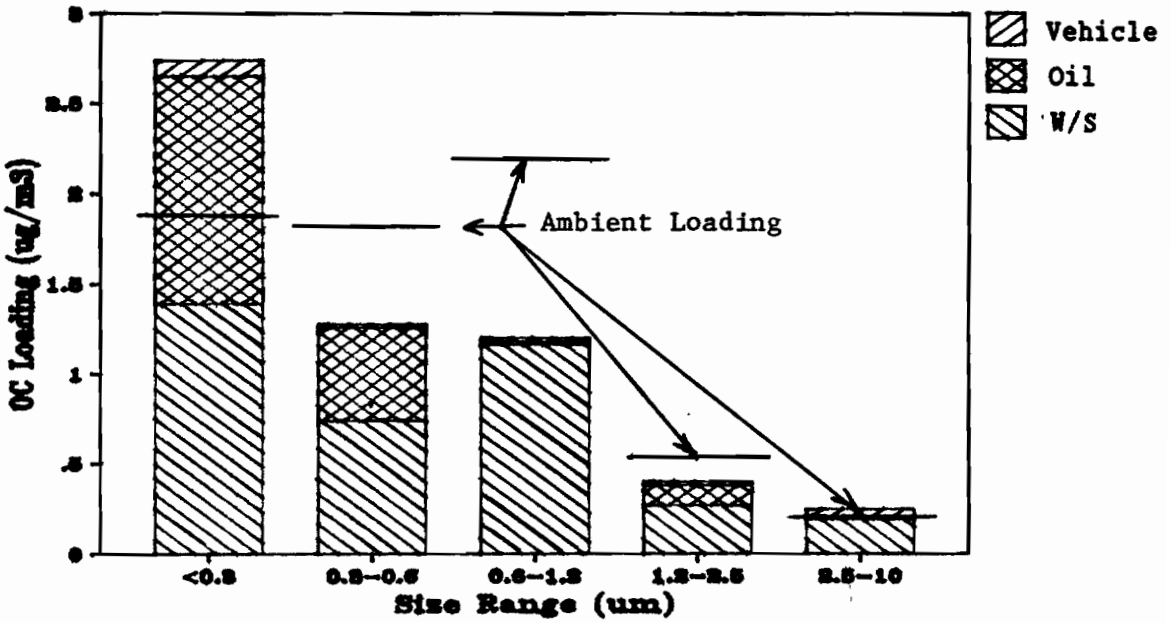

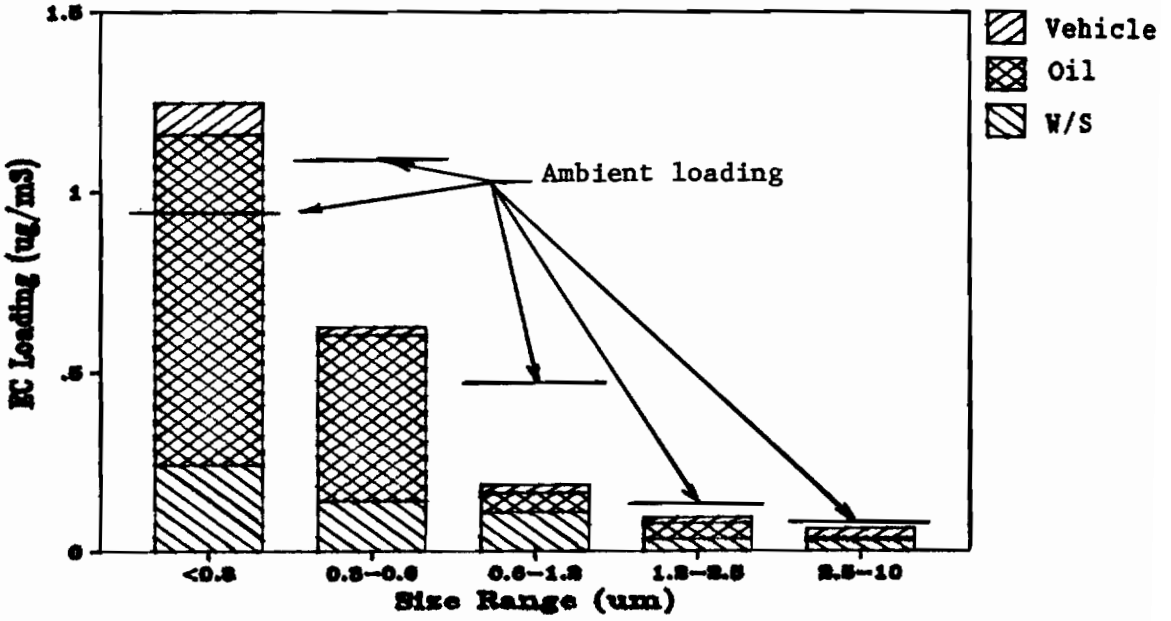

Figure 5.6C. A comparison of ambient organic and elemental carbon loadings with organic and elemental source contributions computed using the CMB model (histogram)(Portland residential area, 02/14/85).

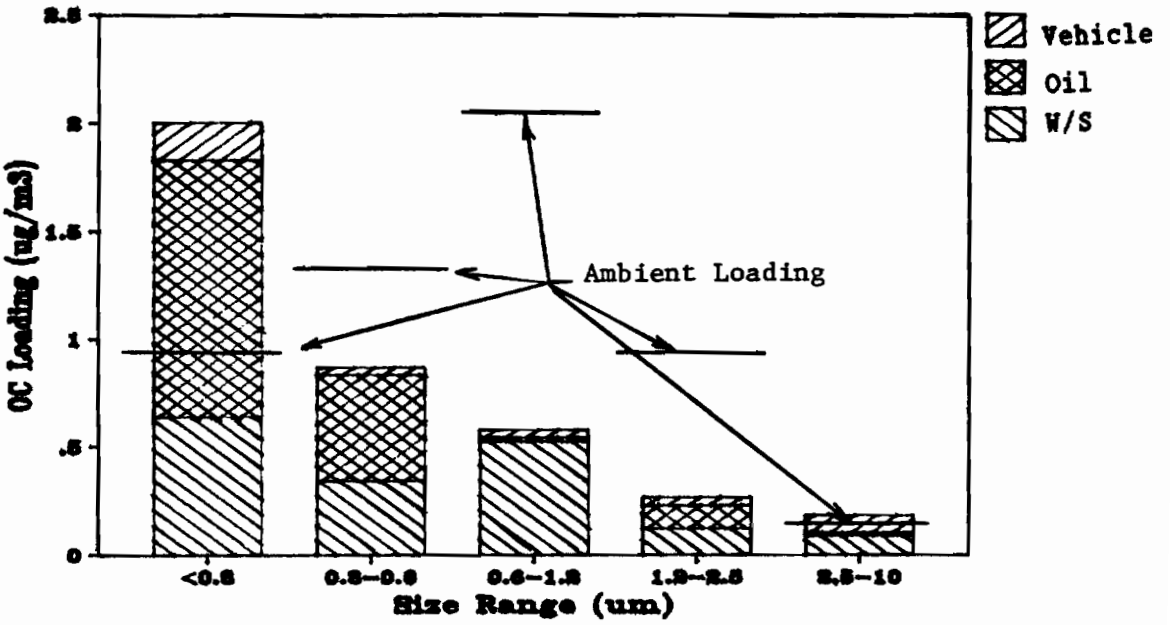

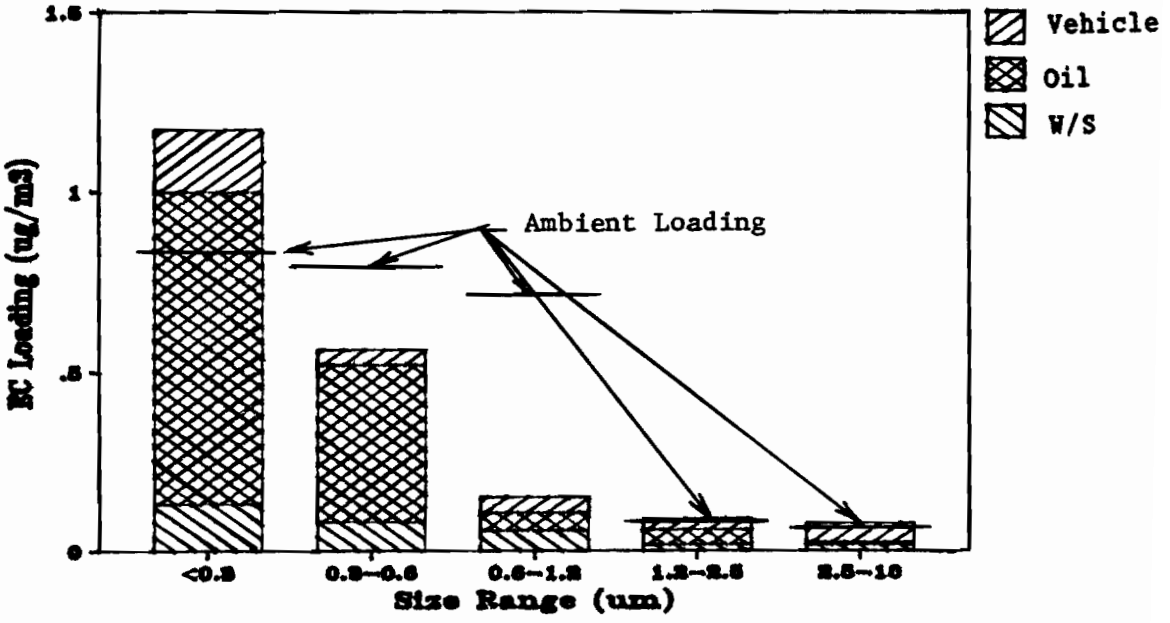

Figure 5.6D. A comparison of ambient organic and elemental carbon loading with organic and elemental source contributions computed using the CMB model (histogram) (Portland residential area, 02/20/85).

μm to above 0.3 μm occurred by coagulation during the atmospheric residence time of these particles. Since heterogeneous coagulation is more likely to occur than homogeneous coagulation particles <0.3 μm are much more likely to coagulate with particles >0.3 μm than they are with particles near their own size. This process transfers mass from <0.3 μm to >0.3 μm.

RWC particles losing organic carbon were mostly from cool burning and can be considered to be spherical particles, i.e., liquid drops which can lose volume as a result of OC loss and still maintain a spherical shape. That cool burn particles are liquid is indicated by the observation that the impaction spot resulting from cool burn particles impacting on an impaction plate looks like a drop of heavy oil and is liquid when smeared. Therefore a 50% OC loss will cause about a 25% decrease in particle volume because OC makes up about 50% of particle volume (assuming the density of all particle constituents are approximately equal). The ratio of new diameter to original diameter for particles losing OC is given by the cube root of the volume loss.

$$d_2/d_1 = (k)^{1/3} \qquad 5.1$$

d_1 = initial particle diameter

d_2 = final particle diameter

k = fraction of the particle remaining after OC loss

A 50% loss of OC for a particle that is 50% OC will reduce the particle

volume by 25% and reduce its diameter to 91% of its initial value. RWC particles in the 0.6-2.5 μm size range whose diameter's are less than 0.67 μm will fall into the 0.3-0.6 μm size range. Assuming that particles in the 0.6 to 2.5 μm size range were mostly in the 0.6 to 1.2 μm size range about 12% of RWC particles in the 0.6-2.5 μm range can be shifted into the 0.3-0.6 μm size range. Since there are essentially no RWC particles above the 2.5 μm size no particles were shifted into the 0.6-2.5 μm range from the size range above 2.5 μm.

For particles in the 0.3-0.6 μm size range particles with diameters between 0.30 and 0.33 μm can be shifted to the <0.3 μm size range; i.e., 10% of RWC particles in the 0.3-0.6 size range can be shifted to <0.3 μm.

Tables 5.11C-D repeat the above analysis for CMB solutions where a 50% organic carbon loss was allowed for the RWC source. Table 5.11C shows higher calculated OC values then shown in Table 5.11A. This resulted because allowing RWC OC loss caused the CMB program to compute larger source contributions to account for the OC in the ambient samples. The effect was to bring calculated and ambient values more into agreement in the 0.3-0.6 and 0.6-2.5 μm size ranges and less into agreement in the <0.3 μm size range. Since the 50% OC loss CMB computations primarily increase RWC source contributions which contain little EC, calculated EC distributions were not significantly changed by allowing RWC OC loss.

Table 5.11C

Comparison of Calculated and Ambient Organic Carbon over the Sampled Size Range (μg/m³)*

Size Range μm.	Calculated	Ambient
Date: 2/5/85.		
<0.3	2.79	1.22
0.3-0.6	1.35	1.87
0.6-1.2	1.63	1.57
1.2-2.5	0.46	0.08
2.5-10	0.31	0.08
Date: 2/8/85		
<0.3	0.86	0.77
0.3-0.6	0.39	0.42
0.6-2.5	0.35	0.20
1.2-2.5	0.12	0.10
2.5-10	0.08	0.06
Date: 2/14/85		
<0.3	3.34	1.81
0.3-0.6	1.60	1.77
0.6-1.2	1.79	1.58
1.2-2.5	0.52	0.57
2.5-10	0.33	0.21
Date: 2/20/85		
<0.3	2.28	0.89
0.3-0.6	1.02	1.29
0.6-2.5	0.86	1.12
1.2-2.5	0.32	0.91
2.5-10	0.23	0.12

* 50% organic carbon loss assumed from hot and cool wood burning

Table 5.11D

Comparison of Calculated and Ambient Elemental Carbon over the Sampled Size Range ($\mu g/m^3$)*

Size Range μm.	Calculated	Ambient
Date: 2/5/85.		
<0.3	0.95	0.85
0.3-0.6	0.46	0.81
0.6-1.2	0.19	0.90
1.2-2.5	0.06	0.03
2.5-10	0.06	0.03
Date: 2/8/85		
<0.3	0.42	0.38
0.3-0.6	0.20	0.18
0.6-1.2	0.06	0.16
1.2-2.5	0.03	0.05
2.5-10	0.02	0.05
Date: 2/14/85		
<0.3	1.24	0.94
0.3-0.6	0.61	1.05
0.6-1.2	0.21	0.33
1.2-2.5	0.08	0.10
2.5-10	0.06	0.07
Date: 2/20/85		
<0.3	1.16	0.79
0.3-0.6	0.55	0.74
0.6-1.2	0.16	0.55
1.2-2.5	0.09	0.08
2.5-10	0.08	0.07

* 50% organic carbon loss assumed for hot and cool wood burning emissions

5.3.3 CMB ANALYSIS ACROSS THE SIZE DISTRIBUTION

Ambient aerosol sample sets were collected with either the #1 (total, 2.5, 1.2, 0.6, 0.3 and 0.1 μm impactors) or #2 (matched 2.5, 0.6 and 0.3 μm impactors) impactor sets. For each sample set the most inclusive member of the set (the total sample for the #1 set and the 2.5 μm sample for the #2 set) was analyzed by CMB modeling to determine the significant sources contributing to the sample. The contributions of this source group to the samples collected behind successively smaller cut-point impactors were then determined with a separate CMB analysis for each sample. These data enabled the atmospheric size distribution of each source to be determined. Knowledge of source atmospheric size distribution is useful to determine the environmental effects of these sources and also can simplify CMB analysis in the case where certain sources do not exist across the whole aerosol size range.

Source compositions that varied as a function of particle size were used where appropriate. Only the motor vehicle emission source showed significant variability as a function of particle size. For this source the composition profiles for the specific size fractions given in Table 3.18 and 3.19 were used. RWC aerosol composition was assumed not to vary as a function of aerosol size for aerosol particles >0.3 μm. The compositions of RWC aerosol particles <0.3 μm had slightly lower carbon values and slightly higher trace element values then particles >0.3 μm. The average of carbon composition values shown in Table 3.6A-B were used. Trace element composition values for RWC particles <0.3 μm were quite variable but seemed generally to be about 20% greater than values for larger particles. Sources whose composition

was not evaluated in this research, i.e., fine soil, distillate oil, Kraft plant, and sea salt were assumed not to vary as a function of particle size.

5.3.3.1 CMB ANALYSIS ACROSS AEROSOL SIZE FOR PORTLAND RESIDENTIAL SAMPLES COLLECTED WITH THE #2 IMPACTOR SET

This section discusses Portland residential area sample sets collected on December 8, 21, and 24 of 1984 using impactor set #2 (paired 2.5, 0.6 and 0.3 μm impactors) where one impactor of each pair was used to collect a sample on a quartz fiber filter and the other was used to collect a sample on a Teflon filter. These samples were used to determine the carbon and trace element compositions of ambient aerosols with diameters <2.5, 0.6 and 0.3 μm.

Tables 5.12A-C to 5.14A-C present CMB results for the above sample sets in terms of μg/m3 rather than in percentages of aerosol mass so that the distributions of the various sources across the aerosol particle size range can be determined. The difference in the $\mu g/m^3$ values for a given source between two points in the size range is the contribution of that source to the size range segment between the two data points. Data presentation is similar to that previously used except that for each date results are presented for particles passing the 2.5, 0.6, and 0.3 μm impactors.

The normal CMB analysis using either the composite or the hot/cool RWC source composition profile showed, analogous to previously discussed samples, that the EC ratio values were lower than the OC

Table 5.12A

Comparisons of CMB Analyses Using Various Wood Smoke Composition Profiles (μg/m³)

Site: SW Portland Residential Area Size: 2.5 μm.		Mass loading = 48 μg/m³		
Date:		12/8/84		
	Normal	-50% *	EPA	Hot/Cool
W/S Comp	21.3±2.6	27.5±3.6	27.3±3.9	-----
Hot burn	-----	-----	-----	2.6±0.7
Cool burn	-----	-----	-----	17.6±2.7
Soil	0.3±0.1	0.2±0.1	0.3±0.1	0.3±0.1
Motor Vehicle	3.0±0.3	3.0±0.3	2.9±0.3	3.0±0.3
Sea salt	0.7±0.2	0.6±0.2	0.5±0.2	0.6±0.2
Oil Furnace	10.2±1.4	9.7±1.5	9.9±1.4	10.3±1.4
X^2	2.112	0.822	0.763	2.147
DF	7	7	7	6
Mass calc.(%)	74.0±17.4	85.4±8.5	85.2	71.6±7.2
OC Ratio**	1.16±0.07	1.02±0.05	1.34±0.6	1.07±0.05
EC Ratio**	0.55±0.10	0.72±0.18	0.96±0.60	0.59±0.08
TC Ratio**	0.97±0.06	0.93±0.05	1.22±0.29	0.92±0.04
K Ratio**	0.81±0.26	1.35±.59	0.92±0.13	1.26±0.43

Uncertainties are standard deviations.

* For CMB analysis organic carbon is decreased by percentage shown for RWC and tunnel sources.

** Ratio of CMB calculated/measured.

DF = Degrees of freedom

Table 5.12B

Comparisons of CMB Analyses Using Various Wood Smoke Composition Profiles (μg/m³)

Site: SW Portland Residential Area Size: 0.6 μm			Mass loading = 22.7 μg/m³	
Date:		12/8/84		
	Normal	-50% *	EPA	Hot/Cool
W/S Comp	17.3±2.0	22.6±2.8	19.8±2.9	-----
Hot burn	-----	-----	-----	1.7±0.5
Cool burn	-----	-----	-----	15.3±2.1
Soil	0.2±0.1	0.2±0.1	0.3±0.1	0.2±0.1
Motor Vehicle	1.5±0.1	1.5±0.1	1.5±0.1	1.5±0.1
Sea salt	0.1±0.05	0.1±0.1	0.2±0.03	0.1±0.05
Oil Furnace	3.5±0.6	3.5±0.6	3.5±0.6	3.5±0.6
X^2	2.265	0.919	0.479	2.880
DF	6	6	6	5
Mass calc.(%)	100.3±10	121.9±12	110.4±11	98.7±9.8
OC Ratio**	1.11±0.06	0.98±0.05	1.17±0.48	1.073±0.04
EC Ratio**	0.48±0.12	0.69±0.20	0.88±0.60	0.51±0.08
TC Ratio**	0.93±0.06	0.90±0.06	1.08±0.26	0.91±0.44
K Ratio**	0.95±0.34	1.62±0.83	0.97±0.15	1.24±0.42

Uncertainties are standard deviations.

* For CMB analysis organic carbon is decreased by percentage shown for RWC and tunnel sources.

** Ratio of CMB calculated/measured.

DF = Degrees of freedom

Table 5.12C

Comparisons of CMB Analyses Using Various Wood Smoke Composition Profiles (μg/m³)

Site: SW Portland Residential Area Size: 0.3 μm.		Mass loading = 7.2 μg/m³		
Date:		12/8/84		
	Normal	-50% *	EPA	Hot/Cool
W/S Comp	4.9±0.7	6.1±0.8	6.4±1.0	-----
Hot burn	-----	-----	-----	0.4±0.1
Cool burn	-----	-----	-----	4.3±0.7
Soil	0.1±0.04	0.1±0.04	0.1±0.04	0.1±0.04
Motor Vehicle	0.6±0.1	0.6±0.1	0.5±0.1	0.6±0.1
Oil Furnace	1.2±0.2	1.1±0.2	1.3±0.2	1.2±0.2
X^2	2.611	1.690	0.502	3.270
DF	7	7	7	6
Mass calc.(%)	93.3±9.3	108.2±11	115.3±11	91.6±9.2
OC Ratio**	1.13±0.10	0.94±0.07	1.46±0.67	1.10±0.05
EC Ratio**	0.43±0.07	0.57±0.12	0.74±0.45	0.43±0.05
TC Ratio**	0.83±0.05	0.76±0.05	1.18±0.29	0.81±0.05
K Ratio**	0.97±0.28	1.55±0.62	0.92±0.13	1.07±0.27

Uncertainties are standard deviations.

* For CMB analysis organic carbon is decreased by percentage shown for RWC and tunnel sources.

** Ratio of CMB calculated/measured.

DF = Degrees of freedom

Table 5.13A

Comparisons of CMB Analyses Using Various Wood Smoke Composition Profiles (μg/m³)

Site: SW Portland Residential Area Size: 2.5 μm.		Mass loading = 17.0 μg/m³		
Date:		12/21/84		
	Normal	-50% *	EPA	Hot/Cool
W/S Comp	4.2±0.6	5.7±0.7	6.5±0.8	-----
Hot burn	-----	-----	-----	0.9±0.2
Cool burn	-----	-----	-----	2.8±0.6
Road Dust	0.3±0.06	0.3±0.1	0.4±0.1	0.3±0.06
Motor Vehicle	0.7±0.09	0.7±0.1	0.8±0.1	0.7±0.09
Diesel	0.7±0.3	0.5±0.4	0.2±0.5	0.7±0.4
Oil Furnace	2.2±0.4	2.2±0.4	2.3±0.4	2.3±0.4
X^2	4.911	1.941	2.881	2.230
DF	7	7	7	6
Mass calc.(%)	48.0±4.8	55.4±5.5	59.1±5.9	44.7±4.4
OC Ratio**	1.27±0.08	1.16±0.07	1.65±0.80	1.03±0.06
EC Ratio**	0.66±0.11	0.72±0.15	0.87±0.48	0.73±0.11
TC Ratio**	1.02±0.08	0.98±0.07	1.34±0.33	0.91±0.07
K Ratio**	0.47±0.12	0.79±0.25	0.62±0.07	1.10±0.36

Uncertainties are standard deviations.

* For CMB analysis organic carbon is decreased by percentage shown for RWC and tunnel sources.

** Ratio of CMB calculated/measured.

DF = Degrees of freedom

Table 5.13B

Comparisons of CMB Analyses Using Various Wood Smoke Composition Profiles ($\mu g/m^3$)

Site: SW Portland Residential Area Size: 0.6 μm.			Mass loading = 11.7 $\mu g/m^3$	
Date:		12/21/84		
	Normal	-50% *	EPA	Hot/Cool
W/S Comp	3.1±0.4	4.0±0.6	3.1±0.5	-----
Hot burn	-----	-----	-----	0.4±0.1
Cool burn	-----	-----	-----	2.4±0.4
Road Dust	0.2±0.04	0.2±0.04	0.2±0.04	0.2±0.04
Motor Vehicle	0.4±0.05	0.4±0.05	0.4±0.05	0.4±0.05
Diesel	0.8±0.3	0.8±0.3	0.7±0.3	0.8±0.3
Oil Furnace	1.3±0.2	1.2±0.2	1.3±0.2	1.3±0.2
X^2	4.395	3.182	5.756	4.184
DF	7	7	7	6
Mass calc.(%)	49.5±4.9	56.6±5.7	48.1±4.8	46.9±4.7
OC Ratio**	1.16±0.07	1.02±0.06	1.06±0.35	1.027±0.06
EC Ratio**	0.69±0.15	0.78±0.17	0.80±0.29	0.73±0.14
TC Ratio**	0.97±1.0	0.93±0.09	0.96±0.17	0.91±0.09
K Ratio**	0.55±0.15	0.89±0.30	0.49±0.05	0.87±0.25

Uncertainties are standard deviations.

* For CMB analysis organic carbon is decreased by percentage shown for RWC and tunnel sources.

** Ratio of CMB calculated/measured.

DF = Degrees of freedom

Table 5.13C

Comparisons of CMB Analyses Using Various Wood Smoke

Composition Profiles (μg/m³)

Site: SW Portland Residential Area Size: 0.3 μm.			Mass loading = 5.3 μg/m³	
Date:		12/21/84		
	Normal	-25% *	EPA	Hot/Cool
W/S Comp	1.0±0.1	1.4±0.2	1.4±0.3	-----
Hot burn	-----	-----	-----	0.1±0.03
Cool burn	-----	-----	-----	0.9±0.1
Road Dust	0.1±0.03	0.1±0.03	0.1±0.03	0.1±0.03
Motor Vehicle	0.2±0.03	0.2±0.03	0.2±0.03	0.2±0.03
Diesel	0.7±0.2	0.8±0.2	0.7±0.2	0.7±0.2
Oil Furnace	0.5±0.1	0.5±0.1	0.5±0.1	0.5±0.1
X^2	1.218	1.160	1.421	1.543
DF	7	7	6	6
Mass calc.(%)	46.5±4.6	49.2±4.9	51.8±5.1	46.5±4.6
OC Ratio**	1.02±0.11	1.00±0.10	1.24±0.42	1.00±0.10
EC Ratio**	1.02±0.31	1.07±0.32	1.11±0.42	1.05±0.32
TC Ratio**	1.00±0.18	1.00±0.18	1.18±0.25	1.00±0.18
K Ratio**	0.87±0.21	1.07±0.30	0.86±0.11	1.02±0.22

Uncertainties are standard deviations.

* For CMB analysis organic carbon is decreased by percentage shown for RWC and tunnel sources.

** Ratio of CMB calculated/measured.

DF = Degrees of freedom

Table 5.14A

Comparisons of CMB Analyses Using Various Wood Smoke Composition Profiles ($\mu g/m^3$)

Site: SW Portland Residential Area Size: 2.5 µm.			Mass loading = 44.0 $\mu g/m^3$	
Date:		12/24/84		
	Normal	-50% *	EPA	Hot/Cool
W/S Comp	22.1±2.8	27.3±3.7	23.2±3.2	-----
Hot burn	-----	-----	-----	2.4±0.6
Cool burn	-----	-----	-----	18.3±3.0
Soil	0.2±0.09	0.2±0.09	0.2±0.09	0.2±0.09
Motor Vehicle	1.8±0.2	1.8±0.2	1.7±0.2	1.8±0.2
Sea Salt	0.7±0.2	0.6±0.2	0.5±0.2	0.6±0.2
Oil Furnace	13.8±1.5	13.0±1.6	13.7±1.5	13.7±1.5
X^2	2.274	1.798	2.256	2.344
DF	9	9	9	8
Mass calc.(%)	87.7±8.8	97.5±9.7	89.5±8.9	84.0±8.4
OC Ratio**	1.11±0.06	0.94±0.5	1.08±0.65	1.02±0.5
EC Ratio**	0.70±0.14	0.88±0.24	1.06±0.65	0.72±0.12
TC Ratio**	1.00±0.06	0.93±0.05	1.08±0.23	0.95±0.05
K Ratio**	0.92±0.32	1.48±0.70	0.87±0.12	1.29±0.45

Uncertainties are standard deviations.

* For CMB analysis organic carbon is decreased by percentage shown for RWC and tunnel sources.

** Ratio of CMB calculated/measured.

DF = Degrees of freedom

Table 5.14B

Comparisons of CMB Analyses Using Various Wood Smoke Composition Profiles ($\mu g/m^3$)

Site: SW Portland Residential Area Size: 0.6 μm.			Mass loading = 22.9 $\mu g/m^3$	
Date:		12/24/84		
	Normal	-50% *	EPA	Hot/Cool
W/S Comp	7.5±1.8	21.9±2.5	14.3±1.5	-----
Hot burn	-----	-----	-----	2.8±0.5
Cool burn	-----	-----	-----	13.3±1.9
Soil	0.2±0.06	0.2±0.07	0.2±0.06	0.2±0.09
Motor Vehicle	0.9±0.1	0.9±0.1	0.8±0.1	0.9±0.1
Oil Furnace	3.6±0.5	3.3±0.5	4.1±0.5	3.6±0.5
X^2	3.019	1.298	5.84	2.866
DF	8	8	8	10
Mass calc.(%)	96.9±9.7	114.5±11	84.6±8.4	90.3±9.0
OC Ratio**	1.20±0.07	1.02±0.05	0.93±0.33	1.03±0.05
EC Ratio**	0.49±0.12	0.70±0.22	0.73±0.44	0.57±0.10
TC Ratio**	1.00±0.07	0.93±0.06	0.88±0.18	0.90±0.04
K Ratio**	0.91±0.33	1.52±0.75	0.68±0.09	1.82±0.87

Uncertainties are standard deviations.

* For CMB analysis organic carbon is decreased by percentage shown for RWC and tunnel sources.

** Ratio of CMB calculated/measured.

Table 5.14C

Comparisons of CMB Analyses Using Various Wood Smoke Composition Profiles ($\mu g/m^3$)

Site: SW Portland Residential Area Size: 0.3 μm.			Mass loading = 10.4 $\mu g/m^3$	
Date:		12/24/84		
	Normal	-50% *	EPA% *	Hot/Cool
W/S Comp	7.8±0.9	9.7±1.2	8.4±1.2	-----
Hot burn	-----	-----	-----	0.5±0.2
Cool burn	-----	-----	-----	7.7±1.0
Soil	0.1±0.04	0.1±0.04	0.1±0.04	0.1±0.04
Motor Vehicle	0.4±0.05	0.4±0.05	0.4±0.05	0.4±0.05
Oil Furnace	1.0±0.9	0.9±0.2	1.1±0.2	1.0±0.2
X^2	1.971	1.369	0.975	2.604
DF	7	7	7	6
Mass calc.(%)	90.1±9.0	106.2±10	96.7±9.7	93.0±9.3
OC Ratio**	1.08±0.10	0.88±0.06	1.18±0.49	1.13±0.10
EC Ratio**	0.49±0.11	0.70±0.19	0.81±0.56	0.49±0.08
TC Ratio**	0.88±0.07	0.78±0.05	1.07±0.26	0.91±0.06
K Ratio**	1.24±0.42	1.99±0.96	0.97±0.15	1.10±0.27

Uncertainties are standard deviations.

* For CMB analysis organic carbon is decreased by percentage shown for RWC and tunnel sources.

** Ratio of CMB calculated/measured.

ratio values. This indicated that the RWC aerosol particles could have lost organic carbon during their atmospheric residence time. RWC organic carbon loss could have been in the range of 50 to 70% for all particles irrespective of size. Smaller particles, on a percentage basis, lose mass by evaporation faster than larger particles. This occurs because evaporative loss on a percentage basis is approximately inversely proportional to surface area. For particles <0.1 μm evaporation is accelerated by the Kelvin effect. In a very fresh aerosol small particles might be expected to exhibit larger organic carbon losses than large particles; however, in an aged aerosol (characterized by organic carbon losses in the 50-70% range) equal organic carbon losses are not unreasonable, i.e., given a reasonable period of time and assuming that plume sampled particles are in similar equilibria with their atmospheric environment, all particles can lose a similar percentage of OC.

Tables 5.12-5.14 show CMB solutions using the RWC composite carbon loss composition profile which was closest to a minimum X^2 value for the given sample. Generally carbon loss values of about 50% were indicated. The magnitude of the various source contributions was not greatly changed by using RWC composition profiles which allowed organic carbon loss. Increasing organic carbon loss mainly tended to increase the RWC contribution and decreased the oil furnace contribution slightly.

Mass data for 12/21 samples might have significant errors because a Mettler mechanical balance was used to obtain mass data instead of the Cahn Electrobalance which was being repaired. In addition filter

mass loading was low and difficult to weight accurately. The fact that TC/M values were low and the CMB model only accounted for about 50% aerosol mass indicates that mass values measured could be lower than the true values.

On a percentage basis, using the 50% OC-loss RWC composite profile, the CMB model indicated that for 12/8/84, 12/21/84, and 12/24/84 RWC contributed respectively 57, 33, and 62% of the fine (<2.5 μm) aerosol at the Portland residential site. Figures 5.7, 5.8, and 5.9 (using the composite RWC profile normal solution) show the percentage contributions of the significant sources to the <2.5, <0.6 and <0.3 μm sample sets. It will be noted RWC was the largest aerosol source and oil furnace emissions were the second largest. RWC, oil furnace emissions, motor vehicle emissions and soil were broadly distributed across the fine aerosol size range. Sea salt did not appear in the <0.6 μm aerosol and diesel emissions were mainly concentrated below 0.3 μm.

CMB analysis using RWC hot/cool composition profiles with 50% OC loss showed that 6% of wood burning air pollution was contributed by hot (damper open) burning on 12/8/84 and 12/24/84 and that 15% was contributed on 12/21/84. The sum of the hot and cool burning contributions given by these CMB analyses was usually in close agreement with the RWC source contributions given by CMB analyses which used the normal composite RWC particulate composition profile.

Figures 5.10A-B to 5.12A-B show source distribution data for the December 1984 samples. The "A" figures used the normal composite RWC profile while the "B" figures used the 50% OC loss RWC composite profile. The most significant difference caused by including organic

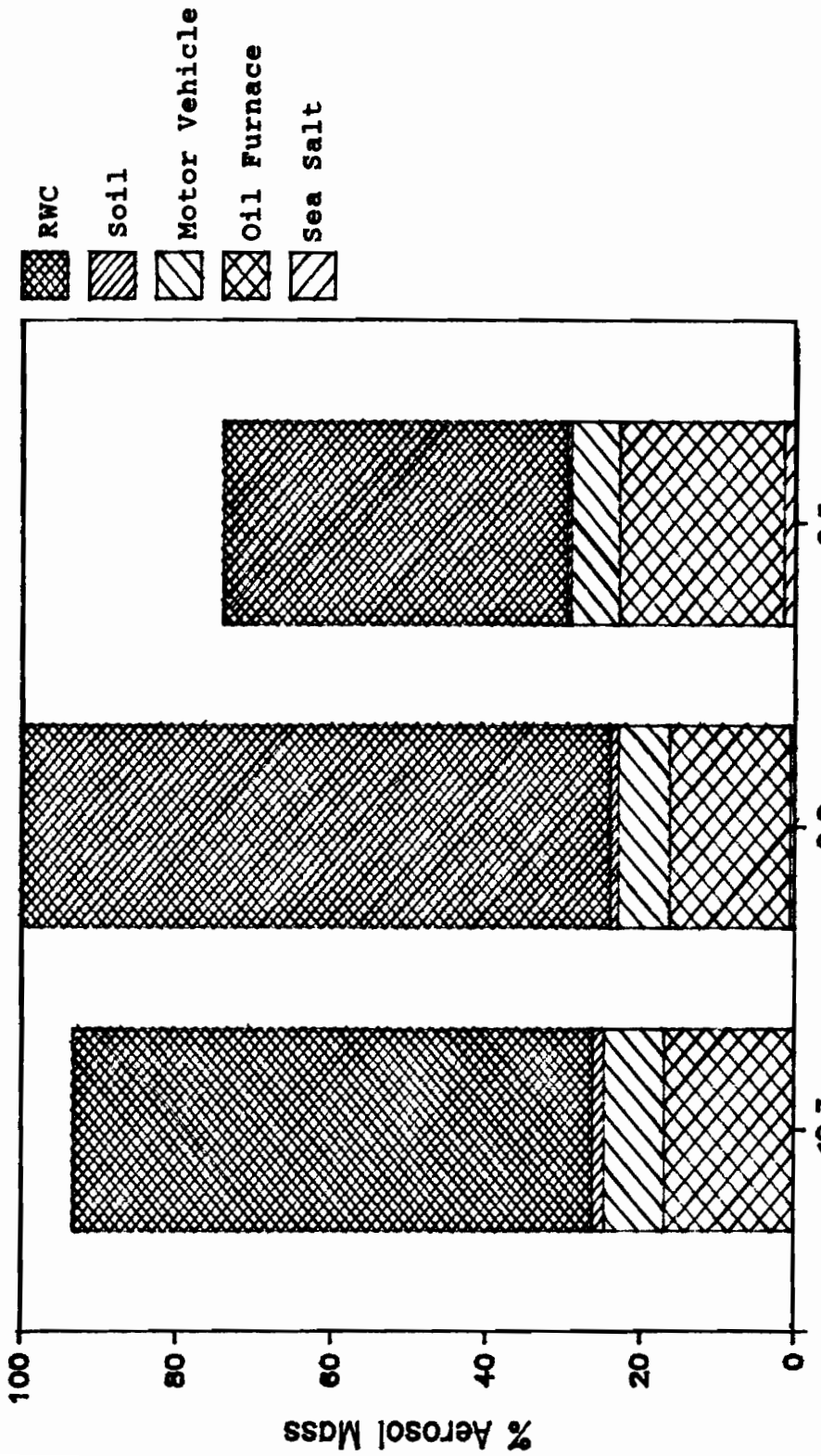

Figure 5.7. CMB source contributions for a Portland residential area aerosol sample (12/08/84) expressed as a percent of aerosol mass in the indicated size range.

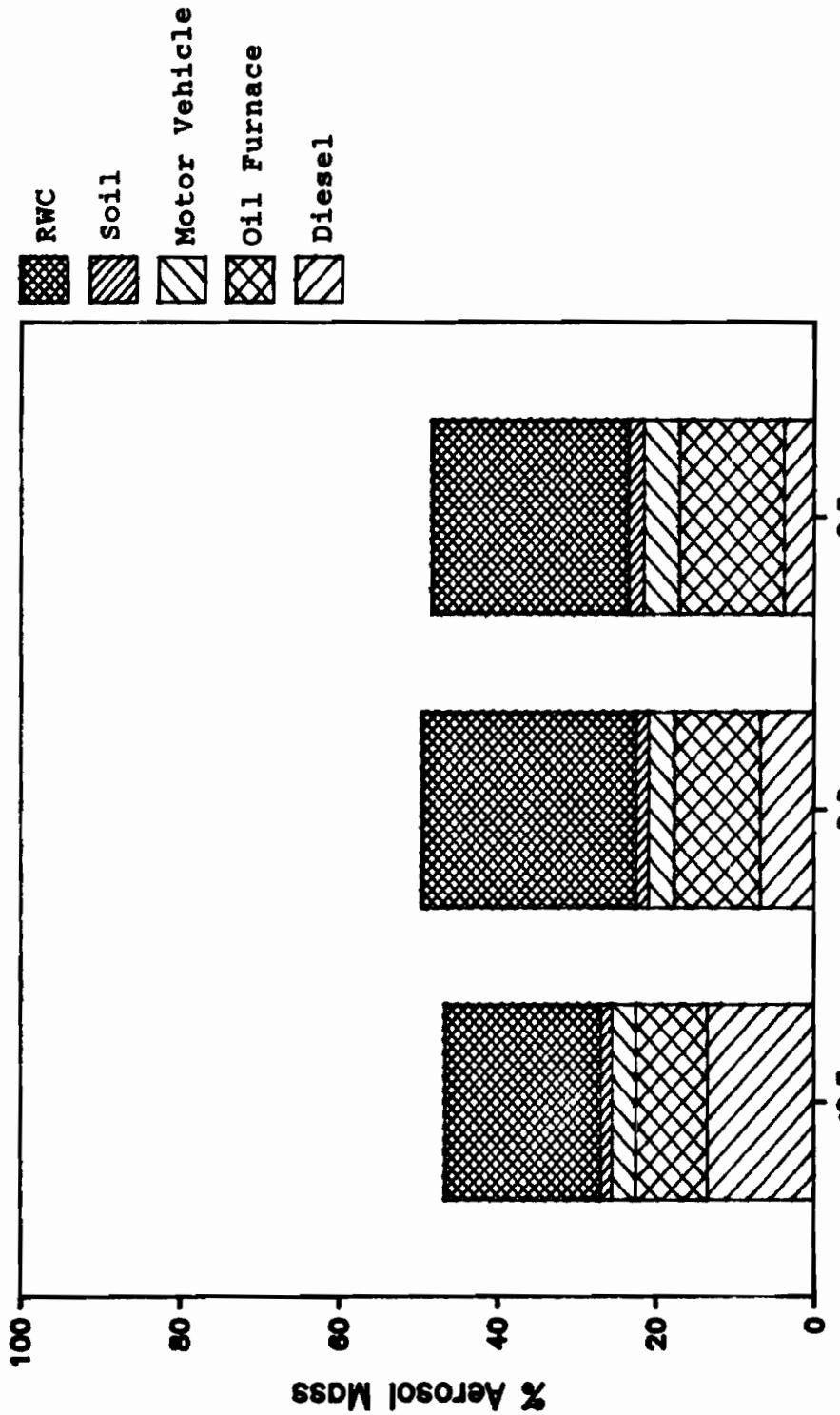

Figure 5.8 CMB Source Contributions Over The Aerosol Size Range, SW Portland (12/21/84)

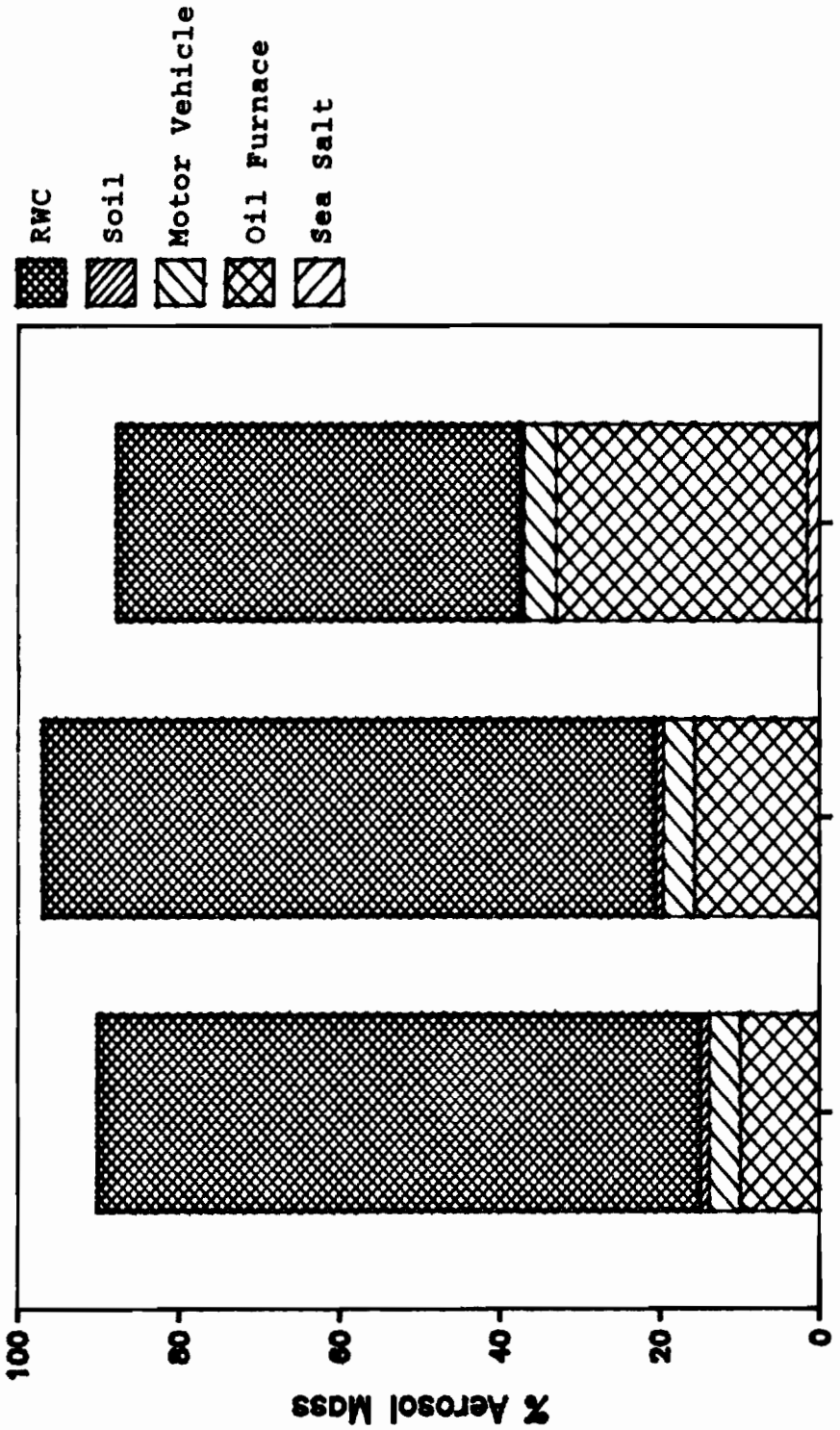

Figure 5.9. CMB source contributions over the aerosol size range (SW Portland, 12/24/84)

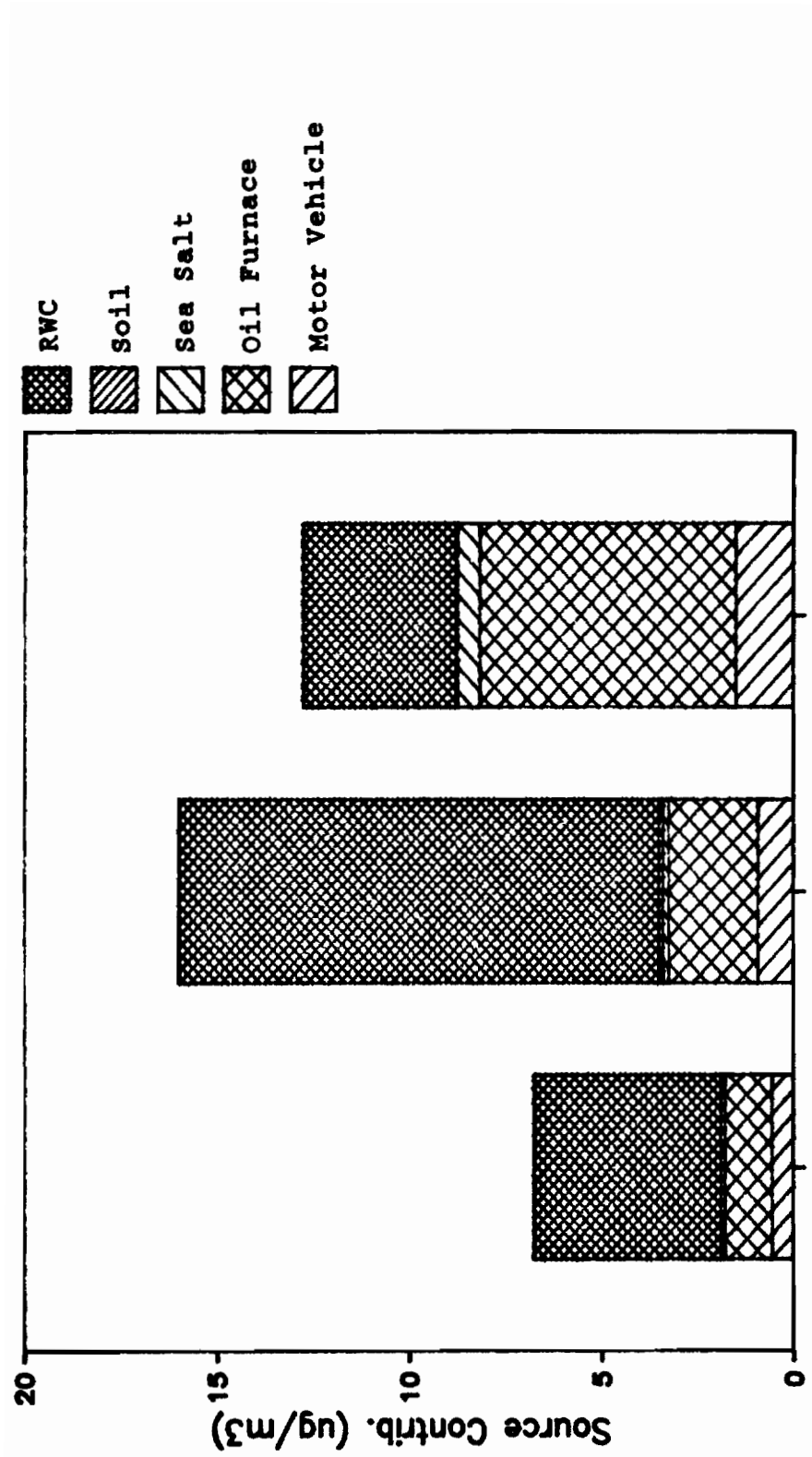

Figure 5.10A. CMB source contributions to the indicated aerosol size ranges (SW Portland, 12/08/84) (normal CMB solution).

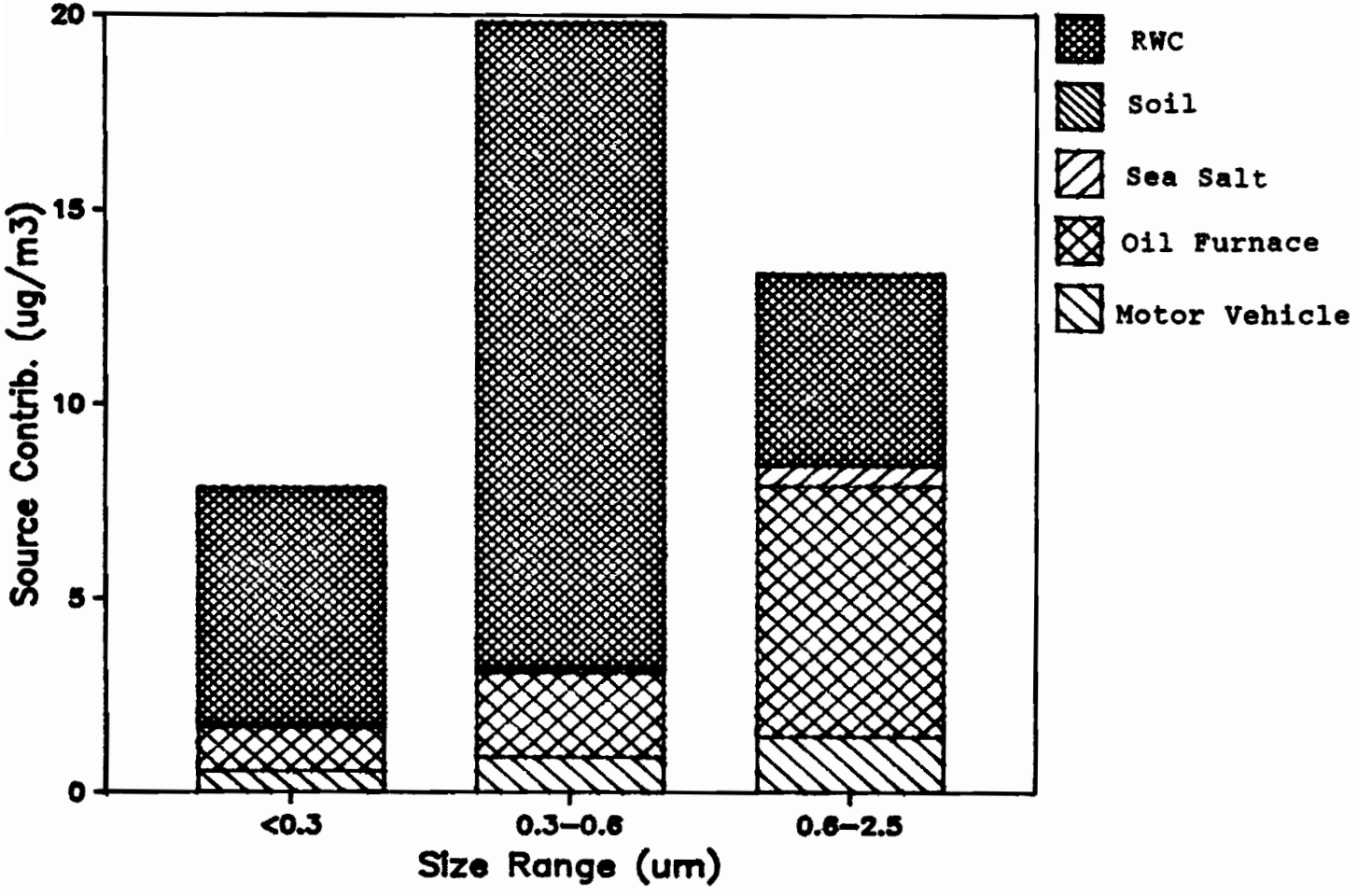

Figure 5.10B. CMB source contributions to indicated aerosol size ranges (SW Portland, 12/08/84). CMB solution used RWC profile with 50% OC loss.

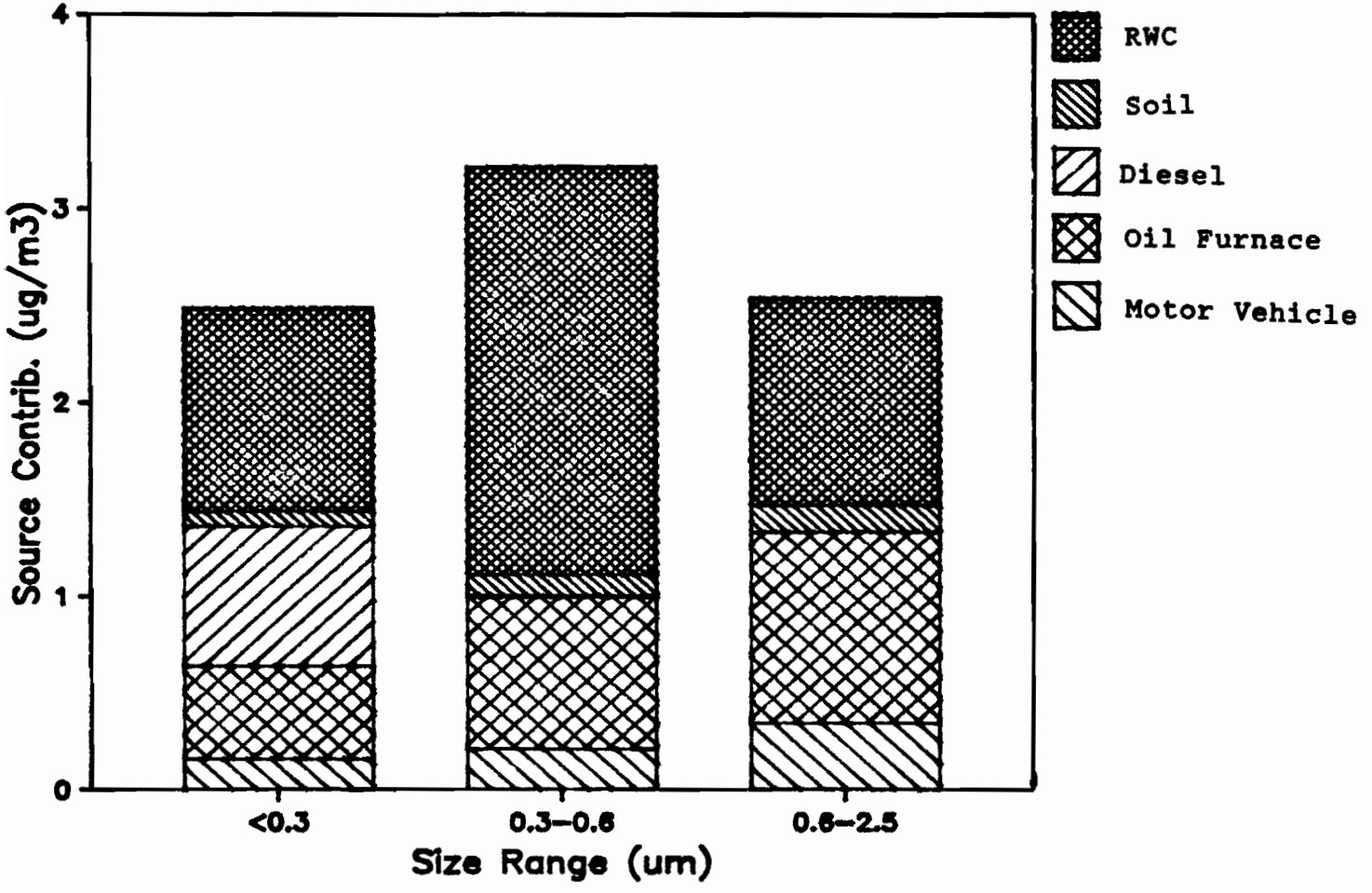

Figure 5.11A. CMB source contributions to indicated aerosol size ranges (SW Portland, 12/21/84) (normal CMB solution).

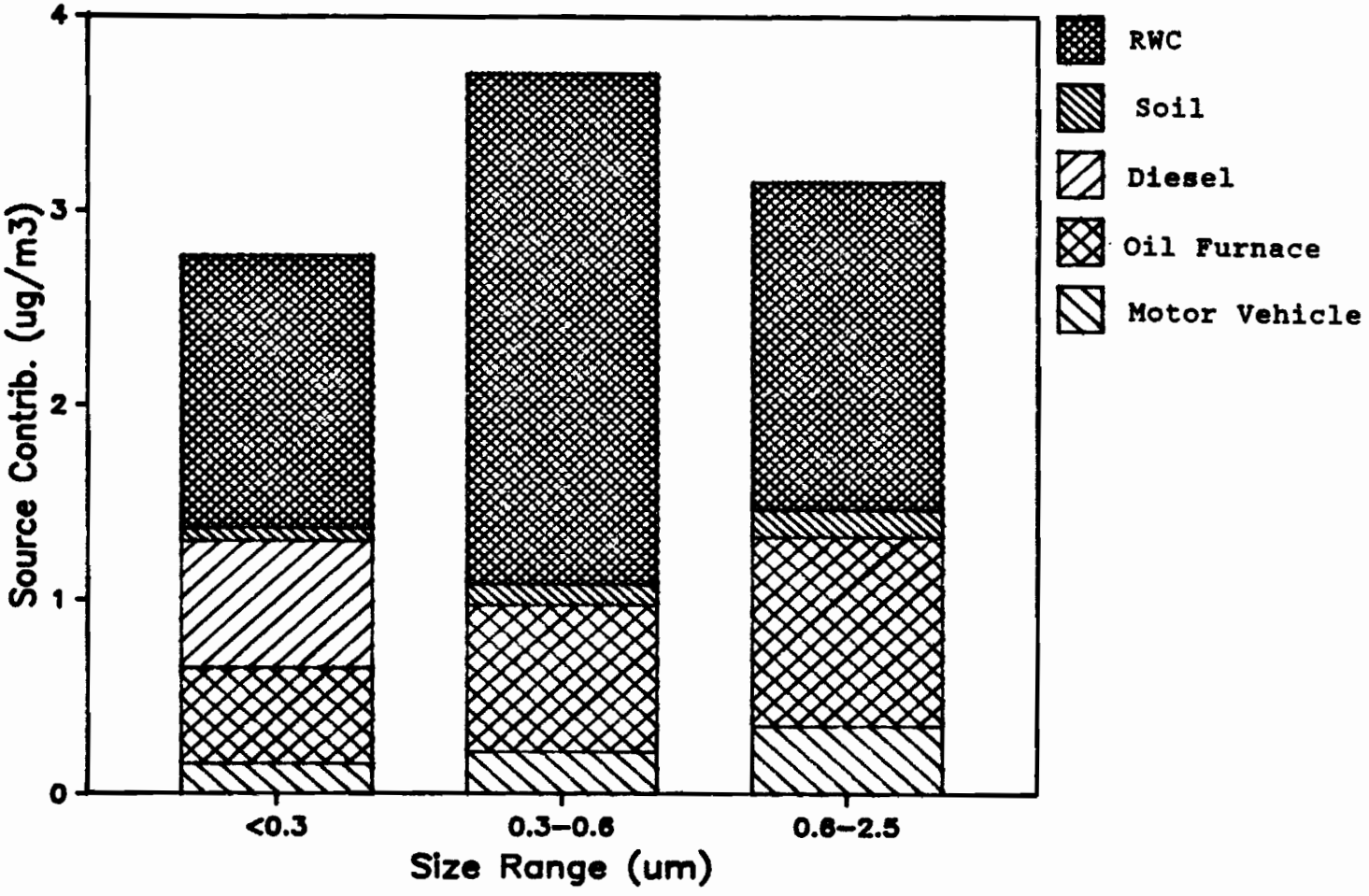

Figure 5.11B. CMB source contributions to indicated aerosol size ranges (SW Portland, 12/21/84). CMB solution used RWC profile with 50% OC loss.

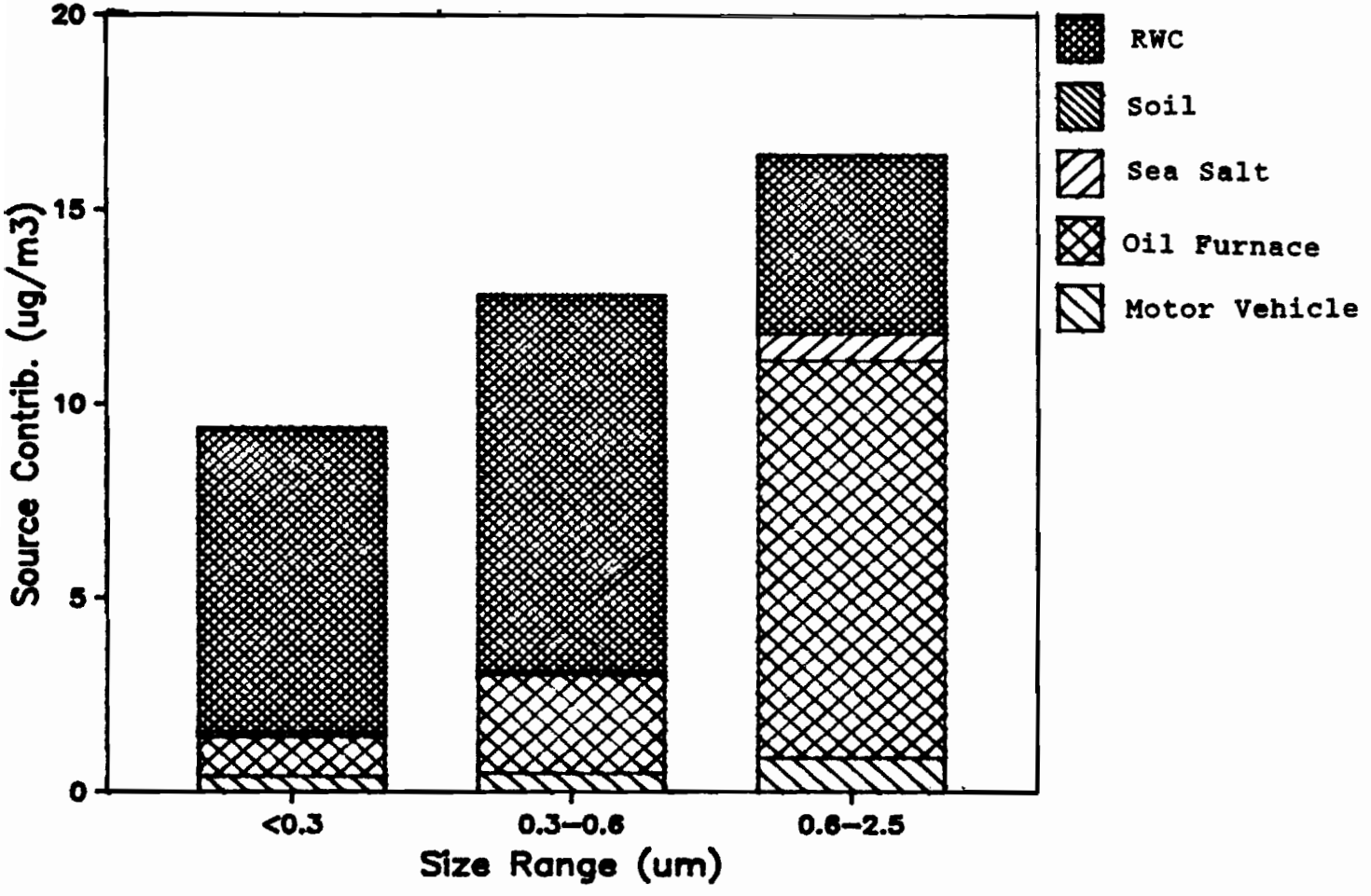

Figure 5.12A. CMB source contributions to the indicated aerosol size ranges (SW Portland, 12/24/84) (normal CMB solution).

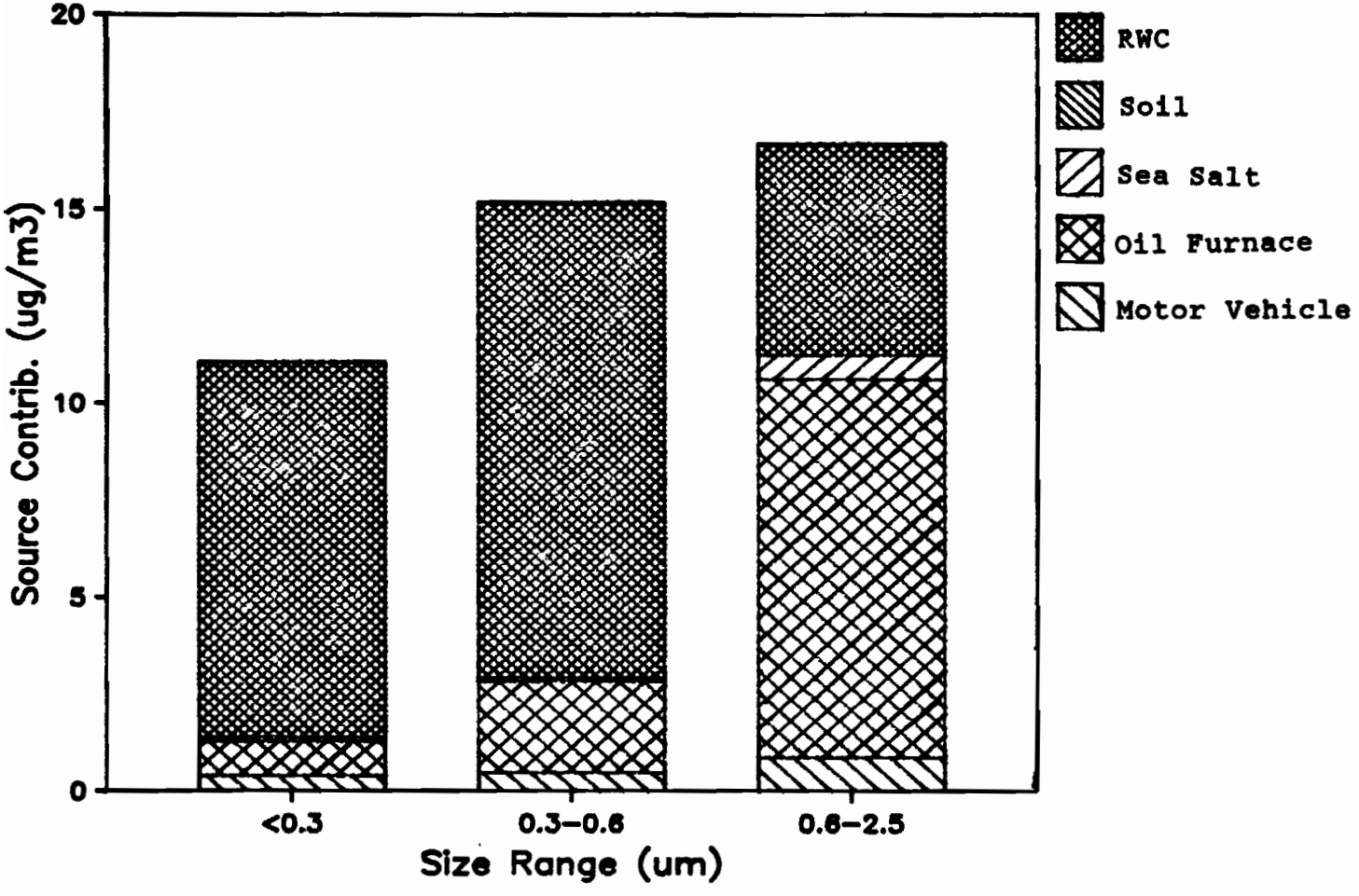

Figure 5.12B. CMB source contributions to indicated aerosol size ranges (SW Portland, 12/24/84). CMB solution used RWC profile with 50% OC loss.

carbon loss was that the RWC contribution was increased. RWC contributions obtained with CMB analyses using RWC profiles which include organic carbon loss can thus be considered to compute the upper limit values for RWC contributions. These figures show $\mu g/m^3$ values for each significant source in the indicated size ranges. RWC emissions were mainly located in size ranges below 0.6 μm while oil furnace emissions were mainly located above 0.6 μm. These data are expected to be typical of residential areas where RWC is a major pollution source.

Comparing the CMB solutions obtained using the EPA CMB profile showed that RWC contributions obtained with this profile were usually not very different from the contributions obtained with either the normal or 50% organic carbon loss composite profiles. Use of the EPA profile always resulted in higher RWC contributions than the normal hot and cool profile CMB solutions. Using hot and cool profile solutions which allowed organic carbon loss would bring these contributions closer together. Usually using the EPA profile did not account for carbon as well as the other RWC profiles.

5.3.3.2 CMB ANALYSIS ACROSS THE AEROSOL SIZE FOR A HILLSBORO WINTERTIME SAMPLE

This section presents CMB analyses across the aerosol size range for a high pollution wintertime sample set collected in Hillsboro, OR on 2/6/84. This sample set was collected with impactor set #1 (Total aerosol and 2.5, 1.2, 0.6, 0.3 and 0.1 μm impactors).

Tables 5.15A-E shows that RWC was by far the largest pollution source contributing to the Hillsboro sample set. This is not surprising

Table 5.15A

Comparisons of CMB Analyses Using Various Wood Smoke Composition Profiles ($\mu g/m^3$)

Site: Hillsboro Residential Area Size: Total		Mass loading = 134 $\mu g/m^3$		
Date:		2/6/84		
	Normal	-25% *	EPA	Hot/Cool
RWC Comp.	82.5±9.6	87.3±10.5	64.2±8.5	-----
Hot burn	-----	-----	-----	5.5±1.5
Cool burn	-----	-----	-----	76.6±10.4
Soil	2.0±0.6	1.9±0.1	2.1±0.6	2.0±0.6
Motor Vehicle	6.1±0.8	6.0±0.1	5.6±0.8	6.1±0.8
Oil Furnace	10.9±2.1	10.3±1.0	13.8±2.0	11.3±2.0
X^2	1.818	1.710	3.385	2.298
DF	9	9	9	8
Mass calc.(%)	75.7±7.6	78.8±7.9	64.0±6.4	75.7±7.5
OC Ratio**	1.02±0.05	0.93±0.05	0.75±0.25	1.02±0.04
EC Ratio**	0.93±0.30	1.06±0.38	1.37±1.20	0.92±0.22
TC Ratio**	1.00±0.07	0.95±0.05	0.85±0.18	1.00±0.05
K Ratio**	1.30±0.56	1.56±0.75	0.93±0.13	1.24±0.41

Uncertainties are standard deviations.

* For CMB analysis organic carbon is decreased by percentage shown for RWC and transportation sources

** Ratio of CMB calculated/measured.

Table 5.15B

Comparisons of CMB Analyses Using Various Wood Smoke Composition Profiles ($\mu g/m^3$)

Site: Hillsboro Residential Area Size: 2.5 μm.		Mass loading = 104 $\mu g/m^3$		
Date:		2/6/84		
	Normal	-25% *	EPA	Hot/Cool
RWC Comp.	75.1±7.9	80.8±8.8	59.0±7.3	-----
Hot burn	-----	-----	-----	4.9±1.3
Cool burn	-----	-----	-----	69.6±8.4
Soil	1.7±0.5	1.6±0.5	1.8±0.5	1.7±0.5
Motor Vehicle	4.1±0.5	4.1±0.5	4.0±0.5	4.1±0.5
Oil Furnace	7.4±1.6	7.0±1.6	9.0±1.6	7.6±1.6
X^2	1.437	1.210	2.134	1.873
DF	9	9	9	8
Mass calc.(%)	85.1±8.5	90.0±9.0	71.1±7.1	84.7±8.5
OC Ratio**	1.05±0.06	0.97±0.05	0.78±0.27	1.04±0.4
EC Ratio**	0.90±0.30	1.05±0.39	1.35±1.22	0.89±0.22
TC Ratio**	1.08±0.08	1.04±0.05	0.91±0.21	1.08±0.06
K Ratio**	1.52±0.73	1.86±1.02	1.10±0.17	1.43±0.52

Uncertainties are standard deviations.

* For CMB analysis organic carbon is decreased by percentage shown for RWC and tunnel sources.

** Ratio of CMB calculated/measured.

Table 5.15C

Comparisons of CMB Analyses Using Various Wood Smoke Composition Profiles ($\mu g/m^3$)

Site: Hillsboro Residential Area Size: 1.2 μm.		Mass loading = 101 $\mu g/m^3$		
Date:		2/6/84		
	Normal	-25% *	EPA	Hot/Cool
RWC Comp.	68.5±7.9	72.4±8.7	56.1±7.8	-----
Hot burn	-----	-----	-----	3.4±1.1
Cool burn	-----	-----	-----	68.3±8.6
Soil	1.9±0.5	1.8±0.5	2.0±0.5	2.0±0.5
Motor Vehicle	4.1±0.5	4.0±0.5	3.9±0.5	4.1±0.5
Oil Furnace	5.7±1.3	5.3±1.3	8.5±1.1	5.8±1.2
X^2	0.664	0.827	1.653	0.739
DF	7	7	7	6
Mass calc.(%)	79.7±8.0	83.1±8.3	70.0±7.0	83.2±8.3
OC Ratio**	0.98±0.05	0.90±0.04	0.76±0.26	1.04±0.04
EC Ratio**	0.84±0.27	0.97±0.35	1.33±1.2	0.82±0.21
TC Ratio**	0.99±0.07	0.93±0.05	0.87±0.19	1.04±0.04
K Ratio**	1.39±0.62	1.61±0.79	1.05±0.16	1.08±0.32

Uncertainties are standard deviations.

* For CMB analysis organic carbon is decreased by percentage shown for RWC and tunnel sources.

** Ratio of CMB calculated/measured.

Table 5.15D

Comparisons of CMB Analyses Using Various Wood Smoke Composition Profiles ($\mu g/m^3$)

Site: Hillsboro Residential Area Size: 0.6 μm.		Mass loading = 60 $\mu g/m^3$		
Date:		2/6/84		
	Normal	-25% *	EPA	Hot/Cool
RWC Comp.	47.5±5.0	52.4±5.6	40.6±4.0	-----
Hot burn	-----	-----	-----	4.6±1.0
Cool burn	-----	-----	-----	40.8±5.4
Soil	1.2±0.3	1.1±0.3	1.3±0.3	1.1±0.3
Motor Vehicle	2.3±0.3	2.3±0.3	2.2±0.3	2.3±0.3
Oil Furnace	3.0±0.9	2.9±0.9	3.3±0.9	3.0±0.9
X^2	1.553	1.287	0.802	1.713
DF	11	11	11	10
Mass calc.(%)	89.5±8.9	97.3±9.7	78.7±7.9	86.0±8.6
OC Ratio**	1.13±0.06	1.07±0.06	0.90±0.33	1.05±0.04
EC Ratio**	0.72±0.22	0.87±0.30	1.17±1.00	0.76±-0.17
TC Ratio**	1.05±0.07	1.03±0.05	0.95±0.22	1.00±0.05
K Ratio**	1.46±0.69	1.83±1.00	1.15±0.19	1.90±0.90

Uncertainties are standard deviations.

* For CMB analysis organic carbon is decreased by percentage shown for RWC and transportation sources.

** Ratio of CMB calculated/measured.

Table 5.15E

Comparisons of CMB Analyses Using Various Wood Smoke Composition Profiles ($\mu g/m^3$)

Site: Hillsboro Residential Area Size: 0.3 μm.		Mass loading = 40 $\mu g/m^3$		
Date:		2/6/84		
	Normal	-25% *	EPA	Hot/Cool
RWC Comp.	32.4±3.6	32.5±4.2	31.1±3.8	-----
Hot burn	-----	-----	-----	2.3±-0.5
Cool burn	-----	-----	-----	30.2±-4.1
Soil	0.4±0.1	0.3±0.1	0.5±0.2	0.4±0.1
Motor Vehicle	0.7±0.1	0.7±0.1	0.7±0.1	0.7±0.1
Oil Furnace	3.9±1.0	4.4±1.0	4.1±1.0	4.0±1.0
X^2	0.590	0.719	1.021	2.637
DF	6	6	6	5
Mass calc.(%)	93.0±9.3	94.5±9.4	90.5±9.5	93.5±9.3
OC Ratio**	1.07±0.09	0.92±0.16	1.04±0.41	1.07±0.09
EC Ratio**	0.07±0.18	0.79±0.24	1.08±0.89	0.71±0.14
TC Ratio**	0.95±0.08	0.86±0.12	1.05±0.26	0.96±0.07
K Ratio**	1.22±0.42	1.39±0.45	0.86±0.12	1.22±0.33

Uncertainties are standard deviations.

* For CMB analysis organic carbon is decreased by percentage shown for RWC and tunnel sources.

** Ratio of CMB calculated/measured.

because Hillsboro is known for a large amount of residential wood burning and there are few other particulate pollution sources. During the heating season there were always many visible RWC plumes from cool wood burning around the sampling site. As was noted for Portland residential area samples, residential oil heating was the second largest pollution source. CMB analyses using the RWC composite or the 25% OC loss composition profiles resulted in lower X^2 values and accounted for more of the aerosol mass than using the EPA RWC composition profile for all members of the sample set but the difference in RWC contributions was not more than about 20%. The CMB solution using the hot/cool RWC composition profiles indicated that about 7% of the RWC aerosol resulted from hot burning. This was similar to the values (7-12% for data where 50% OC loss was assumed) determined for Portland.

Comparing CMB results using the EPA RWC composition profile with the composition profiles developed in this research showed that the EPA RWC profile fitted potassium better than OC or EC. However, since the carbon content of RWC particles has less variability and forms a much larger part of RWC aerosol mass than potassium, using the RWC source profile which most effectively accounts for carbon would be expected to give the most valid RWC contribution estimates.

Tables 5.15A-E show that OC loss values <25% cause OC and EC ratio values to approach 1. This OC loss value which is lower than values indicated for Portland data may be due to the higher levels of RWC emissions measured in Hillsboro; however, the data base is too small to have much confidence in such conclusions.

Figure 5.13 shows the source contributions in given size ranges obtained by subtracting the CMB source contribution obtained from the CMB solution for the lower end of the size range from the CMB source contribution obtained for the upper end of the size range. Wood smoke was by far the largest contributor to aerosol mass for all size ranges and became an increasingly larger contributor as particle size became smaller. This occurs because wood smoke particles are concentrated mainly in the small particle size ranges with usually more than 50% of their mass below 0.3 μm. In contrast motor vehicle emissions which have only 30% of their mass below 0.3 μm contribute a decreasing percentage as aerosol size becomes smaller. Figures 5.14 and 5.15 show Hillsboro OC and EC contributions, respectively, to the same particle size ranges shown in Figure 5.13

5.3.3.3 CMB ANALYSIS ACROSS AEROSOL SIZE FOR PORTLAND RESIDENTIAL SAMPLES COLLECTED WITH THE #1 IMPACTOR SET

This section discusses sample sets collected at a Portland residential site on September 18-20, 1984 (48 hours), July 26-28, 1984 (44 hours), April 28-30, 1984 (41 hours), March 9-11, 1984 (53 hours), March 5-6, 1984 (26 hours), and March 2-4, 1984 (37 hours) using the #1 impactor set. Using this impactor set samples were collected using no impactor (total aerosol) and behind 1.2 and 0.3 μm impactors on quartz filters. At the same time samples were collected behind 2.5, 0.6 and 0.1 μm impactors on Teflon filters. Samples collected on quartz fiber filters were analyzed for carbon and those collected on Teflon filters

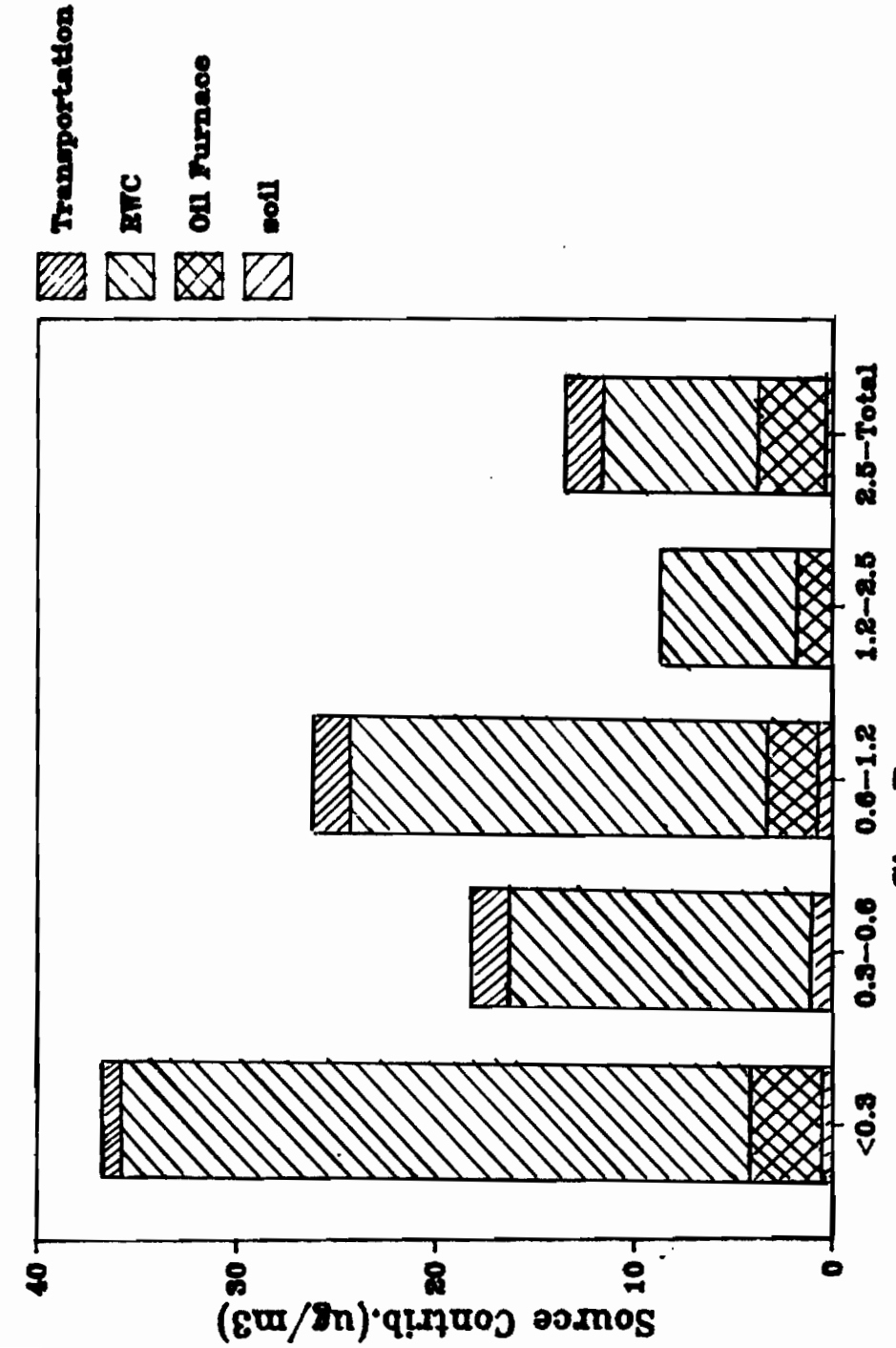

Figure 5.13. CMB source contributions to the indicated aerosol size ranges (Hillsboro, 02/06/84).

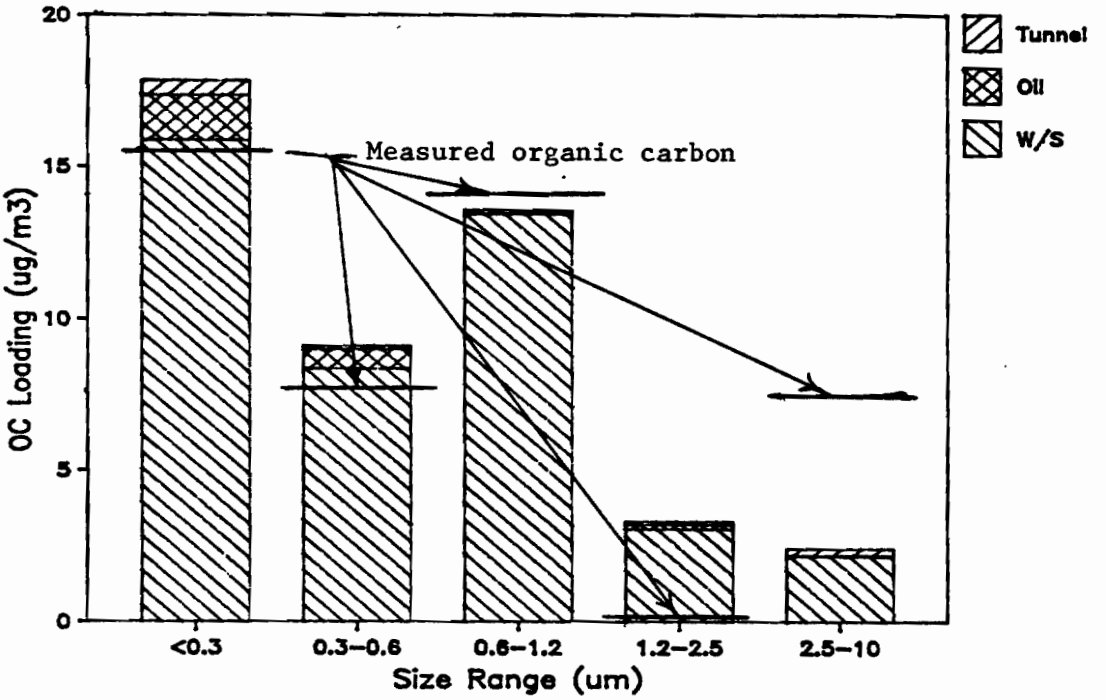

Figure 5.14. A comparison of ambient organic carbon loadings with CMB computed values (Hillsboro, 02/06/84).

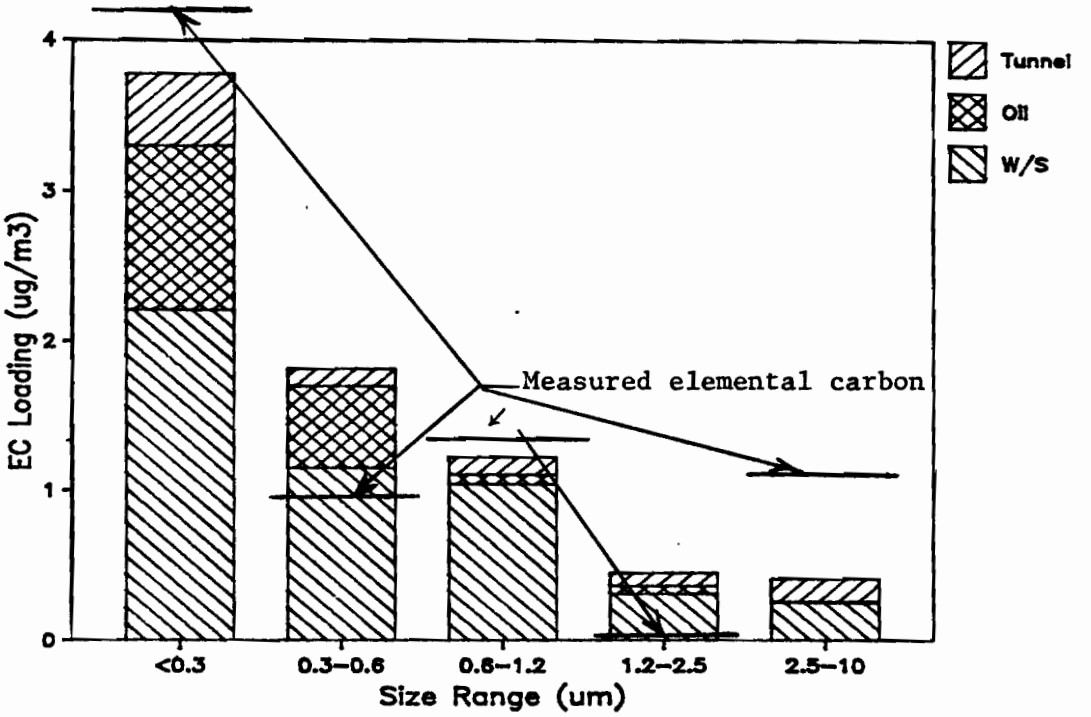

Figure 5.15. A comparison of ambient elemental carbon loadings with CMB computed values (histogram) (Hillsboro, 02/06/84).

were analyzed for trace elements. Thus carbon data was available for the total aerosol and for aerosols <1.2 and 0.3 μm and trace element data was available for aerosols <2.5, 0.6 and 0.1 μm. In order to do CMB analysis for the total aerosol and aerosols <2.5, 1.2, 0.6 and 0.3 μm, for those size cuts where either carbon or trace element data were not available the data above and below the given size-cut were averaged to estimate the missing carbon or trace element data. For example for the sample passing the 2.5 μm impactor the trace element concentrations were known. The carbon concentrations were determined by averaging the carbon concentrations for the total aerosol and the aerosol passing the 1.2 μm impactor. For the aerosol passing the 1.2 μm impactor the carbon data were known and the trace element data were determined by averaging data for aerosols passing the 2.6 and 0.6 μm impactors.

Tables 5.16A-D show CMB results for samples collected on 9/18/84 using impactor set #1. These samples, although collected in late summer, contained reasonably large RWC and residential oil furnace components. The daily minimum temperatures for the sampling period were 61°, 61°, and 53°F. Daily maximum temperature values, respectively, were 83°, 69°, and 71°F. While this sampling period was not very cool, evening wood burning to remove the chill probably occured especially since some of the period was foggy. The presence of a significant EC component confirms the presence of combustion aerosols. The fact that both the RWC and the residential oil furnace sources became a larger part of samples collected behind smaller cut-point impactors also implies that they were combustion aerosols; i.e., the apparent RWC contribution did not result from woody plant dusts in the ambient

Table 5.16A

Comparisons of CMB Analyses Using Various Wood Smoke Composition Profiles ($\mu g/m^3$)

Site: SW Portland Residential Area Size: Total			Mass loading = 38 $\mu g/m^3$	
Date:		9/18/84		
	Normal	-25% *	EPA	Hot/Cool
RWC Comp.	9.0±1.5	9.1±1.6	7.1±1.2	-----
Hot burn	-----	-----	-----	0.6±0.2
Cool burn	-----	-----	-----	8.9±1.8
Road Dust	2.5±0.3	2.5±0.3	2.8±0.3	2.5±0.3
Motor Vehicle	2.2±0.3	2.2±0.2	1.9±0.2	2.2±0.2
Diesel	1.8±0.6	1.8±0.6	2.4±0.6	1.8±0.6
Oil Furnace	9.9±1.0	9.9±1.0	10.0±1.0	9.8±1.0
X^2	1.766	1.877	5.073	2.138
DF	8	8	8	7
Mass calc.(%)	66.5±6.5	66.7±6.7	62.6±6.2	67.8±6.8
OC Ratio**	0.96±0.06	0.88±0.05	0.80±0.18	1.00±0.06
EC Ratio**	1.02±0.20	1.08±0.21	1.18±0.38	1.03±0.19
TC Ratio**	0.99±0.08	0.93±0.07	0.91±0.12	1.02±0.07
K Ratio**	0.84±0.22	0.93±0.26	0.69±0.09	0.83±0.17

Uncertainties are standard deviations.

* For CMB analysis organic carbon is decreased by percentage shown for RWC and tunnel sources.

** Ratio of CMB calculated/measured.

Table 5.16B

Comparisons of CMB Analyses Using Various Wood Smoke Composition Profiles ($\mu g/m^3$)

Site: SW Portland Residential Area Size: 2.5 μm.			Mass loading = 32 $\mu g/m^3$	
Date:		9/18/84		
	Normal	-25% *	EPA	Hot/Cool
RWC Comp.	9.9±1.7	10.1±1.8	6.9±1.2	-----
Hot burn	-----	-----	-----	0.6±0.2
Cool burn	-----	-----	-----	9.9±2.0
Road Dust	2.3±0.3	2.3±0.3	2.4±0.3	2.3±0.3
Motor Vehicle	1.6±0.2	1.6±0.2	1.5±0.2	1.6±0.2
Diesel	1.5±0.5	1.5±0.5	1.5±0.5	1.5±0.5
Oil Furnace	8.3±1.2	8.4±1.2	8.5±1.2	8.3±1.2
X^2	0.911	1.054	2.164	1.016
DF	8	8	8	7
Mass calc.(%)	73.0±7.3	73.6±7.4	64.3±6.4	74.6±7.5
OC Ratio**	1.00±0.10	0.88±0.05	0.72±0.17	1.02±0.05
EC Ratio**	0.91±0.17	0.94±0.18	1.00±0.32	0.91±0.16
TC Ratio**	0.96±0.07	0.91±0.06	0.81±0.11	1.00±0.06
K Ratio**	1.03±0.31	1.16±0.38	0.76±0.10	0.95±0.22

Uncertainties are standard deviations.

* For CMB analysis organic carbon is decreased by percentage shown for RWC and tunnel sources.

** Ratio of CMB calculated/measured.

Table 5.16C

Comparisons of CMB Analyses Using Various Wood Smoke Composition Profiles ($\mu g/m^3$)

Site: SW Portland Residential Area Size: 1.2 μm		Mass loading = 19 $\mu g/m^3$		
Date:		9/18/84		
	Normal	-25% *	EPA	Hot/Cool
RWC Comp.	8.4±1.3	9.0±1.5	7.9±1.4	-----
Hot burn	-----	-----	-----	0.5±0.2
Cool burn	-----	-----	-----	8.3±1.5
Road Dust	2.0±0.3	2.0±0.3	2.0±0.3	2.0±0.3
Motor Vehicle	1.1±0.1	1.1±0.1	1.1±0.1	1.1±0.1
Diesel	0.9±0.4	0.9±0.4	0.8±0.4	0.9±0.4
Oil Furnace	6.0±0.9	5.9±0.9	5.9±0.9	5.9±0.9
X^2	0.906	1.047	0.815	1.005
DF	7	7	7	6
Mass calc.(%)	98.5±9.8	101.3±10	94.9±9.5	100.5±10
OC Ratio**	0.97±0.05	0.91±0.05	0.87±0.25	1.02±0.05
EC Ratio**	0.89±0.16	0.93±0.18	1.08±0.48	0.89±0.15
TC Ratio**	0.96±0.62	0.93±0.05	0.87±0.25	0.99±0.06
K Ratio**	1.16±0.38	1.36±0.50	1.04±0.15	1.02±0.24

Uncertainties are standard deviations.

* For CMB analysis organic carbon is decreased by percentage shown for RWC and tunnel sources.

** Ratio of CMB calculated/measured.

Table 5.16D

Comparisons of CMB Analyses Using Various Wood Smoke Composition Profiles ($\mu g/m^3$)

Site: SW Portland Residential Area Size: 0.6 μm.			Mass loading = 16 $\mu g/m^3$	
Date:		9/18/84		
	Normal	-25% *	EPA	Hot/Cool
RWC Comp.	7.8±1.2	8.4±1.4	7.7±1.4	-----
Hot burn	-----	-----	-----	0.5±0.2
Cool burn	-----	-----	-----	7.4±1.4
Road Dust	2.0±0.3	2.0±0.3	2.1±0.3	2.0±0.3
Motor Vehicle	0.9±0.1	0.9±0.1	0.9±0.1	0.9±0.1
Diesel	0.9±0.3	0.9±0.3	0.8±0.3	0.9±0.4
Oil Furnace	6.5±0.9	6.4±0.9	6.5±0.9	6.4±0.9
X^2	1.162	1.230	1.218	1.324
DF	8	8	8	7
Mass calc.(%)	111.5±11	114.6±11	110.1±11	112.5±11
OC Ratio**	1.00±0.06	0.94±0.05	0.93±0.27	1.02±0.05
EC Ratio**	0.91±0.17	0.95±0.18	1.13±0.49	0.91±0.15
TC Ratio**	0.98±0.06	0.95±0.05	0.99±0.17	1.00±0.06
K Ratio**	1.10±0.35	1.29±0.45	1.02±0.14	1.02±0.24

Uncertainties are standard deviations.

* For CMB analysis organic carbon is decreased by percentage shown for RWC and tunnel sources.

** Ratio of CMB calculated/measured.

sample which would be found mostly in the size range above 2 μm and would have a similar composition as RWC particles. Part of the apparent RWC and residential oil furnace contributions might have come from agricultural burning, residential waste paper burning or commercial oil burning. Note that oil burning was a significant source for the July sample when no residential heating was expected. Therefore the residential oil burning source probably always includes a commercial oil burning component. A secondary sulfur source was not indicated by the CMB model because all sulfur was accounted for by the primary sources.

For the total aerosol the EC ratio was greater than the OC ratio. Therefore using a RWC composition profile which incorporated OC loss would not improve the model fit. CMB solutions for samples <2.5, 1.2, and 0.6 μm showed slightly lower EC than OC ratio values when using the normal composite RWC composition profile but the best model fit was obtained at RWC particle OC loss values of less than 25%. Therefore if RWC particles lost OC during their atmospheric residence time it was less than 25%. This seems to indicate that the atmospheric interaction with the RWC particles was different during mild weather than it was during cold weather. In the absence of other effects OC evaporation would be expected to be greater for RWC particles during warmer weather than during cold weather. RWC particles might have lower OC losses in warmer weather because atmospheric chemistry might convert volatile OC to less volatile OC therefore preventing the wintertime type of OC loss. A second alternative might be that lost organic carbon was replaced by less volatile OC which was formed by gas to particle

conversion on the particle surfaces. Kleindienst et al. (1986) showed that wood smoke, with NO_X added, that was aged and irradiated with sunlight in a Teflon bag showed a factor of 2-3 increase in total aerosol volume. This implies that wood smoke particles can undergo considerable alteration due to atmospheric chemistry. While it is not clear why CMB modeling indicates less OC loss for warmer weather than cold weather, similar results were also noted for early spring and late winter samples.

Figure 5.16 shows how the sources for the 9/18/84 samples collected behind various impactors were distributed as a percentage of aerosol mass passing the indicated impactor. This figure shows that combustion aerosols become a larger part of smaller sized aerosols and that for smaller aerosols the CMB model accounts for a larger fraction of the ambient aerosol. This implies that for aerosols >1.2 μm sources exist which were not characterized or not well characterized. It is also notable that, as was shown for other samples, motor vehicle emissions and road or geological dust contribute only a small amount to even the total aerosol sample and that these contributions on a percentage basis remain fairly constant over the aerosol size range.

Table 5.17 shows CMB results for a summertime sample collected across the particle size range in the SW Portland residential area on 7/26/84 using impactor set #1. This sample was very different from the typical wintertime or spring and fall sample. Neither grass nor slash burning sources provided suitable CMB model fits. The RWC source did not fit the CMB analysis as well as the raw wood source; however, if the RWC source had been used a solution that looked reasonably

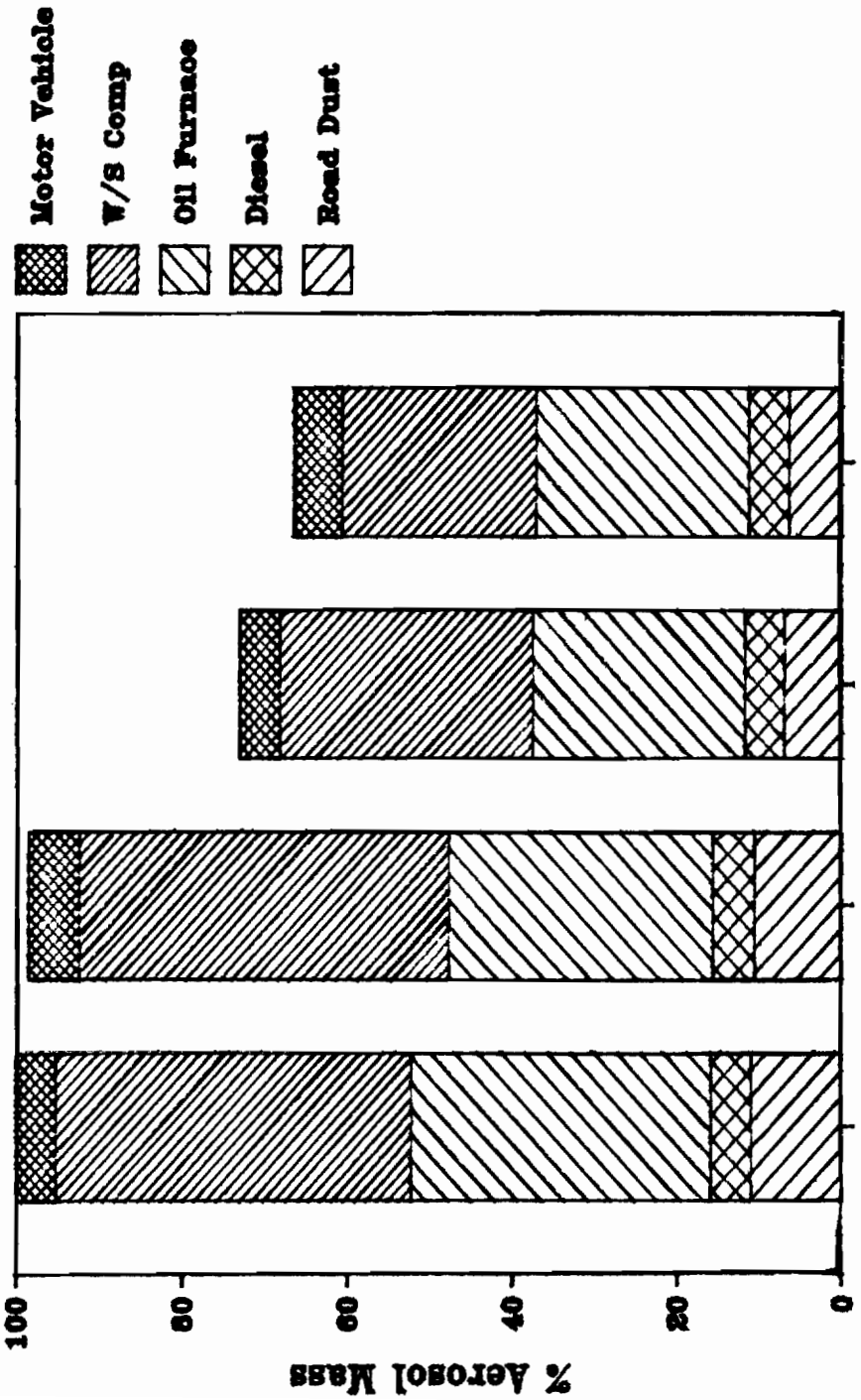

Figure 5.16. CMB source contributions over the aerosol size range for a SW Portland residential area (09/18/84).

Table 5.17

Comparisons of CMB Analyses Across the Aerosol Size Distribution ($\mu g/m^3$)

Site: SW Portland Residential Area Date: 7/26/4			Mass loading = 36 $\mu m/m^3$	
Size	Total	<2.5 um	<1.2 um	<0.6 um
Raw Wood	9.1±2.0	3.2±1.1	1.5±0.9	2.9±0.6
Dist Oil	7.7±1.8	5.9±1.3	5.5±1.3	1.4±0.5
Incinerator	1.1±0.3	0.5±0.1	0.5±0.1	0.5±0.1
Road Dust	4.7±0.6	2.4±0.4	2.5±0.3	2.4±0.3
Motor Vehicle	0.8±0.2	0.3±0.1	0.3±0.1	0.3±0.1
Sec SO4	9.5±1.3	4.5±0.7	3.3±0.5	3.1±0.4
X^2	0.224	0.148	0.134	0.190
DF	5	5	5	5
Mass calc.(%)	91.2±9.1	92.4±9.2	94.0±9.4	90.0±9.0
OC Ratio**	1.00±0.09	1.00±0.12	1.00±0.16	1.00±0.10
EC Ratio**	1.03±0.24	0.99±0.24	0.95±0.22	0.95±0.22
TC Ratio**	1.00±0.13	0.98±0.15	0.99±0.16	0.97±0.21
K Ratio**	1.02±0.15	1.04±0.16	1.00±0.16	0.95±0.15

Uncertainties are standard deviations.

* For CMB analysis organic carbon is decreased by percentage shown for RWC and tunnel sources.

** Ratio of CMB calculated/measured.

acceptable would have been obtained. This sample illustrates the use of particle size information as a guide in CMB source selection. Because the sample had a large coarse OC component (>2.5 μm) it was suspected that it included a coarse aerosol source which contained OC. RWC emissions do not make a significant contribution to the >2.5 μm particle size range and were not expected to be a significant contributor to summertime aerosols. Raw wood particles have a reasonably similar composition profile to cool burning RWC smoke particles. It was assumed that raw wood particles could be used as a surrogate for pollen and plant dust. Using the grass burning source did not provide a suitable CMB model fit.

This sample also showed an apparent large secondary SO_4 component. This was not unusual in summertime aerosols. What was not expected was that half of the SO4 contribution was found in the >2.5 μm size range. Since the SO_4 source contains only sulfur it accounts for sulfur that exists in the sample but is not "used" by the other sources in the model. It does not really identify secondary SO_4. What these results really showed was that there was a source which contained only sulfur and possibly other elements that were not used in fitting and that half of the contribution of this source was in the >2.5 μm size range. This might indicate an industrial sulfur source but the most common industrial source expected, Kraft, did not fit the CMB model. Therefore either some secondary SO_4 had coagulated with large particles or some uncharacterized source of large sulfur particles exists in the airshed. Ion chromatography could be used to definitely identify SO4.

The small incinerator source detected might represent residential

trash burning. Finally in the absence of large combustion components and because summer air was quite stagnant, allowing pollution buildups, a significant diesel emission component was noted. This results when the diesel source contribution was larger than the diesel component that was included in the motor vehicle (tunnel) source.

For this sample the OC ratio, EC ratio and TC ratio values equaled one for all samples across the size range. This indicated that both OC and EC was well accounted for by the model. Any consideration of particle OC loss would not be appropriate.

Figure 5.17 shows how the sources were distributed across the size range as percentages of the total aerosol mass passing the given impactor. It will be noted that the sources were quite uniformly distributed across the particle size range and that the "pollen" component decreased toward smaller sizes while the diesel component increased as might be expected.

Tables 5.18A-D show CMB results for a Portland residential area sample collected on 4/28/84 using impactor set #1. This sample resembles the 9/18/84 sample in that RWC component, based on OC and EC ratio values, did not appear to lose more than 25% OC. The temperature for this sampling period was cooler than for the September sample. Daily low temperatures were 42,° 45° and 47°F and high temperatures were 55,° 54°, and 57°F. The weather was cloudy with light occasional rain and fog.

The RWC contribution computed by using the EPA composition profile was higher than the RWC contributions computed by using either the composite or the hot and cool composition profiles. Using the hot and

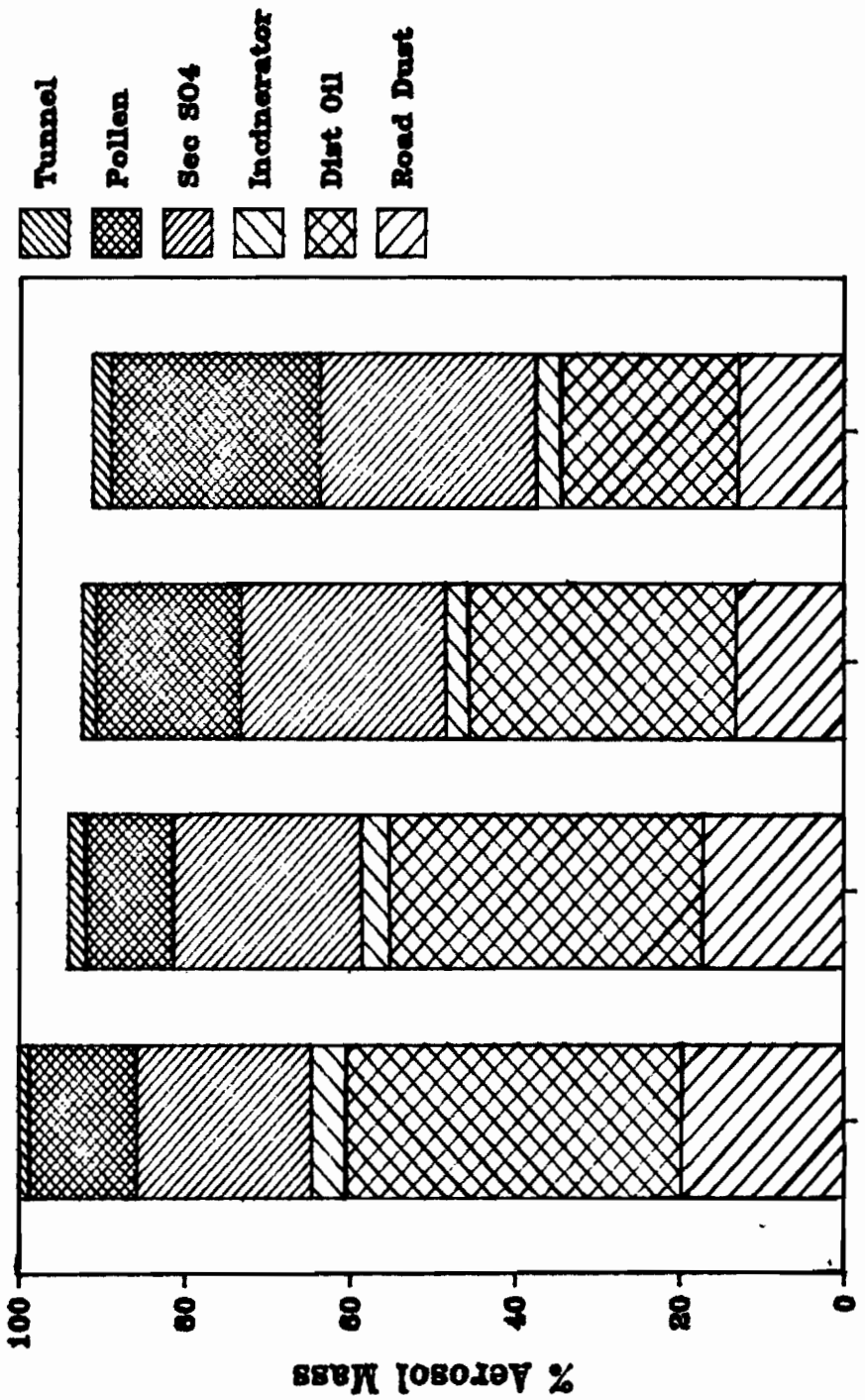

Figure 5.17 CMB Source Contributions Over The Aerosol Size Range for a SW Portland Residential Area (7/26/84)

Table 5.18A

Comparisons of CMB Analyses Using Various Wood Smoke Composition Profiles ($\mu g/m^3$)

Site: SW Portland Residential Area Size: 2.5 μm.		Mass loading = 8.8 $\mu g/m^3$		
Date:		4/28/84		
	Normal	-25% *	EPA	Hot/Cool
RWC Comp.	2.2±0.5	2.5±0.6	3.1±0.8	-----
Hot burn	-----	-----	-----	0.3±0.1
Cool burn	-----	-----	-----	1.6±0.6
Road Dust	0.3±0.1	0.4±0.1	0.3±0.1	0.3±0.1
Motor Vehicle	0.5±0.1	0.5±0.1	0.5±0.1	0.5±0.1
Kraft RB	1.3±0.4	1.1±0.4	1.2±0.4	0.9±0.4
Dist. Oil	2.9±0.9	2.8±0.7	2.7±0.7	3.1±0.7
X^2	1.618	1.410	1.355	1.296
DF	7	7	7	6
Mass calc.(%)	82.0±8.2	83.3±8.3	89.6±8.9	77.0±7.7
OC Ratio**	1.09±0.11	1.06±0.11	1.26±0.42	0.98±0.11
EC Ratio**	1.06±0.22	1.11±0.24	1.42±0.72	1.16±0.24
TC Ratio**	1.08±0.17	1.08±0.16	1.31±0.29	1.03±0.17
K Ratio**	0.78±0.16	0.86±0.19	0.86±0.12	1.04±0.26

Uncertainties are standard deviations.

* For CMB analysis organic carbon is decreased by percentage shown for RWC and tunnel sources.

** Ratio of CMB calculated/measured.

Table 5.18B

Comparisons of CMB Analyses Using Various Wood Smoke Composition Profiles ($\mu g/m^3$)

Site: SW Portland Residential Area Size: 1.2 μm.			Mass loading = 7.8 $\mu g/m^3$	
Date:		4/28/84		
	Normal	-25% *	EPA	Hot/Cool
RWC Comp.	2.3±0.5	2.5±0.5	2.9±0.7	-----
Hot burn	-----	-----	-----	0.4±0.1
Cool burn	-----	-----	-----	1.7±0.5
Road Dust	0.5±0.1	0.5±0.1	0.5±0.1	0.5±0.1
Motor Vehicle	0.5±0.1	0.5±0.1	0.5±0.1	0.5±0.1
Kraft RB	1.0±0.3	0.9±0.3	0.9±0.4	0.7±0.4
Dist. Oil	2.5±0.6	2.5±0.7	2.1±0.8	2.6±0.7
X^2	0.863	0.880	0.830	0.776
DF	7	7	7	6
Mass calc.(%)	86.0±8.6	88.3±8.8	91.2±9.1	82.2±8.2
OC Ratio**	1.08±0.10	1.05±0.10	1.18±0.38	0.98±0.09
EC Ratio**	0.98±0.19	1.04±0.21	1.27±0.63	1.10±0.20
TC Ratio**	1.05±0.15	1.05±0.14	1.21±0.25	1.02±0.15
K Ratio**	0.83±-0.18	0.92±0.22	0.92±0.13	1.06±0.31

Uncertainties are standard deviations.

* For CMB analysis organic carbon is decreased by percentage shown for RWC and tunnel sources.

** Ratio of CMB calculated/measured.

Table 5.18C

Comparisons of CMB Analyses Using Various Wood Smoke Composition Profiles ($\mu g/m^3$)

Site: SW Portland Residential Area Size: 0.6 μm.			Mass loading = 5.4 $\mu g/m^3$	
Date:			4/28/84	
	Normal	-25% *	EPA	Hot/Cool
RWC Comp.	1.5±0.4	1.6±0.4	2.0±0.5	-----
Hot burn	-----	-----	-----	0.2±0.1
Cool burn	-----	-----	-----	1.0±0.4
Road Dust	0.3±0.1	0.3±0.1	0.3±0.05	0.3±0.05
Motor Vehicle	0.4±0.1	0.4±0.1	0.4±0.1	0.4±0.1
Kraft RB	0.6±0.3	0.5±0.2	0.6±0.2	0.4±0.3
Dist. Oil	1.9±0.5	1.9±0.5	1.7±0.6	2.2±0.5
X^2	1.206	1.109	1.122	0.998
DF	7	7	7	6
Mass calc.(%)	85.7±8.6	87.8±8.7	91.7±9.2	81.7±8.2
OC Ratio**	1.09±0.11	1.07±0.11	1.22±0.39	0.98±0.11
EC Ratio**	0.98±0.18	1.04±0.20	1.25±0.56	1.10±0.21
TC Ratio**	1.07±0.16	1.06±0.16	1.23±0.26	1.02±0.17
K Ratio**	0.78±0.16	0.86±0.20	0.88±0.12	1.04±0.27

Uncertainties are standard deviations.

* For CMB analysis organic carbon is decreased by percentage shown for RWC and tunnel sources.

** Ratio of CMB calculated/measured.

Table 5.18D

Comparisons of CMB Analyses Using Various Wood Smoke Composition Profiles ($\mu g/m^3$)

Site: SW Portland Residential Area Size: 0.3 μm.		Mass loading = 3.9 $\mu g/m^3$		
Date:		4/28/84		
	Normal	-25% *	EPA	Hot/Cool
RWC Comp.	1.0±0.3	1.1±0.3	1.3±0.3	-----
Hot burn	-----	-----	-----	0.1±0.04
Cool burn	-----	-----	-----	0.7±0.3
Road Dust	0.3±0.1	0.3±0.1	0.3±0.05	0.3±0.05
Motor Vehicle	0.3±0.05	0.3±0.05	0.3±0.05	0.3±0.05
Kraft RB	0.3±0.2	0.2±0.2	0.4±0.2	0.1±0.2
Dist. Oil	1.3±0.4	1.4±0.3	1.1±0.4	1.6±0.4
X^2	0.567	0.438	0.798	0.417
DF	6	6	6	5
Mass calc.(%)	82.9±8.3	84.5±8.4	85.8±8.6	79.9±8.0
OC Ratio**	1.07±0.12	1.03±0.15	1.17±0.35	0.98±0.12
EC Ratio**	1.01±0.18	1.08±0.20	1.16±0.47	1.10±0.20
TC Ratio**	1.04±0.16	1.03±0.17	1.17±0.23	1.00±0.17
K Ratio**	0.87±0.17	0.94±0.18	0.87±0.11	0.99±0.20

Uncertainties are standard deviations.

* For CMB analysis organic carbon is decreased by percentage shown for RWC and tunnel sources.

** Ratio of CMB calculated/measured.

cool composition profiles best accounted for OC, EC and potassium. As noted for other samples all source contributions except the RWC source contribution were not significantly affected by using different RWC composition profiles.

Figure 5.18 shows the various CMB computed source contributions for samples collected behind each impactor. In a similar manner to other samples all sources were broadly distributed across the aerosol size range. For this sample distillate oil burning contribution was larger than the RWC contribution. This trend would be expected to continue as the weather warms up as wood burning stops and commercial oil burning continues. This sample also showed a significant Kraft recovery boiler component which was unusual at this site but has been noted at other Portland sampling sites.

Tables 5.19A-E, 5.20A-B and 5.21A-E show CMB results for Portland residential area samples collected on 3/9/84, 3/5/84, and 3/2/84, respectively. High and low daily temperature values over the sampling period for the March 2, 5, and 9 were 61°, 32°; 66°, 36°; and 66°,43°F, respectively. March 2 and 9 were high cloud cover days while March 5 was almost cloudless. Figures 5.19 and 5.20 show the distribution of source contributions across the aerosol size range for 3/9/84 and 3/2/84, respectively. Both these figures show that RWC is the largest pollution source and that most of the sources are fairly uniformly distributed across the aerosol size range.

Tables 5.19A-E and 5.21A-E indicate that for 3/9/84 and 3/2/84 samples, respectively, the RWC OC loss values could have ranged from 20-30%, except for the samples collected behind the <0.3 μm impactor

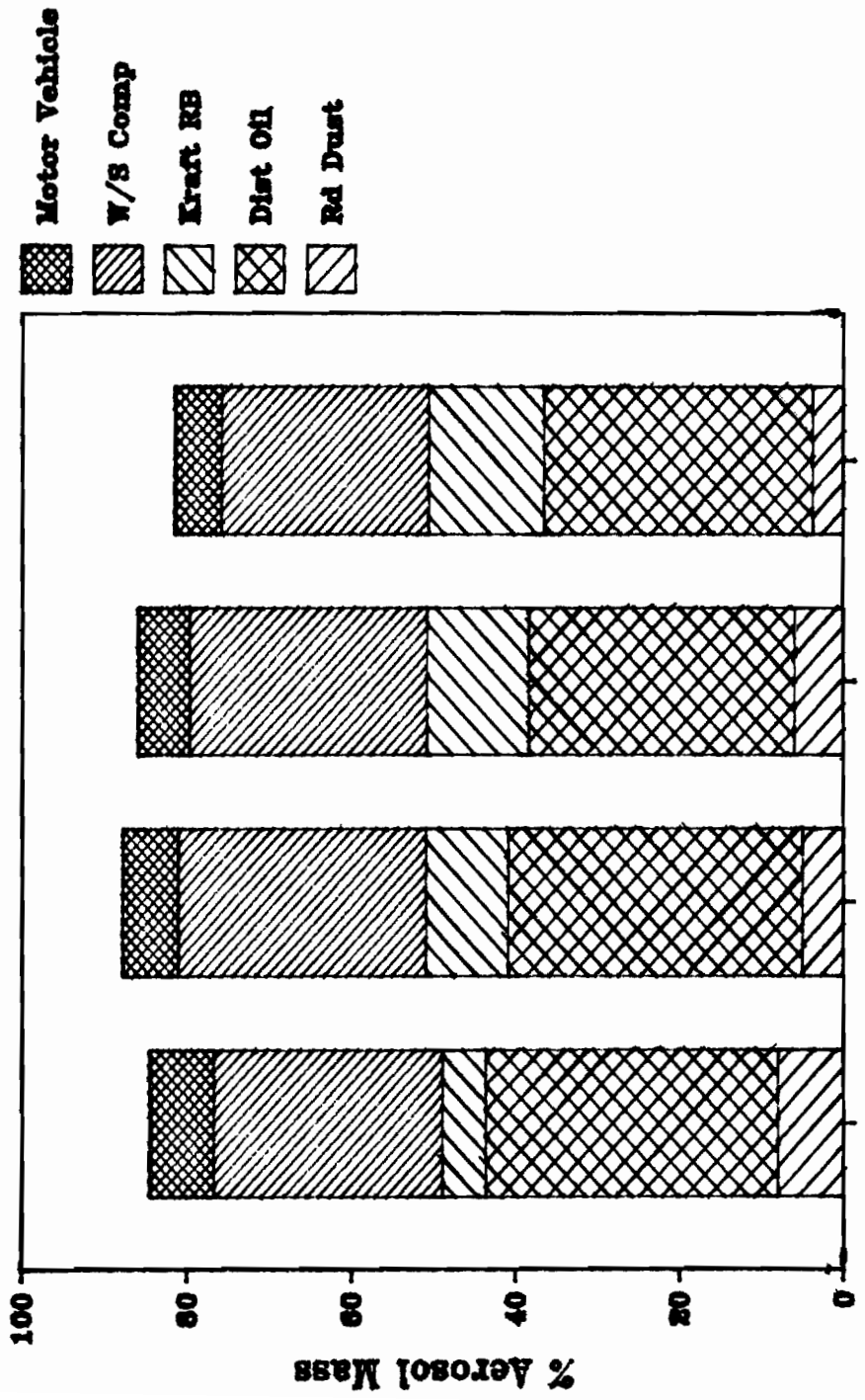

Figure 5.18 CMB Source Contributions Over The Aerosol Size Range For A SW Portland Residential Area (4/28/84)

Table 5.19A

Comparisons of CMB Analyses Using Various Wood Smoke Composition Profiles (μg/m³)

Site: SW Portland Residential Area Size: Total.			Mass loading = 25 μg/m³	
Date:		3/9/84		
	Normal	-25% *	-50% *	Hot/Cool
RWC Comp.	15.7+2.0	17.0+2.2	19.2+2.7	-----
Hot burn	-----	-----	-----	1.2+0.4
Cool burn	-----	-----	-----	14.5+2.1
Soil	0.8+0.3	0.7+0.3	0.7+0.3	0.8+0.3
Motor Vehicle	2.9+0.5	2.8+0.5	2.8+0.5	2.9+0.5
Sea Salt	1.1+0.4	1.1+0.4	1.0+0.4	1.1+0.4
Oil Furnace	2.6+0.7	2.5+0.7	2.4+0.7	2.6+0.7
X^2	0.371	0.407	0.841	0.430
DF	7	7	7	6
Mass calc.(%)	91.8±9.2	96.5±9.6	104.6±10.4	91.8±9.2
OC Ratio**	1.02±0.05	0.97±0.05	0.85±0.04	1.01±0.04
EC Ratio**	0.88±0.23	1.00±0.29	1.19±0.43	0.89±0.17
TC Ratio**	0.99±0.06	0.96±0.04	0.91±0.05	0.99±0.05
K Ratio**	1.00±0.33	1.21±0.45	1.55±0.71	1.05±0.29

Uncertainties are standard deviations.

* For CMB analysis organic carbon is decreased by percentage shown for RWC and tunnel sources.

** Ratio of CMB calculated/measured.

Table 5.19B

Comparisons of CMB Analyses Using Various Wood Smoke Composition Profiles ($\mu g/m^3$)

Site: SW Portland Residential Area Size: 2.5 μm.			Mass loading = 17.7 $\mu g/m^3$	
Date:		3/9/84		
	Normal	-25% *	-50% *	Hot/Cool
RWC Comp.	12.0±1.5	13.4±1.7	15.6±2.1	-----
Hot burn	-----	-----	-----	1.0±0.4
Cool burn	-----	-----	-----	10.6±1.5
Soil	0.4±0.2	0.4±0.1	0.4±0.2	0.4±0.1
Motor Vehicle	2.0±0.3	2.0±0.3	2.0±0.3	2.1±0.3
Sea Salt	0.9±0.3	0.9±0.3	0.8±0.3	0.9±0.3
Oil Furnace	2.2±0.7	2.1±0.7	1.8±0.7	2.2±0.7
X^2	0.924	0.906	0.998	1.184
DF	8	8	8	7
Mass calc.(%)	99.2±9.9	105.7±10.5	116.7±11.7	98.7±9.9
OC Ratio**	1.05±0.06	1.00±0.05	0.92±0.05	1.03±0.04
EC Ratio**	0.86±0.21	0.99±0.28	1.19±0.42	0.90±0.16
TC Ratio**	1.01±0.06	1.00±0.05	0.97±0.06	1.01±0.05
K Ratio**	1.07±0.37	1.32±0.52	1.74±0.88	1.24±0.39

Uncertainties are standard deviations.

* For CMB analysis organic carbon is decreased by percentage shown for RWC and tunnel sources.

** Ratio of CMB calculated/measured.

Table 5.19C

Comparisons of CMB Analyses Using Various Wood Smoke Composition Profiles ($\mu g/m^3$)

Site: SW Portland Residential Area Size: 1.2 μm.			Mass loading = 15.8 $\mu g/m^3$	
Date:		3/9/84		
	Normal	-25% *	-50% *	Hot/Cool
RWC Comp.	11.2±1.4	12.4±1.6	14.4±1.9	-----
Hot burn	-----	-----	-----	1.3±0.5
Cool burn	-----	-----	-----	9.9±1.5
Soil	0.3±0.1	0.3±0.1	0.3±0.1	0.3±0.1
Motor Vehicle	2.0±0.4	2.0±0.4	2.0±0.4	2.0±0.4
Sea Salt	0.5±0.2	0.5±0.2	0.4±0.2	0.4±0.2
Oil Furnace	1.6±0.5	1.4±0.6	1.2±0.6	1.5±0.5
X^2	0.656	0.468	0.616	0.561
DF	7	7	7	6
Mass calc.(%)	99.4±9.9	105.5±10	116.3±11	98.1±9.8
OC Ratio**	1.06±0.06	1.01±0.05	0.92±0.05	1.02±0.04
EC Ratio**	0.81±0.19	0.91±0.25	1.10±0.37	0.91±0.16
TC Ratio**	1.01±0.06	0.99±0.05	0.95±0.06	1.00±0.05
K Ratio**	0.96±0.33	1.19±0.46	1.57±0.76	1.22±0.48

Uncertainties are standard deviations.

* For CMB analysis organic carbon is decreased by percentage shown for RWC and tunnel sources.

** Ratio of CMB calculated/measured.

Table 5.19D

Comparisons of CMB Analyses Using Various Wood Smoke Composition Profiles ($\mu g/m^3$)

Site: SW Portland Residential Area Size: 0.6 μm.			Mass loading = 11.1 $\mu g/m^3$	
Date:		3/9/84		
	Normal	-25% *	-50% *	Hot/Cool
RWC Comp.	8.1±1.0	8.9±1.2	10.2±1.4	-----
Hot burn	-----	-----	-----	0.8±0.3
Cool burn	-----	-----	-----	7.2±1.1
Soil	0.3±0.1	0.3±0.1	0.3±0.1	0.3±0.1
Motor Vehicle	1.7±0.3	1.7±0.3	1.6±0.3	1.7±0.3
Sea Salt	0.04±0.03	0.03±0.03	0.02±0.03	0.03±0.03
Oil Furnace	0.5±0.3	0.4±0.3	-----	0.4±0.3
X^2	0.892	0.784	1.027	0.971
DF	7	8	8	6
Mass calc.(%)	95.0	101.3±10.1	112.0±11.2	93.8±9.4
OC Ratio**	1.04±0.05	0.98±0.05	0.89±0.04	1.01±0.04
EC Ratio**	0.87±0.20	0.9750.26	1.15±0.38	0.91±0.15
TC Ratio**	1.00±0.06	0.98±0.05	0.94±0.06	0.99±0.05
K Ratio**	0.81±0.26	1.00±8.36	1.32±0.57	1.01±0.30

Uncertainties are standard deviations.

* For CMB analysis organic carbon is decreased by percentage shown for RWC and tunnel sources.

** Ratio of CMB calculated/measured.

Table 5.19E

Comparisons of CMB Analyses Using Various Wood Smoke Composition Profiles (μg/m³)

Site: SW Portland Residential Area Size: 0.3 μm.			Mass loading = 9.2 μg/m³	
Date:	3/9/84			
	Normal	-25% *	-50% *	Hot/Cool
RWC Comp.	7.4±1.0	7.8±1.2	8.2±1.3	-----
Hot burn	-----	-----	-----	0.6±0.2
Cool burn	-----	-----	-----	6.7±1.0
Soil	0.05±0.04	0.05±0.04	0.04±0.04	0.05±0.04
Motor Vehicle	1.1±0.2	1.1±0.2	1.1±0.2	1.1±0.2
Sea Salt	-----	-----	-----	-----
Oil Furnace	0.8±0.4	0.8±0.4	0.8±0.4	0.8±0.4
X^2	0.590	0.691	1.370	0.674
DF	6	6	6	5
Mass calc.(%)	101.3±10	105.1±10	109.6±10	100.0±10
OC Ratio**	1.02±0.08	0.92±0.16	0.770.10	1.00±0.08
EC Ratio**	0.99±0.23	1.10±0.31	1.24±0.43	1.00±0.17
TC Ratio**	0.99±0.07	0.92±0.12	0.82±0.11	0.97±0.06
K Ratio**	0.92±0.27	1.09±0.31	1.32±0.36	1.01±0.25

Uncertainties are standard deviations.

* For CMB analysis organic carbon is decreased by percentage shown for RWC and tunnel sources.

** Ratio of CMB calculated/measured.

Table 5.20A

Comparisons of CMB Analyses Using Various Wood Smoke Composition Profiles (μg/m³)

Site: SW Portland Residential Area Size: Total			Mass load = 49.1 μg/m³	
Date:	3/5/84			
	Normal	-25% *	-50% *	Hot/Cool
RWC Comp.	15.1±2.6	16.2±2.9	17.2±3.3	-----
Hot burn	-----	-----	-----	0.8±0.4
Cool burn	-----	-----	-----	15.0±2.7
Road Dust	5.1±0.9	5.0±0.9	5.0±0.9	5.2±0.9
Motor Vehicle	3.4±0.6	3.3±0.6	3.3±0.6	3.4±0.6
Diesel	3.1±1.4	3.0±1.5	2.8±1.5	3.1±1.4
Oil Furnace	5.5±1.0	5.4±1.0	5.3±1.0	5.6±0.4
X^2	1.017	1.173	1.688	1.199
DF	7	7	7	6
Mass calc.(%)	70.0±7.0	71.5±7.1	73.1±7.3	71.5±7.1
OC Ratio**	0.97±0.06	0.90±0.05	0.78±0.05	1.01±0.05
EC Ratio**	1.06±0.25	1.09±0.26	1.14±0.28	1.05±0.23
TC Ratio**	0.99±0.09	0.95±0.08	0.88±0.07	1.02±0.08
K Ratio**	0.93±0.25	1.07±0.32	1.26±0.44	0.83±0.17

Uncertainties are standard deviations.

* For CMB analysis organic carbon is decreased by percentage shown for RWC and tunnel sources.

** Ratio of CMB calculated/measured.

Table 5.20B

Comparisons of CMB Analyses Using Various Wood Smoke Composition Profiles (μg/m³)

Site: SW Portland Residential Area Size: 2.5 μm.			Mass loading = 34.5 μg/m³	
Date:	3/5/84			
	Normal	-25% *	-50% *	Hot/Cool
RWC Comp.	11.2±1.9	12.3±2.1	13.9±2.5	-----
Hot burn	-----	-----	-----	0.9±0.4
Cool burn	-----	-----	-----	10.2±1.9
Road Dust	3.5±0.7	3.5±0.7	3.5±0.7	3.5±0.7
Motor Vehicle	2.4±0.5	2.3±0.5	2.3±0.5	2.3±0.5
Diesel	3.2±1.4	3.1±1.4	2.9±1.4	3.3±1.3
Oil Furnace	3.6±1.0	3.8±1.2	3.6±1.1	3.9±1.0
X^2	0.369	0.370	0.635	0.433
DF	7	7	7	6
Mass calc.(%)	69.7±7.0	72.3±7.2	76.1±7.6	69.4±6.9
OC Ratio**	1.02±0.07	0.97±0.06	0.88±0.06	1.01±0.06
EC Ratio**	1.00±0.25	1.03±0.25	1.08±0.27	1.01±0.24
TC Ratio**	1.02±0.11	0.99±0.10	0.95±0.09	1.01±0.10
K Ratio**	0.97±0.27	1.15±0.36	1.42±0.54	1.02±0.24

Uncertainties are standard deviations.

* For CMB analysis organic carbon is decreased by percentage shown for RWC and tunnel sources.

** Ratio of CMB calculated/measured.

Table 5.21A

Comparisons of CMB Analyses Using Various Wood Smoke Composition Profiles ($\mu g/m^3$)

Site: SW Portland Residential Area Size: Total			Mass loading = 26 $\mu g/m^3$	
Date:	3/2/84			
	Normal	-25% *	-50% *	Hot/Cool
RWC Comp.	10.7±1.9	12.1±2.2	14.2±2.7	-----
Hot burn	-----	-----	-----	1.6±0.6
Cool burn	-----	-----	-----	8.9±1.9
Soil	0.7±0.3	0.7±0.3	0.7±0.2	0.7±0.3
Motor Vehicle	1.5±0.4	1.5±0.4	1.6±0.4	1.5±0.4
Sec SO4	1.7±0.7	1.2±0.8	1.8±0.7	1.7±0.7
Dist. Oil	8.4±2.2	7.8±2.2	7.0±2.4	7.8±2.3
X^2	1.968	1.624	1.527	1.964
DF	6	6	6	5
Mass calc.(%)	88.4±8.8	89.2±8.9	97.0±9.7	85.1±8.5
OC Ratio**	1.10±0.09	1.06±0.08	0.97±0.07	1.02±0.08
EC Ratio**	0.80±0.15	0.84±0.17	0.92±0.22	0.85±0.14
TC Ratio**	0.71±0.12	0.89±0.11	0.95±0.10	0.97±0.12
K Ratio**	0.55±0.21	0.70±0.29	1.19±0.48	1.04±0.31

Uncertainties are standard deviations.

* For CMB analysis organic carbon is decreased by percentage shown for RWC and tunnel sources.

** Ratio of CMB calculated/measured.

Table 5.21B

Comparisons of CMB Analyses Using Various Wood Smoke Composition Profiles (μg/m³)

Site: SW Portland Residential Area Size: 2.5 μm.			Mass loading = 22.8 μg/m³	
Date:		3/2/84		
	Normal	-25% *	-50% *	Hot/Cool
RWC Comp.	7.9±1.5	9.2±1.8	11.3±2.2	-----
Hot burn	-----	-----	-----	1.0±0.4
Cool burn	-----	-----	-----	6.8±1.5
Soil	0.6±0.2	0.6±0.2	0.6±0.2	0.6±0.2
Motor Vehicle	1.3±0.4	1.3±0.3	1.4±0.3	1.3±0.3
Sec SO4	1.4±0.7	1.0±0.8	1.6±0.7	1.4±0.7
Dist. Oil	6.4±1.6	5.8±1.7	5.0±1.8	5.9±1.7
X^2	0.870	0.592	0.473	0.695
DF	6	6	6	5
Mass calc.(%)	77.5±7.7	78.8±7.9	86.7±8.7	75.5±7.5
OC Ratio**	1.07±0.08	1.05±0.08	1.00±0.07	1.02±0.07
EC Ratio**	0.88±0.17	0.91±0.19	0.99±0.24	0.90±0.15
TC Ratio**	1.02±0.12	1.01±0.11	0.99±0.10	0.99±0.11
K Ratio**	0.60±0.17	0.77±0.24	1.19±0.40	0.97±0.29

Uncertainties are standard deviations.

* For CMB analysis organic carbon is decreased by percentage shown for RWC and tunnel sources.

** Ratio of CMB calculated/measured.

Table 5.21C

Comparisons of CMB Analyses Using Various Wood Smoke Composition Profiles ($\mu g/m^3$)

Site: SW Portland Residential Area Size: 1.2 μm.			Mass loading = 20.8 $\mu g/m^3$	
Date:		3/2/84		
	Normal	-25% *	-50% *	Hot/Cool
RWC Comp.	7.8±1.6	9.0±1.8	7.1±1.9	-----
Hot burn	-----	-----	-----	1.3±0.5
Cool burn	-----	-----	-----	6.6±1.5
Soil	0.7±0.2	0.6±0.2	0.6±0.2	0.6±0.2
Motor Vehicle	1.2±0.3	1.2±0.3	1.2±0.3	1.2±0.3
Sec SO4	1.4±0.7	1.0±0.7	1.3±0.7	1.5±0.7
Dist. Oil	6.9±1.7	6.3±1.8	7.0±2.3	5.9±1.8
X^2	0.894	0.605	2.116	0.607
DF	6	6	6	5
Mass calc.(%)	88.8±8.8	90.2±9.0	86.2±8.6	85.5±8.6
OC Ratio**	1.08±0.09	1.05±0.08	0.79±0.07	1.01±0.07
EC Ratio**	0.90±0.18	0.94±0.20	0.97±0.20	0.95±0.16
TC Ratio**	1.03±0.13	1.02±0.12	0.84±0.12	0.99±0.11
K Ratio**	0.60±0.17	0.76±0.23	0.72±0.22	1.00±0.37

Uncertainties are standard deviations.

* For CMB analysis organic carbon is decreased by percentage shown for RWC and tunnel sources.

** Ratio of CMB calculated/measured.

Table 5.21D

Comparisons of CMB Analyses Using Various Wood Smoke Composition Profiles ($\mu g/m^3$)

Site: SW Portland Residential Area Size: 0.6 μm.			Mass loading = 14.6 $\mu g/m^3$	
Date:		3/2/84		
	Normal	-25% *	-50% *	Hot/Cool
RWC Comp.	6.2±1.1	7.0±1.2	8.1±1.4	-----
Hot burn	-----	-----	-----	0.8±0.3
Cool burn	-----	-----	-----	5.2±1.0
Soil	0.4±0.1	0.4±0.1	0.4±0.1	0.4±0.1
Motor Vehicle	0.9±0.2	0.9±0.2	0.9±0.2	0.9±0.2
Sec SO4	1.3±0.5	0.9±0.5	1.3±0.5	1.3±0.5
Dist. Oil	3.9±1.1	3.6±1.2	3.2±1.3	3.5±1.1
X^2	0.749	0.492	0.482	0.450
DF	7	7	7	6
Mass calc.(%)	86.6±8.7	87.6±8.8	95.4±9.5	83.3±8.3
OC Ratio**	1.08±0.08	1.04±0.07	0.95±0.06	1.00±0.06
EC Ratio**	0.97±0.19	1.02±0.22	1.12±0.29	0.99±0.16
TC Ratio**	1.05±0.11	1.02±0.10	0.99±0.09	1.00±0.09
K Ratio**	0.56±0.16	0.68±0.21	0.92±0.32	0.93±0.27

Uncertainties are standard deviations.

* For CMB analysis organic carbon is decreased by percentage shown for RWC and tunnel sources.

** Ratio of CMB calculated/measured.

Table 5.21E

Comparisons of CMB Analyses Using Various Wood Smoke Composition Profiles (μg/m³)

Site: SW Portland Residential Area Size: 0.3 μm.			Mass loading = 9.8 μg/m³	
Date:		3/2/84		
	Normal	-25% *	-50% *	Hot/Cool
RWC Comp.	5.1±0.8	5.5±0.9	5.6±0.9	-----
Hot burn	-----	-----	-----	0.4±0.1
Cool burn	-----	-----	-----	4.7±0.8
Soil	0.1±0.06	0.1±0.06	0.1±0.06	0.1±0.06
Motor Vehicle	0.8±0.2	0.8±0.2	0.8±0.2	0.8±0.2
Sec SO4	0.9±0.3	0.9±0.3	0.9±0.3	0.9±0.3
Dist. Oil	0.6±0.6	0.4±0.7	0.3±0.7	0.6±0.6
X^2	0.299	0.304	0.901	0.361
DF	7	7	7	6
Mass calc.(%)	77.0±7.7	78.7±7.8	78.3±7.8	76.5±7.6
OC Ratio**	1.04±0.09	0.93±0.15	0.74±0.10	1.03±0.08
EC Ratio**	0.94±0.20	1.00±0.27	1.09±0.35	0.94±0.15
TC Ratio**	0.99±0.07	0.91±0.12	0.78±0.10	0.98±0.06
K Ratio**	0.96±0.28	1.14±0.32	1.34±0.36	1.02±0.24

Uncertainties are standard deviations.

* For CMB analysis organic carbon is decreased by percentage shown for RWC and tunnel sources.

** Ratio of CMB calculated/measured.

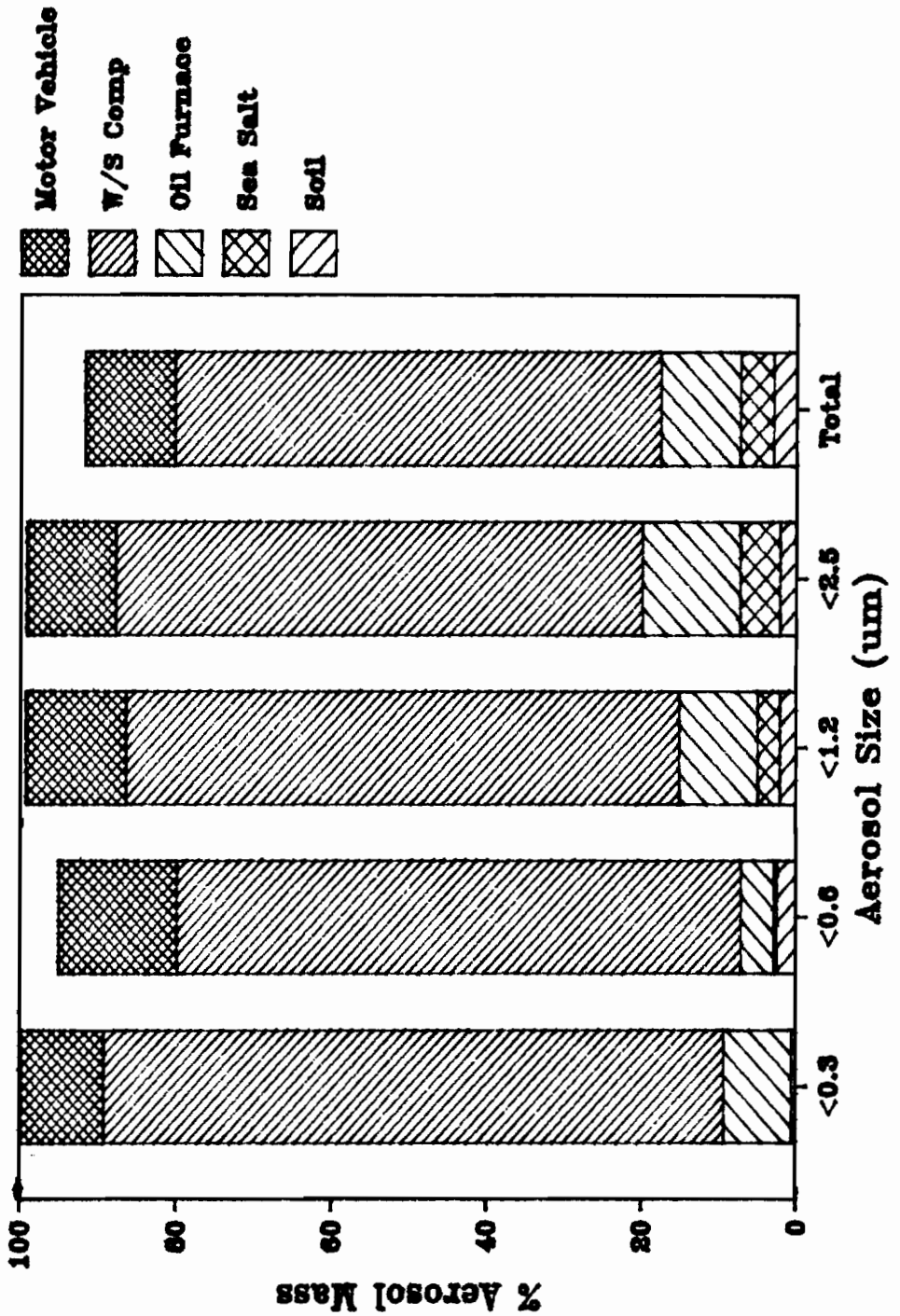

Figure 5.19 CMB Source Contributions Over The Aerosol Size Range For A SW Portland Residential Area (3/9/84)

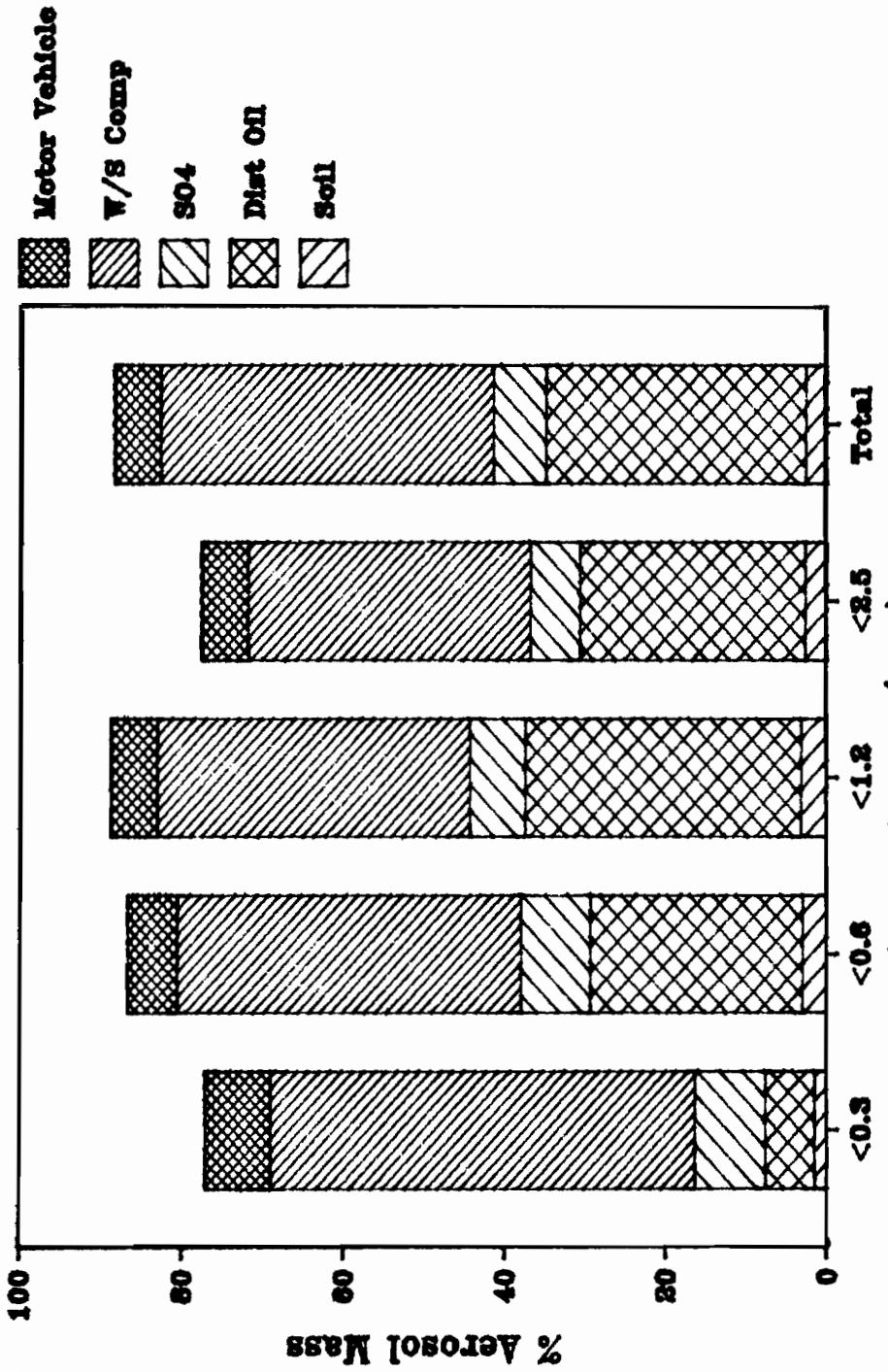

Figure 5.20 CMB Source Contributions Over The Aerosol Size Range For A SW Portland Residential Area (3/2/84)

where indicated OC loss was <25%. These OC losses were higher than noted for the September and April samples but not as high as the 50-70% noted for mid-winter samples. Tables 5.20A-B show a slightly higher EC ratio than OC ratio indicating that the RWC aerosol lost no organic carbon.

The CMB solutions for the 3/2/84 sample are very similar to the 3/9/84 sample except that the solution did accommodate a secondary sulfur source. Excess sulfur that could be attributed to secondary SO_4 was not found in other wintertime residential samples and it probably does not represent secondary SO_4 here since the sampling period was cloudy. If secondary SO_4 existed at all during this time of year it should have been detected in the March 5 sample which was a clear weather sample. Its presence here might indicate a sulfur contribution from an industrial source. It should be noted that when SO_4 was fit by the CMB solution it only indicates that excess sulfur was available in the sample which was not required by the other sources.

CMB analyses of all the forgoing samples have shown that organic and elemental carbon can play an important role in modeling combustion aerosols. RWC aerosols can be quite well fit by using a composite composition profile as long as survey data are available to determine the makeup of the composite. In lieu of survey data separate hot and cool burn RWC composition profiles can be used. This should be demonstrated by independent evaluations of the RWC component such as by using C-14. In the wintertime it may be useful to reduce the RWC OC composition to account for organic vapor loss.

CHAPTER 6: CARBON COMPOSITION OF FOREST SLASH BURNING EMISSIONS

6.1 SMOLDERING AND FLAMING FOREST SLASH BURNING EMISSIONS

Combustion particulate emission composition and size distribution of flaming and smoldering combustion emissions from forest slash burning and perhaps from various types of agricultural burning are expected to be similar to hot and cool burning wood stove emissions, respectively. Ward (1986) noted that smoldering forest slash burning emissions were tan while emissions from flaming combustion were black. He also noted that the concentration of potassium in flaming emissions was much higher than it was in smoldering emissions. In chapter one it was indicated that Radke et al.(1978) observed a monomodal particulate mass distribution for hot burning forest slash and a bimodal distribution for cooler burning slash. These distributions were similar to those measured for hot and cool burning stove emissions. Figure 6.1 and 6.2 show thermo-optical carbon analysis results for flaming and smoldering slash burning emissions, respectively. It will be noted that these figures are similar to figures 2.8 and 2.9. The cool stove burn and smoldering slash burn data showed that the particulate material was primarily organic carbon and that a large amount of the organic carbon pyrolyzes. In contrast, the graphs for hot burning stove emissions and for flaming slash combustion show comparatively lower OC and higher EC contents and low amounts of OC that volatilizes at the lowest analysis temperature. The similarities between wood burning in stoves and slash burning will be noted despite the fact that the cool and hot burn stove and slash burning profiles are not as similar as they might be because the slash burning aerosols were sampled on glass fiber filter material and

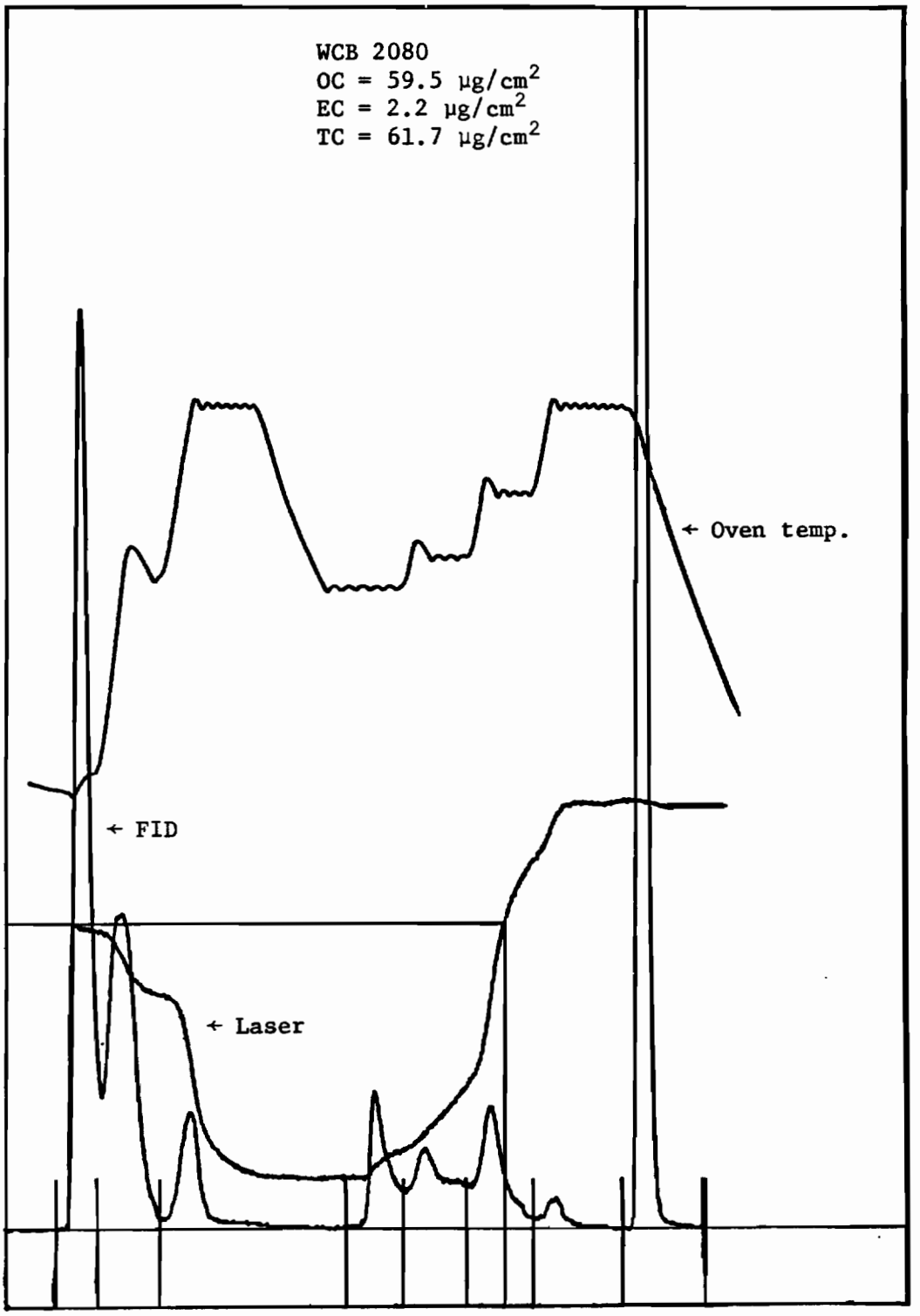

Figure 6.1. Thermo-optical carbon analyzer output for a smoldering slash burn sample.

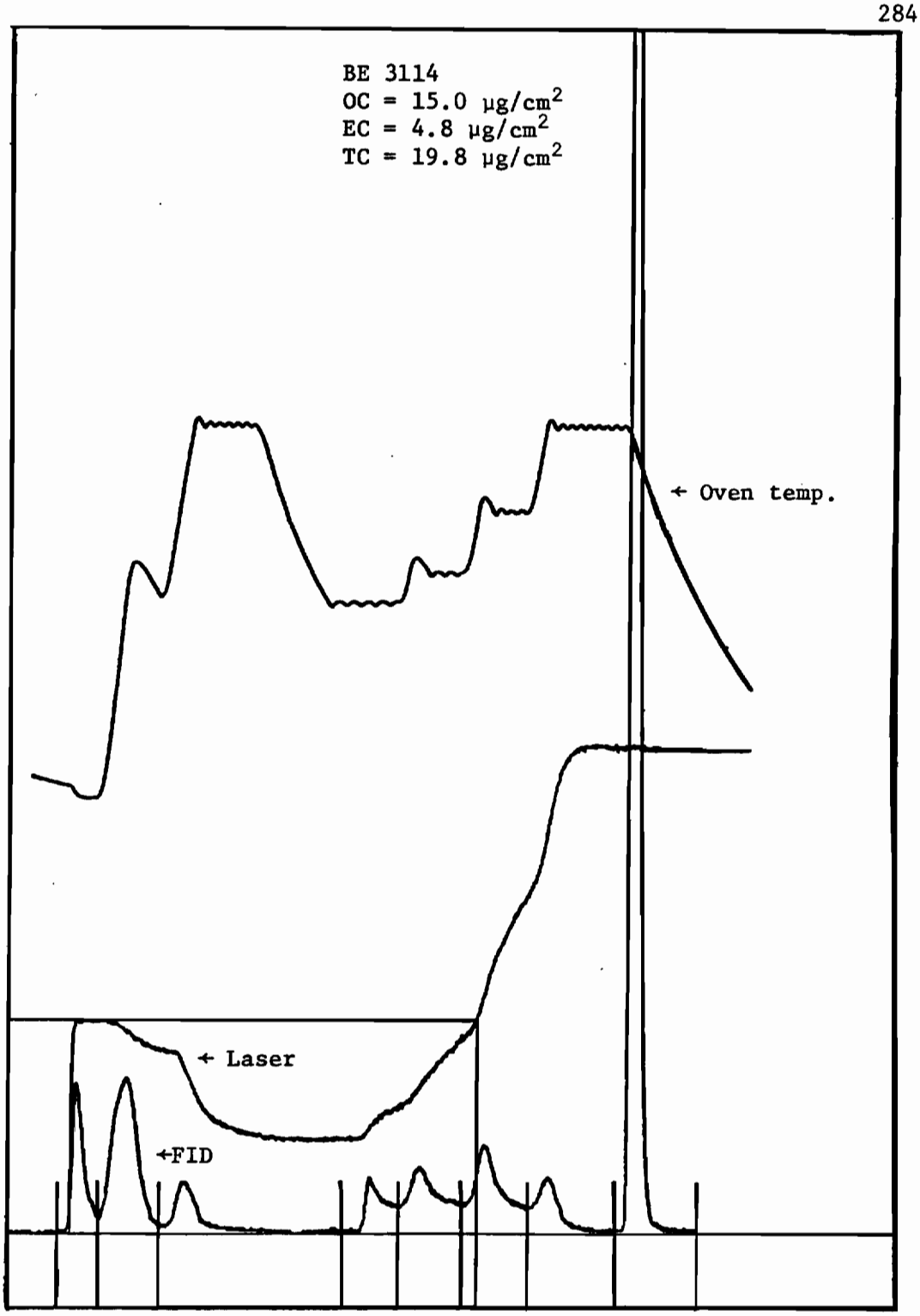

Figure 6.2. Thermo-optical carbon analyzer output for a flaming slash burn sample.

therefore require a lower temperature heating profile than the stove samples which were sampled on quartz.

Because of the similarities between stove and slash burning emissions it would seem that the uncertainty in CMB modeling of slash emissions can be reduced by using separate flaming and smoldering emission source composition profiles as was done for stove emissions. This is especially applicable when the burning consists of smoldering and flaming combustion with adequate combustion air availability. Flaming combustion can also be hot and air starved. This type of combustion occurs when the fuel is finely divided such as in dry twig or grass burning where the amount of burning surface is large. For this type of combustion large amounts of highly elemental carbon particulate material is produced by flaming combustion and the ratio of elemental carbon to potassium will be higher than it would be for emissions from flaming combustion with adequate combustion air. Perhaps future CMB modeling of slash burn could consider using a smoldering emission profile and two separate composition profiles that characterize hot burning. If the emissions from different phases of combustion can be separated then burning practices can be altered to minimize those combustion phases which produce the highest emission levels. Since the relative EC content of slash burn aerosol is proportional to combustion temperature and inversely proportional to particulate emission rates this parameter together with potassium concentrations could be used to measure the average combustion efficiency and average relative emission levels of slash burns.

CHAPTER 7: SUMMARY AND RECOMMENDATIONS FOR FURTHER RESEARCH

7.1 Summary

This study determined the composition of aerosol particles emitted by residential wood burning stoves and fireplaces as a function of particle size. It also determined the distribution of particulate mass, carbon and trace element species as a function of particle size. Sampling was done from smoke plumes which had been cooled and diluted by ambient air to insure that the composition data obtained represented particle composition as it left the source, i.e., condensible organic vapor was allowed to condense naturally onto particles. For stove burning, in order to limit sample variability, sampling was done under two conditions: hot burning (damper open and low fuel load) and cool burning (damper closed). RWC aerosol composition was primarily controlled by burn temperature and the associated flame turbulence. Combustion air availability determined flame temperature and in turn flame turbulence. It was assumed that the compositions of hot and cool burn aerosols provided limits within which the compositions of all RWC aerosols could be found. These two conditions bound the types of stove operation that residential stove users have available. They can burn with the damper closed or mostly closed (usually with a large fuel load to reduce the number of times that the stove must be attended) or they can burn with the damper open using a small fuel load. Using a large fuel load with the damper open usually results in excessive heat output and can result in cool, air-starved burning if the amount of burning wood surface is too large for the available combustion air supply. It

is suspected that emissions from newly designed clean burning stoves which incorporate secondary combustion, catalysts, or high temperature combustion would have compositions bounded by hot burning conventional stoves and industrial wood burning furnaces.

In Portland survey data indicated that 75% of people burn with their dampers closed or mostly closed and 25% burn with dampers open. Table 5.4 gives the composite composition of stove emissions resulting from this mix of burning. Portland data also indicated that about one third of the wood burned in the area was burned in fireplaces. Table 5.6 gives composite RWC compositions taking fireplace burning into account.

A small amount of source testing was also done on traffic aerosols collected in a highway tunnel and on residential oil burning emissions. The purpose of collecting these data was to determine particulate organic and elemental carbon concentrations using thermo-optical analysis and to determine composition variability as a function of particle size for these sources. RWC, distillate oil burning and motor vehicle emissions where broadly distributed in the <2.5 μm size range.

Damper open stove burning (hot burning) consisted of turbulent, flaming combustion with bright yellow flames and with appropriate combustion air availability. Damper closed stove burning (cool burning) consisted of smoldering, air starved combustion with smoky orange flames and little turbulence. Temperatures at the entrance of the flue in the stove were about 250°C for cool burning and 500-600°C for hot burning. Fireplace burning allowed no control over combustion conditions and was conducted with typical fuel loads.

Wood type and stove design were found to be minor factors in

determining emission compositions for wood burning in common box type air tight stoves. Wood moisture content was not considered as an experimental variable because most wood burners tend to use adequately aged wood. The wood used was well aged and had a moisture content of about 15%.

All source and ambient sample analyses placed special emphasis on the determination of organic and elemental carbon. This was done because the thermo-optical carbon analysis system developed at the Oregon Graduate Center is believed to determine a more accurate split between organic and elemental carbon than analysis methods which do not correct for sample pyrolysis during the analysis process. The sampling artifact of organic vapor adsorption on the quartz filters used to collect aerosol particles was also taken into account. Organic vapor adsorption on quartz filters usually ranges from 4 to 7 ug/cm2. This sampling artifact can cause errors in particulate organic carbon concentrations ranging from 5% for data obtained from heavily loaded filters to over 100% for data obtained from lightly loaded filters.

Both the appearance of smoke plumes and the composition of particles from hot and cool burning were found to be very different. Hot burning resulted in essentially invisible plumes while cool burning resulted in the highly visible blue-gray plumes. This type of plume is commonly associated with wood burning. Cool burn aerosol particles were, within very narrow limits, 58% carbon. This carbon was primarily organic carbon with no more than 5% of the carbon in the form of elemental carbon. Cool burn particles collected on filters were tan and had a strong, pleasant wood smoke odor. Hot burn particles contained less

than 58% carbon (could be as low as 25% carbon) and up to 80% of this carbon was in the form of elemental carbon. Hot burn particles collected on a filter were black and had a mild acrid odor. On the average, for similar fuel loads, particulate emissions were 4.8 times greater for cool burning than for hot burning. Fireplace emissions for similar fuel loads were on average 1.2 times greater than for cool burning stove combustion. While fireplace burning would seem to have ample combustion air available, it actually has too much combustion air available so that the flames are cooled and the particles produced are very similar in composition to cool burning stove emissions.

The chemical composition of wood stove hot burn emissions were highly variable because they were very sensitive to changes in hot burning conditions i.e. temperature, turbulence, and residence time in the flame and because hot burning conditions were difficult to reproduce exactly from one run to the next. Hotter burning produced higher trace elemental concentrations. This resulted because higher burn temperature caused a decrease in particulate carbon content, therefore reducing particulate mass and increasing the relative concentration of trace elements. Also, higher burn temperatures caused more trace elemental species originally in the wood to enter the vapor phase rather than remaining in the ash therefore making them available for aerosol formation. In contrast, cool burning wood smoke aerosols showed little composition variability. They consistently had very low trace elemental concentrations and almost constant carbon concentrations. Fireplace emissions compositions also showed relatively little composition variability.

Compositions of wood stove emissions are found in table 5.1 for damper open and closed burning of hard and soft wood. It will be noted that trace element concentrations for cool burn aerosols are roughly one to two orders of magnitude less than for hot burn aerosols. In some wood stove hot burn tests potassium concentrations were obtained as high as 25%. Stiles (1983) measured values as high as 32%. It would be expected that the trace elemental composition of aerosols from an industrial wood fired boiler would represent a practical upper limit for values of trace elemental concentrations to be found in residential wood smoke. The differences associated with wood type should be viewed with caution. They probably resulted primarily from differences in burn temperature that may have been a consequence of the hardwood burning slightly hotter than softwood. Only very carefully controlled laboratory burn tests can establish emission differences associated with wood type because of the overwhelming effects contributed by burn temperature.

The composition of both RWC and distillate oil burning emissions does not appear to a strong function of particle size. Wood smoke particles less than 0.3 μm had slightly lower carbon concentrations and slightly higher trace elemental concentrations than larger particles. The high variability of trace element data for <0.3 μm aerosols may make the indication of higher trace element concentrations in RWC particles <0.3 μm of questionable significance. Only motor vehicle (tunnel) aerosols showed a significant composition variation as a function of aerosol size. For these aerosols the concentrations of lead, bromine and sulfur increased with decreasing particle size.

Because the composition of motor vehicle emitted aerosol was composed of a mixture of geological materials and vehicle emissions it did vary with particle size. Larger particle sizes were dominated by trace elements found in geological material while smaller sized particles were dominated by lead and bromine from vehicle emissions. Motor vehicle aerosols were distributed about 50% below 0.3 μm.

The mass and carbon distributions of hot and cool burn stove emissions were also quite different. The hot burn aerosol distribution was monomodal with the particle concentration increasing as particle size decreased. In contrast, cool burn emissions where bimodally distributed with one mode <0.3 μm and one mode between 0.6 and 1.2 μm. It is believed that the bimodal distribution results from organic vapor condensation on both particles produced in combustion and on particles initially present in the combustion air. In both hot and cool stove burning emissions about half of the particulate material was found below 0.3 μm.

The principal findings of the source study part of this research were: (1) RWC, residential oil furnace, and motor vehicle generated aerosols were mainly carbonaceous; (2) adsorbed organic carbon can be a significant artifact in sampling carbonaceous aerosols; (3) measured aerosol elemental carbon concentrations were significantly influenced by the correction for organic carbon pyrolysis during carbon analysis; (4) there were significant differences between hot and cool burn RWC aerosols in both chemical composition and size distribution; (5) fireplace emissions had compositions intermediate between hot and cool wood stove burning and tended to be more like cool burning wood stoves.

7.2 CMB RESULTS

This research pioneered three new aspects of CMB modeling: (1) the use of two separate RWC composition profiles, hot burning and cool burning, to represent RWC emissions; (2) the combination of hot and cool burning RWC composition profiles in proportion to expected emission rates determined by survey data to produce a composite RWC composition; and (3) CMB modeling across the fine mode aerosol size range. Both item one and two reduce the uncertainty in modeling RWC emissions, as compared to using the EPA RWC composition profile, by separating the analytic uncertainty in measuring RWC particulate composition from the uncertainty associated with process variation. Item three examined how the contribution of various sources to ambient particulate loading varied across the fine aerosol size range. This examination showed that for combustion sources such as RWC, distillate oil burning and motor vehicle emissions the contributions were spread relatively uniformly across the fine particulate size range. It was thus not possible to use sampling in a particular segment of the fine particle range to isolate sampling to a particular source. It also showed that sea salt aerosol and summertime plant dusts appeared, as expected, mainly in the coarse mode while diesel emissions were found in the <0.6 μm size range. Size data were sometimes useful in selecting sources in CMB modeling. For example the presence of a coarse carbon component might indicate the presence of plant dusts rather than RWC emissions in an ambient particulate sample. Both have similar compositions.

The composite RWC profile given is useful when the fraction of wood

burners burning in the hot and cool manner is approximately split 25/75%. When the split is not known separate hot and cool composition profiles can be used. The compositions of hot burn and cool burn particles are sufficiently different so that no multicolinearity effects in CMB analysis result. By representing the RWC source by two separate sources, hot and cool burning, the CMB model has a greater freedom to fit both carbon and trace element species especially potassium in ambient aerosol samples.

By using the RWC composite composition profile developed in this study, organic and elemental carbon are usually better fit than potassium. On the other hand, using the EPA composite composition profile given in Core (1984) usually results in a good fit of potassium data and a poorer fit of carbon data. This problem results both because wood burners may not be split into 75% cool burners and 25% hot burners and because ambient RWC hot burning trace element concentrations, being highly variable, might be different from the trace element composition values used in RWC source profiles. For the ambient data examined in this study, using the EPA RWC composition profile usually resulted in higher estimates of RWC contributions to ambient aerosols than using either the composite RWC composition profile or separate hot and cool RWC composition profiles. This is not an intrinsic property of the RWC source profiles but depends mainly on ambient trace element concentrations. Because carbon forms a major part of RWC particles and is reasonably stable over a wide variety of burn conditions it is expected that CMB analyses which best explain ambient carbon concentrations will give the most accurate estimates of RWC

contributions.

For the ambient samples examined in this research it was found that from 7 to 18% of RWC emissions resulted from hot burning. Based on emissions data of hot and cool burning and survey data, 3 to 7% of ambient aerosols would be expected to be contributed by hot stove burning. While this was reasonably good agreement, the differences can be explained by considering that there might have been more damper open burning than reported, or that for some stoves hot burning occurs at higher temperature levels than those used in this research and therefore produces higher trace element concentrations. More measurement of stove emission compositions under normal operating conditions could resolve this question.

The ratio of hot burn to cool burn emissions also has utility in evaluating the effectiveness of burner education programs which encourage damper open burning or evaluating the effectiveness of replacing conventional airtight stoves with new, cleaner burning stoves. Cleaner burning stoves would be expected to emit particles whose composition approached that of wood burning industrial furnace emissions; however, this must be established by source testing of these stoves.

For many CMB analyses in this study it was observed that the ratio of measured to calculated OC was greater than one and the ratio of measured to calculated EC was less than one. Both of these ratios could be made to approach one by allowing the RWC source to lose OC. Since RWC particles have an odor and it is known that the particles contain a large proportion of OC volatile species it seemed reasonable to

consider that RWC particles might lose OC during their atmospheric residence time. The RWC composition profiles were modified to remove 25, 50, and 65% of the OC in the particle. Concentrations of other composition species were also modified to reflect the loss of particle mass due to OC loss. Using these modified RWC composition profiles in CMB analyses usually showed that, at some value of OC loss, the OC and EC ratio values approached one and at the same time the value of X^2, the measure of model fit, was lowest indicating the best possible model fit. It was found that for aerosol samples collected in the winter when temperatures were lowest, CMB solutions had the their lowest X^2 value for RWC organic carbon loss values of about 50%. For spring and fall samples which were collected at higher temperatures it was found that the lowest X^2 values occurred at carbon loss values of 25% or less. That OC losses should be higher during colder weather than during warmer weather seems counter intuitive; however, if carbon losses as supposed do actually occur, the complexities of atmospheric chemistry certainly will provide an explanation. These CMB analyses do not prove that organic carbon losses as high as 50% do occur for RWC particles during their atmospheric residence time but they do show how CMB results would be affected if such losses did occur. The major point to note is that even with an assumed organic carbon loss of 50%, the RWC contributions are not very different from what they are when no carbon loss is considered.

In contrast to the SW Portland samples, where using the normal composite RWC profile resulted in lower RWC contributions than using the EPA profile, for the Hillsboro sample the highest RWC contribution

was obtained by using the normal composite RWC profile. The difference between RWC source contributions given by using the composite RWC profile and the EPA RWC profile results because the composite RWC profile more strongly utilizes carbon information than does the EPA RWC profile, i.e., carbon uncertainty values are lower for the composite RWC profile. When ambient carbon data, as viewed by the CMB program, tend to give a different RWC contribution than ambient trace element data, then characterizing RWC pollution with the composite profile will cause the program to compute a somewhat different RWC contribution than if RWC pollution were characterized by the EPA profile. The determination of which solution is more valid ultimately depends on the accuracy with which source contributions at the receptor and ambient aerosol compositions are known. Since carbon can be analytically well quantified and composes usually about half of the RWC aerosol it seems reasonable that the CMB solution which best accounts for carbon should give the most valid CMB results, assuming that there are no significant unknown carbon sources.

7.3 FUTURE RESEARCH DIRECTIONS

The RWC composition profiles developed in this research have improved the accuracy with which CMB analyses can be used to determine the contribution of RWC emissions to residential area air pollution. Because the composition of wood smoke particles is highly variable, it will always be desirable to obtain more wood smoke composition data especially for regions where temperatures or stove usage patterns are significantly different from those found in the Pacific Northwest.

The problems caused by high levels of RWC air pollution has caused the wood stove industry to develop a variety of cleaner burning stoves. All of these stoves aim at combusting particulate and vapor carbon before it can leave the stove in the flue gas. As a consequence, emissions from these stoves when they are operating correctly would be expected to be like emissions from hot burning conventional stoves; however, this should be evaluated. Emission composition should also be determined under conditions where the stove is not operating as designed. As these stoves replace conventional stoves, the compositions of their particulate emissions should be appropriately incorporated into CMB modeling.

The use of flaming and smoldering combustion emission composition profiles in CMB modeling of forest slash burning should be developed. This should include the determination of composition profiles for both flaming combustion with ample combustion air supply and air starved flaming combustion such as occurs when dry, high surface area materials such as brush and grass are burned.

REFERENCES

Adams, F., Van Epsen, P., & Maehaut, W. (1983). "Aerosol Composition at Chacaltaya, Bolivia, as Determined by Size-Fractionated Sampling." Atmos. Env., 8, 1521-1536.

Albrechcinski, T. M., Michalovic, J. G., Wattle, B. J., & Wilkinson, E. P. (1984). "Chamber Investigations of the Physical, Chemical and Biological Fate of Diesel Exhaust Emissions in the Atmosphere." In: Aerosols: Science, Technology, and Industrial Applications of Airborne Particles, Liu, B. Y. H., Pui, D. Y. H., and Fissan, H. J. (eds.), 761-64, Elsevier Press.

Alfheim, I., Becher, G., Hongslo, J. K., & Ramdahl, T. (1984a). "Mutagenicity Testing of High Performance Liquid Cromatography Fractions From Wood Stove Emission Samples Using a Modified Samonella Assay Requiring Smaller Sample Volumes." Environmental Mutagenesis, 6, 91-102.

Alfheim, I., & Ramdahl, T. (1984b). "Environmental Impact of Residential Wood Heating in Scandinavia." Presented at the 77th Meeting of the Air Pollution Control Association, San Francisco, CA., June.

Alfheim,I., & Ramdahl, T. (1984c). "Contribution of Wood Combustion to Indoor Air Pollution as Measured by Mutagenicity in Salmonella and Polycyclic Aromatic Hydrocarbon Concentration." Env. Mutagenesis, 6, 121-130.

Bailey, M. R., & Wheeling, P. R. (1982a). "Wood and Energy in Vermont." Natural Resource Economics Division, Economics Research Division, U. S. Department of Agriculture, Washington, D. C., April, ERS Staff Report No. Ages 820126,

Bailey, M. R., & Wheeling, P. R. (1982b). "Wood and Energy in New Hamshire." Natural Resource Economics Division, Economics Research Service, U. S. Dept. of Agriculture, Washington, D. C., June, ERS Staff Report No. AGES 820604.

Barnett, S. G., & Shea, D. (1982). "Effects of Woodstove Design and Operation on Condensable Particulate Emissions." In: Residential Solid Fuels, Cooper, J. A. and Malek, D., (eds.), 227-266, published by Oregon Graduate Center, Beaverton, OR.

Bell, D. A., Rives, G., Kamens, R. M., Perry, J. M., Saucy, D., & Claxton, L. (1983). "Mutagenic Changes of Dilute Wood and Peat Smoke Under Simulated Atmospheric Conditions: An Outdoor Chamber Study." Proc. of the 8th International Battelle Symposium on Polynuclear Aromatic Hydrocarbons.

Berner, A., & Lurzer, C. (1980). "Mass Size Distributions of Traffic Aerosols at Vienna." J. Phys. Chem., 84, 2079-2083.

Bergstrom, R. W., Ackerman, T. P., & Richards, L. W. (1982). "The Optical Properties of Particulate Elemental Carbon." In: Particulate Carbon: Atmospheric Life Cycle, Wolff, G. T. and Klimisch, R. L. (eds.), 43-51, Plenum Press.

Boubel, R. W., & Junge, D. C. (1981). "Emissions of Polynuclear Organic Materials from Industrial Spreader-Stoker Boilers Fired with Wood and Bark Residue." Presented at the Annual meeting of the Pacific Northwest International Section-Air Pollution Control Association, Spokane, Washington, November.

Browne, F. L. (1958). "Theories of the Combustion of Wood and Its Control." United States Department of Argrculture,Report No. 2136.

Butcher, S. S., & Buckley, D. I. (1977). "Preliminary Study of Particulate Emissions from Small Wood Stoves." J. Air Pollut. Control Assoc., 27, 346-348.

Butcher, S. S., (1978). "The Impact of Residential Heating by Wood Stoves on Ambient Air Quality." A report to the Maine Department of Environmental Protection, April.

Butcher, S. S., & Sorenson, E. M. (1979). "Study of Wood Stove Particulate Emissions," J. of the Air Pollut. Control Assoc., 29, 724-728.

Butcher, S. S., & Ellenbecker. M. J. (1982). "Particulate Emission Factors for Small Wood and Coal Stoves." In: Residential Solid Fuels, Cooper, J. A. and Malek, D. (eds.), 289-303, published by Oregon Graduate Center, Beaverton, OR.

Cadle, S. H., & Groblicki, P. J. (1982). "An Evaluation of Methods for the Determination of Organic and Elemental Carbon in Particulate Samples." In: Particulate Carbon: Atmospheric Life Cycle, Wolff, G. T. and Klimisch, R. L. (eds.), 89-109, Plenum Press.

Cadle, S. H., Groblicki, P. J., & Mulawa, P. A. (1983). "Problems in the Sampling and Analysis of Carbon Particulate." Atmos. Environ., 17, 593-600.

Cannon. J. A. (1984). "Air Quality Effects of Residential Wood Combustion." J. Air Pollut. Control Assoc., 34, 895-897.

Carlson, J. H. (1982). "Residential Wood Combustion in Missoula, Montana: An Overview of its Air Pollution Contributions, Health Effects, and Proposed Regulatory Solutions." In: Residential Solid Fuels, Cooper, J. A. and Malek, D. (eds.), 539-550, published by Oregon Graduate Center.

Carnow, B. W. (1978). "The "Urban Factor" and Lung Cancer: Cigarette Smoking or Air Pollution?" Environ. Health Perspectives, 22, 17-21.

Carnow, B. W., & Meir, P. (1973). "Air Pollution and Pulmonary Cancer." Arch. Environ Health, 27, 207-217.

Carroll, J. J., Miller, G. E., Thompson, J. F., & Darley, E. F. (1977). "The Dependence of Open Field Burning Emissions and Plume Concentrations on Meteorology, Field Conditions and Ignition Technique." Atmos. Environ., 11, 1037-1050.

Chan, T. L., & Lawson, D. R. (1981). "Characteristics of Cascade Impactors in Size Determination of Diesel Particles. "Atmos. Environ, 15, 1273-1279.

Chang, S. G., Brodzinsky, R., Gundel, L. A., & Novakov, T. (1982). "Chemical and Catalytic Properties of Elemental Carbon." In: Particulate Carbon: Atmospheric Life Cycle, Wolff, G. T. and Klimisch, R. L. (eds.), 159-181, Plenum Press.

Charlson, R. J., & Ogren, J. A. (1982). "The Atmospheric Cycle of Elemental Carbon." In Particulate Carbon: Atmospheric Life Cycle, Wolff, G. T. and Klimisch, R. L. (eds.), 3-18, Plenum Press.

Cheng, Y. S., & Yeh, H. C. (1979). "Particle Bounce in Cascade Impactors." Environ. Sci. Technol., 13, 1392-1396.

Cooke, W. M., Allen, J. M., & Hall, R. E. (1982). "Characterization of Emissions from Residential Wood Combustion Sources." In: Residential Solid Fuels, Cooper, J. A. and Malek, D. (eds.), 139-163, published by Oregon Graduate Center.

Cooper, J. A., Currie, L. A., & Klouda, G. A. (1979a). "Evaluation of Carbon-14 as a Unique Tracer to Determine the Maximum Impact of Contemporary Carbon Sources of Atmospheric Particulates in the Portland and Eugene Airsheds." Final Report to U. S. Environmental Protection Agency.

Cooper, J. A. (1980). "Environmental Impact of Residential Wood Combustion Emissions and Its Implications." J. Air Pollut. Control Assoc., 30, 855-861.

Cooper, J. A., & Watson, J. G. Jr. (1980). "Receptor Oriented Methods of Air Particulate Source Apportionment." J. Air Pollut. Control Assoc., 30, 1116-1125.

Cooper, J. A., Currie, L. A., & Klouda, G. A. (1981). "Assessment of Contemporary Carbon Combustion Source Contributions to Urban Air Particulate Levels Using Carbon-14 Measurements." Environ. Sci. Technol. 15, 1045-1050.

Cooper, J. A., Watson, J. G., & Huntzicker, J. J. (1979). "Summary of the Portland Aerosol Characterization Study (PACS)." Final Report to the Oregon State Department of Environmental Quality.

Core, J. E. (1983). "Combustion Process and Emission Characteristics." Presented at the Workshop on Residential Wood and Coal Combustion, Portland, OR, November, 1983.

Core, J. E., Shah, J. J., & Cooper, J. A. (1984). "Receptor Model Source Composition Library." EPA-450/4-85-002. Office of Air Quality Planning and Standards, Research Triangle Park, NC.

Core, J. E., Cooper, J. A., & Neulicht, R. M. (1984). "Current and Projected Impacts of Residential Wood Combustion on Pacific Northwest Air Quality." J. Air Pollut. Control Assoc., 31, 139-143.

Countess, R. J., Wolf, G. T., & Cadle, S. H. (1980). "The Denver Winter Aerosol: A Comprehensive Chemical Characterization." J. Air Pollut Control Assoc., 30, 1194-1200.

Countess, R. J., Wolf, G. T., & Cadle, S. H. (1980). "Denver Aerosol -- A Comprehensive Chemical Characterization." Environmental Science Department, General Motors Research Laboratories, Warren, MI., GMR-3210. ENV #72.

Courtney, J. W., Tesch, J. W., Russwurm, R. K., Stevens, R. K., & Dzubay, T. G. (1980). "Characterization of the Denver Aerosol Between December 1978 and December 1979." Paper #80.58.1 presented at the 73rd Annual Meeting of APCA, Montreal, Quebec, Canada, June 22-27.

Cummings, C. (1982). "Portland Area Wood Heating Survey." Oregon Department of Environmental Quality.

Currie, L. A. (1982). "Contemporary Particulate Carbon" In: Particulate Carbon: Atmospheric Life Cycle, Wolff, G. T. and Klimisch, R. L. (eds.), 245-260, Plenum Press.

Currie, L. A., Gerlach, R. W., Lewis, C. W., Balfour, W. D., Cooper, J. A., Dattner, S. L., DeCesar, R. T., Gordon, G. E., Heisler, S. L., Hopkle, P. K., Shah, J. J., Thurston, G. D., & Williamson, H. J. (1984). "Interlaboratory Comparison of Source Apportionment Procedures: Results for Simulated Data Sets." Atmos. Environ., 18, 1517-1537.

Daisey, J. M. (1980). "Organic Compounds in Urban Aerosols." Annals New York Academy of Sciences, 50-69.

Dalton, M. M., Durgin, O. B., Herrington, J. H., & Andrews, R. A. (1977). "Household Fuel Wood Use and Procurement in New Hamshire." research report No. 59, New Hamshire Agricultural Experiment Station, University of New Hampshire, Durham, New Hamshire.

Dasch, J. M. (1982). "Particulate and Gaseous Emissions from Wood-Burning Fireplaces." Environ. Sci and Technol., 16, 639-645.

DeAngelis, D. G., Ruffin, D. S., Peters, J. A., & Reznik, R. B. (1981). "Source Assessment: Residential Combustion of Wood." Prepared by Monsanto Research Corporation (Dayton, Ohio) for the U. S. Environmental Protection Agency under Contract No. 68-02-1874, March 1980. Report No. EPA-600/2-80-042B., 91 pp.

DeCesar, R. T. & Cooper, J. A. (1982). "The Quantitative Impact of Residential Wood Combustion and Vegetative Burning on the Air Quality in Medford, Oregon." In: Residential Solid Fuels, Cooper, J. A. and Malek, D (eds.), 551-565, Published by Oregon Graduate Center, Beaverton, OR

Duce, R. A. (1978). "Speculations on the Buget of Particulate and Vapor Phase Non-Methane Organic Carbon in the Global Troposphere." Pageoph., 116, 244-273.

Dzubay, T. G. (1980). "Chemical Element Balance Method Applied to Dichotomous Sampler Data." Annals New York Academy of Sciences, 126-145.

Eaton, F., & Wendler, G. (1983). "Some Environmental Effects of Forest Fires in Interior Alaska." Atmos. Environ., 17, 1331-1337.

Esmen, N. A., Ziegler, P., & Whitfield, R. (1978). "The Adhesion of Particles upon Impaction," J. Aerosol Sci., 9, 547-556.

Fitch, W. L., & Smith, D. H. (1979). "Analysis of Adsorption Properties and Adsorbed Species on Commercial Polymeric Carbons." Environ. Sci. Technol., 13, 341-346.

Fitzgerald, M. (1985). "Portland Area Wood Heating Survey." Oregon Department of Environmental Quality.

Flocchini, R. G., Cahill, T. A., Shadoan, D. J., Lange, S. J., Eldred, R. A., Feeney, P. J., Wolfe, G. W., Simmeroth, D. C., & Suder, J. K. (1976). "Monitoring California's Aerosols by Size and Elemental Composition." Env. Sci and Technol., 10, 76-82.

Friedlander, S. K. (1973). "Chemical Element Balances and Identification of Air Pollution Sources." Environ. Sci. and Technol., 7, 235-240.

Friedlander. S. K. (1977). "Smoke, Dust, and Haze." John Wiley & Sons.

Giaque, R. D. (1974). "Characterization of Aerosols in California by X-Ray Induced X-Ray Fluorescence Analysis," Environ. Sci. and Technol., 8 436.

Gladney, E. S,, Zoller, W. H., & Gordon, G. E. (1974). "Composition and Size Distributions of Atmospheirc Particulate Matter in Boston Area."Env. Sci. and Technol., 8, 551-557.

GMA, (1979) "Oregon Residential Energy Conservation Survey." Prepared by GMA Research Corp., Portland, OR for the Oregon Department of Energy.

Gordon, G. E. (1980). "Techniques for Treating Multielement Particulate Data to Obtain Information on Sources: Overview." Annals of New York Academy of Sciences, 93-101.

Green, W. T. (1980). "Wood Space Heating Emissions and Control Strategies in Portland-Vancouver Air Quality Maintenance Area." Oregon Department of Environmental Quality, January.

Groblicki, P. J., Wolff, G. T., & Countess, R. J. (1981). "Visibility-Reducing Species in the Denver "Brown Cloud" --I. Relationships between Extinction and Chemical Composition." Atmos. Env., 15, 2473-2484.

Grosjean, D. (1983). "Polycyclic Aromatic Hydrocarbons in Los Angeles Air From Samples Collected on Teflon, Glass and Quartz." Atmos. Env., 17, 2565-2573.

Hall, R. E., & DeAngelis, D. G. (1980). "EPA's Research Program for Controlling Residential Wood Combustion Emissions." J. Air Pollut. Control Assoc., 30, 862-867.

Hatchard, R. E., & Day, T. D. (1979). Survey conducted by Talbot, Wong & Assoc., Portland, OR for Oregon Department of Environmental Quality.

Heindryckx, R. (1976). "Comparison of the Mass-size Functions of the Elements in the Aerosols of the Gent Industrial District with Data from Other Areas. Some Physico-Chemical Implications." Atmos. Environ., 10, 65-71.

Henry, R. C. (1982). "Stability Analysis of Receptor Models that Use Least Squares Fitting." In Receptor Models Applied to Contemporary Air Pollution Problems, Air Pollution Control Association, Pittsburg, PA.

Henry, R. C., Lewis, C. W., Hopke, P. K., & Willimson, H. J. (1984). "Review of Receptor Model Fundamentals." Atmos. Environ., 18, 1507-1515.

Hester, N. E. (1979). "Evaluation of Techniques to Determine the Impact of Particulate Matter from Field and Slash Burning on Urban Areas," Prepared by Rockwell International, Environmental Monitoring & Services Center, Newbury Park, CA. for Oregon Department of Environmental Quality, No. AMC58001.15FR.

Hering, S. V., Flagan, R. C., & Friedlander, S. K. (1978). "Design and Evaluation of New Low-Pressure Impactor. 1." Env. Sci and Technol., 12, 667-673.

Hering, S. V., Miguel, A. H., Dod, R. L., & Daisey, J. M. (1985). "Receptor Modeling for Carbonaceous Aerosols: Source Characterization." Atmospheric Sciences Research Laboratory, Office of Research and Development, U. S. Environmental Protection Agency, Research Triangle Park, NC, Report No. EPA/600/D-85/004.

Himel, J. H., Moyer, R. H., & Cook J. D. (1978). "Forestry Burning Emissions & Potential Air Quality Impacts in the Pacific Northwest." Presented at the Pollution Control Seminar for the Pacific Northwest Forest Industry, Portland, OR, April.

Hinds, W. C. (1978). "Size Characteristics of Cigarette Smoke." Am. Ind. Hyg. Assoc. J., 39, 48-54.

Howard, P. H., Santodonata, J., Basu, D., & Bruce, R. (1982). "Multimedia Human Exposure to Polycyclic Aromatic Hydrocarbons and Their Association with Cancer Risk." In: Residential Solid Fuels, 79-138, Cooper, J. A. and Malek, D. (eds.), published by the Oregon Graduate Center, Beaverton, OR.

Howland, D. E., & Kowalczyk, G. S. (1984). "An Assessment of the Relative Source Impact of Residential Woodburning on the Ambient Total Suspended Particulate Levels in Western Massachusetts." Paper #84.70.12 presented at the 77th Annual Meeting of APCA, San Francisco, CA June 24-29.

Hubble, B. R., Stetter, J. R., Gebert, E, Harkness, J. B. L., & Flotard, R. D. (1982). "Experimental Measurements of Emissions from Residential Wood-Burning Stoves." In: Residential Solid Fuels, Cooper, J. A. and Malek, D., (eds.), 79-138, Published by Oregon Graduate Center, Beaverton, OR.

Huntzicker, J. J., Johnson, R. L., Shah, J. J., & Cary, R. A. (1982). "Analysis of Organic and Elemental Carbon in Ambient Aerosols by a Thermal-Optical Method."In: Particulate Carbon: Atmospheric Life Cycle, Wolff, G. T. and Klimisch (eds.), Plenum , New York, 79-88.

Imhoff, R. E., Manning, J. A., Cook, W. M., & Hayes, T. L. (1982). "Preliminary Report on a Study of the Impact of Residential Wood Combustion in Petersville, Alabama." In: Residential Solid Fuels, Cooper, J. A. and Malek, D (eds.), 520-537, published by Oregon Graduate Center, Beaverton, OR.

Imhoff, R. E., Manning, J. A., & Bontrager, P. J. (1984). "The Contribution of Residential Wood Combustion to Ambient Air Pollution in Nashville, Tennesee - A Case Study."Paper #84.70.9 presented at the 77th Annual Meeting of APCA, Montreal, Quebec, Canada, June 22-27.

Jahnson, V. (1961). "The Chemical Composition of Hardwood Smoke." Ph.D. Dissertation, Purdue University.

Japar, S. J., Szkarlat, A. C., Gorse, R. A. Jr., Heyerdahl, E. K., Johnson, R. L., Rau, J. A., & Huntzicker, J. J. (1984). "Comparison of Solvent Extraction and Thermal-optical Carbon Analysis Methods: Application to Diesel Vehicle Exhaust Aerosol." Environ. Sci. Technol., 18, 231-234.

Johnson, R. L., Shah, J. J., Cary, R. A., & Huntzicker, J. J. (1981). "An Automated Thermo-optical Method for the Analysis of Carbonaceous Aerosol." In: Atmospheric Aerosol Source/Air Quality Relationships, Macias, E. S., and Hopke, P. K. (eds.), ACS Symposium Series 167, 223-283.

Khalil, M. A. K., Edgerton, S. A., & Rasmussen, R. A. (1983). "A Gaseous Tracer Model for for Air Pollution from Residential Wood Burning." Env. Sci and Tech., 17, 555-559.

Kamens, R. M., Rives, G.D., Perry J. M., Goodman, R. G., Bell, D. A., & Saucy D. A. (1983). "Mutagenic and Chemical Changes in Dilute Wood Smoke as it Ages and Reacts in the Atmosphere: An Outdoor Chamber Study." Presented at the 76th Meeting of the Air Pollution Control Association, Atlanta, Georgia, June 1983.

Kamens, R. M., Perry, J. M., Saucy, D. A., Bell, D. A., Newton, D. L., & Brand, B. (1984a). "Factors which Influence PAH Decomposition on Wood Smoke Particle." Presented at the 77th Annual Meeting of the Air Pollution Control Association, San Francisco, CA., June.

Kamens, R. M., Rives, G. D., Perry, J. M., Bell, D. A., Paylor, R. F., Goodman, R. G., & Claxton, L. D. (1984b). "Mutagenic Changes in Dilute Wood Smoke as it Ages and Reacts with Ozone and Nitrogen Dioxide: An Outdoor Chamber Study." Environ. Sci Technol., 18, 523-530.

Kamens, R. M., Bell, D. A., Dietrich, A., Perry, J., Goodman, R. G., Claxton, L. D., & Tejada, S. (1985). "Mutagenic Transformations of Dilute Wood Smoke Systems in the Presence of Ozone and Nitrogen Dioxide. Analysis of Selected High-Pressure Liquid Chromatography Fractions from Wood Smoke Particle Extracts." Environ. Sci. Technol., 19, 63-69.

Kelsey, M. I., & Kraybill, H. F. (1982). "A Data Base of Organic Pollutants that have been Evaluated for Carcinogenicity and Mutagenicity." In: Residential Solid Fuels, Cooper, J. A. and Malek, D. (eds.), 577-605, Published by Oregon Graduate Center, Beaverton, OR.

Kowalczyk, G. S., Choquette, C. E., & Gordon, G. E. (1978). "Chemical Element Balances and Identification of Air Pollution Sources in Washington, D. C." Atmos. Env., 12, 1143-1153.

Kowalczyk, J. F., Bosserman, P. B., & Tombleson, B. J. (1982). "Particulate Emissions from New Low Emission Wood Stove Designs Measured by EPA Method V." In: Residential Solid Fuels, Cooper, J. A. and Malek, D. (eds.), 54-78, published by Oregon Graduate Center, Beaverton, OR.

Kowalczyk, J. F., & Green, W. T. (1982). "New Techniques for Identifying Ambient Air Impacts from Residential Wood heating." In: Residential Solid Fuels, Cooper, J. A. and Malek, D. (eds.), 469-494, published by the Oregon Graduate Center, Beaverton, OR.

Kowalczyk, J. F., & Tombleson, B. J. (1985). "Oregon's Woodstove Certification Program." J. Air Pollut. Control Assoc., 35, 619-625.

Kuhlmey, G. A., Liu, B. Y. H., & Marple, V. A. (1981). "A Micro-orfice Impactor for Sub-micron Aerosol Size Classification." Am. Ind. Hyg. Assoc. J. 42, 790-795.

Lahaye, J., & Prado, G. (1974). "Formation of Carbon Particles from a Gas Phase: Nucleation Phenomenon." Water, Air, and Soil Pollution, 3, 473-481.

Laresgoiti, A, Loos, A. C., & Springer, G. S. (1977). "Particulate and Smoke Emission from a Light Duty Diesel Engine." Environ. Sci. Technol., 11, 973-978.

Lee, R. E. Jr., & Goranson, S. S. (1972). "National Air Surveillance Cascade Impactor Network. I. Size Distribution Measurements of Suspended Particulate Matter in Air," Env. Sci and Technol., 6, 1019-1024.

Lee, R. E. Jr. Goranson, S. S., Enrione, R. E., & Morgan, G. B. (1972). "National Air Surveillance Cascade Impactor Network. II: Size Distribution Measurements of Trace Metal Components." Env. Sci. and Technol., 6, 1025-1030.

Lee, M. L., Prado, G. P., Howard, J. B., & Hites, R. A. (1977). "Source Identification of Urban Airborne Polycyclic Aromatic Hydrocarbons by Gas Chromatographic Mass Spectrometry and High Resolution Mass Spectrometry." Biomedical Mass Spectrometry, 4, 182-186.

Lewtas, J. (1982). "Comparison of the Mutagenic and Potentially Carciongenic Activity of Particle Bound Organics for Wood Stoves, Residential Oil Furnaces, and Other Combustion Sources." In: Residential Solid Fuels, Cooper, J. A. and Malek, D. (eds.), 606-619, Published by Oregon Graduated Center, Beaverton, OR.

Lipari, F., Dasch, J. M., & Scruggs, W. F. (1984). Aldehyde Emissions from Wood-Burning Fireplaces." Environ. Sci. Technol., 18, 326-329.

Lipfert, F. W., & Dungan J. L. (1983). "Residential Firewood Use in the United States." Science, 219, 1425-1426.

Marple, V. A., Liu, B. Y. H., & Whitby, K. T. (1974a). "Fluid Mechanics of the Laminar Flow Aerosol Impactor." Aerosol Sci., 5, 1-16.

Marple, V. A., & Liu, B. Y. H. (1974b). "Characteristics of Laminar Jet Impactors." Environ. Sci. and Technol., 8, 648-654.

Marple, V. A., & Liu, B. Y. H. (1975). "On Fluid Flow and Aerosol Impaction in Inertial Impactors." J. Colloid and Interface Sci., 53, 31-34.

Mast, T. J., Hsieh, D. P., & Seiber, J. N. (1984). "Mutagenicity and Chemical Characterization of Organic Constituents in Rice Straw Smoke Particulate Matter." Environ.Sci.Technol., 18, 338-347.

Masumder, M. K., Ware, R. E., Wilson, J. D., Renninger, R. G., Hiller, F. C., McLeod, P. C., Riable, R. W., & Testerman, M. K. (1979). "Spart Analyzer: Its Application to Aerodynamic Size Distribution Measurement." J. Aerosol. Sci., 10, 561-569.

McCrillis, R. C., & Merrill, R. G. (1985). "Emission Control Effectiveness of a Woodstove Catalyst and Emission Measurement Methods Comparison." Presented at the 78th Meeting of the Air Pollution Control Association, Detroit, Michigan, June.

McDow, S. R. (1986). "The Effect of Sampling Proceedures on Organic Aerosol Measurement." PhD dissertation, Oregon Graduate Center, Beaverton, OR.

Miguel, A. H., & Friedlander, S. K. (1985). "Size Distributions of Elemental Carbon in Atmospheric Aerosols." Atmospheric Sciences Research Laboratory, Office of Research and Development, U.S. Environmental Protection Agency, Research Triangle Park, NC, Report No. EPA/600/D-85-003.

Miller, D. F., Levy, A., Pui, D. Y. H., Whitby, K. T., & Wilson, W. E. Jr. (1976). "Combustion and Photochemical Aerosols Attributable to Automobiles." J. Air Pollut. Control Assoc., 26, 576-581.

Miller, F. J., Gardner, D. E., Graham, J. A., Lee, R. E. Jr., Wilson, W. E., & Bachman, J. D. (1979). "Size Considerations for Establishing a Standard for Inhalable Particles." J. Air Pollution Control Assoc., 29, 610-615.

Miller, M. S., Friedlander, S. K., Hidy, & G. M. (1972). "A Chemical Element Balance for the Pasadena Aerosol," J. Colloid and Interface Sci., 39, 165.

Mueller, P. K., Fung, K. K., Heisler, S. J., Grosjean, D., & Hidy, G. M. (1982). "Atmospheric Particulater Carbon Observations in Urban and Rural Areas of the United States." In: Particulate Carbon: Atmospheric Life Cycle, Wolff, G. T. and Klimisch, R. L. (eds.), Plenum Press.

Muhlbaier, J. L. (1981). "Particulate and Gaseous Emissions from Natural Gas Furnaces and Water Heaters." J. Air Pollut. Control Assoc., 31, 1268-1273.

Nero & Assoc. (1984) "Air Pollution Effects of Residential Wood Combustion: Data Collection and Analysis." EPA Contract No. 68-0106543.

Olson, D. B., & Calcote, H. F. (1981). "Ionic Mechanisms of Soot Nucleationin Premixed Flames." In: Particulate Carbon: Formation During Combustion, Siegla, D. C. and Smith, G. W. (eds.), Plenum Press.

Ogren, J. A., & Charlson, R. J. (1983). "Elemental Carbon in the Atmosphere: Cycle and Lifetime." Tellus, 35B, 241-254.

Ondov, J. M., Zoller, W. H., & Gordon, G. E. (1982). "Trace Element Emissions on Aerosols from Motor Vehicles." Environ. Sci. Technol., 16, 318-327.

Otis, T. (1977). "Wood Burning and Particulate Air Pollution in the Missoula Valley." Missoula, Montana, Missoula City-County Health Department, Air Pollution Control Division, September.

Paciga, J. J., Roberts, T. M., & Jervis, R. E. (1975). "Particle Size Distributions of Lead, Bromine, and Chlorine in Urban-Industrial Aerosols." Environ. Sci. and Technol., 9, 1141-1144.

Paciga, J. J., & Jervis, R. E. (1976). "Multielement Size Characterization of Urban Aerosols." Environ. Sci. and Technol., 10, 1124-1127.

Packham, D. R., & Vines, R. G. (1978). "Properties of Bushfire Smoke: The Reduction in Visibility Resulting from Prescribed Fires in Forests." J. Air Pollut. Control Assoc., 28, 790-795.

Palmer, L., McKusick, R., & Bailey, M. (1980). "Wood and Energy in New England: A Review and Bibliography." Bibliographies and Literature of Agriculture No. 7, U. S. Dept. of Agriculture.

Peters, J. A. (1982). "POM Emissions from Residential Woodburning: An Environmental Assessment." In: Residential Solid Fuels, Cooper, J. A. and Malek, D. (eds.), 267-284, Published by Oregon Graduate Center, Beaverton, OR.

Patterson, R. K., & Wagman, J. (1977). "Mass and Composition of an Urban Aerosol as a Function of Particle Size for Several Visibility Levels." J. Aerosol Sci., 8, 269-279.

Pierson, W. R. (1980). "Particulate Matter and Total Carbon from Vehicles on the Road." Technical Report #SR-80-34, Scientific Laboratory, Ford Motor Co. Dearborn, MI.

Pimentel, D., Moran, M. A., Fast, S., Weber, G., Bukantis, R., Balliett, L., Boveng, P., Cutler, C., Hindman, S., & Young, M. (1981). "Biomass Energy from Crop and Forest Residues." Science, 212, 1110-1114.

Prado, G., & Lahaye, J. (1981). "Physical Aspects of Nucleation and Growth of Soot Particles." In: Particulate Carbon Formation During Combustion, Siegla D. C. and Smith G. W. (eds.), 143-175, Published by Plenum Press, NY.

Prakash, C. B., & Murray, F. E. (1972). "Studies on Air Emissions from Combustion of Wood-Waste." Combustion Sci. and Technol., 6, 81-88.

Radke, L. F., Slith, J. L., Hegg, D. A., & Hobbs, P. V. (1978) "Airborne Studies of Particles and Gases from Forest Fires." J. Air Pollut. Control Assoc., 28, 30-34.

Rahn, K. A., Brosset. C., Ottar, B., & Patterson, E. M. (1982). "Black and White Episode, Chemical Evolution of Eurasian Air Masses and Long-Range Transport of Carbon to the Artic." In: Particulate Carbon Atmospheric Life Cycle, Wolff G. T. and Klimisch, R. L. (eds.), 327-342, Plenum Press.

Ramdahl, T., Alfheim, I., Rustad, S., & Olsen, T. (1982). "Chemical and Biological Characterization of Emissions from Small Residential Stoves Burning Wood and Charcoal." Chemoshere, 11, 601-611.

Ramdahl, T., Schjoldager, J., Currie, L. A. Hanssen, J. E., Moller, M., Klouda, G. A., & Alfheim, I (1984). "Ambient Impact of Residential Wood Combustion in Elverum, Norway." Sci. Total Environ., 36, 81-90.

Romero, A. E. Buchan R. M., & Fox, D. G. (1978). "Study of Air Pollution from Fireplace Emissions at Vail Ski Resort." J. Env. Health 41, 117-119.

Rosen, H., Hansen, A. D. A., Dod, R. L., & Novakov, T. (1980). "Soot in Urban Atmospheres: Determination by an Optical Adsorption Technique." Science, 208, 297-314.

Rudling, L., & Ahling, B. (1982). "Chemical and Biological Characterization of Emissions from Combustion of Wood and Woodchips in Small Furnaces and Stoves." In: Residential Solid Fuels, Cooper, J. A. and Malek, D. (eds.), 34-53, Published by Oregon Graduate Center, Beaverton OR.

Sandborn, C. R., & Blanchet, M. A. (1982). " Particulate Emissions from Residential Wood Combustion in Vermont." In: Residential Solid Fuels, Cooper, J. A. and Malek, D. (eds.), 188-198, Published by the Oregon Graduate Center,Beaverton, OR.

Schwartz, G. P., Daisey, J. M., & Lioy, P. J. (1981). "Effect of Sampling Duration on the Concentration of Particulate Organics collected on Glass Fiber Filters." Am. Ind. Hyd. Assoc. J., 42, 258-263.

Seizinger, D. E. (1978). "Analysis of Carbonaceous Diesel Emissions." Presented at: Conference on Carbonaceous Particles in the Atmosphere, Lawerence Berkeley Laboratory, Berkeley, CA, March.

Sexton, K., Liu, K., Hayward, S. B., & Spengler, J. D. (1984). "Organic and Elemental Characterization of Wintertime Aerosol in a Wood-Burning Community." Presented at the 77th Annual Meeting of the Air Pollution Control Association, San Francisco, CA, June.

Sexton, K., Spengler, J. D., & Treitman, R. D. (1984). "Effects of Residential Wood Combustion on Indoor Air Quality: A Case Study in Waterbury, Vermont" Atmos. Environ., 18, 1371-1383.

Shah, J. J. (1981). "Measurements of Carbonaceous Aerosol Across the U. S.: Sources and Role in Visibility Degradation." Ph.D. dissertation, Oregon Graduate Center, Beaverton, OR.

Shah, J. J., Watson, J. G. Jr., Cooper, J. A., & Huntzicker, J. J. (1984). "Aerosol Chemical Composition and Light Scattering in Portland, Oregon: The Role of Carbon." Atm. Environ., 18, 235-240.

Shani, G. S., Haccoun, A., & Kuscheevsky, A. (1984). Aerosol and Air Pollution Size Distribution." Atmos. Environ., 18, 2223-2229.

Smith, R. D., Campbell, J. A., & Nielson K. K. (1979). "Concentration Dependence upon Particle Size of Volatilized Elements in Fly Ash." Environ. Sci. Technol., 13, 553-558.

Smith, K. R., Aggarwal, A. L., & Dave, R. M. (1983). "Air Pollution and Rural Biomass Fuels in Developing Countries: A Pilot Village Study in India and Implications for Research and Policy." Formerly East-West Resource Systems Institute, Working papers WP-82-17 and WP-83-2, Atmos. Env., 17, 2343-2362.

Smith, K. R., Apte, M., Menon, P., & Shrestha, M. (1984). "Carbon Monoxide and Particles from Cooking Stoves: Results from a Simulated Village Kitchen." Presented at the Third International Conference on Indoor Air Quality and Climate, Stockholm, Sweden, August, 1984.

Smith, K. R.(1984). "Air Pollutant Emissions, Concentrations, and Exposures from Biomass Combustion: The Cigarette Analogy, "American Chemical Society Meeting, Philadelphia, August.

Stevens, R. K., Dzubay, T. G., Shaw, R. W. Jr., McClenny, W. A., Lewis, C. W., & Wilson, W. E. (1980). "Characterization of the Aerosol in the Great Smoky Mountains." Environ. Sci. Technol., 14, 1491-1498.

Stevens, R. K., McClenny, W. A., & Dzubay, T. G. (1982). "Analytical Methods to Measure the Carbonaceous Content of Aerosols." In Particulate Carbon: Atmospheric Life Cycle, Wolff, G. T. and Klimisch, R. L. (eds.), 111-129, Plenum Press.

Stevens, R. K. (1983). "Analytical Measurements for Use in Source Apportionment Studies to Determine Impact of Wood Burning on Visibility and Fine Particle Mass." Presented at the workshop on Residential Wood and Coal Combustion co-sponsored by the US EPA and the University of Washington, Portland, OR, November 30-December 1.

Stiles, D. C. (1983). "Evaluation of an S2 Sampler for Receptor Modeling of Wood Smoke Emissions." Paper #83-54.6 presented at the 76th Annual Meeting of the Air Pollution Control Association, Atlanta, GA., June 19-20.

Stith, J. L., Radke, L. F., & Hobbs, P. V. (1981). "Particle Emissions and the Production of Ozone and Nitrogen Oxides from the Burning of Forest Slash." Atmos. Environ., 15, 73-82.

Thomson, V. E., Jones, A., Haemisegger, E., & Steigerwald, B. (1985). "The Air Toxics Problem in the United States: An Analysis of Cancer Risks Posed by Selected Air Pollutants." J. Air Pollut. Control Assoc., 36, 535-540.

Thornton, M. M., & Malte, P. C. (1982). "Combustion Rate of Model Wood Volatiles." In: Residential Solid Fuels, Cooper, J. A. and Malek, D., (eds.), 851-872, published by Oregon Graduate Center, Beaverton. OR.

Truesdale, R. S., Mack, J. B., White, K. E., Leese, K. E., & Cleland, J. G. (1984). "Characterization of Emissions from the Combustion of Wood and Alternative Fuels in a Residential Woodstove." United States Environmental Protection Agency, Industrial Environmental Research Laboratory, EPA-600/S7-84-094

Van Vaeck, L., Broddin, G., & Cauvenberghe, K. (1979). "Differences in Particle Size Distributions of Major Organic Pollutants in Ambient Aerosols in Urban, Rural, and Seashore Areas." Environ. Sci. and Technol., 13, 1494-1502.

Van Vaeck, K. Van Cauwenberghe, K., & Janssens, J. (1984). "The Gas-Particle Distribution of Organic Aerosol Consituents: Measurement of the Volatilisation Artifact in Hi-Vol Cascade Impactor Sampling." Atmos. Environ., 18, 417-430.

Wagner, H. Gr. (1981). "Soot Formation An Overview." In: Particulate Carbon Formation During Combustion, Siegla, D. C.and Smith, G. W. (eds), 1-29, Published by Plenum Press, NY.

Ward, D. E., Core, J. E. (1986). "Does a Signature Exist for Source Apportionment of Emissions for Prescribed Fires?" Paper #1B4 presented at the 1986 Annual Meeting of the Pacific Northwest International Section of the Air Pollution Control Association, Eugene, OR, Nov. 19-21.

Watson, J. G. Jr. (1979). "Chemical Element Balance Receptor Model Methodology for Assessing the Sources of Fine and Total Suspended Particulate Matter in Portland, Oregon." Ph. D. dissertation. Oregon Graduate Center, Beaverton, Oregon.

Watson, J. G. Jr., Cooper, J. A., & Huntzicker, J. J. (1984). "The Effective Variance Weighting for Least Squares Calculations Applied to the Mass Balance Receptor Model." Atmos. Environ., 18, 1347-1355.

Willeke, K., & Whitby, K. T. (1975). "Atmospheric Aerosols: Size Distribution Interpretation." J. Air Pollut. Control Assoc., 25, 529-534.

Wolff, G. T., Countess, R. J., Groblicki, P. J., Ferman, S. H., Cadle, S. H., & Muhlbaier, J. L. (1981). "Visibility - Reducing Species in the Denver "Brown Cloud" -II Sources and Patterns." Atm. Environ., 15, 2485-2502.

Wolff, G. T. (1981). "Particulate Elemental Carbon in the Atmosphere." J. Air Pollut. Control Assoc. 31, 935-937.

Wolff, G. T., Groblicki, P. J., Cadle, S. H., & Countess, R. J. (1982). "Particulate Carbon at Various Locations in the United States." In: Particulate Carbon: Atmospheric Life Cycle, Wolf, G. T. and Klimisch, R. L., (eds.), Plenum Press.

APPENDIX ONE

A1.1 RESIDENITAL WOOD BURING IN OREGON, VERMONT AND NATIONALLY

Oregon and Vermont lead the nation in levels of RWC. Oregonians have responded to the increase in energy prices during the 1970's by a dramatic increase in wood burning. This occurred despite the fact that only 25% of the Oregon residential heating load is supplied by oil. Various surveys have attempted to evaluate the magnitude of RWC. According to a GMA Research Corporation survey (1978) 53% of Oregonians use a secondary heat source. Nine percent of secondary heat sources were wood stoves and 23% were fireplaces. The survey also found that 10% of Oregonians use wood as their primary heating fuel. Those Oregonians who use wood used an average of 2.7 cords of wood per year. Wood heating is principally used by home owners living in single family homes.

Hatchard and Day (1979) found that in the Portland/Vancouver area 10% of all households had at least one wood stove and 35% had at least one fireplace. These households burned on the average of 1.4 cords of wood annually. The wood used was 40% fir, 30% alder, 9% cedar and 8% pressed logs

In a survey of the Portland area Cummings (1982) found that 56% of those surveyed burned wood in their residence. Of these, 12% used wood stoves, 9% used fireplace inserts, 34% used fireplaces and 1% used wood burning furnaces. Three percent of the respondents used wood as their only heat source, while 36% used wood as either a major or a secondary heat source. This survey indicated that over a third of fireplaces were

used for heating. The average age of wood stoves was 5.3 years, while the average age of fireplaces was 20 years. This indicates that wood stove usage was a response to the oil embargo, whereas fireplace usage has a much older history rooted in aesthetics. On the average 1.4 cords of wood were burned per household per year. Annual wood usage for stove users was 2.3 cords, for fireplace insert users 2.0 cords and for fireplace users 0.85 cords. Fifty percent of wood-burners burned a mixture of hardwood and soft wood, while 27% burned only hardwood and 17% burned only fir. Fifty-six percent cut their own wood. Both wood stoves and fireplaces each burned 37% of the total amount of wood burned, while 24% was burned in fireplace inserts. Compared to earlier surveys these results indicate that wood-burning for heat did not increase greatly from 1979 to 1982.

Most stove and fireplace insert users indicated that they usually operated their stove with the damper mostly closed or closed. Emission estimates for the 1981-82 heating season indicate that wood stove and fireplace inserts together contributed 6512 tons of particulate matter and fireplaces contributed 1962 tons to the greater Portland airshed.

A1.2 RESIDENTIAL WOOD BURNING IN VERMONT

Vermont, like Oregon, has a very heavy dependence on the use of wood as a residential heating fuel. Prior to 1900 wood was the major energy source in the area even though forests covered only 20% of the land area due to the need for farmland (Bailey and Wheeling, 1982). After 1900 the use of wood as a heating fuel declined sharply after the widespread adoption of oil burning furnaces. By 1970 agricultural land

widespread adoption of oil burning furnaces. By 1970 agricultural land use had decreased greatly. Eighty percent of the land area was now forested. About 15% of residents were using some wood heating, primarily non-airtight stoves. At this time nationally only 1% of homes used wood heat. Residential wood-burning was mainly recreational. As a result of the 1973-74 oil embargo oil prices increased by 240% in terms of constant dollars from 1972 to 1979. Since Vermont's heating requirements are 167% of the national average (on a per unit area heated basis) and oil supplied 70-80% of residential heat, a strong motivation to return to wood heating was created. About 20,000 new stoves have been installed per year. In 1979 40% of all households and 55% of owner-occupied households were using wood-burning stoves or central wood-fired heating systems. Those homeowners who used airtight wood stoves burned an average of 4.4 cords of wood per heating season and derived 60% of their space heat from this source.

A1.3 WOOD BURNING ON A NATIONAL LEVEL

Significant amounts of wood burning occur in all states of the Union except Hawaii. Table A.1 (Nero and Assoc., 1984) gives RWC levels on a per household and per state basis. The level of air pollution associated with RWC burning depends both on the amounts of wood burned, on burning practices and on the local meteorological conditions which determine smoke dispersion. RWC has become an air pollution problem in those areas which have high levels of wood burning and also poor meteorological dispersion.

Table A-1

Fuelwood Consumption by State 1980-81

State	Number of Households (10×10^6)	Percent burning	Average burned (Cords)	Total burned (Cords $\times 10^6$)
Alabama	1.324	28	2.0	0.76
Arizona	0.963	24	1.0	
Arkansas	0.821	42	2.5	0.85
California	8.633	28	0.8	1.84
Colorado	1.059	35	1.0	0.39
Connecticut	1.094	30	1.3	0.44
Deleware	0.207	29		
Washington,DC	0.253			
Florida	3.743	11	1.5	0.62
Georgia	1.872	28	1.4	0.73
Idaho	0.323	46	2.6	0.39
Illinois	4.051	22	1.8	1.58
Indiana	1.936	23	1.9	0.86
Iowa	1.056	21	1.9	
Kansas	0.870	21	1.9	
Kentucky	1.264	26	2.5	
Louisiana	1.421	13	1.8	
Maine	0.397	54	3.9	0.84
Maryland	1.466	21	1.6	0.49
Massachusetts	2.027	29	1.8	1.07
Michigan	3.193	25	2.2	1.79
Minnesota	1.442	35	1.9	1.92

Mississippi	0.830	27		
Missouri	1.792	36	1.9	1.23
Montana	0.286	38	2.4	0.26
Nebraska	0.572	14		
Nevada	0.305		2.2	
New Hamshire	0.324	47	3.0	0.46
New Jersey	2.551	18	0.9	0.41
New Mexico	0.444	43	1.2	0.23
New York	6.332	18	1.7	2.21
North Carolina	2.047	46	2.0	1.92
North Dakota	0.229	36	1.7	0.14
Ohio	3.837	30	1.8	2.09
Oklahoma	1.114	22		0.57
Oregon	0.993	58	2.7	1.55
Pennslvania	4.213	23	2.2	2.20
Rhode Island	0.339	25		
South Carolina	1.031	36	1.6	0.61
South Dakota	0.244	27	3.3	0.22
Tennessee	1.615	38	2.4	1.47
Texas	4.945	25	1.1	1.32
Utah	0.448	32	2.0	
Vermont	0.178	58	4.0	0.41
Virginia	0.857	46	2.1	1.76
Washington	1.540	53	2.1	1.67
West Virginia	0.687	35	2.7	0.64
Wisconsin	1.653	28	2.7	1.28

APPENDIX TWO

This appendix describes the modifications made to the thermo-optical carbon analysis system which contributed significantly to the quality of carbon data obtained in this research.

1. The flow controller system which controls the flow of gases to the analysis oven and temperature control system which controls the temperatures of the analysis and oxidation ovens and the methanator were redesigned and compactly packaged into two separate modules. The methanator and the flame ionization detector (FID) were mounted on top of the temperature controller.

2. Modifications in the system flows were made to eliminate changes in gas flows seen by the FID, during various parts of the analysis cycle. These modifications eliminated shifts in the FID baseline output. Two flow modifications were made:

(A) The flow system was modified to reintroduce the bypassed helium or helium/oxygen streams back into the carrier gas flow stream going through the FID. In the organic carbon analysis part of the analysis cycle the carrier stream is composed of two streams of pure helium: the main stream and the make-up stream. The flow rate of the make-up stream is exactly equal to the flow rate of the 10% oxygen in helium stream. For elemental analysis the makeup stream was replaced by the 10% oxygen in helium stream thus changing the oxygen concentration in the total carrier stream to 1-2% oxygen but maintaining the same volumetric flow

rate. In the earlier design the make-up stream or the 10% oxygen in helium streams were dumped when they were not used. In the new flow configuration the formerly dumped streams were reintroduced into the carrier stream beyond the analysis oven but ahead of the FID so that both the make-up stream and the 10% oxygen in helium stream were always going to the FID.

(B) Similarly the backflow stream was also reintroduced into the gas stream going to the FID. It is necessary to direct part of the carrier stream (the back-flow stream) entering the analysis oven back through the sample loading area and out through the back end of the oven to remove ambient air that has entered the oven during sample loading. In the earlier design the backflow stream was vented. Since the backflow stream carries part of the calibration gas it was necessary to accurately know the volume of this flow stream and enter it into calculations when the backflow stream was vented. By reintroducing the back flow stream into the carrier stream ahead of the FID it was no longer necessary to know the magnitude of the backflow stream and errors in knowing its value are eleminated. A judicious choice of flows and tubing lengths insures that the calibration gas slug going through the oven arrives at the FID at the same time as the slug carried by the back flow stream.

3. The FID power supply was changed from a rectified AC system to a high voltage battery. This reduced FID noise.

4. The optical system was changed from a lens and mirror configuration

to a fiber optic configuration. This greatly simplified the optical system and resulted in a stronger laser signal. This modification allowed the optical signal to be caried to the computer interface with an optical cable rather than an electrical one, thus eleminating electrical interference with the laser signal.

5. Optical quality quartz rods were substituted for the commercial quality quartz rods that were fomerly used. Both "Amersil" and "Homosil" were found to work well. This greatly increased the laser output signal. "Amersil" is by far the least expensive material. These rods can be obtained from GM Associates, 9803 Kitty Lane, Oakland, CA 94603.

6. It was determined that internal flaws in the quartz rod caused by prolonged heating were responsible for degradation of rod performance rather than defects in the polished ends of the rods. It was also determined that rod ends could be machine polished with sanding wheels used to prepare metal microscope specimens.

7. The ceramic rod and rubber septum at the sample loading end of the oven was replaced with a stainless steel rod and a Teflon septum. This reduced the need for septum changes and eliminated the introduction of carbon from the septum into the oven.

8. It was determined that a Supelco oxygen scrubber would be useful to remove trace amounts of oxygen from the helium carrier gas. It was also

determined that the Supelco scrubber had to be initially and periodically activated by passing a helium stream which contained a few percent of hydrogen through the scrubber. The hydrogen concentration can be increased toward the end of the activation process, but in no event should more than a few percent hydrogen be used during the majority of the activation process and pure hydrogen should not be used.

9. The rear oven heater was changed from a nichrome wound heater to a commercial cavity heater (Watlow ceramic fiber heater, model VC401A060A, manufactured by Watlow Electric Mfg. Co., 12001 Lackland Road, St. Louis MI 63146). The 1000 C. temperature requirement of the rear oven caused frequent failures of the wound heaters.

10. It was determined that the wound heater used for the front oven could be constructed by winding the nichrome wire in tight contact with adjacent wire coils rather than the previous winding technique which sought to prevent contact between adjacent coils of wire. This resulted in lower wire operating temperatures for the same heat output and longer oven lifetimes.

APPENDIX 3

SOURCE DATA FOR: Residential Wood Stoves and Fireplaces, a Residential Oil Furnace, and Motor Vehicle Emissions Collected in a Highway Tunnel.

Mass loading = Particulate loading sampled ($\mu g/m^3$)

Cut-point = Impactor cut-point behind which the sample was collected

Adsorbed OC = Vapor organic carbon adsorbed on a quartz filter located behind a Teflon filter that was sampling particulate material

Mass = Mass of particulate material collected (M) (mg)

OC = Organic Carbon

EC = Elemental Carbon

TC = Total carbon (EC + OC)

SOURCE DATA
Type: Earthstove, fir, damper closed
Date: 2/14/84

Mass loading: 5542 $\mu g/m^3$
Adsorbed OC: 5.90 $\mu g/cm^2$
Sampling time = 20 minutes

Cut Pt. (μm)	Filter	Mass (mg)	OC ($\mu g/cm^2$)	EC ($\mu g/cm^2$)	OC/M (%)	EC/M (%)
0.1	Q320	0.11	5.31	0.16	38.2	3.4
0.3	Q306	0.32	21.78	1.76	37.5	4.2
0.6	Q298	0.31	20.09	2.08	38.9	5.7
1.2	Q296	0.86	55.95	2.37	49.8	2.3
2.5	Q337	0.90	57.94	2.09	49.1	2.0
None	Q332	0.92	58.41	2.93	48.5	2.7

Carbon Size Distribution (%) (μm)	OC	EC	TC
<0.1	9.4	15.2	9.7
0.1-0.3	17.5	38.2	18.6
0.3-0.6	0.1	17.5	1.0
0.6-1.2	68.3	9.9	65.2
1.2-2.5	3.8	-9.6	3.1
>2.5	0.9	28.7	2.4

Mass Distribution (μm)	(%)
<0.1	12.0
0.1-0.3	22.8
0.3-0.6	-1.1
0.6-1.2	59.8
1.2-2.5	4.3
<2.5	2.2

SOURCE DATA
Type: Earthstove, fir damper open
Date: 2/14/84

Mass loading: 2650 $\mu g/m^3$
Adsorbed OC: 4.2 $\mu g/cm^2$
Sampling time = 20 minutes

Cut Pt. (μm)	Filter	Mass (mg)	OC ($\mu g/cm^2$)	EC ($\mu g/cm^2$)	OC/M (%)	EC/M (%)
0.1	Q330	0.14	2.95	0.57	6.6	9.7
0.3	Q327	0.17	10.17	6.03	26.2	26.8
0.6	Q323	0.35	13.37	14.87	22.1	36.1
1.2	Q328	0.44	17.88	18.15	26.3	35.1
2.5	Q324	0.44	15.81	21.12	22.3	40.8
None	Q321	0.44	18.18	20.10	26.9	38.8

Carbon Size Distribution (%) (μm)	OC	EC	TC
<0.1	7.8	7.9	7.9
0.1-0.3	30.0	18.8	23.4
0.3-0.6	27.7	47.3	39.3
0.6-1.2	32.4	16.3	22.9
1.2-2.5			3.6
>2.5			4.0

Mass Distribution (μm)	(%)
<0.1	32
0.1-0.3	7
0.3-0.6	41
0.6-1.2	20
1.2-2.5	0
<2.5	0

SOURCE DATA
Type: Earthstove, fir, damper open
Date: 3/13/88

Mass loading: 2289 $\mu g/m^3$
Adsorbed OC: 5.2 $\mu g/cm^2$
Sampling time = 20 minutes

Cut Pt. (μm)	Filter	Mass (mg)	OC ($\mu g/cm^2$)	EC ($\mu g/cm^2$)	OC/M (%)	EC/M (%)
0.1	T135	0.06				
0.3	Q413	0.15	9.15	5.08	25.6	45.5
0.6	T143	0.22				
1.2	Q370	0.30	15.00	8.59	27.8	24.3
2.5	T147	0.31				
None	Q407	0.38	17.46	10.69	27.4	23.9

	Al/M (%)	Si/M (%)	P/M (%)	S/M (%)	Cl/M (%)	K/M (%)
0.1	0.45	0.95	0.00	0.65	0.00	0.93
0.6	0.15	0.23	0.08	0.35	0.47	2.00
2.5	0.04	0.17	0.07	0.34	0.51	1.56

	Ca/M (%)	Ti/M (%)	V/M (%)	Mn/M (%)	Fe/M (%)	Ni/M (%)
0.1	0.20	0.05	0.01	0.11	0.14	0.00
0.6	0.30	0.02	0.01	0.02	0.02	0.00
2.5	0.38	0.01	0.00	0.03	0.00	0.00

	Cu/M (%)	Zn/M (%)	Br/M (%)	Rb/M (%)	Pb/M (%)
0.1	0.02	0.01	0.00	0.00	0.00
0.6	0.01	0.09	0.01	0.00	0.00
2.5	0.00	0.08	0.00	0.00	0.00

Carbon Size Distribution (%)

(μm)	OC	EC	TC
<0.3	28.7	42.3	35.0
0.3-1.2	51.3	38.1	45.1
>1.2	20.1	19.6	19.8

Mass Distribution

(μm)	(%)
<0.1	15.8
0.1-0.3	23.7
0.3-0.6	18.4
0.6-1.2	21.0
1.2-2.5	18.4
<2.5	

Trace Element Size Distributions

(μm)	S (%)	Cl (%)	K (%)	Ca (%)	Zn (%)	Ti (%)
<0.1	36.9	0.0	11.5	10.2	1.5	74.7
0.1-0.6	36.7	65.6	79.4	45.4	72.5	11.0
0.6-2.5	26.4	34.4	9.1	44.4	25.9	14.3

SOURCE DATA
Type: Earthstove, fir, damper open
Date: 3/22/84

Mass loading: 963 $\mu g/m^3$
Adsorbed OC: 2.88 $\mu g/cm^2$
Sampling time = 20 minutes

Cut Pt. (μm)	Filter	Mass (mg)	OC ($\mu g/cm^2$)	EC ($\mu g/cm^2$)	OC/M (%)	EC/M (%)
0.1	T57	0.06				
0.3	Q377	0.12	4.00	5.83	7.1	36.7
0.6	T139	0.15				
1.2	Q364	0.15	3.93	8.90	5.9	50.4
2.5	T142	0.16				
None	Q363	0.16	4.31	10.81	7.6	57.4

	Al/M (%)	Si/M (%)	P/M (%)	S/M (%)	Cl/M (%)	K/M (%)
0.1						
0.6	0.08	0.00	0.00	0.89	2.53	4.63
2.5	0.37	0.13	0.12	1.06	2.17	4.46

	Ca/M (%)	Ti/M (%)	V/M (%)	Mn/M (%)	Fe/M (%)	Ni/M (%)
0.1	0.22					
0.6	0.14					
2.5	0.38	0.01	0.00	0.03	0.00	0.00

	Cu/M (%)	Zn/M (%)	Br/M (%)	Rb/M (%)	Pb/M (%)
0.1					
0.6		0.32			
2.5		0.30			

Carbon Size Distribution (%)

(μm)	OC	EC	TC
<0.3	69.7	48.0	50.4
0.3-1.2	3.7	34.3	30.8
>1.2	26.6	17.7	18.7

Mass Distribution

(μm)	(%)
<0.1	37.5
0.1-0.3	37.5
0.3-0.6	18.7
0.6-1.2	0.0
1.2-2.5	6.2
<2.5	0.0

SOURCE DATA
Type: Earthstove, fir, damper closed
Date: 3/22/88

Mass loading: 8915 $\mu g/m^3$
Adsorbed OC: 5.82 $\mu g/cm^2$
Sampling time = 20 minutes

Cut Pt. (μm)	Filter	Mass (mg)	OC ($\mu g/cm^2$)	EC ($\mu g/cm^2$)	OC/M (%)	EC/M (%)
0.1	T145	0.42				
0.3	Q349	0.68	56.96	2.10	56.9	2.3
0.6	T140	0.79				
1.2	Q411A	1.01	72.93	4.11	56.5	3.5
2.5	T137	1.32				
None	Q365	1.48	103.37	3.71	56.0	2.1

	Al/M (%)	Si/M (%)	P/M (%)	S/M (%)	Cl/M (%)	K/M (%)
0.1						
0.6						
2.5						

	Ca/M (%)	Ti/M (%)	V/M (%)	Mn/M (%)	Fe/M (%)	Ni/M (%)
0.1						
0.6						
2.5						

	Cu/M (%)	Zn/M (%)	Br/M (%)	Rb/M (%)	Pb/M (%)
0.1					
0.6					
2.5					

Carbon Size Distribution (%)

Size (μm)	OC	EC	TC
<0.3	46.7	50.4	46.8
0.3-1.2	22.1	60.4	23.5
>1.2	31.2	-10.8	29.7

Mass Distribution

Size (μm)	(%)
<0.1	28.4
0.1-0.3	17.6
0.3-0.6	7.4
0.6-1.2	14.9
1.2-2.5	20.9
<2.5	10.8

SOURCE DATA
Type: Earth Stove, fir, damper closed
Date: 4/5/84

Mass loading: 6024 $\mu g/m^3$
Adsorbed OC: 5.1 $\mu g/cm^2$
Sampling time = 20 minutes

Cut Pt. (μm)	Filter	Mass (mg)	OC ($\mu g/cm^2$)	EC ($\mu g/cm^2$)	OC/M (%)	EC/M (%)
0.1	T64	0.42				
0.3	Q423	0.58	37.23	3.11	41.9	4.06
0.6	T76	0.59				
1.2	Q449	1.00	57.40	4.60	44.4	3.91
2.5	T122	1.00				
None	Q443	0.98	58.98	4.51	46.7	3.91

	Al/M (%)	Si/M (%)	P/M (%)	S/M (%)	Cl/M (%)	K/M (%)
0.1	0.00	0.00	0.00	0.31	0.36	0.31
0.6	0.04	0.00	0.00	0.07	0.10	0.09
2.5	0.00	0.00	0.00	0.04	0.08	0.08

	Ca/M (%)	Ti/M (%)	V/M (%)	Mn/M (%)	Fe/M (%)	Ni/M (%)
0.1	0.03					
0.6	0.01					
2.5	0.01					

	Cu/M (%)	Zn/M (%)	Br/M (%)	Rb/M (%)	Pb/M (%)
0.1		0.14			
0.6		0.04			
2.5		0.02			

Carbon Size Distribution (%)

(μm)	OC	EC	TC
<0.3	53.0	61.3	53.6
0.3-1.2	44.0	40.6	43.8
>1.2	2.9	-2.0	2.5

Mass Distribution

(μm)	(%)
<0.1	43
0.1-0.3	16
0.3-0.6	1
0.6-1.2	42
1.2-2.5	0
<2.5	-2

Trace Element Size Distributions

(μm)	S (%)	Cl (%)	K (%)	Ca (%)	Fe (%)	Ni (%)
<0.1						
0.1-0.6						
0.6-2.5						

SOURCE DATA
Type: Earth Stove, fir, damper open
Date: 4/5/84

Mass loading: 1997 $\mu g/m^3$
Adsorbed OC: 4.9 $\mu g/cm^2$
Sampling time = 20 minutes

Cut Pt. (μm)	Filter	Mass (mg)	OC ($\mu g/cm^2$)	EC ($\mu g/cm^2$)	OC/M (%)	EC/M (%)
0.1	T153	0.03				
0.3	Q431	0.17	12.35	3.93	33.1	17.5
0.6	T152	0.21				
1.2	Q436	0.24	14.76	6.76	34.9	23.9
2.5	T70	0.24				
None	Q425	0.29	16.09	8.34	32.8	24.4

	Al/M (%)	Si/M (%)	P/M (%)	S/M (%)	Cl/M (%)	K/M (%)
0.1	2.89	0.74	0.14	1.03	1.00	0.85
0.6	0.18	0.04	0.00	0.17	0.90	0.80
2.5	0.21	0.07	0.01	0.22	0.73	0.72

	Ca/M (%)	Ti/M (%)	V/M (%)	Mn/M (%)	Fe/M (%)	Ni/M (%)
0.1	0.00					
0.6	0.18					
2.5	0.20					

	Cu/M (%)	Zn/M (%)	Br/M (%)	Rb/M (%)	Pb/M (%)
0.1		1.57			
0.6		0.18			
2.5		0.14			

Carbon Size Distribution (%)

(μm)	OC	EC	TC
<0.3	59.2	41.9	51.9
0.3-1.2	28.9	39.1	33.2
>1.2	11.9	18.9	14.9

Mass Distribution

(μm)	(%)
<0.1	10
0.1-0.3	48
0.3-0.6	14
0.6-1.2	10
1.2-2.5	0
<2.5	17

Trace Element Size Distributions

(μm)	S (%)	Cl (%)	K (%)	Ca (%)	Fe (%)	Ni (%)
<0.1	57.5		14.8	0.0		
0.1-0.6	9.3		88.5	78.1		
0.6-2.5	33.2		2.6	21.9		

SOURCE DATA
Type: Earthstove, fir, damper almost closed
Date: 4/5/84

Mass loading: 2957 $\mu g/m^3$
Adsorbed OC: 6.5 $\mu g/cm^2$
Sampling time = 20 minutes

Cut Pt. (μm)	Filter	Mass (mg)	OC ($\mu g/cm^2$)	EC ($\mu g/cm^2$)	OC/M (%)	EC/M (%)
0.1	T7	0.25				
0.3	Q439	0.32	22.41	1.86	37.6	4.4
0.6	T11	0.37				
1.2	Q415	0.52	36.32	3.49	48.7	5.7
2.5	T158	0.49				
None	Q444	0.54	39.18	3.12	51.4	4.9

	Al/M (%)	Si/M (%)	P/M (%)	S/M (%)	Cl/M (%)	K/M (%)
0.1	0.00	0.00	0.00	0.00	1.30	0.83
0.6	0.06	0.00	0.00	0.24	0.49	0.69
2.5	0.05	0.00	0.01	0.17	0.45	0.57

	Ca/M (%)	Ti/M (%)	V/M (%)	Mn/M (%)	Fe/M (%)	Ni/M (%)
0.1	0.11					
0.6	0.06					
2.5	0.09					

Carbon Size Distribution (%)

(μm)	OC	EC	TC
<0.3	43.3	53.1	44.2
0.3-1.2	47.9	58.8	48.9
>1.2	8.7		6.9

Mass Distribution

(μm)	(%)
<0.1	46.3
0.1-0.3	13.0
0.3-0.6	9.2
0.6-1.2	27.8
1.2-2.5	
<2.5	9.2

Trace Element Size Distributions

(μm)	S (%)	Cl (%)	K (%)	Ca (%)	Fe (%)	Ni (%)
<0.1			74.1			
0.1-0.6			16.2			
0.6-2.5			9.7			

SOURCE DATA
Type: Earthstove, alder, damper open
Date: 4/13/84

Mass loading: 855 $\mu g/m^3$
Adsorbed OC: 2.10 $\mu g/cm^2$
Sampling time = 20 minutes

Cut Pt. (μm)	Filter	Mass (mg)	OC ($\mu g/cm^2$)	EC ($\mu g/cm^2$)	OC/M (%)	EC/M (%)
0.1	T91	0.02				
0.3	Q487	0.15	3.73	2.81	8.2	14.2
0.6	T150	0.17				
1.2	Q518	0.18	3.71	3.72	7.6	17.6
2.5	T165	0.18				
None	Q488	0.22	3.74	3.43	6.3	13.2

	Al/M (%)	Si/M (%)	P/M (%)	S/M (%)	Cl/M (%)	K/M (%)
0.1	2.03	2.04	0.11	3.63	3.54	15.78
0.6	0.14	0.67	0.34	5.12	7.19	18.49
2.5	0.91	0.62	0.39	5.09	7.66	18.89

	Ca/M (%)	Ti/M (%)	V/M (%)	Mn/M (%)	Fe/M (%)	Ni/M (%)
0.1	0.00	0.00	0.00	0.00	0.00	0.00
0.6	0.04	0.01	0.00	0.01	0.19	0.01
2.5	0.00	0.01	0.00	0.01	0.00	0.01

	Cu/M (%)	Zn/M (%)	Br/M (%)	Rb/M (%)	Pb/M (%)
0.1	0.00	0.53	0.18	0.00	0.00
0.6	0.01	0.49	0.02	0.06	0.09
2.5	0.03	0.52	0.02	0.07	0.11

Carbon Size Distribution (%)

(μm)	OC	EC	TC
<0.3	88.5	72.9	77.9
0.3-1.2	9.7	35.5	27.2
>1.2	1.8		

Mass Distribution

(μm)	(%)
<0.1	9.1
0.1-0.3	59.1
0.3-0.6	9.1
0.6-1.2	4.6
1.2-2.5	0.0
<2.5	18.2

Trace Element Size Distributions

(μm)	S (%)	Cl (%)	K (%)	Ca (%)	Fe (%)	Ni (%)
<0.1						
0.1-0.6						
0.6-2.5						

SOURCE DATA
Type: Earthstove, alder, damper closed Mass loading: 6084 $\mu g/m^3$
Date: 4/13/84 Adsorbed OC: 6.70 $\mu g/cm^2$
Sampling time = 20 minutes

Cut Pt. (μm)	Filter	Mass (mg)	OC ($\mu g/cm^2$)	EC ($\mu g/cm^2$)	OC/M (%)	EC/M (%)
0.1	T53	0.33				
0.3	Q522	0.59	48.03	1.80	53.0	2.3
0.6	T73	0.50				
1.2	Q505	0.99	71.00	2.56	55.2	2.2
2.5	T151	0.98				
None	Q519	1.01	74.19	2.52	56.8	2.1

	Al/M (%)	Si/M (%)	P/M (%)	S/M (%)	Cl/M (%)	K/M (%)
0.1	0.00	0.00	0.00	0.00	0.03	0.21
0.6	0.02	0.00	0.02	0.05	0.05	0.19
2.5	0.02	0.00	0.01	0.04	0.04	0.18

	Ca/M (%)	Ti/M (%)	V/M (%)	Mn/M (%)	Fe/M (%)	Ni/M (%)
0.1	0.00	0.00	0.00	0.00	0.00	0.00
0.6	0.01	0.00	0.00	0.00	0.00	0.00
2.5	0.00	0.00	0.00	0.00	0.00	0.00

	Cu/M (%)	Zn/M (%)	Br/M (%)	Rb/M (%)	Pb/M (%)
0.1	0.00	0.00	0.00	0.00	0.00
0.6	0.00	0.00	0.00	0.00	0.00
2.5	0.00	0.00	0.00	0.00	0.00

Carbon Size Distribution (%)

(μm)	OC	EC	TC
<0.3	54.5	63.6	54.8
0.3-1.2	38.0	40.7	40.6
>1.2	4.7		4.5

Mass Distribution

(μm)	(%)
<0.1	
0.1-0.3	
0.3-0.6	
0.6-1.2	
1.2-2.5	
<2.5	

Trace Element Size Distributions

	S (%)	Cl (%)	K (%)	Ca (%)	AL (%)
<0.1	0.0	25.5	41.0	0.0	0.0
0.1-0.6	68.0	32.8	15.2	94.9	70.8
0.6-2.5	32.0	41.8	43.8	5.1	29.2

SOURCE DATA
Type: Earth Stove, fir, damper closed
Date: 4/13/84

Mass loading: 8590 $\mu g/m^3$
Adsorbed OC: 7.50 $\mu g/cm^2$
Sampling time - 20 minutes

Cut Pt. (μm)	Filter	Mass (mg)	OC ($\mu g/cm^2$)	EC ($\mu g/cm^2$)	OC/M (%)	EC/M (%)
0.1	T180	0.73				
0.3	Q428	0.73	54.07	3.03	48.3	3.2
0.6	T168	0.73				
1.2	Q480	1.41	93.78	3.08	52.0	1.9
2.5	T172	1.40				
None	Q499	1.68	110.34	4.17	53.3	2.2

	Al/M (%)	Si/M (%)	P/M (%)	S/M (%)	Cl/M (%)	K/M (%)
0.1	0.08	0.14	0.00	0.02	0.06	0.05
0.6	0.04	0.14	0.01	0.05	0.05	0.12
2.5	0.00	0.03	0.00	0.02	0.03	0.08

	Ca/M (%)	Ti/M (%)	V/M (%)	Mn/M (%)	Fe/M (%)	Ni/M (%)
0.1	0.00					
0.6	0.02					
2.5	0.00					

	Cu/M (%)	Zn/M (%)	Br/M (%)	Rb/M (%)	Pb/M (%)
0.1		0.00			
0.6		0.00			
2.5		0.00			

Carbon Size Distribution (%)

(μm)	OC	EC	TC
<0.3	40.3	64.7	41.2
0.3-1.2	43.6	9.2	42.2
>1.2	16.1	26.1	16.5

Mass Distribution

(μm)	(%)
<0.1	44.5
0.1-0.3	0.0
0.3-0.6	0.0
0.6-1.2	41.4
1.2-2.5	0.0
<2.5	14.0

Trace Element Size Distributions

(μm)	S (%)	Cl (%)	K (%)	Ca (%)	AL (%)	Ni (%)
<0.1			34.7			
0.1-0.6			42.0			
0.6-2.5			23.3			

SOURCE DATA

Type: Earthstove, oak planks, damper — Mass loading: 3548 $\mu g/m^3$
Date: 4/13/84 open — Adsorbed OC: 1.40 $\mu g/cm^2$
Note: high surface area, hot burn — Sampling time = 20 minutes

Cut Pt. (μm)	Filter	Mass (mg)	OC ($\mu g/cm^2$)	EC ($\mu g/cm^2$)	OC/M (%)	EC/M (%)
0.1	T178	0.17				
0.3	Q537	0.26	5.20	14.78	11.1	43.0
0.6	T162	0.39				
1.2	Q531	0.51	7.66	24.73	10.4	41.2
2.5	T169	0.44				
None	Q540	0.53	6.25	25.67	7.8	41.2

	Al/M (%)	Si/M (%)	P/M (%)	S/M (%)	Cl/M (%)	K/M (%)
0.1	0.00	0.07	0.00	1.43	1.79	3.70
0.6	0.91	0.79	0.14	4.50	6.33	13.02
2.5	0.99	0.80	0.15	4.22	6.26	13.27

	Ca/M (%)	Ti/M (%)	V/M (%)	Mn/M (%)	Fe/M (%)	Ni/M (%)
0.1	0.00					
0.6	0.02					
2.5	0.00					

	Cu/M (%)	Zn/M (%)	Br/M (%)	Rb/M (%)	Pb/M (%)
0.1		0.17			1.40
0.6		0.44			0.89
2.5		0.45			0.88

Carbon Size Distribution (%)

(μm)	OC	EC	TC
<0.3		51.2	54.2
0.3-1.2		45.1	47.4
>1.2		26.1	

Mass Distribution

(μm)	(%)
<0.1	
0.1-0.3	
0.3-0.6	
0.6-1.2	
1.2-2.5	
<2.5	

Trace Element Size Distributions

(μm)	S (%)	Cl (%)	K (%)	Zn (%)	AL (%)	Si (%)
<0.1	13.1	11.0	10.8	14.3	0.0	3.4
0.1-0.6	81.4	78.6	76.1	72.9	81.5	83.6
0.6-2.5	5.5	10.3	13.1	12.8	18.5	13.0

	Cu	Br	RB	Mn	Fe	Pb
<0.1						61.4
0.1-0.6						28.5
0.6-2.5						10.1

SOURCE DATA

Type: Earthstove, alder, damper
Date: 4/13/84 closed

Mass loading: 9236 $\mu g/m^3$
Adsorbed OC: 6.23 $\mu g/cm^2$
Sampling time = 20 minutes

Cut Pt. (μm)	Filter	Mass (mg)	OC ($\mu g/cm^2$)	EC ($\mu g/cm^2$)	OC/M (%)	EC/M (%)
0.1	T174	0.06				
0.3	Q539	0.11	12.05	1.69	40.0	11.6
0.6	T171	0.28				
1.2	Q528	0.84	78.78	8.87	73.4	9.0
2.5	T177	0.87				
None	Q383	0.98	88.46	9.96	71.3	8.7

	Al/M (%)	Si/M (%)	P/M (%)	S/M (%)	Cl/M (%)	K/M (%)
0.1	0.00	0.00	0.00	0.32	0.00	0.78
0.6	0.04	0.19	0.00	0.20	0.08	0.76
2.5	0.03	0.07	0.02	0.13	0.07	0.59

	Ca/M (%)	Ti/M (%)	V/M (%)	Mn/M (%)	Fe/M (%)	Ni/M (%)
0.1						
0.6						
2.5						

	Cu/M (%)	Zn/M (%)	Br/M (%)	Rb/M (%)	Pb/M (%)
0.1		0.47			
0.6		0.01			
2.5		0.00			

Carbon Size Distribution (%)

(μm)	OC	EC	TC
<0.3	6.3	15.1	7.5
0.3-1.2	81.9	73.8	81.5
>1.2	11.8	11.1	11.7

Mass Distribution

(μm)	(%)
<0.1	6.1
0.1-0.3	5.1
0.3-0.6	17.3
0.6-1.2	57.1
1.2-2.5	3.1
<2.5	11.2

Trace Element Size Distributions

(μm)	S (%)	Cl (%)	K (%)	Zn (%)	AL (%)	Si (%)
<0.1	17.6	0.0	9.1		0.0	0.0
0.1-0.6	32.9	37.0	32.3		44.5	81.7
0.6-2.5	49.6	63.0	58.5		55.5	18.2

	P	Br	RB	Mn	Fe	Pb
<0.1	0.0					
0.1-0.6	8.1					
0.6-2.5	91.9					

SOURCE DATA
Type: Earthstove, fir, damper open
Date: 4/18/84

Mass loading: 1285 $\mu g/m^3$
Adsorbed OC: 4.00 $\mu g/cm^2$
Sampling time = 20 minutes

Cut Pt. (μm)	Filter	Mass (mg)	OC ($\mu g/cm^2$)	EC ($\mu g/cm^2$)	OC/M (%)	EC/M (%)
0.1	T154	0.14				
0.3	Q523	0.15	4.38	10.29	1.9	51.9
0.6	T50	0.14				
1.2	Q476	0.24	7.09	14.04	10.9	49.7
2.5	T155	0.20				
None	Q542	0.32	9.79	17.42	15.4	46.3

	Al/M (%)	Si/M (%)	P/M (%)	S/M (%)	Cl/M (%)	K/M (%)
0.1	0.17	0.99	0.00	0.86	0.65	1.51
0.6	0.90	1.53	0.16	4.99	4.24	9.54
2.5	0.65	1.24	0.16	4.38	3.69	7.82

	Ca/M (%)	Ti/M (%)	V/M (%)	Mn/M (%)	Fe/M (%)	Ni/M (%)
0.1	0.00					
0.6	0.52					
2.5	0.52					

	Cu/M (%)	Zn/M (%)	Br/M (%)	Rb/M (%)	Pb/M (%)
0.1		0.04			
0.6		0.72			
2.5		0.51			

Carbon Size Distribution (%)

(μm)	OC	EC	TC
<0.3	5.8	52.6	40.9
0.3-1.2	47.5	28.0	32.9
>1.2	46.6	19.4	26.2

Mass Distribution

(μm)	(%)
<0.1	
0.1-0.3	
0.3-0.6	
0.6-1.2	
1.2-2.5	
<2.5	

Trace Element Size Distributions

(μm)	S (%)	Cl (%)	K (%)	Ca (%)	AL (%)	Ni (%)
<0.1	13.8	12.3	13.5	0.0	17.9	
0.1-0.6	65.9	68.1	71.9	69.7	78.9	
0.6-2.5	20.3	19.6	14.6	30.3	3.2	

SOURCE DATA
Type: Earthstove, oak/alder, damper
Date: 4/19/84 open

Mass loading: 1446 $\mu g/m^3$
Adsorbed OC: 1.30 $\mu g/cm^2$
Sampling time = 20 minutes

Cut Pt. (μm)	Filter	Mass (mg)	OC ($\mu g/cm^2$)	EC ($\mu g/cm^2$)	OC/M (%)	EC/M (%)
0.1	T170	0.06				
0.3	Q527	0.06	1.46	0.60	2.0	7.6
0.6	T167	0.18				
1.2	Q367	0.24	2.19	1.47	3.1	5.2
2.5	T176	0.24				
None	Q432	0.24	2.30	1.66	7.8	5.9

	Al/M (%)	Si/M (%)	P/M (%)	S/M (%)	Cl/M (%)	K/M (%)
0.1	0.00	0.93	0.00	1.33	0.56	4.87
0.6	1.32	1.22	0.16	7.36	2.99	25.27
2.5	1.40	1.11	0.10	7.38	2.78	24.66

	Ca/M (%)	Ti/M (%)	V/M (%)	Mn/M (%)	Fe/M (%)	Ni/M (%)
0.1	0.00					
0.6	0.50					
2.5	0.52					

	Cu/M (%)	Zn/M (%)	Br/M (%)	Rb/M (%)	Pb/M (%)
0.1		0.09			0.00
0.6		0.59			0.13
2.5		0.56			0.18

Carbon Size Distribution (%)

(μm)	OC	EC	TC
<0.3	14.2	32.2	25.4
0.3-1.2	74.8	56.39	63.3
>1.2	11.0	11.4	11.3

Mass Distribution

(μm)	(%)
<0.1	25.0
0.1-0.3	0.0
0.3-0.6	50.0
0.6-1.2	25.0
1.2-2.5	0.0
<2.5	0.0

Trace Element Size Distributions

(μm)	S (%)	Cl (%)	K (%)	Zn (%)	AL (%)	Si (%)
<0.1	4.5	5.0	4.9	3.8	0.0	21.0
0.1-0.6	70.3	75.4	71.9	74.7	70.6	61.0
0.6-2.5	25.1	19.5	23.1	21.5	29.3	17.9

	Cu	Br	RB	Mn	Fe	Pb
<0.1						0.0
0.1-0.6						71.9
0.6-2.5						28.1

SOURCE DATA

Type: Earthstove, alder, damper — Mass loading: 2209 $\mu g/m^3$

Date: 4/19/84 open — Adsorbed OC: 3.40 $\mu g/cm^2$

Sampling time = 20 minutes

Cut Pt. (μm)	Filter	Mass (mg)	OC ($\mu g/cm^2$)	EC ($\mu g/cm^2$)	OC/M (%)	EC/M (%)
0.1	T166	0.11				
0.3	Q535	0.11	5.89	0.85	17.1	5.8
0.6	T175	0.19				
1.2	Q506	0.30	9.89	3.78	18.1	10.7
2.5	T179	0.28				
None	Q389	0.33	10.07	3.76	17.2	9.7

	Al/M (%)	Si/M (%)	P/M (%)	S/M (%)	Cl/M (%)	K/M (%)
0.1	0.22	0.14	0.07	1.11	0.32	3.41
0.6	1.32	1.05	0.09	6.33	2.02	22.67
2.5	1.08	0.86	0.09	5.51	1.82	20.19

	Ca/M (%)	Ti/M (%)	V/M (%)	Mn/M (%)	Fe/M (%)	Ni/M (%)
0.1	0.00					
0.6	0.00					
2.5	0.02					

	Cu/M (%)	Zn/M (%)	Br/M (%)	Rb/M (%)	Pb/M (%)
0.1		0.17			
0.6		0.37			
2.5		0.24			

Carbon Size Distribution (%)

(μm)	OC	EC	TC
<0.3	33.2	20.1	28.5
0.3-1.2	62.7	80.4	69.1
>1.2	4.5		2.4

Mass Distribution

(μm)	(%)
<0.1	
0.1-0.3	
0.3-0.6	
0.6-1.2	
1.2-2.5	
<2.5	

Trace Element Size Distributions

(μm)	S (%)	Cl (%)	K (%)	Zn (%)	AL (%)	Si (%)
<0.1	7.9	7.0	6.6	27.4	8.0	6.3
0.1-0.6	69.9	68.3	69.6	76.9	74.8	76.7
0.6-2.5	22.1	24.7	23.8		17.2	17.0

(μm)	P	Br	RB	Mn	Fe	Pb
<0.1	29.3					
0.1-0.6	35.9					
0.6-2.5	34.2					

SOURCE DATA
Type: Earthstove, alder, damper Mass loading: 4698 $\mu g/m^3$
Date: 5/2/84 open Adsorbed OC: 6.90 $\mu g/cm^2$
Sampling time = 20 minutes

Cut Pt. (μm)	Filter	Mass (mg)	OC ($\mu g/cm^2$)	EC ($\mu g/cm^2$)	OC/M (%)	EC/M (%)
0.1						
0.3	Q614	0.41	26.10	6.53	35.4	12.1
0.6	T173	0.68				
1.2	Q623	0.69	46.78	12.45	49.1	15.3
2.5	T202	0.68				
None	Q633	0.78	45.63	12.32	42.2	13.4

	Al/M (%)	Si/M (%)	P/M (%)	S/M (%)	Cl/M (%)	K/M (%)
0.1						
0.6						
2.5	0.03	0.39	0.07	0.76	1.00	3.18

	Ca/M (%)	Ti/M (%)	V/M (%)	Mn/M (%)	Fe/M (%)	Ni/M (%)
0.1						
0.6						
2.5	0.02	0.00	0.00	0.00	0.00	0.00

	Cu/M (%)	Zn/M (%)	Br/M (%)	Rb/M (%)	Pb/M (%)
0.1					
0.6					
2.5	0.00	0.04	0.00	0.02	0.00

Carbon Size Distribution (%)

(μm)	OC	EC	TC
<0.3	44.1	47.1	44.9
0.3-1.2	58.8	53.8	57.6
>1.2			

Mass Distribution

(μm)	(%)
<0.1	0.0
0.1-0.3	52.6
0.3-0.6	34.6
0.6-1.2	1.3
1.2-2.5	
<2.5	12.8

Trace Element Size Distributions

(μm)	S (%)	Cl (%)	K (%)	Zn (%)	AL (%)	Si (%)
<0.1						
0.1-0.6						
0.6-2.5						

SOURCE DATA
Type: Earthstove, alder, damper
Date: 5/2/84 closed

Mass loading: 3433 $\mu g/m^3$
Adsorbed OC: 7.30 $\mu g/cm^2$
Sampling time = 20 minutes

Cut Pt. (μm)	Filter	Mass (mg)	OC ($\mu g/cm^2$)	EC ($\mu g/cm^2$)	OC/M (%)	EC/M (%)
0.1	T194	0.22				
0.3	Q630	0.29	24.34	3.20	44.4	8.3
0.6	T205	0.26				
1.2	Q613	0.50	37.78	4.15	51.8	7.0
2.5	T201	0.53				
None	Q624	0.57	41.71	3.75	51.3	5.6

	Al/M (%)	Si/M (%)	P/M (%)	S/M (%)	Cl/M (%)	K/M (%)
0.1						
0.6						
2.5						

	Ca/M (%)	Ti/M (%)	V/M (%)	Mn/M (%)	Fe/M (%)	Ni/M (%)
0.1						
0.6						
2.5						

	Cu/M (%)	Zn/M (%)	Br/M (%)	Rb/M (%)	Pb/M (%)
0.1					
0.6					
2.5					

Carbon Size Distribution (%)

(μm)	OC	EC	TC
<0.3	44.1		47.2
0.3-1.2	44.5		43.5
>1.2	11.4		9.2

Mass Distribution

(μm)	(%)
<0.1	38.6
0.1-0.3	12.3
0.3-0.6	
0.6-1.2	42.11
1.2-2.5	5.3
<2.5	7.2

Trace Element Size Distributions

(μm)	S (%)	Cl (%)	K (%)	Zn (%)	AL (%)	Si (%)
<0.1						
0.1-0.6						
0.6-2.5						

SOURCE DATA
Type: Earthstove, fir/alder, damper
Date: 5/4/84
open

Mass loading: 1144 $\mu g/m^3$
Adsorbed OC: 3.38 $\mu g/cm^2$
Sampling time = 20 minutes

Cut Pt. (μm)	Filter	Mass (mg)	OC ($\mu g/cm^2$)	EC ($\mu g/cm^2$)	OC/M (%)	EC/M (%)
0.1	Q603	0.02	1.48	0.12		14.3
0.3	Q632	0.12	5.02	1.74	10.3	11.0
0.6	Q635	0.18	5.27	2.73	8.9	12.9
1.2	Q619	0.18	5.28	3.14	9.0	14.8
2.5	Q616	0.18	5.21	3.14	8.6	14.8
None	Q636	0.19	5.78	2.94	10.7	13.1

Carbon Size Distribution (%) (μm)	OC	EC	TC
<0.1	0	11	6
0.1-0.3	61	41	50
0.3-0.6	16	40	30
0.6-1.2	0	14	8
1.2-2.5	0	0	
>2.5	23		7

Mass Distribution (μm)	(%)
<0.1	11
0.1-0.3	53
0.3-0.6	31
0.6-1.2	0
1.2-2.5	0
<2.5	5

SOURCE DATA
Type: Earthstove, fir/alder, damper closed
Date: 5/4/84

Mass loading: 4337 $\mu g/m^3$
Adsorbed OC: 5.30 $\mu g/cm^2$
Sampling time = 20 minutes

Cut Pt. (μm)	Filter	Mass (mg)	OC ($\mu g/cm^2$)	EC ($\mu g/cm^2$)	OC/M (%)	EC/M (%)
0.1	Q653	0.22	7.68	1.98	48.5	21.3
0.3	Q627	0.42	30.80	3.76	45.9	6.8
0.6	Q664	0.49	40.23	3.37	60.6	5.8
1.2	Q657	0.67	51.82	4.31	59.0	5.8
2.5	Q659	0.67	53.62	4.28	61.3	5.4
None	Q604	0.72	54.07	5.80	57.6	6.8

Carbon Size Distribution (%) (μm)	OC	EC	TC	Mass Distribution (μm)	(%)
<0.1	25.7		33.1	<0.1	31
0.1-0.3	20.8		14.6	0.1-0.3	28
0.3-0.6	25.1		22.6	0.3-0.6	10
0.6-1.2	23.7		22.9	0.6-1.2	25
1.2-2.5	3.7		3.2	1.2-2.5	0
>2.5	0.9		3.6	<2.5	7

SOURCE DATA
Type: Earthstove, oaks/fir, damper
Date: 5/4/84 open

Mass loading: 1095 $\mu g/m^3$
Adsorbed OC: 4.48 $\mu g/cm^2$
Sampling time - 20 minutes

Cut Pt. (μm)	Filter	Mass (mg)	OC ($\mu g/cm^2$)	EC ($\mu g/cm^2$)	OC/M (%)	EC/M (%)
0.1	T190	0.03				
0.3	Q662	0.10	5.63	1.48	8.7	11.2
0.6	T187	0.17				
1.2	Q663	0.18	6.24	3.52	8.3	16.6
2.5	T196	0.20				
None	Q661	0.19	6.75	3.58	10.2	16.0

	Al/M (%)	Si/M (%)	P/M (%)	S/M (%)	Cl/M (%)	K/M (%)
0.1						
0.6						
2.5	0.02	0.84	0.35	5.97	2.72	23.41

	Ca/M (%)	Ti/M (%)	V/M (%)	Mn/M (%)	Fe/M (%)	Ni/M (%)
0.1						
0.6						
2.5	0.21	0.00	0.00	0.01	0.00	0.00

	Cu/M (%)	Zn/M (%)	Br/M (%)	Rb/M (%)	Pb/M (%)
0.1					
0.6					
2.5	0.02	0.23	0.00	0.08	0.07

Carbon Size Distribution (%)

(μm)	OC	EC	TC
<0.3	45.1	36.8	40.0
0.3-1.2	32.4	61.5	50.2
>1.2	22.8	1.7	9.7

Mass Distribution

(μm)	(%)
<0.1	16
0.1-0.3	37
0.3-0.6	37
0.6-1.2	5
1.2-2.5	11
<2.5	-5

Trace Element Size Distributions

(μm)	S (%)	Cl (%)	K (%)	Zn (%)	AL (%)	Si (%)
<0.1						
0.1-0.6						
0.6-2.5						

SOURCE DATA
Type: Earthstove, oaks/fir, damper closed
Date: 5/4/84
Mass loading: 5180 $\mu g/m^3$
Adsorbed OC: 8.34 $\mu g/cm^2$
Sampling time = 20 minutes

Cut Pt. (μm)	Filter	Mass (mg)	OC ($\mu g/cm^2$)	EC ($\mu g/cm^2$)	OC/M (%)	EC/M (%)
0.1	T206	0.33				
0.3	Q660	0.61	46.46	3.81	47.3	4.7
0.6	T189	0.67				
1.2	Q626	1.13	84.54	5.72	57.3	4.3
2.5	T211	1.21				
None	Q656	1.29	93.95	4.27	56.4	2.8

	Al/M (%)	Si/M (%)	P/M (%)	S/M (%)	Cl/M (%)	K/M (%)
0.1						
0.6						
2.5						

	Ca/M (%)	Ti/M (%)	V/M (%)	Mn/M (%)	Fe/M (%)	Ni/M (%)
0.1						
0.6						
2.5						

	Cu/M (%)	Zn/M (%)	Br/M (%)	Rb/M (%)	Pb/M (%)
0.1					
0.6					
2.5					

Carbon Size Distribution (%)

(μm)	OC	EC	TC
<0.3	39.6		41.5
0.3-1.2	49.4		49.6
>1.2	11.0		8.97

Mass Distribution

(μm)	(%)
<0.1	26
0.1-0.3	22
0.3-0.6	5
0.6-1.2	36
1.2-2.5	6
<2.5	6

Trace Element Size Distributions

(μm)	S (%)	Cl (%)	K (%)	Zn (%)	AL (%)	Si (%)
<0.1						
0.1-0.6						
0.6-2.5						

SOURCE DATA
Type: Earthstove, alder/fir, damper open
Date: 5/14/84
Mass loading: 2078 $\mu g/m^3$
Adsorbed OC: 4.0 $\mu g/cm^2$
Sampling time = 20 minutes

Cut Pt. (μm)	Filter	Mass (mg)	OC ($\mu g/cm^2$)	EC ($\mu g/cm^2$)	OC/M (%)	EC/M (%)
0.1	T191	0.08				
0.3	Q687	0.12	4.14	1.33	0.9	8.3
0.6	T214	0.39				
1.2	Q688	0.52	10.22	4.45	10.2	7.3
2.5	T210	0.52				
None	Q696	0.53	12.78	6.03	14.1	9.7

	Al/M (%)	Si/M (%)	P/M (%)	S/M (%)	Cl/M (%)	K/M (%)
0.1						
0.6						
2.5						

	Ca/M (%)	Ti/M (%)	V/M (%)	Mn/M (%)	Fe/M (%)	Ni/M (%)
0.1						
0.6						
2.5						

	Cu/M (%)	Zn/M (%)	Br/M (%)	Rb/M (%)	Pb/M (%)
0.1					
0.6					
2.5					

Carbon Size Distribution (%)

(μm)	OC	EC	TC
<0.3	1.4	19.6	8.8
0.3-1.2	69.4	54.2	63.2
>1.2	29.2	26.2	27.9

Mass Distribution

(μm)	(%)
<0.1	15
0.1-0.3	8
0.3-0.6	51
0.6-1.2	25
1.2-2.5	0
<2.5	2

Trace Element Size Distributions

(μm)	S (%)	Cl (%)	K (%)	Ca (%)	Fe (%)	Ni (%)
<0.1						
0.1-0.6						
0.6-2.5						

SOURCE DATA
Type: Earthstove, fir, damper closed
Date: 12/6/84

Mass loading: 4216 $\mu g/m^3$
Adsorbed OC: 5.22 $\mu g/cm^2$
Sampling time = 20 minutes

Cut Pt. (μm)	Filter	Mass (mg)	OC ($\mu g/cm^2$)	EC ($\mu g/cm^2$)	OC/M (%)	EC/M (%)
0.3A	T287	0.37				
0.3B	Q833	0.38	30.66	2.76	50.7	5.5
0.6A	T286					
0.6B	Q885	0.48	32.79	3.15	48.9	5.6
2.5A	T285					
2.5B	Q879	0.70	49.45	4.17	53.7	5.1

	Al/M (%)	Si/M (%)	P/M (%)	S/M (%)	Cl/M (%)	K/M (%)
0.3A						
0.6A						
2.5A						

	Ca/M (%)	Ti/M (%)	V/M (%)	Mn/M (%)	Fe/M (%)	Ni/M (%)
0.3A						
0.6A						
2.5A						

	Cu/M (%)	Zn/M (%)	Br/M (%)	Rb/M (%)	Pb/M (%)
0.3A					
0.6A					
2.5A					

Carbon Size Distribution (%) (μm)	OC	EC	TC	Mass Distribution (%) T mass	Q mass
<0.3	51.2	58.9	51.9		54
0.3-0.6	11.1	16.6	11.6		14
0.6-2.5	37.6	24.5	36.5		31

Trace Element Size Distributions

(μm)	S (%)	Cl (%)	K (%)	Ca (%)	Fe (%)	Ni (%)
<0.3						
0.3-0.6						
0.6-2.5						

SOURCE DATA
Type: Earthstove, fir, damper open
Date: 12/6/84

Mass loading: 586 $\mu g/m^3$
Adsorbed OC: 3.98 $\mu g/cm^2$
Sampling time = 20 minutes

Cut Pt. (μm)	Filter	Mass (mg)	OC ($\mu g/cm^2$)	EC ($\mu g/cm^2$)	OC/M (%)	EC/M (%)
0.3A	T295	0.09				
0.3B	Q427	0.12	7.90	2.32	24.7	14.6
0.6A	T294	0.17				
0.6B	Q880	0.16	8.48	2.58	23.9	13.7
2.5A	T207					
2.5B						

	Al/M (%)	Si/M (%)	P/M (%)	S/M (%)	Cl/M (%)	K/M (%)
0.3A						
0.6A	0.13	0.00	0.05	0.75	1.08	3.02
2.5A						

	Ca/M (%)	Ti/M (%)	V/M (%)	Mn/M (%)	Fe/M (%)	Ni/M (%)
0.3A						
0.6A	0.32	0.02	0.01	0.02	0.03	0.01
2.5A						

	Cu/M (%)	Zn/M (%)	Br/M (%)	Rb/M (%)	Pb/M (%)
0.3A					
0.6A	0.02	0.11	0.00	0.01	0.05
2.5A					

Carbon Size Distribution (%)				Mass Distribution (%)	
(μm)	OC	EC	TC	T mass	Q mass
<0.3					
0.3-0.6					
0.6-2.5					

Trace Element Size Distributions

	S	Cl	K	Ca	Fe	Ni
(μm)	(%)	(%)	(%)	(%)	(%)	(%)
<0.3						
0.3-0.6						
0.6-2.5						

SOURCE DATA
Type: Earthstove, fir, damper closed
Date: 12/6/84

Mass loading: 17951 $\mu g/m^3$
Adsorbed OC: 6.4 $\mu g/cm^2$
Sampling time = 20 minutes

Cut Pt. (μm)	Filter	Mass (mg)	OC ($\mu g/cm^2$)	EC ($\mu g/cm^2$)	OC/M (%)	EC/M (%)
0.3A	T260	1.55				
0.3B	Q232	1.61	128.47	4.52	57.4	2.1
0.6A	T267	1.57				
0.6B	Q760	1.57	105.79	5.86	53.8	3.2
2.5A	T269	2.98				
2.5B	Q435	2.90	191.06	9.23	54.1	2.7

	Al/M (%)	Si/M (%)	P/M (%)	S/M (%)	Cl/M (%)	K/M (%)
0.3A	0.02	0.01	0.02	0.03	0.01	0.02
0.6A	0.03	0.06	0.02	0.03	0.00	0.03
2.5A	0.03	0.02	0.02	0.06	0.01	0.02

	Ca/M (%)	Ti/M (%)	V/M (%)	Mn/M (%)	Fe/M (%)	Ni/M (%)
0.3A	0.01	0.00	0.00	0.00	0.00	0.00
0.6A	0.02	0.00	0.00	0.00	0.01	0.00
2.5A	0.01	0.00	0.00	0.00	0.00	0.00

	Cu/M (%)	Zn/M (%)	Br/M (%)	Rb/M (%)	Pb/M (%)
0.3A	0.00	0.00	0.00	0.00	0.00
0.6A	0.00	0.00	0.00	0.00	0.00
2.5A	0.00	0.00	0.00	0.00	0.00

Carbon Size Distribution (%)				Mass Distribution (%)	
(μm)	OC	EC	TC	T mass	Q mass
<0.3	58.8	43.6	58.1	52	55
0.3-0.6	-5.0	19.9	-3.8	1	-1
0.6-2.5	46.2	36.5	45.7	47	46

Trace Element Size Distributions

	S (%)	Cl (%)	K (%)	P (%)	Al (%)	Zn (%)
(μm)						
<0.3	23		46	53	37	24
0.3-0.6	7		12	3	6	17
0.6-2.5	69		41	44	57	59

	Cu	Br	RB	Mn	Fe	Pb
<0.3						0
0.3-0.6						21
0.6-2.5						78

SOURCE DATA
Type: Earthstove, fir, damper open
Date: 12/6/84

Mass loading: 1058 $\mu g/m^3$
Adsorbed OC: 4.77 $\mu g/cm^2$
Sampling time - 20 minutes

Cut Pt. (μm)	Filter	Mass (mg)	OC ($\mu g/cm^2$)	EC ($\mu g/cm^2$)	OC/M (%)	EC/M (%)
0.3A	T266	0.14				
0.3B	Q206	0.20	8.30	10.72	13.3	40.6
0.6A	T280	0.26				
0.6B	Q822	0.28	9.68	14.01	14.9	42.5
2.5A	T281	0.28				
2.5B	Q877	0.28	9.75	14.82	15.1	45.0

	Al/M (%)	Si/M (%)	P/M (%)	S/M (%)	Cl/M (%)	K/M (%)
0.3A	0.45	0.34	0.17	0.98	2.68	5.53
0.6A	0.31	0.28	0.15	0.69	2.47	4.78
2.5A	0.26	0.27	0.16	0.95	2.55	4.84

	Ca/M (%)	Ti/M (%)	V/M (%)	Mn/M (%)	Fe/M (%)	Ni/M (%)
0.3A	0.17	0.00	0.00	0.00	0.07	0.00
0.6A	0.17	0.01	0.00	0.00	0.03	0.00
2.5A	0.25	0.00	0.00	0.01	0.01	0.00

	Cu/M (%)	Zn/M (%)	Br/M (%)	Rb/M (%)	Pb/M (%)
0.3A	0.01	0.15	0.02	0.00	0.13
0.6A	0.01	0.13	0.00	0.01	0.00
2.5A	0.00	0.00	0.00	0.00	0.14

Carbon Size Distribution (%)				Mass Distribution (%)	
(μm)	OC	EC	TC	T mass	Q mass
<0.3	63.1	64.4	64.0	50	71
0.3-0.6	35.5	30.2	31.5	43	28
0.6-2.5	1.4	5.5	4.4	7	0

Trace Element Size Distributions

	S	Cl	K	P	Cl	Zn
(μm)	(%)	(%)	(%)	(%)	(%)	(%)
<0.3	52	52	57	52	53	
0.3-0.6	15	38	35	35	38	
0.6-2.5	33	10	8	13	10	

	Cu	Br	RB	Mn	Fe	Pb
<0.3						48
0.3-0.6						13
0.6-2.5						39

SOURCE DATA
Type: Earthstove, oak, damper closed
Date: 12/6/84

Mass loading: 9414 $\mu g/m^3$
Adsorbed OC: 6.86 $\mu g/cm^2$
Sampling time = 20 minutes

Cut Pt. (μm)	Filter	Mass (mg)	OC ($\mu g/cm^2$)	EC ($\mu g/cm^2$)	OC/M (%)	EC/M (%)
0.3A	T284	0.93				
0.3B	Q625	0.93	80.82	4.27	60.2	3.5
0.6A	T298	1.11				
0.6B	Q834	1.05	77.33	6.57	57.0	5.3
2.5A	T297	1.72				
2.5B	Q212	1.72	120.06	9.49	55.9	4.7

	Al/M (%)	Si/M (%)	P/M (%)	S/M (%)	Cl/M (%)	K/M (%)
0.3A	0.03	0.05	0.02	0.04	0.02	0.10
0.6A	0.04	0.00	0.01	0.02	0.02	0.09
2.5A						

	Ca/M (%)	Ti/M (%)	V/M (%)	Mn/M (%)	Fe/M (%)	Ni/M (%)
0.3A	0.02	0.00	0.00	0.00	0.02	0.00
0.6A	0.01	0.00	0.00	0.00	0.01	0.00
2.5A						

	Cu/M (%)	Zn/M (%)	Br/M (%)	Rb/M (%)	Pb/M (%)
0.3A	0.00	0.00	0.00	0.00	0.01
0.6A	0.00	0.00	0.00	0.00	0.00
2.5A					

Carbon Size Distribution (%)				Mass Distribution (%)	
(μm)	OC	EC	TC	T mass	Q mass
<0.3	58.1	40.0	56.7	54	54
0.3-0.6	4.1	29.2	6.0	10	7
0.6-2.5	37.8	30.8	37.2	35	40

Trace Element Size Distributions

	S	Cl	K	P	Cl	Zn
(μm)	(%)	(%)	(%)	(%)	(%)	(%)
<0.3						
0.3-0.6						
0.6-2.5						

SOURCE DATA
Type: Earthstove, oak, damper open
Date: 12/6/84

Mass loading: 2982 $\mu g/m^3$
Adsorbed OC: 8.03 $\mu g/cm^2$
Sampling time = 20 minutes

Cut Pt. (μm)	Filter	Mass (mg)	OC ($\mu g/cm^2$)	EC ($\mu g/cm^2$)	OC/M (%)	EC/M (%)
0.3A	T293	0.49				
0.3B	Q876A	0.49	39.88	7.96	49.2	12.3
0.6A	T289	0.91				
0.6B	Q881	0.89	56.41	12.90	46.2	12.3
2.5A	T288	0.95				
2.5B	Q875	0.96	58.45	13.43	43.2	11.5

	Al/M (%)	Si/M (%)	P/M (%)	S/M (%)	Cl/M (%)	K/M (%)
0.3A	0.20	0.22	0.07	1.06	0.53	3.62
0.6A	0.13	0.17	0.08	1.10	0.52	3.37
2.5A	0.17	0.16	0.09	1.16	0.55	3.63

	Ca/M (%)	Ti/M (%)	V/M (%)	Mn/M (%)	Fe/M (%)	Ni/M (%)
0.3A	0.10	0.00	0.00	0.01	0.02	0.00
0.6A	0.02	0.00	0.00	0.00	0.01	0.00
2.5A	0.10	0.00	0.00	0.00	0.01	0.00

	Cu/M (%)	Zn/M (%)	Br/M (%)	Rb/M (%)	Pb/M (%)
0.3A	0.00	0.04	0.00	0.01	0.01
0.6A	0.00	0.02	0.00	0.01	0.01
2.5A	0.00	0.02	0.00	0.01	0.02

Carbon Size Distribution (%)				Mass Distribution (%)	
(μm)	OC	EC	TC	T mass	Q mass
<0.3	56.3	52.7	55.5	52	50
0.3-0.6	39.8	43.3	40.5	44	40
0.6-2.5	3.9	3.9	3.9	4	10

Trace Element Size Distributions

	S	Cl	K	P	Cl	Al
(μm)	(%)	(%)	(%)	(%)	(%)	(%)
<0.3	47	51	47	38	51	58
0.3-0.6	44	41	42	43	48	15
0.6-2.5	9	8	11	19	8	27

	Cu	Br	RB	Mn	Fe	Pb
(μm)	(%)	(%)	(%)	(%)	(%)	(%)
<0.3			50			37
0.3-0.6			22			38
0.6-2.5			28			25

SOURCE DATA
Type: Earthstove, fir, damper open
Date: 1/23/85

Mass loading: 1588 $\mu g/m^3$
Adsorbed OC: 2.42 $\mu g/cm^2$
Sampling time = 20 minutes

Cut Pt. (μm)	Filter	Mass (mg)	OC ($\mu g/cm^2$)	EC ($\mu g/cm^2$)	OC/M (%)	EC/M (%)
0.3A	T316	0.21				
0.3B	Q919	0.21	4.78	6.33	8.5	22.8
0.6A	T335	0.27				
0.6B	Q918	0.25	4.52	8.09	7.1	27.5
2.5A	T320	0.29				
2.5B	Q925	0.29	4.77	8.89	6.9	26.1

	Al/M (%)	Si/M (%)	P/M (%)	S/M (%)	Cl/M (%)	K/M (%)
0.3A	0.55	0.55	0.23	3.95	5.77	15.29
0.6A	0.81	0.83	0.35	5.24	8.10	19.78
2.5A	0.77	0.64	0.39	4.99	7.97	19.55

	Ca/M (%)	Ti/M (%)	V/M (%)	Mn/M (%)	Fe/M (%)	Ni/M (%)
0.3A	0.00	0.00	0.00	0.01	0.02	0.00
0.6A	0.00	0.00	0.00	0.02	0.03	0.00
2.5A	0.00	0.00	0.00	0.02	0.03	0.00

	Cu/M (%)	Zn/M (%)	Br/M (%)	Rb/M (%)	Pb/M (%)
0.3A	0.00	0.15	0.02	0.03	0.14
0.6A	0.01	0.19	0.03	0.03	0.22
2.5A	0.01	0.19	0.03	0.03	0.20

Carbon Size Distribution (%)

(μm)	OC	EC	TC
<0.3	89.4	63.4	68.8
0.3-0.6	0.0	27.6	21.8
0.6-2.5	10.6	9.0	9.3

Mass Distribution (%)

T mass	Q mass
72	72
21	14
7	14

Trace Element Size Distributions

(μm)	S (%)	Cl (%)	K (%)	P (%)	Cl (%)	Fe (%)
<0.3	57	52	56	42	52	42
0.3-0.6	41	42	38	40	42	49
0.6-2.5	2	5	6	18	5	8

(μm)	Zn (%)	Al (%)	RB (%)	Mn (%)	Br (%)	Pb (%)
<0.3	61	52	53	35	51	53
0.3-0.6	36	45	18	31	36	48
0.6-2.5	3	3	28	34	13	0

SOURCE DATA
Type: Earthstove, oak, damper closed
Date: 1/23/85

Mass loading: 15120 $\mu g/m^3$
Adsorbed OC: 5.43 $\mu g/cm^2$
Sampling time = 20 minutes

Cut Pt. (μm)	Filter	Mass (mg)	OC ($\mu g/cm^2$)	EC ($\mu g/cm^2$)	OC/M (%)	EC/M (%)
0.3A	T319	0.92				
0.3B	Q242	1.17	94.64	5.15	57.7	3.3
0.6A	T313	1.27				
0.6B	Q898	1.27	87.86	4.79	55.2	3.2
2.5A	T318	2.26				
2.5B	Q895	2.51	143.41	5.62	46.7	1.9

	Al/M (%)	Si/M (%)	P/M (%)	S/M (%)	Cl/M (%)	K/M (%)
0.3A	0.01	0.02	0.02	0.01	0.01	0.19
0.6A	0.02	0.03	0.01	0.03	0.03	0.15
2.5A	0.02	0.02	0.02	0.02	0.01	0.15

	Ca/M (%)	Ti/M (%)	V/M (%)	Mn/M (%)	Fe/M (%)	Ni/M (%)
0.3A	0.01	0.00	0.00	0.00	0.00	0.00
0.6A	0.01	0.00	0.00	0.00	0.00	0.00
2.5A	0.00	0.00	0.00	0.00	0.00	0.00

	Cu/M (%)	Zn/M (%)	Br/M (%)	Rb/M (%)	Pb/M (%)
0.3A	0.00	0.00	0.00	0.00	0.00
0.6A	0.00	0.00	0.00	0.00	0.00
2.5A	0.00	0.00	0.00	0.00	0.00

Carbon Size Distribution (%)				Mass Distribution (%)	
(μm)	OC	EC	TC	T mass	Q mass
<0.3	36.4	46.0	44.6	46	46
0.3-0.6	38.0	40.7	40.3	33	36
0.6-2.5	25.6	13.2	15.1	21	18

Trace Element Size Distributions

	S	Cl	K	P	Al	Fe
(μm)	(%)	(%)	(%)	(%)	(%)	(%)
<0.3	34		51	47	13	
0.3-0.6	61		5	2	68	
0.6-2.5	5		44	51	18	

SOURCE DATA
Type: Earthstove, fir, damper open Mass loading: 888 $\mu g/m^3$
Date: 1/23/85 Adsorbed OC: 5.31 $\mu g/cm^2$
Charcoal burning (late in burn cycle) Sampling time = 20 minutes

Cut Pt. (μm)	Filter	Mass (mg)	OC ($\mu g/cm^2$)	EC ($\mu g/cm^2$)	OC/M (%)	EC/M (%)
0.3A	T312	0.14				
0.3B	Q916	0.14	8.34	2.11	16.3	11.4
0.6A	T322	0.28				
0.6B	Q914	0.28	8.16	4.86	8.6	14.7
2.5A	T339	0.28				
2.5B	Q905	0.28	7.77	12.68	7.5	14.9

	Al/M (%)	Si/M (%)	P/M (%)	S/M (%)	Cl/M (%)	K/M (%)
0.3A	0.95	0.66	0.28	3.50	2.03	24.56
0.6A	0.68	0.72	0.31	3.27	1.73	23.00
2.5A	0.72	0.57	0.34	3.65	1.77	25.77

	Ca/M (%)	Ti/M (%)	V/M (%)	Mn/M (%)	Fe/M (%)	Ni/M (%)
0.3A	0.00	0.00	0.00	0.04	0.00	0.00
0.6A	0.19	0.00	0.00	0.06	0.04	0.00
2.5A	0.29	0.01	0.00	0.09	0.07	0.00

	Cu/M (%)	Zn/M (%)	Br/M (%)	Rb/M (%)	Pb/M (%)
0.3A	0.01	0.25	0.00	0.04	0.23
0.6A	0.01	0.24	0.00	0.04	0.22
2.5A	0.01	0.26	0.00	0.05	0.27

Carbon Size Distribution (%)				Mass Distribution (%)	
(μm)	OC	EC	TC	T mass	Q mass
<0.3		38.2	62.1	50	50
0.3-0.6		60.7	42.5	50	50
0.6-2.5		1.0	-4.6	0	0

Trace Element Size Distributions

	S	Cl	K	P	Al	Fe
(μm)	(%)	(%)	(%)	(%)	(%)	(%)
<0.3	48	58	48	41	65	0
0.3-0.6	42	40	42	50	29	66
0.6-2.5	10	2	11	9	5	34

	Zn	Sr	RB	Mn	Ca	Pb
(μm)	(%)	(%)	(%)	(%)	(%)	(%)
<0.3	50	68	41	22	0	42
0.3-0.6	45	21	33	51	63	39
0.6-2.5	5	11	27	27	37	18

SOURCE DATA
Type: Earthstove, fir, damper closed
Date: 1/23/85

Mass loading: 8273 $\mu g/m^3$
Adsorbed OC: 5.06 $\mu g/cm^2$
Sampling time = 20 minutes

Cut Pt. (μm)	Filter	Mass (mg)	OC ($\mu g/cm^2$)	EC ($\mu g/cm^2$)	OC/M (%)	EC/M (%)
0.3A	T314	0.98				
0.3B	Q943	1.08	86.78	6.75	57.2	4.7
0.6A	T317	1.12				
0.6B	Q927	1.07	81.95	4.84	61.1	3.8
2.5A	T315	1.86				
2.5B	Q939	2.06	145.81	6.70	58.1	2.8

	Al/M (%)	Si/M (%)	P/M (%)	S/M (%)	Cl/M (%)	K/M (%)
0.3A	0.04	0.17	0.02	0.04	0.01	0.10
0.6A	0.13	0.03	0.02	0.02	0.02	0.07
2.5A	0.02	0.03	0.02	0.01	0.02	0.07

	Ca/M (%)	Ti/M (%)	V/M (%)	Mn/M (%)	Fe/M (%)	Ni/M (%)
0.3A	0.02	0.00	0.00	0.00	0.02	0.00
0.6A	0.01	0.00	0.00	0.00	0.01	0.00
2.5A	0.00	0.00	0.00	0.00	0.00	0.00

	Cu/M (%)	Zn/M (%)	Br/M (%)	Rb/M (%)	Pb/M (%)
0.3A	0.00	0.00	0.00	0.00	0.00
0.6A	0.00	0.00	0.00	0.00	0.00
2.5A	0.00	0.00	0.00	0.00	0.00

Carbon Size Distribution (%)				Mass Distribution (%)	
(μm)	OC	EC	TC	T mass	Q mass
<0.3	55.7	89.7	53.4	53	52
0.3-0.6	3.0	-17.4	2.0	8	0
0.6-2.5	27.8	27.8	44.6	40	48

Trace Element Size Distributions

	S	Cl	K	P	Al	Fe
(μm)	(%)	(%)	(%)	(%)	(%)	(%)
<0.3		34	71	60		
0.3-0.6		11	-7	-5		
0.6-2.5		54	36	45		

SOURCE DATA
Type: Earthstove, oak, damper open
Date: 1/23/85

Mass loading: 1987 $\mu g/m^3$
Adsorbed OC: 5.79 $\mu g/cm^2$
Sampling time = 20 minutes

Cut Pt. (μm)	Filter	Mass (mg)	OC ($\mu g/cm^2$)	EC ($\mu g/cm^2$)	OC/M (%)	EC/M (%)
0.3A	T338	0.30				
0.3B	Q902	0.30	8.48	18.55	6.7	46.0
0.6A	T336	0.52				
0.6B	Q935	0.54	10.68	31.11	7.7	49.0
2.5A	T340	0.66				
2.5B	Q889	0.66	12.36	35.85	8.5	46.2

	Al/M (%)	Si/M (%)	P/M (%)	S/M (%)	Cl/M (%)	K/M (%)
0.3A	0.43	0.32	0.15	2.75	1.46	8.39
0.6A	0.40	0.50	0.19	2.98	1.61	8.37
2.5A	0.39	0.38	0.19	3.10	1.96	9.25

	Ca/M (%)	Ti/M (%)	V/M (%)	Mn/M (%)	Fe/M (%)	Ni/M (%)
0.3A	0.00	0.01	0.00	0.00	0.01	0.00
0.6A	0.00	0.00	0.00	0.00	0.01	0.00
2.5A	0.00	0.00	0.00	0.01	0.01	0.00

	Cu/M (%)	Zn/M (%)	Br/M (%)	Rb/M (%)	Pb/M (%)
0.3A	0.01	0.07	0.00	0.02	0.07
0.6A	0.00	0.06	0.01	0.01	0.07
2.5A	0.00	0.07	0.01	0.02	0.09

Carbon Size Distribution (%)				Mass Distribution (%)	
(μm)	OC	EC	TC	T mass	Q mass
<0.3	36.4	46.0	44.6	46	46
0.3-0.6	38.0	40.7	40.3	33	36
0.6-2.5	25.6	13.2	15.1	21	18

Trace Element Size Distributions

	S	Cl	K	P	Al	Fe
(μm)	(%)	(%)	(%)	(%)	(%)	(%)
<0.3	41	34	42	38	50	56
0.3-0.6	35	30	29	38	29	33
0.6-2.5	24	35	29	23	20	10

	Zn	Sr	Rb	Br	Ca	Pb
(μm)	(%)	(%)	(%)	(%)	(%)	(%)
<0.3	46	30	39	2		38
0.3-0.6	29	25	5	54		21
0.6-2.5	25	45	56	44		40

SOURCE DATA
Type: Blazequeen stove, alder, damper open
Date: 6/8/84

Mass loading: 3493 $\mu g/m^3$
Adsorbed OC: 4.55 $\mu g/cm^2$
Sampling time = 20 minutes

Cut Pt. (μm)	Filter	Mass (mg)	OC ($\mu g/cm^2$)	EC ($\mu g/cm^2$)	OC/M (%)	EC/M (%)
0.1	T242	0.03				
0.3	Q731	0.28	9.02	2.75	12.1	7.4
0.6	T240	0.45				
1.2	Q706	0.48	12.33	8.80	13.8	15.6
2.5	T241	0.58				
None	Q757	0.58	13.60	10.12	13.3	14.8

	Al/M (%)	Si/M (%)	P/M (%)	S/M (%)	Cl/M (%)	K/M (%)
0.1	0.92			2.73		11.97
0.6	0.96	0.79	0.05	3.27	2.09	13.49
2.5	0.97	0.76	0.08	3.22	2.12	13.85

	Ca/M (%)	Ti/M (%)	V/M (%)	Mn/M (%)	Fe/M (%)	Ni/M (%)
0.1						
0.6	3.04					
2.5	3.06					

	Cu/M (%)	Zn/M (%)	Br/M (%)	Rb/M (%)	Pb/M (%)
0.1					
0.6		0.19			
2.5		0.14			

Carbon Size Distribution (%)

(μm)	OC	EC	TC
<0.3	44.0	24.2	33.5
0.3-1.2	42.0	62.8	53.0
>1.2	14.0	13.0	13.5

Mass Distribution

(μm)	(%)
<0.1	5
0.1-0.3	43
0.3-0.6	30
0.6-1.2	5
1.2-2.5	17
<2.5	0

Trace Element Size Distributions

(μm)	S (%)	Cl (%)	K (%)	Zn (%)	AL (%)	Si (%)
<0.1	4.3	0.0	4.4			
0.1-0.6	74.5	76.6	71.1			
0.6-2.5	21.2	23.4	24.4			

SOURCE DATA
Type: Blazequeen stove, alder, damper closed
Date: 6/8/84

Mass loading: 2108 $\mu g/m^3$
Adsorbed OC: 7.4 $\mu g/cm^2$
Sampling time = 20 minutes

Cut Pt. (μm)	Filter	Mass (mg)	OC ($\mu g/cm^2$)	EC ($\mu g/cm^2$)	OC/M (%)	EC/M (%)
0.1	T231	0.11				
0.3	Q761	0.16	18.18	1.96	51.0	9.3
0.6	T232	0.25				
1.2	Q750	0.30	25.56	2.92	51.4	8.3
2.5	T229	0.35				
None	Q762	0.35	29.32	3.88	53.2	9.4

	Al/M (%)	Si/M (%)	P/M (%)	S/M (%)	Cl/M (%)	K/M (%)
0.1						
0.6						
2.5	0.04	0.47	0.03	0.11	0.00	0.44

	Ca/M (%)	Ti/M (%)	V/M (%)	Mn/M (%)	Fe/M (%)	Ni/M (%)
0.1						
0.6						
2.5	0.01	0.00	0.00	0.00	0.00	0.00

	Cu/M (%)	Zn/M (%)	Br/M (%)	Rb/M (%)	Pb/M (%)
0.1					
0.6					
2.5	0.00	0.00	0.00	0.00	0.00

Carbon Size Distribution (%)

(μm)	OC	EC	TC
<0.3	43.8	45.0	44.0
0.3-1.2	39.1	30.3	37.8
>1.2	17.1	24.7	18.3

Mass Distribution

(μm)	(%)
<0.1	31
0.1-0.3	14
0.3-0.6	26
0.6-1.2	14
1.2-2.5	14
<2.5	0

Trace Element Size Distributions

(μm)	S (%)	Cl (%)	K (%)	Zn (%)	AL (%)	Si (%)
<0.1						
0.1-0.6						
0.6-2.5						

SOURCE DATA
Type: Fisher Stove, oak damper almost closed
Date: 4/28/84

Mass loading: 3554 $\mu g/m^3$
Adsorbed OC: 4.12 $\mu g/cm^2$
Sampling time = 20 minutes

Cut Pt. (μm)	Filter	Mass (mg)	OC ($\mu g/cm^2$)	EC ($\mu g/cm^2$)	OC/M (%)	EC/M (%)
0.1	T204	0.28				
0.3	Q571	0.35	26.94	2.06	49.3	4.4
0.6	T199	0.57				
1.2	Q596	0.57	37.98	2.76	50.5	4.1
2.5	T200	0.57				
None	Q586	0.59	41.76	3.45	54.2	5.0

	Al/M (%)	Si/M (%)	P/M (%)	S/M (%)	Cl/M (%)	K/M (%)
0.1						
0.6						
2.5						

	Ca/M (%)	Ti/M (%)	V/M (%)	Mn/M (%)	Fe/M (%)	Ni/M (%)
0.1						
0.6						
2.5						

	Cu/M (%)	Zn/M (%)	Br/M (%)	Rb/M (%)	Pb/M (%)
0.1					
0.6					
2.5					

Carbon Size Distribution (%)

(μm)	OC	EC	TC
<0.3	54.0	53.1	53.9
0.3-1.2	36.0	26.9	35.2
>1.2	10.0	20.0	10.9

Mass Distribution

(μm)	(%)
<0.1	47
0.1-0.3	12
0.3-0.6	37
0.6-1.2	0
1.2-2.5	0
<2.5	3

Trace Element Size Distributions

(μm)	S (%)	Cl (%)	K (%)	Ca (%)	Fe (%)	Ni (%)
<0.1						
0.1-0.6						
0.6-2.5						

SOURCE DATA
Type: Fisher Stove, oak damper almost closed
Date: 4/28/84

Mass loading: 1445 $\mu g/m^3$
Adsorbed OC: 3.86 $\mu g/cm^2$
Sampling time = 20 minutes

Cut Pt. (μm)	Filter	Mass (mg)	OC ($\mu g/cm^2$)	EC ($\mu g/cm^2$)	OC/M (%)	EC/M (%)
0.1	T157	0.16				
0.3	Q577	0.16	11.65	0.93	36.8	4.4
0.6	T163	0.21				
1.2	Q578	0.21	14.28	1.45	42.2	5.9
2.5	T203	0.24				
None	Q566	0.24	19.20	1.84	54.3	6.5

	Al/M (%)	Si/M (%)	P/M (%)	S/M (%)	Cl/M (%)	K/M (%)
0.1						
0.6						
2.5						

	Ca/M (%)	Ti/M (%)	V/M (%)	Mn/M (%)	Fe/M (%)	Ni/M (%)
0.1						
0.6						
2.5						

	Cu/M (%)	Zn/M (%)	Br/M (%)	Rb/M (%)	Pb/M (%)
0.1					
0.6					
2.5					

Carbon Size Distribution (%)

(μm)	OC	EC	TC
<0.3	45.2	45.0	45.2
0.3-1.2	22.7	33.8	23.9
>1.2	32.1	21.2	30.9

Mass Distribution

(μm)	(%)
<0.1	67
0.1-0.3	0
0.3-0.6	21
0.6-1.2	0
1.2-2.5	12
<2.5	0

Trace Element Size Distributions

(μm)	S (%)	Cl (%)	K (%)	Ca (%)	Fe (%)	Ni (%)
<0.1						
0.1-0.6						
0.6-2.5						

SOURCE DATA
Type: Fischer stove, oak, damper closed
Date: 6/13/84

Mass loading: 31084 $\mu g/m^3$
Adsorbed OC: 8.3 $\mu g/cm^2$
Sampling time = 20 minutes

Cut Pt. (μm)	Filter	Mass (mg)	OC ($\mu g/cm^2$)	EC ($\mu g/cm^2$)	OC/M (%)	EC/M (%)
0.1	T247	0.45				
0.3	Q771	0.39	27.80	2.65	37.8	5.1
0.6	T249	1.03				
1.2	Q767	3.02	215.36	11.04	58.3	3.1
2.5	T244	4.53				
None	Q787	5.16	344.73	14.27	55.4	2.3

	Al/M (%)	Si/M (%)	P/M (%)	S/M (%)	Cl/M (%)	K/M (%)
0.1						
0.6	0.03	0.22	0.02	0.15	0.03	0.44
2.5	0.01	0.05	0.02	0.07	0.01	0.22

	Ca/M (%)	Ti/M (%)	V/M (%)	Mn/M (%)	Fe/M (%)	Ni/M (%)
0.1						
0.6	0.00	0.00	0.00	0.00	0.00	0.00
2.5	0.00	0.00	0.00	0.00	0.00	0.00

	Cu/M (%)	Zn/M (%)	Br/M (%)	Rb/M (%)	Pb/M (%)
0.1					
0.6	0.00	0.00	0.00	0.00	0.01
2.5	0.00	0.00	0.00	0.00	0.00

Carbon Size Distribution (%)

(μm)	OC	EC	TC
<0.3	5.2	16.5	5.6
0.3-1.2	56.4	60.8	56.6
>1.2	38.5	22.6	37.8

Mass Distribution

(μm)	(%)
<0.1	9
0.1-0.3	0
0.3-0.6	12
0.6-1.2	38
1.2-2.5	29
<2.5	12

Trace Element Size Distributions

(μm)	S (%)	Cl (%)	K (%)	Zn (%)	AL (%)	Si (%)
<0.1						
0.1-0.6						
0.6-2.5						

SOURCE DATA

Type: Fireplace insert, alder, damper open
Date: 4/25/84
(damper open but cool burn)

Mass loading: 1807 $\mu g/m^3$
Adsorbed OC: 5 $\mu g/cm^2$
Sampling time = 20 minutes

Cut Pt. (μm)	Filter	Mass (mg)	OC ($\mu g/cm^2$)	EC ($\mu g/cm^2$)	OC/M (%)	EC/M (%)
0.1	Q582	0.17	5.93	0.38	40.9	5.3
0.3	Q570	0.17	12.10	1.92	31.6	8.5
0.6	Q575	0.23	16.61	2.21	42.9	8.2
1.2	Q561	0.29	17.37	2.44	36.3	7.1
2.5	Q576	0.29	16.38	2.46	33.4	7.2
None	Q585	0.29	18.93	2.40	40.8	7.0

Carbon Size Distribution (%) (μm)	OC	EC	TC
<0.1	58.7	44.2	56.6
0.1-0.3	-13.3	27.0	-7.4
0.3-0.6	38.0	20.9	35.5
0.6-1.2	5.5	9.5	6.1
1.2-2.5	-7.1	0.8	-5.9
>2.5	18.3	-2.5	15.25

Mass Distribution (μm)	(%)
<0.1	58
0.1-0.3	0
0.3-0.6	21
0.6-1.2	21
1.2-2.5	0
<2.5	0

SOURCE DATA
Type: Fireplace insert, alder
Date: 4/25/84
(damper open but burn was cool)

Mass loading: $\mu g/m^3$
Adsorbed OC: $\mu g/cm^2$
Sampling time = 20 minutes

Cut Pt. (μm)	Filter	Mass (mg)
0.1	T193	0.36
0.3	T192	0.36
0.6	T197	0.56
1.2	T185	0.51
2.5	T195	0.50
None	T181	0.73

	Al/M (%)	Si/M (%)	P/M (%)	S/M (%)	Cl/M (%)	K/M (%)
0.1	0.00	0.17	0.04	0.02	0.25	1.13
0.3	0.03	0.35	0.01	0.17	0.30	1.30
0.6	0.07	0.53	0.03	0.16	0.31	1.30
1.2	0.04	0.08	0.02	0.19	0.35	1.41
2.5	0.00	0.06	0.03	0.25	0.38	1.46
None	0.02	0.06	0.02	0.15	0.29	1.03

	Ca/M (%)	Ti/M (%)	V/M (%)	Mn/M (%)	Fe/M (%)	Ni/M (%)
0.1	0.04					
0.3	0.01					
0.6	0.02					
1.2	0.00					
2.5	0.00					
None	0.02					

	Cu/M (%)	Zn/M (%)	Br/M (%)	Rb/M (%)	Pb/M (%)
0.1					
0.3					
0.6					
1.2					
2.5					

SOURCE DATA
Type: Earthstove, fir, fireplace mode Mass loading: 2350 $\mu g/m^3$
Date: 3/22/88 Adsorbed OC: 7.5 $\mu g/cm^2$
(stove door removed) Sampling time = 20 minutes

Cut Pt. (μm)	Filter	Mass (mg)	OC ($\mu g/cm^2$)	EC ($\mu g/cm^2$)	OC/M (%)	EC/M (%)
0.1	T156	0.08				
0.3	Q373	0.23	16.65	3.25	30.1	10.7
0.6	T148	0.26				
1.2	Q382	0.29	17.81	6.08	30.2	17.8
2.5	T159	0.33				
None	Q413A	0.39	19.15	7.76	25.4	16.9

	Al/M (%)	Si/M (%)	P/M (%)	S/M (%)	Cl/M (%)	K/M (%)
0.1						
0.6						
2.5						

	Ca/M (%)	Ti/M (%)	V/M (%)	Mn/M (%)	Fe/M (%)	Ni/M (%)
0.1						
0.6						
2.5						

	Cu/M (%)	Zn/M (%)	Br/M (%)	Rb/M (%)	Pb/M (%)
0.1					
0.6					
2.5					

Carbon Size Distribution (%) (μm)	OC	EC	TC
<0.3	69.9	37.3	56.9
0.3-1.2	18.6	41.1	27.6
>1.2	11.5	21.6	15.6

Mass Distribution (μm)	(%)
<0.1	20
0.1-0.3	17
0.3-0.6	7
0.6-1.2	7
1.2-2.5	10
<2.5	15

SOURCE DATA
Type: Fireplace, alder
Date: 4/13/84

Mass loading: 8614 $\mu g/m^3$
Adsorbed OC: 5.40 $\mu g/cm^2$
Sampling time = 20 minutes

Cut Pt. (μm)	Filter	Mass (mg)	OC ($\mu g/cm^2$)	EC ($\mu g/cm^2$)	OC/M (%)	EC/M (%)
0.1	T149	0.22				
0.3	Q495	0.80	59.02	4.22	50.7	4.0
0.6	T127	1.23				
1.2	Q515	1.40	86.00	9.05	48.9	5.5
2.5	T106	1.40				
None	Q497	1.40	92.18	8.96	52.7	5.4

	Al/M (%)	Si/M (%)	P/M (%)	S/M (%)	Cl/M (%)	K/M (%)
0.1	0.10	0.16	0.06	0.31	0.00	0.40
0.6	0.04	0.07	0.04	0.17	0.92	0.45
2.5	0.05	0.06	0.04	0.14	0.90	0.38

	Ca/M (%)	Ti/M (%)	V/M (%)	Mn/M (%)	Fe/M (%)	Ni/M (%)
0.1	0.03	0.00	0.00	0.00	0.00	0.00
0.6	0.03	0.00	0.00	0.00	0.00	0.00
2.5	0.05	0.00	0.00	0.00	0.00	0.00

	Cu/M (%)	Zn/M (%)	Br/M (%)	Rb/M (%)	Pb/M (%)
0.1	0.00	0.03	0.00	0.00	0.00
0.6	0.00	0.04	0.01	0.00	0.08
2.5	0.00	0.04	0.01	0.00	0.06

Carbon Size Distribution (%)

(μm)	OC	EC	TC
<0.3	55.0	41.9	53.8
0.3-1.2	37.9	59.1	39.9
>1.2	7.1		6.4

Mass Distribution

(μm)	(%)
<0.1	15.7
0.1-0.3	41.4
0.3-0.6	30.7
0.6-1.2	12.1
1.2-2.5	0.0
<2.5	0.0

Trace Element Size Distributions

(μm)	S (%)	Cl (%)	K (%)	Ca (%)	AL (%)	P (%)
<0.1	33.9	0.0	16.8	10.8	29.7	24.6
0.1-0.6	69.4	89.3	87.1	39.1	30.8	66.3
0.6-2.5		10.6		50.0	39.6	9.1

(μm)	Ca (%)	Br (%)	RB (%)	Mn (%)	Fe (%)	Pb (%)
<0.1	10.8					
0.1-0.6	39.1					
0.6-2.5	50.0					

SOURCE DATA
Type: Fireplace, alder
Date: 4/13/84

Mass loading: 10506 $\mu g/m^3$
Adsorbed OC: 5.90 $\mu g/cm^2$
Sampling time = 20 minutes

Cut Pt. (μm)	Filter	Mass (mg)	OC ($\mu g/cm^2$)	EC ($\mu g/cm^2$)	OC/M (%)	EC/M (%)
0.1	Q491	0.36	9.58	1.71	39.8	11.3
0.3	T161	1.08				
0.6	T79	1.59				
1.2	Q496	2.09	137.96	10.89	53.7	4.4
2.5	T483	2.18	152.83	12.79	57.3	5.0
None	Q500	2.16	143.59	11.06	54.2	4.3

	Al/M (%)	Si/M (%)	P/M (%)	S/M (%)	Cl/M (%)	K/M (%)
0.3	0.00	0.02	0.01	0.09	0.26	0.50
0.6	0.02	0.03	0.01	0.13	0.40	0.64
2.5						

	Ca/M (%)	Ti/M (%)	V/M (%)	Mn/M (%)	Fe/M (%)	Ni/M (%)
0.3	0.00					
0.6	0.00					
2.5						

	Cu/M (%)	Zn/M (%)	Br/M (%)	Rb/M (%)	Pb/M (%)
0.3		0.01			
0.6		0.02			
2.5					

Carbon Size Distribution (%)				Mass Distribution	
(μm)	OC	EC	TC	(μm)	(%)
<0.3				<0.1	17
0.3-1.2				0.1-0.3	33
>1.2				0.3-0.6	24
				0.6-1.2	23
				1.2-2.5	4
				<2.5	-1

SOURCE DATA
Type: Fireplace, alder
Date: 4/13/84

Mass loading: 19366 $\mu g/m^3$
Adsorbed OC: 5.90 $\mu g/cm^2$
Sampling time = 20 minutes

Cut Pt. (μm)	Filter	Mass (mg)	OC ($\mu g/cm^2$)	EC ($\mu g/cm^2$)	OC/M (%)	EC/M (%)
0.1	T136	0.14				
0.3	Q485	0.71	51.76	6.60	48.8	7.0
0.6	T75	1.72				
1.2	Q484	2.17	131.37	24.67	49.1	9.6
2.5	T45	2.17				
None	Q503	2.17	148.48	27.18	55.8	10.6

	Al/M (%)	Si/M (%)	P/M (%)	S/M (%)	Cl/M (%)	K/M (%)
0.1	0.00	0.00	0.11	0.21	0.82	1.36
0.6	0.13	0.07	0.04	0.42	1.84	1.01
2.5	0.12	0.07	0.05	0.38	1.60	0.88

	Ca/M (%)	Ti/M (%)	V/M (%)	Mn/M (%)	Fe/M (%)	Ni/M (%)
0.1	0.00	0.00	0.00	0.00	0.00	0.00
0.6	0.00	0.00	0.00	0.00	0.00	0.00
2.5	0.02	0.00	0.00	0.00	0.00	0.00

	Cu/M (%)	Zn/M (%)	Br/M (%)	Rb/M (%)	Pb/M (%)
0.1	0.00	0.03	0.00	0.00	0.00
0.6	0.00	0.05	0.01	0.00	0.08
2.5	0.00	0.05	0.01	0.00	0.06

Carbon Size Distribution (%)

(μm)	OC	EC	TC
<0.3	28.6	21.6	27.5
0.3-1.2	59.4	69.2	60.9
>1.2	11.9	9.2	11.5

Mass Distribution

(μm)	(%)
<0.1	6.4
0.1-0.3	26.3
0.3-0.6	46.5
0.6-1.2	20.7
1.2-2.5	0.0
<2.5	0.0

Trace Element Size Distributions

(μm)	S (%)	Cl (%)	K (%)	Ca (%)	AL (%)	P (%)
<0.1	3.5	3.3	10.0	0.0	0.0	15.9
0.1-0.6	84.2	87.9	80.5	1.1	86.9	56.5
0.6-2.5	12.3	8.7	9.5	98.9	13.1	27.6

SOURCE DATA
Type: Fireplace, fir/alder
Date: 4/13/84

Mass loading: 28072 $\mu g/m^3$
Adsorbed OC: 10.80 $\mu g/cm^2$
Sampling time = 20 minutes

Cut Pt. (μm)	Filter	Mass (mg)	OC ($\mu g/cm^2$)	EC ($\mu g/cm^2$)	OC/M (%)	EC/M (%)
0.1	T215	1.28				
0.3	Q740	1.45	127.74	14.87	61.0	7.8
0.6	T208	3.49				
1.2	Q724	4.48	303.71	53.01	55.57	10.1
2.5	T223	4.60				
None	Q743	4.60	300.14	51.48	53.46	9.5

	Al/M (%)	Si/M (%)	P/M (%)	S/M (%)	Cl/M (%)	K/M (%)
0.1	0.03		0.05	0.15	0.10	0.58
0.6	0.02	0.09	0.03	0.12	0.14	0.49
2.5	0.03	0.05	0.02	0.10	0.11	0.43

	Ca/M (%)	Ti/M (%)	V/M (%)	Mn/M (%)	Fe/M (%)	Ni/M (%)
0.1	0.02	0.00	0.00	0.00	0.00	0.00
0.6	0.05	0.00	0.00	0.00	0.00	0.00
2.5	0.06	0.00	0.00	0.00	0.00	0.00

	Cu/M (%)	Zn/M (%)	Br/M (%)	Rb/M (%)	Pb/M (%)
0.1	0.00	0.02	0.00	0.00	0.01
0.6	0.00	0.01	0.00	0.00	0.00
2.5	0.00	0.01	0.00	0.00	0.00

Carbon Size Distribution (%)

(μm)	OC	EC	TC
<0.3	36.0	25.7	34.4
0.3-1.2	65.3	77.3	67.1
>1.2	-1.2	-3.0	-1.5

Mass Distribution

(μm)	(%)
<0.1	28
0.1-0.3	4
0.3-0.6	44
0.6-1.2	22
1.2-2.5	2
<2.5	0

Trace Element Size Distributions

(μm)	S (%)	Cl (%)	K (%)	Ca (%)	AL (%)	P (%)
<0.1	43.3	25.4	37.3	8.1	32.6	15.9
0.1-0.6	47.8	69.0	49.6	48.9	32.9	33.5
0.6-2.5	8.9	5.6	13.1	43.0	34.5	10.5

SOURCE DATA
Type: Fireplace, fir/alder
Date: 5/14/84

Mass loading: 3833 $\mu g/m^3$
Adsorbed OC: 6.0 $\mu g/cm^2$
Sampling time = 20 minutes

Cut Pt. (μm)	Filter	Mass (mg)	OC ($\mu g/cm^2$)	EC ($\mu g/cm^2$)	OC/M (%)	EC/M (%)
0.1	T184					
0.3	Q679	0.19	16.61	4.18	42.4	16.6
0.6	T209	0.54				
1.2	Q686	0.58	29.11	13.39	33.9	19.6
2.5	T182	0.58				
None	Q675	0.70	35.40	18.94	35.7	22.3

	Al/M (%)	Si/M (%)	P/M (%)	S/M (%)	Cl/M (%)	K/M (%)
0.1						
0.6						
2.5						

	Ca/M (%)	Ti/M (%)	V/M (%)	Mn/M (%)	Fe/M (%)	Ni/M (%)
0.1						
0.6						
2.5						

	Cu/M (%)	Zn/M (%)	Br/M (%)	Rb/M (%)	Pb/M (%)
0.1					
0.6					
2.5					

Carbon Size Distribution (%)

(μm)	OC	EC	TC
<0.3	32.1	20.3	27.6
0.3-1.2	46.5	52.7	48.9
>1.2	21.4	27.0	23.5

Mass Distribution

(μm)	(%)
<0.1	0
0.1-0.3	27
0.3-0.6	50
0.6-1.2	6
1.2-2.5	0
<2.5	17

Trace Element Size Distributions

(μm)	S (%)	Cl (%)	K (%)	Ca (%)	AL (%)	P (%)
<0.1	3.5	3.3	10.0	0.0	0.0	15.9
0.1-0.6	84.2	87.9	80.5	1.1	86.9	56.5
0.6-2.5	12.3	8.7	9.5	98.9	13.1	27.6

SOURCE DATA
Type: Fireplace, oak/alder
Date: 5/14/84

Mass loading: 4337 $\mu g/m^3$
Adsorbed OC: 6.0 $\mu g/cm^2$
Sampling time = 20 minutes

Cut Pt. (μm)	Filter	Mass (mg)	OC ($\mu g/cm^2$)	EC ($\mu g/cm^2$)	OC/M (%)	EC/M (%)
0.1	Q689	0.18	5.85	2.03	29.6	26.7
0.3	Q677	0.27	20.65	5.06	41.0	14.2
0.6	Q667	0.46	33.99	6.55	51.6	12.1
1.2	Q672	0.60	37.33	8.91	44.4	12.6
2.5	Q668	0.62	40.01	9.37	46.6	12.8
None	Q678	0.72	45.31	10.31	46.4	12.2

Carbon Size Distribution (%) (μm)	OC	EC	TC	Mass Distribution (μm)	(%)
<0.1	15.9	54.9	24.0	<0.1	25
0.1-0.3	17.2	-11.2	11.3	0.1-0.3	13
0.3-0.6	37.9	19.8	34.1	0.3-0.6	26
0.6-1.2	8.7	22.9	11.6	0.6-1.2	19
1.2-2.5	6.8	4.5	6.3	1.2-2.5	3
>2.5	13.5	9.1	12.6	<2.5	14

SOURCE DATA
Type: Fireplace, fir/alder
Date: 5/17/84

Mass loading: 20421 $\mu g/m^3$
Adsorbed OC: 10.8 $\mu g/cm^2$
Sampling time = 20 minutes

Cut Pt. (μm)	Filter	Mass (mg)	OC ($\mu g/cm^2$)	EC ($\mu g/cm^2$)	OC/M (%)	EC/M (%)
0.1	Q739	0.81	27.89	2.67	62.7	7.8
0.3	Q737	1.09	93.38	7.15	57.3	5.0
0.6	Q742	2.61	210.90	9.83	65.2	3.2
1.2	Q736	3.13	231.82	13.28	60.0	3.6
2.5	Q733	3.39	247.51	13.36	59.3	3.3
None	Q734	3.39	246.51	14.49	59.1	3.6

Carbon Size Distribution (%) (μm)	OC	EC	TC	Mass Distribution (μm)	(%)
<0.1	25.3	51.4	26.8	<0.1	24
0.1-0.3	5.8	-7.5	5.1	0.1-0.3	8
0.3-0.6	53.7	23.9	52.0	0.3-0.6	45
0.6-1.2	8.9	23.8	9.8	0.6-1.2	15
1.2-2.5	6.6	0.5	6.3	1.2-2.5	8
>2.5	-0.4	7.8	0.05	<2.5	0

SOURCE DATA
Type: Fireplace, oak/fir
Date: 6/20/84

Mass loading: 5686 $\mu g/m^3$
Adsorbed OC: 7.22 $\mu g/cm^2$
Sampling time = 20 minutes

Cut Pt. (μm)	Filter	Mass (mg)	OC ($\mu g/cm^2$)	EC ($\mu g/cm^2$)	OC/M (%)	EC/M (%)
0.1	T235	0.08				
0.3	Q749	0.82	72.58	10.80	60.3	10.0
0.6	T250	1.06				
1.2	Q798	1.10	76.03	8.98	53.2	6.9
2.5	T256	1.10				
None	Q807	1.18	76.40	19.42	49.8	6.8

	Al/M (%)	Si/M (%)	P/M (%)	S/M (%)	Cl/M (%)	K/M (%)
0.1						
0.6						
2.5						

	Ca/M (%)	Ti/M (%)	V/M (%)	Mn/M (%)	Fe/M (%)	Ni/M (%)
0.1						
0.6						
2.5						

	Cu/M (%)	Zn/M (%)	Br/M (%)	Rb/M (%)	Pb/M (%)
0.1					
0.6					
2.5					

Carbon Size Distribution (%)

(μm)	OC	EC	TC
<0.3	84.1		86.2
0.3-1.2	15.4		12.7
>1.2	.5		1.0

Mass Distribution

(μm)	(%)
<0.1	7
0.1-0.3	63
0.3-0.6	20
0.6-1.2	3
1.2-2.5	0
<2.5	7

SOURCE DATA
Type: Fireplace, oak/fir
Date: 6/20/84

Mass loading: 6517 $\mu g/m^3$
Adsorbed OC: 7.42 $\mu g/cm^2$
Sampling time - 20 minutes

Cut Pt. (μm)	Filter	Mass (mg)	OC ($\mu g/cm^2$)	EC ($\mu g/cm^2$)	OC/M (%)	EC/M (%)
0.1	T257	0.06				
0.3	Q804	0.66	42.54	6.60	51.6	5.6
0.6	T258	0.88				
1.2	Q811	0.93	64.89	10.55	52.5	9.6
2.5	T234	1.22				
None	Q793	1.22	81.66	11.55	51.7	8.0

	Al/M (%)	Si/M (%)	P/M (%)	S/M (%)	Cl/M (%)	K/M (%)
0.1						
0.6						
2.5						

	Ca/M (%)	Ti/M (%)	V/M (%)	Mn/M (%)	Fe/M (%)	Ni/M (%)
0.1						
0.6						
2.5						

	Cu/M (%)	Zn/M (%)	Br/M (%)	Rb/M (%)	Pb/M (%)
0.1					
0.6					
2.5					

Carbon Size Distribution (%)

(μm)	OC	EC	TC
<0.3	54.0	50.9	53.6
0.3-1.2	23.4	40.5	25.7
>1.2	22.6	8.7	20.7

Mass Distribution

(μm)	(%)
<0.1	5
0.1-0.3	49
0.3-0.6	18
0.6-1.2	4
1.2-2.5	24
<2.5	0

SOURCE DATA
Type: Fireplace, fir
Date: 6/20/84

Mass loading: 20000 $\mu g/m^3$
Adsorbed OC: 8.4 $\mu g/cm^2$

Cut Pt. (μm)	Filter	Mass (mg)	OC ($\mu g/cm^2$)	EC ($\mu g/cm^2$)	OC/M (%)	EC/M (%)
0.1	T255	0.28				
0.3	Q808	1.30	106.36	6.33	57.0	3.7
0.6	T218	2.49				
1.2	Q806	3.22	242.85	14.00	61.9	3.7
2.5	T216	3.15				
None	Q799	3.32	240.42	16.13	59.4	4.1

	Al/M (%)	Si/M (%)	P/M (%)	S/M (%)	Cl/M (%)	K/M (%)
0.1			0.00	0.35	0.00	0.09
0.6	0.02	0.22	0.02	0.06	0.06	0.10
2.5	0.03	0.05	0.02	0.06	0.05	0.08

	Ca/M (%)	Ti/M (%)	V/M (%)	Mn/M (%)	Fe/M (%)	Ni/M (%)
0.1		0.00	0.01	0.01	0.00	0.00
0.6	0.00	0.00	0.00	0.00	0.00	0.00
2.5	0.01	0.00	0.00	0.00	0.00	0.00

	Cu/M (%)	Zn/M (%)	Br/M (%)	Rb/M (%)	Pb/M (%)
0.1	0.00	0.01	0.00	0.00	0.00
0.6	0.00	0.01	0.00	0.00	0.01
2.5	0.00	0.00	0.00	0.00	0.00

Carbon Size Distribution (%)

(μm)	OC	EC	TC
<0.3	37.6	34.9	37.4
0.3-1.2	63.5	51.9	62.7
>1.2	-1.0	13.2	0.0

Mass Distribution

(μm)	(%)
<0.1	8
0.1-0.3	31
0.3-0.6	36
0.6-1.2	22
1.2-2.5	-2
<2.5	5

Trace Element Size Distributions

(μm)	S (%)	Cl (%)	K (%)	Zn (%)	AL (%)	Si (%)
<0.1	55.8	0.0	10.3			
0.1-0.6	25.4	88.6	91.3			
0.6-2.5	18.8	11.4	-1.7			

SOURCE DATA
Type: Backyard brush
Date: 3/22/84
(apple tree prunings)

Mass loading: 10120 $\mu g/m^3$
Adsorbed OC: 7.8 $\mu g/cm^2$
Sampling time = 20 minutes

Cut Pt. (μm)	Filter	Mass (mg)	OC ($\mu g/cm^2$)	EC ($\mu g/cm^2$)	OC/M (%)	EC/M (%)
0.1	Q416A	0.39	11.17	1.22	39.5	7.4
0.3	Q406A	0.48	39.99	4.75	50.7	7.5
0.6	Q407A	1.19	91.99	10.39	60.1	7.4
1.2	Q408A	1.32	87.07	9.88	51.0	6.4
2.5	Q410A	1.58	115.98	12.56	58.2	6.8
None	Q412A	1.68	114.68	11.80	54.1	6.0

Carbon Size Distribution (%) (μm)	OC	EC	TC	Mass Distribution (μm)	(%)
<0.1	16.9	28.8	18.1	<0.1	23
0.1-0.3	9.9	7.0	9.6	0.1-0.3	5
0.3-0.6	52.0	52.2	52.0	0.3-0.6	42
0.6-1.2	-4.6	-4.3	-4.6	0.6-1.2	8
1.2-2.5	27.0	22.7	26.6	1.2-2.5	15
>2.5	-1.2	-6.4	-1.7	<2.5	6

SOURCE DATA
Type: Residential oil furnace
Date: 4/1/85
Sampling time = 1 hour

Mass loading: 376 $\mu g/m^3$
Adsorbed OC: 3.71 $\mu g/cm^2$

Cut Pt. (μm)	Filter	Mass (mg)	OC ($\mu g/cm^2$)	EC ($\mu g/cm^2$)	OC/M (%)	EC/M (%)
0.3	Q941	0.12	6.57	1.92	18.03	12.1
0.6	Q974	0.17	7.30	2.57	18.0	12.8
1.2	Q529	0.22	7.34	2.67	14.0	10.3
2.5	Q973	0.23	7.57	2.75	14.3	10.2
10	Q883	0.25	7.60	2.76	13.2	9.4
10	T895	0.25				

	Al/M (%)	Si/M (%)	P/M (%)	S/M (%)	Cl/M (%)	K/M (%)
10	0.57	0.98	0.30	11.51	0.00	0.07

	Ca/M (%)	Ti/M (%)	V/M (%)	Mn/M (%)	Fe/M (%)	Ni/M (%)
10	0.04	0.00	0.01	0.01	0.11	0.00

	Cu/M (%)	Zn/M (%)	Br/M (%)	Rb/M (%)	Pb/M (%)
10	0.04	0.06	0.01	0.00	0.07

Carbon Size Distribution (%) (μm)	OC	EC	TC	Mass Distribution (%) Q mass
<0.3	65.5	61.8	64.0	48
0.3-0.6	27.0	31.2	28.7	20
0.6-1.2	1.0	3.6	2.0	20
1.2-2.5	5.8	3.0	4.7	4
2.5-10	0.7	0.4	0.6	8

SOURCE DATA
Type: Residential oil furnace
Date: 4/1/85
Sampling time = 1 hour

Mass loading: 602 $\mu g/m^3$
Adsorbed OC: 3.79 $\mu g/cm^2$

Cut Pt. (μm)	Filter	Mass (mg)	OC ($\mu g/cm^2$)	EC ($\mu g/cm^2$)	OC/M (%)	EC/M (%)
0.3	T344	0.12				
0.6	T309	0.17				
1.2	T341	0.22				
2.5	T346	0.23				
10	Q979	0.30	10.24	3.03	18	9
10	T343	0.29				

	Al/M (%)	Si/M (%)	P/M (%)	S/M (%)	Cl/M (%)	K/M (%)
0.3	0.43	0.42	0.30	11.82	0.00	0.02
0.6	0.38	0.41	0.27	10.86	0.00	0.00
1.2	0.48	0.42	0.34	11.66	0.00	0.00
2.5	0.45	0.43	0.31	12.16	0.00	0.01
10	0.54	0.60	0.33	12.12	0.00	0.02

	Ca/M (%)	Ti/M (%)	V/M (%)	Mn/M (%)	Fe/M (%)	Ni/M (%)
0.3	0.00	0.01	0.00	0.00	0.03	0.00
0.6	0.01	0.00	0.00	0.00	0.04	0.00
1.2	0.00	0.00	0.00	0.00	0.04	0.00
2.5	0.01	0.00	0.00	0.00	0.04	0.00
10	0.01	0.00	0.00	0.00	0.07	0.00

	Cu/M (%)	Zn/M (%)	Br/M (%)	Rb/M (%)	Pb/M (%)
0.3	0.02	0.06	0.00	0.00	0.00
0.6	0.02	0.04	0.00	0.00	0.04
1.2	0.02	0.05	0.00	0.00	0.00
2.5	0.01	0.05	0.00	0.00	0.01
10	0.00	0.04	0.01	0.01	0.06

Elemental Size Distribution

	Al (%)	Si (%)	P (%)	S (%)	Mass (%)
<0.3	35	31	37	43	45
0.3-0.6	21	23	44	27	34
0.6-1.2	21	6	0	12	7
1.2-2.5	-2	4	12	7	3
2.5-10	25	36	7	10	10

SOURCE DATA
Type: Oil furnace
Date: 5/14/84
Sampling time = 1 hour

Mass loading: 602 $\mu g/m^3$
Adsorbed OC: 5.48 $\mu g/cm^2$

Cut Pt. (μm)	Filter	Mass (mg)	OC ($\mu g/cm^2$)	EC ($\mu g/cm^2$)	OC/M (%)	EC/M (%)
0.1	T221	0.03 mass est.				
0.3	Q699	0.16	6.07	0.92	2.8	4.3
0.6	T222	0.20				
1.2	Q705	0.20	7.33	2.44	7.9	10.4
2.5	T200	0.23				
None	Q704	0.26	9.85	3.13	14.3	10.2

	Al/M (%)	Si/M (%)	P/M (%)	S/M (%)	Cl/M (%)	K/M (%)
0.1	0.31	2.10	0.24	13.16	0.19	0.07
0.6	0.46	0.83	0.37	12.67	0.00	0.00
2.5	0.59	0.87	0.34	12.98	0.00	0.03

	Ca/M (%)	Ti/M (%)	V/M (%)	Mn/M (%)	Fe/M (%)	Ni/M (%)
0.1	0.04	0.11	0.01	0.11	0.00	0.02
0.6	0.01	0.00	0.00	0.00	0.04	0.00
2.5	0.00	0.00	0.00	0.00	0.03	0.00

	Cu/M (%)	Zn/M (%)	Br/M (%)	Rb/M (%)	Pb/M (%)
0.1	0.23	0.04	0.00	0.00	0.00
0.6	0.21	0.06	0.00	0.00	0.02
2.5	0.23	0.04	0.00	0.00	0.05

Carbon Size Distribution (%)

(μm)	OC	EC	TC
<0.3	12.0	26.2	17.9
0.3-1.2	30.3	51.8	39.3
>1.2	57.7	22.0	42.8

Mass Distribution

(μm)	(%)
<0.1	12
0.1-0.3	50
0.3-0.6	15
0.6-1.2	0
1.2-2.5	11
<2.5	11

Trace Element Size Distributions

(μm)	S (%)	P (%)	Pb (%)	Zn (%)	AL (%)	Si (%)
<0.1	13	9	0		6	31
0.1-0.6	71	85	30		61	52
0.6-2.5	15	6	70		32	17

SOURCE DATA Sampling time = 32.6 hours
Type: Motor Vehicle (Tunnel) Mass loading: 26.5 $\mu g/m^3$
Date: 7/17/84 Adsorbed OC: 6.65 $\mu g/cm^2$

Cut Pt. (μm)	Filter	Mass (mg)	OC ($\mu g/cm^2$)	EC ($\mu g/cm^2$)	OC/M (%)	EC/M (%)
0.1	T237	0.09				
0.3	Q818	0.17	12.08	6.33	20.5	28.2
0.6	T263	0.25				
1.2	Q730	0.27	13.24	5.64	20.7	17.8
2.5	T262	0.36				
None	Q780	0.43	16.80	8.46	20.1	16.7

	Al/M (%)	Si/M (%)	P/M (%)	S/M (%)	Cl/M (%)	K/M (%)
0.1	1.10	1.53	0.00	5.26	0.88	0.22
0.6	0.74	1.16	0.00	5.09	0.31	0.20
2.5	0.77	1.12	0.00	4.44	1.73	0.24

	Ca/M (%)	Ti/M (%)	V/M (%)	Mn/M (%)	Fe/M (%)	Ni/M (%)
0.1	0.66	1.29	0.09	0.15	0.59	0.04
0.6	0.62	0.17	0.01	0.21	1.35	0.03
2.5	0.49	0.12	0.01	0.23	1.34	0.02

	Cu/M (%)	Zn/M (%)	Br/M (%)	Rb/M (%)	Pb/M (%)
0.1	0.09	0.26	2.48	0.00	6.79
0.6	0.05	0.25	2.85	0.00	6.02
2.5	0.05	0.44	2.23	0.00	4.54

Carbon Size Distribution (%)

(μm)	OC	EC	TC
<0.3	40.4	66.6	52.3
0.3-1.2	24.5	0.1	13.4
>1.2	35.1	33.3	34.3

Mass Distribution

(μm)	(%)
<0.1	21
0.1-0.3	19
0.3-0.6	18
0.6-1.2	5
1.2-2.5	21
<2.5	16

Trace Element Size Distributions

(μm)	S (%)	Cl (%)	K (%)	Ca (%)	Fe (%)	Ni (%)
<0.1	30	13	23	33	12	47
0.1-0.6	50	0	35	54	59	37
0.6-2.5	20	87	41	12	29	17

	Cu (%)	Br (%)	Al (%)	Mn (%)	Fe (%)	Pb (%)
<0.1	46	28	36	17	11	37
0.1-0.6	24	61	31	49	59	54
0.6-2.5	29	12	33	34	30	8

SOURCE DATA
Type: Motor Vehicle (Tunnel)
Date: 7/18/84
Sampling time = 36.6 hours

Mass loading: 36.6 $\mu g/m^3$
Adsorbed OC: 5.8 $\mu g/cm^2$

Cut Pt. (μm)	Filter	Mass (mg)	OC ($\mu g/cm^2$)	EC ($\mu g/cm^2$)	OC/M (%)	EC/M (%)
0.1	Q847	0.07	4.26	0.45	26.4	15.2
0.3	Q842	0.12	9.31	3.59	22.1	22.6
0.6	Q845	0.18	10.00	5.40	19.8	25.5
1.2	Q849	0.23	10.06	6.09	15.7	22.5
2.5	Q840	0.30	10.74	6.76	14.0	19.1
None	Q839	0.41	12.19	7.72	13.2	16.0

Carbon Size Distribution (%) (μm)	OC	EC	TC	Mass Distribution (μm)	(%)
<0.1	34	16	24	<0.1	17
0.1-0.3	15	25	20	0.1-0.3	12
0.3-0.6	16	29	23	0.3-0.6	15
0.6-1.2	1	9	5	0.6-1.2	12
1.2-2.5	11	9	10	1.2-2.5	17
>2.5	23	12	17	<2.5	27

SOURCE DATA
Type: Motor Vehicle (Tunnel) Mass loading: 25.2 $\mu g/m^3$
Date: 7/19/84
Sampling time = 23 hours

Cut Pt. (μm)	Filter	Mass (mg)
0.1	T265	0.03
0.3	T261	0.09
0.6	T238	0.12
1.2	T259	0.17
2.5	T243	0.20
None	T245	0.29

	Al/M (%)	Si/M (%)	P/M (%)	S/M (%)	Cl/M (%)	K/M (%)
0.1				0.15		
0.3	0.70			4.33	0.56	0.14
0.6	0.82			5.30	0.35	0.12
1.2	0.42	0.21		5.28	0.29	0.12
2.5	0.53	0.53		5.41	0.53	0.21
None	0.59	2.44		4.17	2.02	0.27

	Ca/M (%)	Ti/M (%)	V/M (%)	Mn/M (%)	Fe/M (%)	Ni/M (%)
0.1	0.66				0.72	
0.3	0.56	0.41		0.11	0.99	0.03
0.6	0.53	0.32		0.16	0.94	0.02
1.2	0.42	0.22		0.16	0.66	0.02
2.5	0.67	0.19		0.21	1.10	0.02
None	1.29	0.31		0.19	2.35	0.01

	Cu/M (%)	Zn/M (%)	Br/M (%)	Rb/M (%)	Pb/M (%)
0.1			6.64		14.89
0.3	0.07	0.17	4.34		9.77
0.6	0.04	0.15	3.16		7.28
1.2	0.04	0.16	2.65		5.95
2.5	0.05	0.22	2.63		5.83
None	0.06	0.24	2.06		4.59

Elemental Size Distributions

	S (%)	Cl (%)	Ca (%)	Fe (%)	Zn (%)	Br (%)	Pb (%)
0.1	24	13	5	3	14	33	33
0.3	8	-5	8	10	7	32	33
0.6	20	-1	4	3	5	-2	0
1.2	22	1	2	0	13	12	10
2.5	15	10	17	16	24	13	12
None	11	82	64	68	37	12	12

SOURCE DATA
Type: Motor Vehicle (Tunnel) Mass loading: 38.8 $\mu g/m^3$
Date: 7/20/84 Adsorbed OC: 7.4 $\mu g/cm^2$
Sampling time = 39.3 hours

Cut Pt. (μm)	Filter	Mass (mg)	OC ($\mu g/cm^2$)	EC ($\mu g/cm^2$)	OC/M (%)	EC/M (%)
0.1	T275	0.06				
0.3	Q835	0.22	15.22	6.65	26.7	22.9
0.6	T271	0.36				
1.2	Q827	0.45	18.29	11.31	20.5	21.4
2.5	T272	0.59				
None	Q852	0.76	22.89	15.11	17.3	16.9

	Al/M (%)	Si/M (%)	P/M (%)	S/M (%)	Cl/M (%)	K/M (%)
0.1	0.00	0.00	0.00	14.14	0.00	0.99
0.6	0.84	0.73	0.00	6.32	0.51	0.41
2.5	0.37	0.31	0.00	6.76	0.49	0.48

	Ca/M (%)	Ti/M (%)	V/M (%)	Mn/M (%)	Fe/M (%)	Ni/M (%)
0.1	0.66	0.00	0.00	0.00	0.39	0.00
0.6	0.35	0.00	0.00	0.04	0.57	0.02
2.5	0.32	0.00	0.00	0.03	0.56	0.01

	Cu/M (%)	Zn/M (%)	Br/M (%)	Rb/M (%)	Pb/M (%)
0.1	0.00	0.23	9.11		23.54
0.6	0.02	0.14	4.21		8.57
2.5	0.03	0.18	3.32		6.42

Carbon Size Distribution (%)

(μm)	OC	EC	TC
<0.3	44.8	39.2	42.0
0.3-1.2	25.4	35.7	30.5
>1.2	29.5	25.1	27.5

Mass Distribution

(μm)	(%)
<0.1	8
0.1-0.3	21
0.3-0.6	18
0.6-1.2	12
1.2-2.5	18
<2.5	22

Trace Element Size Distributions

(μm)	S (%)	Cl (%)	K (%)	Ca (%)	Fe (%)	Ni (%)	Zn (%)	Br (%)	Pb (%)
<0.1	21	0	21	21	7	0	13	28	37
0.1-0.6	36	63	32	46	55	90	33	49	44
0.6-2.5	43	37	47	33	38	10	53	27	18

VITA

John A. Rau was born in Albany, N. Y., on May 28, 1935. He graduated from Vincentian Institute High School in 1953 and obtained a B. S. in Mechanical Engineering from Rensselaer Polyhtechnic Institute in 1958. He worked for the Boeing Company from 1958 to 1963 and then for the Pratt and Whitney Aircraft Company from 1963 to 1966. He obtained an M. S. in Mechanical Engineering from the University of Michigan in 1967, after which he worked for Eastman Kodak Company until 1970. He then worked for the Reed College Physics Department until 1974. In 1977 he entered the Oregon Graduate Center and obtained an M. S. in Environmental Science in 1981.